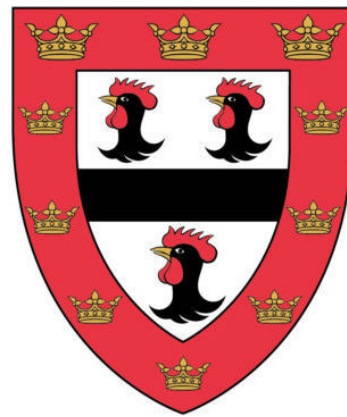
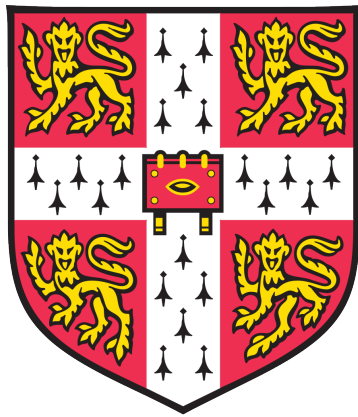


A dissertation submitted for the degree of Doctor of Philosophy

# Identifying regulators of neural stem cell fate and tumourigenesis



**Anna Elizabeth Hakes**

Supervisor: Professor Andrea H. Brand

Jesus College  
University of Cambridge

Wellcome Trust / Cancer Research UK Gurdon Institute  
Department of Physiology, Development and Neuroscience

September 2018



## **DECLARATION**

This dissertation is the result of my own work and includes nothing which is the outcome of work done in collaboration except as declared in the Preface and specified in the text.

It is not substantially the same as any that I have submitted, or, is being concurrently submitted for a degree or diploma or other qualification at the University of Cambridge or any other University or similar institution except as declared in the Preface and specified in the text. I further state that no substantial part of my dissertation has already been submitted, or, is being concurrently submitted for any such degree, diploma or other qualification at the University of Cambridge or any other University or similar institution except as declared in the Preface and specified in the text

It does not exceed the prescribed word limit of 60,000 words.

Anna Elizabeth Hakes



## SUMMARY

### Identifying regulators of neural stem cell fate and tumourigenesis

Anna Elizabeth Hakes

The proliferation of neural stem cells (NSCs) must be regulated precisely in order to generate a functional nervous system. Mis-regulated NSC division can lead to the inadequate production of differentiated progeny or to ectopic NSCs and tumour formation. As such, genes that promote the proliferative capacity of NSCs must be maintained in NSCs but down regulated in post-mitotic progeny.

In vertebrates, the orphan nuclear receptor TLX (also known as nuclear receptor subfamily 2, group E, member 1 or NR2E1) is expressed in NSCs both during development and in adults. TLX mutations are linked to microcephaly and hereditary cases of bipolar disorder, whereas high TLX expression is a diagnostic marker of aggressive glioblastoma tumours and is correlated with poor patient prognosis. Despite the developmental and clinical importance of this gene, the molecular mechanisms through which it acts are not understood well.

I have identified the *Drosophila* gene *tailless* (*tll*), the counterpart of TLX, as a key regulator of a subset of NSCs (known as type II) that divide in a manner analogous to mammalian NSCs. Human TLX and *tll* are highly conserved: the DNA binding domains share 81 % amino acid identity and conserved cofactors, such as Atrophin, mediate their activity as transcriptional repressors. During development, type II NSCs express Tll and divide to give rise to intermediate progenitors, which down-regulate Tll. In the absence of Tll, type II NSCs convert into a more restricted progenitor and are unable to generate full neuronal lineages. To identify the genes regulated by Tll in type II NSCs I used Targeted DamID to determine the genome-wide binding sites of Tll *in vivo*. My results showed that Tll binds to many of the genes required for type II NSC identity, suggesting that Tll is a master regulator of type II NSC fate.

To test if the tumourigenic capacity of Tll/TLX was conserved in flies I expressed Tll or human TLX at high levels in the *Drosophila* brain, which resulted in large tumours consisting of type II NSCs. Through lineage analysis, I showed that Tll/TLX causes intermediate progenitors to revert to a NSC fate, thereby preventing differentiation and creating large tumours. This suggests that TLX and Tll act through conserved mechanisms to control NSC fate and implicates intermediate progenitors as the cell type of origin of TLX-induced tumours. Identifying the tumour-initiating cell for glioblastoma is vital for developing effective cell-type-specific treatments.

Many distinct types of NSCs, which have different developmental and tumourigenic capacities, act in a coordinated manner to generate the *Drosophila* brain. The optic lobe neuroepithelium generates the NSCs that produce the adult visual system. The neuroepithelium is formed in the embryo but is not thought to generate NSCs until larval stages. I observed that many of the genes that regulate type II NSCs, such as *tll*, are also expressed in the optic lobe neuroepithelium. I identified that a marker of type II lineages (a regulatory fragment of the Fezf transcription factor *earmuff*) can also be used to follow the transition from neuroepithelium to NSCs in the optic lobe. Analysis of the division mode of the neuroepithelium (carried out in collaboration with Dr. Leo Otsuki) identified a new, embryonic phase of optic lobe NSC production. This finding shows that the neuroepithelium and NSCs co-exist throughout the majority of development and highlights the common genetic mechanisms that regulate different NSC populations.



## ACKNOWLEDGEMENTS

First and foremost I should like to thank Andrea for her support and guidance during my PhD. Thank you for creating a great working environment, for giving me the freedom to pursue my own ideas, and for providing encouragement when I needed it.

Thank you to all the members of the Brand Lab, past and present. I feel very fortunate to have been able to work alongside so many talented scientists from whom I have learnt so much. The support and enthusiasm of the whole lab has kept me going throughout the ups and downs of my PhD. In particular, thank you to Libby and Esteban for being fantastic mentors; to Leo, who was there from the beginning, for all the fun times, coffee club, and for EONs; and to Chloe, Janina, Seth, and Steph, I am so grateful to have shared the PhD experience with friends like you. Thanks also go to Jelle for his infectious enthusiasm and to Robert for his bioinformatics expertise.

I am thankful to those who were kind enough to share reagents with me: Benjamin Altenhein, Konrad Basler, Sarah Bray, Richard Carthew, Chris Doe, Ted Erclik Lily Jan and Yuh Nung Jan, Yuu Kimata, Golnar Kolahgar, Jurgen Knoblich, Mitsuhiro Kurusu, Cheng-Yu Lee, Tzumin Lee, Gwo-Jen Liaw, Makoto Sato, Jim Skeath, Ryohei Yagi, Sijun Zhu. The fly community is a generous group. Thanks to everyone who has helped me at the Gurdon Institute; especially to Admin, Media, I.T., and the Imaging Facility. Thank you to the Wellcome Trust for funding my PhD studentship and to Daniel, Clare, and Sarah for running a great programme. And to Steve for supporting me from the start.

Thanks to Mike, for being my partner in crime, and to the Wellcome Gals, Bean, Surangi, and Tara, for their friendship and mutual enthusiasm for gin.

And, finally, to my Mum and Dad for providing me with every opportunity and supporting me unconditionally. I couldn't have done it without you.



# TABLE OF CONTENTS

|                                                                                                                                                         |             |
|---------------------------------------------------------------------------------------------------------------------------------------------------------|-------------|
| <b>Declaration</b> .....                                                                                                                                | <b>i</b>    |
| <b>Summary</b> .....                                                                                                                                    | <b>iii</b>  |
| <b>Acknowledgements</b> .....                                                                                                                           | <b>v</b>    |
| <b>Table of Contents</b> .....                                                                                                                          | <b>vii</b>  |
| <b>Table of Figures</b> .....                                                                                                                           | <b>xi</b>   |
| <b>List of Tables</b> .....                                                                                                                             | <b>xii</b>  |
| <b>Glossary</b> .....                                                                                                                                   | <b>xiii</b> |
| <b>Terms</b> .....                                                                                                                                      | <b>xiii</b> |
| <b>Protein abbreviations</b> .....                                                                                                                      | <b>xiv</b>  |
| <br>                                                                                                                                                    |             |
| <b>Chapter 1: Introduction</b> .....                                                                                                                    | <b>1</b>    |
| 1.1 Brain tumours can arise from NSC lineages .....                                                                                                     | 1           |
| 1.1.1 Glioblastoma multiforme tumours are heterogeneous and difficult to treat.....                                                                     | 1           |
| 1.2 TLX is an important regulator of NSCs .....                                                                                                         | 3           |
| 1.2.1 TLX in brain tumours .....                                                                                                                        | 3           |
| 1.2.2 TLX structure and regulation .....                                                                                                                | 4           |
| 1.3 <i>tailless</i> is the <i>Drosophila</i> homologue of TLX.....                                                                                      | 6           |
| 1.3.1 <i>tailless</i> specifies NSC fate in the embryo .....                                                                                            | 6           |
| 1.4 <i>Drosophila</i> neurogenesis .....                                                                                                                | 7           |
| 1.4.1 Multiple types of NSCs generate the <i>Drosophila</i> brain .....                                                                                 | 7           |
| 1.4.2 Type II neuroblasts .....                                                                                                                         | 8           |
| 1.5 Project aims .....                                                                                                                                  | 11          |
| 1.5.1 The characterisation of Tll in type II neuroblasts and tumourigenesis.....                                                                        | 11          |
| 1.5.2 Characterising the early stages of optic lobe neuroepithelium development.....                                                                    | 12          |
| <br>                                                                                                                                                    |             |
| <b>Chapter 2: Tll is required to maintain type II neuroblast and lineage identity</b> .....                                                             | <b>15</b>   |
| 2.1 Tll is expressed in type II neuroblasts .....                                                                                                       | 16          |
| 2.1.1 Assessing the expression of <i>tll</i> .....                                                                                                      | 16          |
| 2.1.2 Examining the expression patterns of <i>tll</i> -GAL4 lines .....                                                                                 | 18          |
| 2.2 Determining the role of Tll in type II lineages .....                                                                                               | 23          |
| 2.2.1 Tll is required for type II lineage maintenance.....                                                                                              | 23          |
| 2.2.2 Creating an immortalised type II-specific GAL4 .....                                                                                              | 25          |
| 2.2.3 Type II neuroblasts switch to type I neuroblasts in the absence of <i>tll</i> .....                                                               | 27          |
| 2.2.4 Removing <i>tll</i> prevents <i>brat</i> tumour formation.....                                                                                    | 29          |
| 2.2.5 Repression of <i>ase</i> is downstream of <i>tll</i> .....                                                                                        | 29          |
| 2.3 Chapter 2 discussion.....                                                                                                                           | 32          |
| <br>                                                                                                                                                    |             |
| <b>Chapter 3: Targeted DamID reveals the genome-wide binding sites of Tll <i>in vivo</i></b> .....                                                      | <b>35</b>   |
| 3.1 Designing the Tll Targeted DamID experiment.....                                                                                                    | 36          |
| 3.1.1 Creating a type II-specific GAL4 for Targeted DamID .....                                                                                         | 37          |
| 3.2 Profiling Tll binding sites in type II neuroblasts .....                                                                                            | 39          |
| 3.2.1 Tll TaDa shows cell type specific binding .....                                                                                                   | 39          |
| 3.2.2 Tll binds to AS-C genes.....                                                                                                                      | 42          |
| 3.2.3 Tll binds to genes that are expressed differentially in type II lineages: <i>pros</i> , <i>pntP1</i> , <i>erm</i> , <i>btd</i> , <i>Sp1</i> ..... | 43          |

|                                                                                                                     |            |
|---------------------------------------------------------------------------------------------------------------------|------------|
| 3.2.4 Tll binds to canonical NSC genes.....                                                                         | 47         |
| 3.3 Tll binds to a subset of TLX orthologues.....                                                                   | 48         |
| 3.4 Chapter 3 discussion.....                                                                                       | 50         |
| 3.4.1 Tll binds to many genes throughout the genome.....                                                            | 50         |
| 3.4.2 Implications for vertebrate TLX.....                                                                          | 51         |
| <b>Chapter 4: Tll/TLX initiates tumourigenesis from intermediate neural progenitors .....</b>                       | <b>53</b>  |
| 4.1 Assessing the tumourigenic capacity of Tll in <i>Drosophila</i> type II lineages.....                           | 54         |
| 4.1.1 High levels of Tll in type II lineages results in tumours.....                                                | 55         |
| 4.1.2 Tll can generate type II neuroblasts from INPs.....                                                           | 55         |
| 4.2 Tll/TLX causes INPs to revert to type II neuroblast fate.....                                                   | 57         |
| 4.2.1 G-TRACE shows that Tll causes INPs to revert to neuroblasts.....                                              | 58         |
| 4.2.2 GAL4 immortalisation reveals tumourigenic capacity of Tll from INPs.....                                      | 59         |
| 4.2.3 Non-autonomous contribution to tumourigenesis.....                                                            | 60         |
| 4.2.4 Human TLX can induce tumours from <i>Drosophila</i> INPs.....                                                 | 62         |
| 4.3 Assessing the tumourigenic capacity of Tll in other <i>Drosophila</i> neural progenitors.....                   | 64         |
| 4.3.1 Tll and TLX induce type II neuroblast fate from type I neuroblasts.....                                       | 64         |
| 4.3.2 Co-operativity with <i>btd</i> is required for <i>tll</i> to induce tumours.....                              | 65         |
| 4.4 Tll-induced tumours are prevented by promoting differentiation.....                                             | 70         |
| 4.4.1 Ase can rescue Tll tumours.....                                                                               | 70         |
| 4.4.2 Differentiating cells are resistant to Tll-induced tumourigenesis.....                                        | 72         |
| 4.5 TLX has a stronger tumourigenic capacity than Tll.....                                                          | 73         |
| 4.6 Chapter 4 discussion.....                                                                                       | 74         |
| <b>Chapter 5: The optic lobe generates a newly discovered neural stem cell population during embryogenesis.....</b> | <b>77</b>  |
| 5.1 The optic lobe and type II neuroblasts are regulated by common factors.....                                     | 77         |
| 5.1.1 Earmuff is an optic lobe transition zone marker.....                                                          | 78         |
| 5.2 The optic lobe neuroepithelium divides in the embryo.....                                                       | 80         |
| 5.2.1 Neuroepithelial cells divides throughout embryogenesis.....                                                   | 80         |
| 5.2.2 The embryonic neuroepithelium generates neuroblasts.....                                                      | 82         |
| 5.3 Characterising EON production.....                                                                              | 85         |
| 5.3.1 EONs derive from two spatial domains of the neuroepithelium.....                                              | 85         |
| 5.3.2 The embryonic neuroepithelium expresses transition zone markers.....                                          | 85         |
| 5.3.3 EONs generate neurons and glia.....                                                                           | 86         |
| 5.4 EONs in the post-embryonic brain.....                                                                           | 90         |
| 5.4.1 EONs undergo G <sub>0</sub> quiescence and persist into the larval brain.....                                 | 90         |
| 5.4.2 EONs turn off R9D11-mCD8-GFP before they re-enter the cell cycle.....                                         | 90         |
| 5.4.3 The fate of EONs after reactivation is unclear.....                                                           | 92         |
| 5.5 Early larval neuroblast transition.....                                                                         | 94         |
| 5.5.1 Early larval optic lobe neuroblasts come from the <i>wg</i> domains.....                                      | 96         |
| 5.6 Chapter 5 discussion.....                                                                                       | 97         |
| <b>Chapter 6: Discussion.....</b>                                                                                   | <b>99</b>  |
| 6.1 Common genetic mechanisms regulate different NSC populations.....                                               | 99         |
| 6.2 <i>Drosophila</i> Tll: implications for brain disorders and tumour initiation.....                              | 101        |
| 6.2.1 A conserved route to tumourigenesis.....                                                                      | 103        |
| 6.2.2 TLX as a therapeutic target.....                                                                              | 105        |
| 6.2.3 <i>Drosophila</i> as a drug screening system.....                                                             | 106        |
| 6.3 Concluding remarks.....                                                                                         | 106        |
| <b>Chapter 7: Materials and methods.....</b>                                                                        | <b>107</b> |
| 7.1 Fly stocks and husbandry.....                                                                                   | 107        |
| 7.1.1 GAL4 driver lines.....                                                                                        | 107        |

|                                                                                                                                                                           |            |
|---------------------------------------------------------------------------------------------------------------------------------------------------------------------------|------------|
| 7.1.2 UAS-driven transgenes.....                                                                                                                                          | 107        |
| 7.1.3 Reporter lines.....                                                                                                                                                 | 108        |
| 7.1.4 MARCM clones.....                                                                                                                                                   | 108        |
| 7.1.5 FLEXAMP lineage tracing.....                                                                                                                                        | 108        |
| 7.2 Protocols for imaging techniques.....                                                                                                                                 | 109        |
| 7.2.1 Embryo fixation and immunostaining.....                                                                                                                             | 109        |
| 7.2.2 Larval brain fixation and immunostaining.....                                                                                                                       | 109        |
| 7.2.3 Adult brain fixation and immunostaining.....                                                                                                                        | 110        |
| 7.2.4 <i>tll</i> RNA FISH.....                                                                                                                                            | 110        |
| 7.2.5 Image acquisition and processing.....                                                                                                                               | 111        |
| 7.2.6 Quantification and statistical analysis.....                                                                                                                        | 111        |
| 7.3 <i>Drosophila</i> transgenesis.....                                                                                                                                   | 111        |
| 7.3.1 Generation of UAS- <i>TLX</i> .....                                                                                                                                 | 111        |
| 7.3.2 Generation of UAS-LT3-NDam- <i>tll</i> .....                                                                                                                        | 112        |
| 7.4 Targeted DamID.....                                                                                                                                                   | 113        |
| 7.4.1 <i>Drosophila</i> genetics for Targeted DamID.....                                                                                                                  | 113        |
| 7.4.2 Targeted DamID protocol.....                                                                                                                                        | 113        |
| 7.4.3 Targeted DamID analysis.....                                                                                                                                        | 115        |
| <b>Appendix.....</b>                                                                                                                                                      | <b>117</b> |
| Appendix 1: Sequence conservation between human <i>TLX</i> and <i>Drosophila</i> Tll.....                                                                                 | 117        |
| Appendix 2: Tll target genes in type II neuroblasts identified by Targeted DamID.....                                                                                     | 119        |
| Appendix 3: <i>Drosophila</i> genotypes and temperature conditions.....                                                                                                   | 133        |
| Appendix 4: A newly discovered neural stem cell population is generated by the optic lobe<br>neuroepithelium during embryogenesis in <i>Drosophila melanogaster</i> ..... | 139        |
| <b>References.....</b>                                                                                                                                                    | <b>147</b> |



## TABLE OF FIGURES

|                                                                                                                   |           |
|-------------------------------------------------------------------------------------------------------------------|-----------|
| <b>Chapter 1: Introduction</b> .....                                                                              | <b>1</b>  |
| Figure 1.1: NSC fate and differentiation must be balanced during brain development.....                           | 2         |
| Figure 1.2: TLX in brain homeostasis.....                                                                         | 4         |
| Figure 1.3: Human TLX and <i>Drosophila</i> Tll are highly conserved.....                                         | 5         |
| Figure 1.4: Division modes of <i>Drosophila</i> NSCs.....                                                         | 7         |
| Figure 1.5: The anatomy of the <i>Drosophila</i> larval CNS.....                                                  | 8         |
| Figure 1.6: Differential gene expression between type II and type I neuroblast lineages.....                      | 10        |
| Figure 1.7: The development of the <i>Drosophila</i> optic lobe.....                                              | 13        |
| <br>                                                                                                              |           |
| <b>Chapter 2: Tll is required to maintain type II neuroblast and lineage identity</b> .....                       | <b>15</b> |
| Figure 2.1: <i>tll</i> reporters are expressed in type II neuroblasts.....                                        | 17        |
| Figure 2.2: <i>tll</i> mRNA and protein is expressed in type II neuroblasts.....                                  | 18        |
| Figure 2.3: Expression of <i>tll</i> -GAL4 drivers in the larval CNS.....                                         | 20        |
| Figure 2.4: Type II <i>tll</i> fragments map to overlapping genomic regions.....                                  | 22        |
| Figure 2.5: Knockdown to <i>tll</i> results in the loss of all type II neuroblasts.....                           | 24        |
| Figure 2.6: <i>tll</i> null type II neuroblast clones cannot be recovered.....                                    | 25        |
| Figure 2.7: <i>pntP1&gt;act</i> -GAL4 – an immortalised type II GAL4 driver.....                                  | 26        |
| Figure 2.8: Loss of <i>tll</i> causes type II lineages to transform to type I identity.....                       | 28        |
| Figure 2.9: Removing <i>tll</i> rescues <i>brat</i> tumours.....                                                  | 30        |
| Figure 2.10: Tll acts upstream of <i>ase</i> repression in type II neuroblasts.....                               | 31        |
| <br>                                                                                                              |           |
| <b>Chapter 3: Tll is required to maintain type II neuroblast and lineage identity</b> .....                       | <b>35</b> |
| Figure 3.1: TaDa allows low, cell-type-specific expression of Dam-fusion proteins.....                            | 36        |
| Figure 3.2: Available type II GAL4s are not suitable for TaDa.....                                                | 37        |
| Figure 3.3: Testing the expression of <i>stg</i> $\cap$ <i>dpn</i> -GAL4.....                                     | 38        |
| Figure 3.4: Tll binds to previously determined target genes.....                                                  | 40        |
| Figure 3.5: Tll binds to <i>ase</i> and <i>l'sc</i> , two AS-C genes.....                                         | 41        |
| Figure 3.6: Tll binds at the <i>pros</i> locus.....                                                               | 43        |
| Figure 3.7: Tll binds to genes required for INP specification.....                                                | 44        |
| Figure 3.8: Tll binds to <i>btd</i> and <i>Sp1</i> .....                                                          | 46        |
| Figure 3.9: Tll binds to canonical NSC genes.....                                                                 | 47        |
| <br>                                                                                                              |           |
| <b>Chapter 4: Tll/TLX initiates tumourigenesis from intermediate neural progenitors</b> .....                     | <b>53</b> |
| Figure 4.1: Molecular markers for following type II lineage progression.....                                      | 54        |
| Figure 4.2: High levels of Tll cause tumours in type II lineages.....                                             | 55        |
| Figure 4.3: Tll is sufficient to induce type II neuroblast fate from INPs.....                                    | 56        |
| Figure 4.4: G-TRACE reveals that INPs revert to type II neuroblast fate in response to Tll.....                   | 58        |
| Figure 4.5: R9D11> <i>act</i> -GAL4 is an immortalised INP driver.....                                            | 60        |
| Figure 4.6: Immortalised INP GAL4 results in large Tll OE tumours.....                                            | 61        |
| Figure 4.7: Tll and TLX show comparable expression in NSC lineages.....                                           | 62        |
| Figure 4.8: Human TLX initiates tumourigenesis from type II INPs.....                                             | 63        |
| Figure 4.9: Type II INPs revert to neuroblast fate in response to human TLX.....                                  | 64        |
| Figure 4.10: Tll can induce tumours outside of type II lineages.....                                              | 65        |
| Figure 4.11: Tll tumours lack Ase and Pros.....                                                                   | 66        |
| Figure 4.12: Tumour initiation by Tll occurs in <i>btd</i> <sup>+</sup> VNC lineages.....                         | 67        |
| Figure 4.13: Loss of <i>ase</i> from type I lineages is not sufficient to induce type II fate.....                | 69        |
| Figure 4.14: Tll OE in <i>btd</i> <sup>+</sup> type I neuroblasts generates large type II neuroblast tumours..... | 69        |
| Figure 4.15: Expressing Ase in Tll tumours prevents tumour formation.....                                         | 71        |
| Figure 4.16: Differentiating cells do not generate tumours in response to high levels of Tll.....                 | 72        |
| Figure 4.17: TLX induces tumours from type I neuroblasts and GMCs but not from neurons.....                       | 73        |

|                                                                                                                                                   |            |
|---------------------------------------------------------------------------------------------------------------------------------------------------|------------|
| <b>Chapter 5: The optic lobe generates a newly discovered neural stem cell population during embryogenesis .....</b>                              | <b>77</b>  |
| <b>Figure 5.1:</b> Division modes of stem cells in the optic lobe and type II neuroblasts.....                                                    | 78         |
| <b>Figure 5.2:</b> Maturing type II INPs and the optic lobe transition zone express Erm and L'sc .....                                            | 79         |
| <b>Figure 5.3:</b> Existing model of neuroepithelium dynamics .....                                                                               | 81         |
| <b>Figure 5.4:</b> The neuroepithelium divides throughout embryogenesis .....                                                                     | 81         |
| <b>Figure 5.5:</b> The embryonic neuroepithelium divides to give rise to EONs.....                                                                | 83         |
| <b>Figure 5.6:</b> The <i>dVsx1</i> and <i>wg</i> domains of the embryonic neuroepithelium produce EONs.....                                      | 84         |
| <b>Figure 5.7:</b> Transition zone markers are expressed in the embryonic neuroepithelium at sites of EON production.....                         | 86         |
| <b>Figure 5.8:</b> EONs generate neurons and glia.....                                                                                            | 87         |
| <b>Figure 5.9:</b> Lineage tracing confirms that EONs generate neuronal progeny that lie in close contact with the larval visual system .....     | 88         |
| <b>Figure 5.10:</b> EONs persist in the larval brain in G <sub>0</sub> quiescence .....                                                           | 89         |
| <b>Figure 5.11:</b> EONs turn off R9D11-mCD8-GFP before re-entering the cell cycle.....                                                           | 91         |
| <b>Figure 5.12:</b> Tracing the fate of EONs and their progeny is not possible with the tools available.....                                      | 93         |
| <b>Figure 5.13:</b> All neuroblasts surrounding the neuroepithelium re-enter the cell cycle .....                                                 | 94         |
| <b>Figure 5.14:</b> R9D11-mCD8-GFP labels neuroblasts in close contact with the neuroepithelium before the progression of the proneural wave..... | 95         |
| <b>Figure 5.15:</b> The <i>wg</i> domain expresses the transition zone marker R9D11-mCD8-GFP during early larval development .....                | 96         |
| <b>Figure 5.16:</b> Summary of transition zones in the neuroepithelium throughout development.....                                                | 98         |
| <br>                                                                                                                                              |            |
| <b>Chapter 6: Discussion .....</b>                                                                                                                | <b>99</b>  |
| <b>Figure 6.1:</b> Common molecular mechanisms regulate NSC transitions in the developing optic lobe and type II neuroblast lineages .....        | 100        |
| <b>Fig. 6.2:</b> Targeting GSCs with differentiation therapy .....                                                                                | 104        |
| <br>                                                                                                                                              |            |
| <b>LIST OF TABLES</b>                                                                                                                             |            |
| <br>                                                                                                                                              |            |
| <b>Chapter 2: Tll is required to maintain type II neuroblast and lineage identity.....</b>                                                        | <b>15</b>  |
| <b>Table 2.1:</b> Expression patterns of <i>tll</i> GAL4 lines .....                                                                              | 21         |
| <br>                                                                                                                                              |            |
| <b>Chapter 3: Tll is required to maintain type II neuroblast and lineage identity.....</b>                                                        | <b>35</b>  |
| <b>Table 3.1:</b> GO term analysis of genome-wide Tll protein-coding targets .....                                                                | 39         |
| <b>Table 3.3:</b> Tll binds to a subset of TLX targets .....                                                                                      | 49         |
| <br>                                                                                                                                              |            |
| <b>Chapter 7: Materials and methods.....</b>                                                                                                      | <b>109</b> |
| <b>Table 7.1:</b> Primary antibodies used for immunostaining.....                                                                                 | 113        |
| <br>                                                                                                                                              |            |
| <b>Appendix .....</b>                                                                                                                             | <b>119</b> |
| <b>Appendix Table 1:</b> <i>Drosophila</i> genotypes and experimental conditions.....                                                             | 135        |

## GLOSSARY

### Terms

|                |                                                                   |               |                                                   |
|----------------|-------------------------------------------------------------------|---------------|---------------------------------------------------|
| <b>ALH</b>     | After larval hatching                                             | <b>LT3</b>    | Low level translation version 3                   |
| <b>AS-C</b>    | Achaete-scute complex                                             | <b>MARCM</b>  | Mosaic analysis with a repressible cell marker    |
| <b>bp</b>      | Base pair                                                         | <b>MaTaDa</b> | Mammalian TaDa                                    |
| <b>BrdU</b>    | 5-bromo-2'-deoxyuridine                                           | <b>mRNA</b>   | Messenger RNA                                     |
| <b>CB</b>      | Central brain                                                     | <b>NB</b>     | Neuroblast                                        |
| <b>cDNA</b>    | complementary DNA                                                 | <b>NE</b>     | Neuroepithelium                                   |
| <b>ChIP</b>    | Chromatin immunoprecipitation                                     | <b>NGS</b>    | Next-generation sequencing                        |
| <b>CNS</b>     | Central nervous system                                            | <b>NSC</b>    | Neural stem cell                                  |
| <b>CyO</b>     | Curly of Oster (second chromosome balancer)                       | <b>OE</b>     | Over expression                                   |
| <b>Dam</b>     | DNA adenine methyltransferase                                     | <b>OL</b>     | Optic lobe                                        |
| <b>DamID</b>   | DNA adenine methyltransferase identification                      | <b>ORF</b>    | Open reading frame                                |
| <b>DBD</b>     | DNA binding domain                                                | <b>PBS</b>    | Phosphate buffered saline                         |
| <b>DL</b>      | Dorsolateral                                                      | <b>PBTx</b>   | Phosphate buffered saline with 0.3 % Triton X-100 |
| <b>DM</b>      | Dorsomedial                                                       | <b>PCR</b>    | Polymerase chain reaction                         |
| <b>DNA</b>     | Deoxyribonucleic acid                                             | <b>pH3</b>    | Phosphorylated H3                                 |
| <b>EON</b>     | Embryonic optic neuroblast                                        | <b>RFP</b>    | Red fluorescent protein                           |
| <b>FISH</b>    | Fluorescence <i>in situ</i> hybridisation                         | <b>RNA</b>    | Ribonucleic acid                                  |
| <b>FLEXAMP</b> | Flip-out LexA amplification                                       | <b>RNAi</b>   | RNA interference                                  |
| <b>FM7</b>     | First multiple 7 (X chromosome balancer)                          | <b>RT-PCR</b> | Reverse transcription PCR                         |
| <b>G-TRACE</b> | GAL4 technique for real-time and clonal expression                | <b>SGZ</b>    | Subgranular zone                                  |
| <b>GBM</b>     | Glioblastoma multiforme                                           | <b>shRNA</b>  | Short hairpin RNA                                 |
| <b>GMC</b>     | Ganglion mother cell                                              | <b>SSC</b>    | Saline-sodium citrate                             |
| <b>GMR</b>     | Gerald Mayer Rubin (identifier for <i>Janelia</i> FlyLight GAL4s) | <b>SVZ</b>    | Subventricular zone                               |
| <b>GO</b>      | Gene ontology                                                     | <b>TaDa</b>   | Targeted DamID                                    |
| <b>GSC</b>     | Glioblastoma stem cell                                            | <b>TM6B</b>   | Third multiple 6B (third chromosome balancer)     |
| <b>HDAC</b>    | Histone deacetylase                                               | <b>TSS</b>    | Transcription start site                          |
| <b>INP</b>     | Intermediate neural progenitor                                    | <b>txn</b>    | Transcription                                     |
| <b>kb</b>      | Kilobase                                                          | <b>TZ</b>     | Transition zone                                   |
| <b>LBD</b>     | Ligand binding domain                                             | <b>UAS</b>    | Upstream activating sequence                      |
| <b>lof</b>     | Loss of function                                                  | <b>VNC</b>    | Ventral nerve cord                                |
|                |                                                                   | <b>VT</b>     | Vienna Tiles                                      |
|                |                                                                   | <b>YFP</b>    | Yellow fluorescent protein                        |

## Protein names

|                |                                                  |               |                                 |
|----------------|--------------------------------------------------|---------------|---------------------------------|
| <b>22C10</b>   | Futsch                                           | <b>Pnt</b>    | Pointed                         |
| <b>Ac</b>      | Achaete                                          | <b>Pros</b>   | Prospero                        |
| <b>ASCL1</b>   | Achaete-scute family bHLH transcription factor 1 | <b>Prox 1</b> | Prospero-related homeobox 1     |
| <b>Ase</b>     | Asense                                           | <b>PTEN</b>   | Phosphatase and tensin homolog  |
| <b>BCL11A</b>  | B-cell lymphoma/leukemia 11A                     | <b>Repo</b>   | Reversed polarity               |
| <b>Brat</b>    | Brain tumour                                     | <b>RFP</b>    | Red fluorescent protein         |
| <b>Btd</b>     | Buttonhead                                       | <b>Sc</b>     | Scute                           |
| <b>CycA</b>    | Cyclin A                                         | <b>Sna</b>    | Snail                           |
| <b>Dfd</b>     | Deformed                                         | <b>Sp1</b>    | Specificity protein 1           |
| <b>Dpn</b>     | Deadpan                                          | <b>Stg</b>    | String                          |
| <b>Dpp</b>     | Decapentaplegic                                  | <b>Tll</b>    | Tailless                        |
| <b>EGFP</b>    | Enhanced green fluorescent protein               | <b>VGlut</b>  | Vesicular glutamate transporter |
| <b>EGFR</b>    | Epidermal growth factor receptor                 | <b>Vsx</b>    | Visual system homeobox          |
| <b>Elav</b>    | Embryonic lethal abnormal vision                 | <b>Wg</b>     | Wingless                        |
| <b>Erm</b>     | Earmuff                                          | <b>Wor</b>    | Worniu                          |
| <b>Esg</b>     | Escargot                                         | <b>β-Gal</b>  | Beta galactosidase              |
| <b>Eya</b>     | Eyes absent                                      |               |                                 |
| <b>FasII</b>   | Fasciclin II                                     |               |                                 |
| <b>GFP</b>     | Green fluorescent protein                        |               |                                 |
| <b>Hb</b>      | Hunchback                                        |               |                                 |
| <b>Hh</b>      | Hedgehog                                         |               |                                 |
| <b>hTLX</b>    | Human TLX                                        |               |                                 |
| <b>Kni</b>     | Knirps                                           |               |                                 |
| <b>Kr</b>      | Krüppel                                          |               |                                 |
| <b>L'sc</b>    | Lethal of scute                                  |               |                                 |
| <b>L(3)mbt</b> | Lethal(3)malignant brain tumour                  |               |                                 |
| <b>Lola</b>    | Longitudinals lacking                            |               |                                 |
| <b>LSD1</b>    | Lysine-specific demethylase 1                    |               |                                 |
| <b>Mira</b>    | Miranda                                          |               |                                 |
| <b>N</b>       | Notch                                            |               |                                 |
| <b>N-CAM</b>   | Neural cell adhesion molecule                    |               |                                 |
| <b>NR2E1</b>   | Nuclear Receptor Subfamily 2 Group E Member 1    |               |                                 |
| <b>Ogre</b>    | Optic ganglion reduced                           |               |                                 |

# Chapter 1

## Introduction

The division mode of neural stem cells (NSCs) must be regulated throughout development and in adult life. During development, NSCs divide symmetrically to expand the NSC pool or asymmetrically to generate neurons and glia that will form the nervous system. A small population of NSCs are maintained into adulthood, which divide to maintain brain homeostasis (for a review see (Götz et al., 2016)). Importantly, asymmetric NSC divisions do not give rise to neurons directly but rather generate intermediate progenitors (**Fig. 1.1A**). Intermediate progenitors maintain some properties of NSCs but are more committed to differentiation.

The genetic programmes that control NSC fate must be downregulated in their progeny so that differences between NSCs and their daughter cells can be established. These differences allow both the maintenance of the NSC pool and for differentiation to progress in their progeny. Insufficient NSC divisions or precocious differentiation can occur if the genes controlling NSC fate are downregulated, which can result in the failure to produce the correct neural circuitry. Conversely, failure to downregulate NSC genes could lead to the expansion of the NSC population and be an initiating step in tumorigenesis (**Fig. 1.1B**). Therefore, understanding the genetic mechanisms that control NSC fate is essential for improving our understanding of normal brain development and the events that can lead to cancer.

### **1.1 Brain tumours can arise from NSC lineages**

Tumours affecting the central nervous system (CNS) are among the most poorly understood and difficult to treat. This is in part due to the huge diversity of tumours as well as the lack of understanding surrounding tumour-initiating events. The recent identification of genetic markers, in combination with histopathological analysis, has allowed for the classification of CNS tumours to be refined (Louis et al., 2016). Increased understanding of the genetic signatures of different tumours provides more specific diagnostic techniques but developing treatments for CNS tumours remains extremely challenging despite these advances.

#### **1.1.1 Glioblastoma multiforme tumours are heterogeneous and difficult to treat**

Glioblastoma multiforme (GBM) is the most common malignant tumour that affects the adult CNS. Unfortunately, GBM has remained resistant to conventional therapies and patient survival has not improved beyond 15 months since the 1980s (Bondy et al., 2008). One of the

reasons that GBM is difficult to treat is because the premalignant lesions that develop into malignant tumours are not known. Identifying the tumour cell of origin is challenging across the cancer field (Blanpain, 2013) but the diversity of GBM tumours makes this particularly challenging. GBMs display heterogeneity in genetic mutations and cell type composition, both between patients and within individuals, which makes studying the early stages of tumour initiation a daunting task. However, determining which cell types are affected by different tumourigenic mutations that are found in distinct GBM subtypes is essential for improving the diagnostic tools for precancerous lesions and for the design of targeted cell-type-specific cancer treatments (Pisapia, 2017).

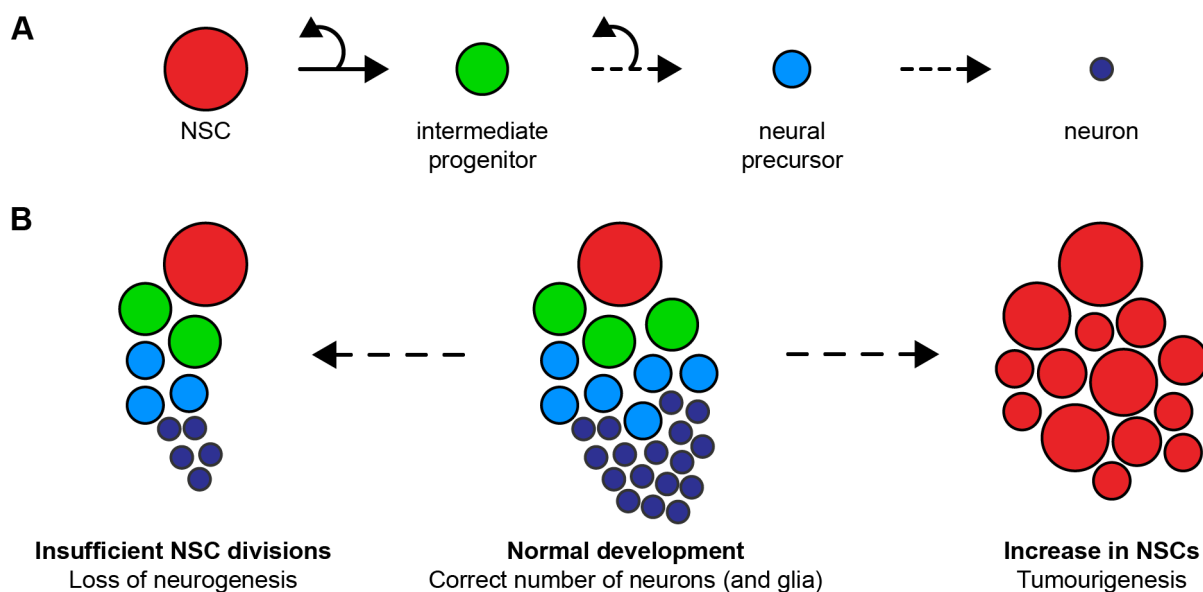


**Figure 1.1: NSC fate and differentiation must be balanced during brain development**

(A) NSCs (red) divide asymmetrically to give rise to an intermediate progenitor (green). Intermediate progenitors more committed to neuronal fate than NSCs but often maintain the ability to self-renew. Neural precursors (blue) produce neurons (navy) either by differentiation or terminal division.

(B) NSC fate must be balanced during development in order to produce the correct neurons and glia at the correct time and place to generate a functioning brain (centre). Reduction in the self-renewal capacity of NSCs can result in the failure to produce sufficient progeny (left). Conversely, aberrant activation of NSC fate can result in ectopic NSCs and tumour initiation (right).

There are many candidates for the GBM cell of origin. Mature glial cells were once believed to be the only dividing cells in the adult brain and so were designated as the cell of origin for gliomas (review in (Stiles and Rowitch, 2008; Zong et al., 2012)). However, the identification of NSCs with glial identity in the adult brain provided an attractive alternative candidate for the GBM cell of origin (Doetsch et al., 1999; Reynolds and Weiss, 1992; Seri et al., 2001). This discovery suggested that aberrant reactivation of NSCs could be an important tumour initiating event for GBM and highlighted the importance of exploring the role of NSCs in the early stages of GBM generation (Sanai et al., 2005). In addition, analysis of the cell type

heterogeneity within GBMs led to the isolation of stem cell-like cells that were required for tumour growth and propagation (Johnson et al., 2014; Singh et al., 2004; Sottoriva et al., 2013). These cells were designated glioblastoma stem cells (GSCs) because they shared many similarities with NSCs, namely the expression of NSC genes and their self-renewal capacity (Chen et al., 2012; Singh et al., 2004). It is thought that GSCs are resistant to treatment and so act as a reservoir of cells that can regenerate tumours following therapy (Reya et al., 2001; Singh et al., 2003). Understanding the genes that control GSC proliferation and survival is essential for developing effective treatments for GBM. The similarities between GSCs and NSCs suggest that many of the genetic programmes that regulate NSCs also play a role in cancer.

## **1.2 TLX is an important regulator of NSCs**

The orphan nuclear receptor TLX, or NR2E1 (Nuclear Receptor Subfamily 2 Group E Member 1) is expressed in NSCs in the developing and adult brain (Li et al., 2008; Liu et al., 2008; Monaghan et al., 1995; Shi et al., 2004; Yu et al., 1994). Mice that lack TLX during embryonic development exhibit defects in neocortex development due to decreased proliferation of periventricular NSCs but otherwise show no obvious defects at birth (Li et al., 2008; Monaghan et al., 1997). However, adolescent and adult TLX null mice have smaller cerebral hemispheres, exhibit aggressive and hyper-excitable behaviour (Monaghan et al., 1997; O'Leary et al., 2016; Roy et al., 2002; Young et al., 2002), and suffer from visual impairment (Holleman et al., 1998; Yu et al., 2000). The majority of the defects affecting the CNS are due to the requirement of TLX in post-embryonic NSCs; TLX expression maintains NSCs in an undifferentiated, proliferative state (Li et al., 2012; Niu et al., 2011; Obernier et al., 2011; Qu et al., 2010; Shi et al., 2004) and is necessary for adult neurogenesis in both the subventricular zone (SVZ) and subgranular zone (SGZ) (Elmi et al., 2010; Liu et al., 2008; Zhang et al., 2008). In humans, mutations in TLX have been linked to microcephaly (Kumar et al., 2007a; Kumar et al., 2007b) and hereditary cases of bipolar disorder and schizophrenia (Dick et al., 2003; McQueen et al., 2005; Middleton et al., 2004; Wong et al., 2010), indicating a conserved requirement of TLX for proper neurogenesis.

### **1.2.1 TLX in brain tumours**

In addition to the requirement of TLX for normal brain homeostasis, TLX has also been implicated in GBM initiation and malignancy. TLX expression is elevated in GBM (Park et al., 2010; Zou et al., 2012) and aggressive neuroblastomas (Chavali et al., 2014), but is absent from many other CNS tumours (such as medulloblastoma and lower-grade gliomas) (Zou et

al., 2012). The expression of TLX in brain tumours correlates with poor patient survival and, as such, TLX is an important diagnostic marker and a potential therapeutic target for malignant brain tumours (Chavali et al., 2014; Park et al., 2010).

Animal models of glioma have shown that expressing TLX in NSCs at high levels is sufficient to induce NSC expansion and, when combined with other genetic lesions, can induce malignant gliomas (Liu et al., 2010; Park et al., 2010; Zou et al., 2012). TLX is also expressed in GSCs (Zhu et al., 2014) and the downregulation of TLX inhibits GSC self-renewal and tumour reinitiation (Cui et al., 2016). Understanding how TLX promotes NSC fate is key for improving treatments for brain tumours associated with high levels of TLX. It is also unclear if TLX acts through common genetic pathways in development and tumorigenesis (**Fig. 1.2**).

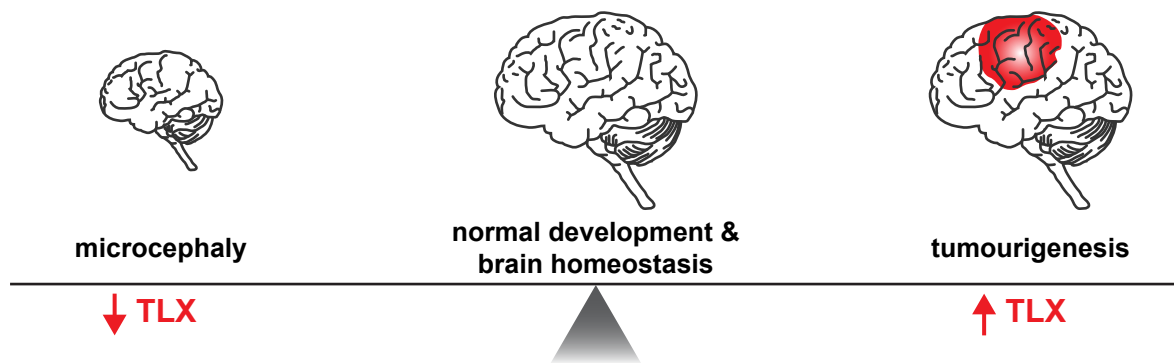


**Figure 1.2: TLX in brain homeostasis**

TLX levels must be balanced to ensure correct brain development and homeostasis. TLX mutations are associated with microcephaly and the loss of TLX in adult mice results in decreased neurogenesis. Elevated levels of TLX cause the NSC pool to expand, which can be an initiating step in tumourigenesis.

### **1.2.2 TLX structure and regulation**

TLX is a member of the orphan nuclear receptor sub-family of transcription factors. Its structure consists of a DNA binding domain (DBD) and a ligand binding domain (LBD). Unlike other nuclear receptors, whose activity is regulated by steroid hormones, no physiological ligand that binds to TLX has been identified.

TLX can repress or activate the transcription of its target genes. The repressive function of TLX is mediated by a number of co-repressors, such as Atrophin (Haecker et al., 2007; Wang et al., 2006; Zhang et al., 2006; Zhi et al., 2015), B-cell lymphoma/leukemia 11A (BCL11A) (Estruch et al., 2012), lysine-specific histone demethylase 1 (LSD1) (Sun et al., 2010; Sun et al., 2011; Yokoyama et al., 2008), as well as some histone deacetylases (HDACs) (Haecker et

al., 2007; Sun et al., 2010; Sun et al., 2011; Wang et al., 2006; Yokoyama et al., 2008) (**Fig. 1.3A**). TLX co-repressors either confer repressive chromatin marks directly (e.g. LSD1) or recruit additional factors to do so (e.g. Atrophin recruits HDACs to TLX target genes). The ability of TLX to promote the transcription of its target genes is a more recent discovery and so far no co-activators have been identified. Both positive and negative regulation of gene expression by TLX is mediated through the binding of TLX to its consensus binding motif (AAGTCA) upstream of the transcriptional start site (Wang and Xiong, 2016; Yu et al., 1994).

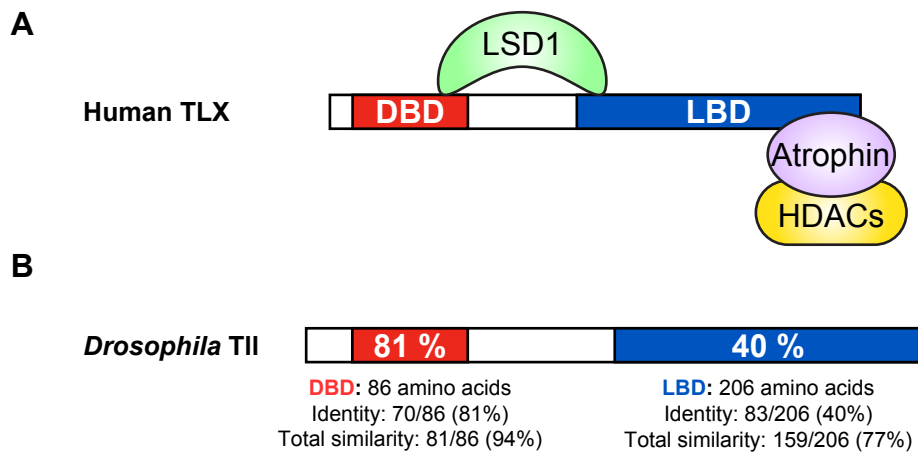


**Figure 1.3: Human TLX and *Drosophila* Tll are highly conserved**

(A) TLX consists of a DBD and LBD; both domains mediate interactions with transcriptional corepressors (Sun et al., 2010; Wang et al., 2006; Wang et al., 2008).

(B) Amino acid conservation between human TLX and *Drosophila* Tll. Sequence alignment of TLX and Tll performed using EMBOSS Needle and UniProt alignment tools. See **Appendix 1** for full sequence alignment. Human TLX amino acid sequence from Jackson et al., 1998.

The molecular mechanism through which TLX regulates NSC fate and tumourigenesis is not fully understood. The number of TLX target genes that has been identified is small and many targets have been identified in cell culture (reviewed in (Wang and Xiong, 2016)). This is in part due to the absence of genome-wide binding data for TLX, which would allow greater insight into its transcriptional targets in different cell types. In general, TLX is considered to repress genes that negatively regulate the cell cycle and activate the expression of genes that promote NSC proliferation; the proliferation of NSCs is reduced in the absence of TLX and neurogenesis is reduced significantly (Li et al., 2012; Li et al., 2008; Liu et al., 2008; Niu et al., 2011; Shi et al., 2004).

However, the effect of the loss or overexpression of TLX on NSC fate and lineage progression is not known. Manipulating NSCs at the single cell level *in vivo* is difficult and performing genetic lineage tracing of NSCs in the adult mammalian brain remains technically challenging (Bonaguidi et al., 2011; Hippenmeyer, 2013; Zong et al., 2005).

Therefore, studying the regulation of NSCs in a less complex organism has many benefits for investigating the fundamentals of NSC behaviour *in vivo*. The CNS of the fruit fly *Drosophila melanogaster* presents a comparatively simple system for studying NSCs; there are many lineage tracing techniques available, as well as many cell fate markers that allow lineage progression to be followed (for a review, see (del Valle Rodriguez et al., 2011)). Furthermore, nearly 75 % of disease-causing human genes have functional homologues in *Drosophila* (Pandey and Nichols, 2011).

### **1.3 tailless is the *Drosophila* homologue of TLX**

Human TLX and its *Drosophila* counterpart Tailless (Tll) are highly conserved (**Fig. 1.3B**). Their DBDs share 81 % identical amino acids (conservation increases to 94 % when similar amino acid substitutions are included) and can bind to the same DNA consensus sequence (AAGTCA) (Jackson et al., 1998; Yu et al., 1994). The LBDs have lower amino acid identity at 40 % (77 % amino acid similarity) but bind to the co-repressor Atrophin via conserved amino acid residues in both species (Zhi et al., 2015). The high molecular conservation of TLX and its cofactors in *Drosophila* suggests that studying the function of Tll could provide valuable insight into the role of TLX in development and tumourigenesis.

#### **1.3.1 tailless specifies NSC fate in the embryo**

In *Drosophila*, *tll* was first identified as a gene required for correct body pattern formation during embryogenesis (Jürgens et al., 1984). During the early stages of embryo development, *tll* functions as one of the final products of the terminal system to promote the formation of the most anterior (head) and most posterior (tail) structures of the embryo (Jürgens et al., 1984; Pignoni et al., 1990; Strecker et al., 1986). In the head region, *tll* expression is enriched in the proneural regions of the neuroectoderm from which NSCs delaminate (Pignoni et al., 1990; Rudolph et al., 1997; Urbach and Technau, 2003; Younossi-Hartenstein et al., 1997) and loss of *tll* results in the loss of NSCs (Younossi-Hartenstein et al., 1997). As embryonic development progresses, *tll* expression becomes more restricted until it is maintained in only a subset of NSCs (Urbach and Technau, 2003).

The role of Tll later in brain development is not well understood and appears to have diverse roles. The loss of *tll* in the NSCs that generate the olfactory system of the adult brain causes minor defects in the division of NSC progeny (Kurusu et al., 2009). In contrast, the loss of Tll in progenitors that generate the optic lobe (the visual processing centre of the brain) results in a major reduction in the visual ganglia (Guillermin et al., 2015). However, the high degree of

molecular conservation with mammalian TLX suggests that *Drosophila* Tll could have additional roles in NSC regulation, which have not yet been discovered, that more closely mirror the function of mammalian TLX.

## **1.4 *Drosophila* neurogenesis**

### **1.4.1 Multiple types of NSCs generate the *Drosophila* brain**

The *Drosophila* CNS is generated in two distinct phases of neurogenesis: an embryonic phase (that forms the larval nervous system) and a larval phase (that forms the adult nervous system). There are three main types of NSCs that produce neurons and glia in *Drosophila*: type 0 neuroblasts, type I neuroblasts, and type II neuroblasts (**Fig. 1.4A**).

All neuroblasts divide asymmetrically to self-renew and to generate a more differentiated daughter cell, but the neurogenic potential of neuroblasts differs between lineages. Type 0 neuroblasts have the most restricted division mode because their progeny differentiate directly to neuronal fate (**Fig. 1.4Ai**). Type 0 division mode is rare in the *Drosophila* CNS; it occurs at the end of embryogenesis and in a small population of optic lobe NSCs (Baumgardt et al., 2014; Bertet et al., 2014; Karcavich and Doe, 2005; Ulvklo et al., 2012). Type I neuroblasts are the most prevalent NSC in the *Drosophila* CNS. Asymmetric division of type I neuroblasts generates ganglion mother cells (GMCs), which undergo terminal division to produce two neurons (**Fig. 1.4Aii**) (Buescher et al., 1998). In contrast, type II neuroblasts exhibit a relatively rare NSC division mode, with only 16 type II neuroblasts per brain. Type II neuroblasts give rise to transit amplifying intermediate neural progenitors (INPs) that in turn divide asymmetrically to produce GMCs, which generate two neurons (**Fig. 1.4Aiii**). As such, type II neuroblasts are able to generate much larger lineages compared to type 0 and type I neuroblasts (**Fig. 1.4B**). The generation of INPs from type II neuroblasts makes their division mode analogous to that of mammalian NSCs.

### **1.4.2 Type II neuroblasts**

The *Drosophila* brain is a well-established system for studying NSCs (Brand and Livesey, 2011; Doe, 2008). There are extensive genetic tools that can be used to manipulate NSC lineages *in vivo* as well as many molecular markers for following cell fate changes. The advanced genetic toolbox combined with the relative simplicity of the CNS makes *Drosophila* an excellent organism in which to study NSCs *in vivo*.

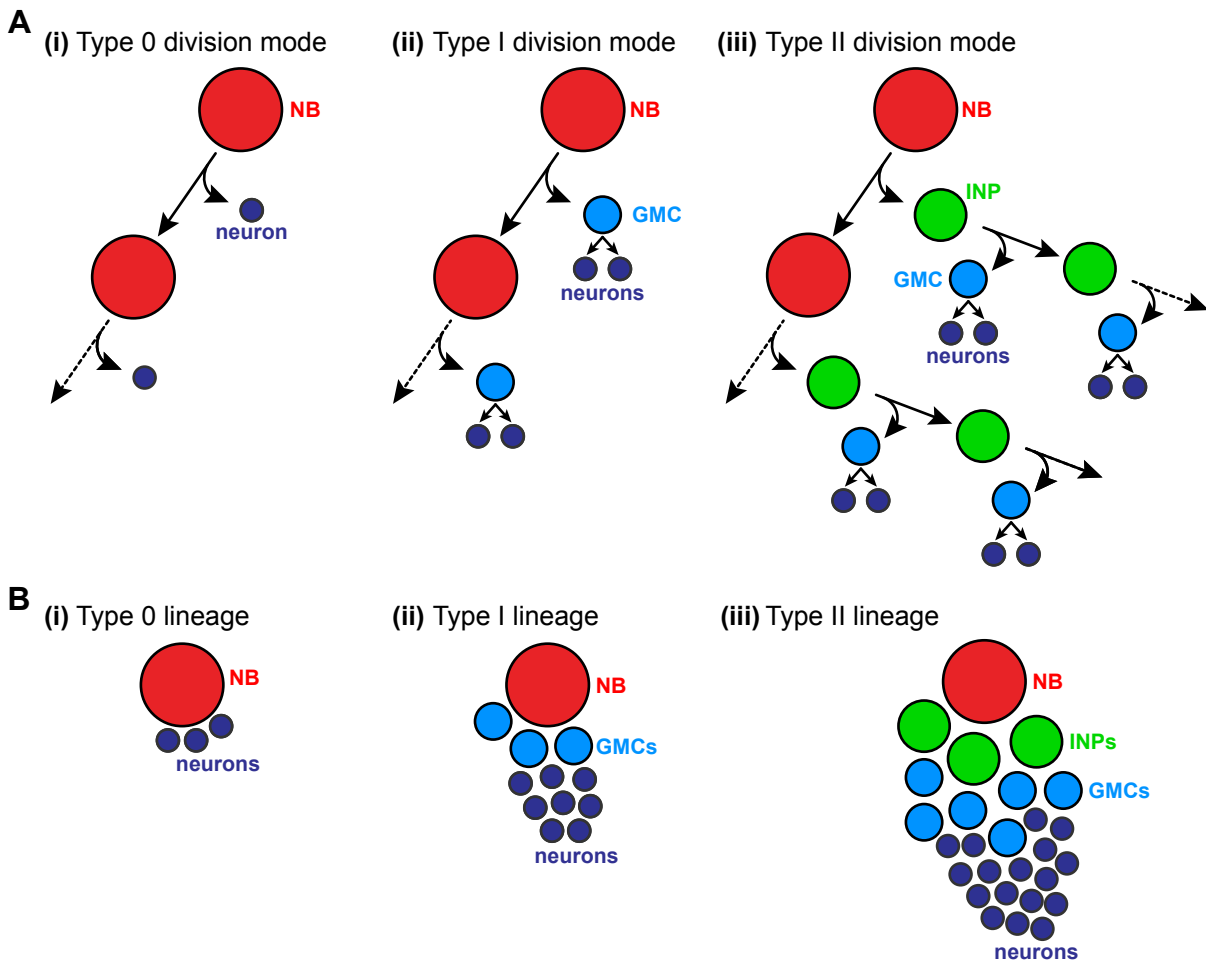


**Figure 1.4: Division modes of *Drosophila* NSCs**

(A) (i) Type 0 neuroblasts divide asymmetrically to self-renew and generate one neuron; (ii) Asymmetric division of type I neuroblasts generates a GMC, which undergoes terminal division to produce two neurons; (iii) Type II neuroblasts generate INPs, which maintain self-renewal capacity and divide asymmetrically to produce a GMC that generates two neurons.

(B) (i) Type 0 lineages contain the smallest number of neuronal progeny; (ii) Type I lineages contain more neurons than type 0 lineages due to the presence of GMCs. (iii) Type II lineages have the greatest neuronal output as a result of transit amplifying INPs, which undergo multiple rounds of asymmetric cell division to generate GMCs.

NB: neuroblast; INP: intermediate neural progenitor; GMC: ganglion mother cell. Schematic adapted from Doe, 2017.

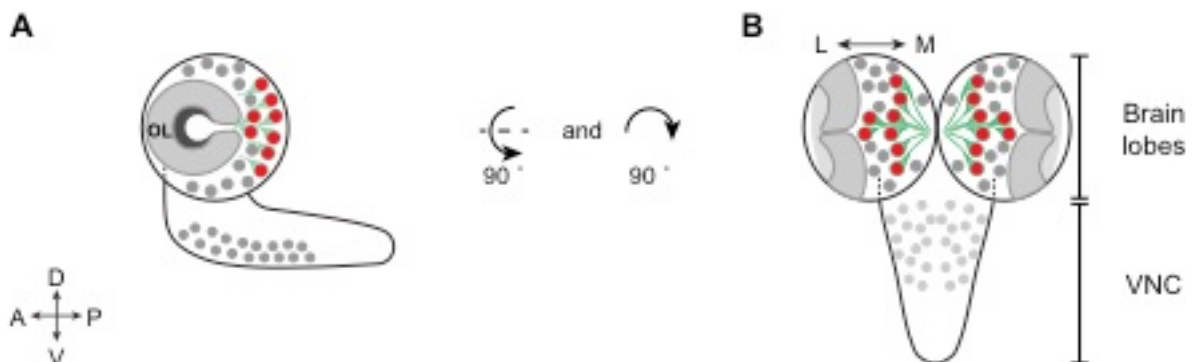


**Figure 1.5: The anatomy of the *Drosophila* larval CNS**

(A) Orientation of the CNS within a larva; (B) The view of a brain mounted for imaging (with the VNC facing into the page). The majority of neuroblasts in the brain lobes, optic lobe (OL) and ventral nerve cord (VNC) are type I (grey). Type II neuroblasts (red) are found in the posterior region of the brain lobes and their lineages (green) project medially. A: anterior; P: posterior; D: dorsal; V: ventral; L: lateral; M: medial.

The division mode of type II neuroblasts is rare within the *Drosophila* brain; they are the only type of *Drosophila* NSC that divide asymmetrically to give rise to progenitors that can also self-renew (Bello et al., 2008; Boone and Doe, 2008; Bowman et al., 2008). There are only eight type II lineages in each lobe of the developing brain, which are found in stereotyped positions throughout development (**Fig. 1.5A-B**) (Bello et al., 2008; Boone and Doe, 2008; Bowman et al., 2008). In contrast, there are approximately ~85 central brain type I neuroblasts (Ito and Hotta, 1992). As such, type II neuroblasts have an increased proliferative capacity and neurogenic potential compared to the majority of neuroblasts. Identifying the genes that regulate the division mode and identity of type II neuroblasts will help to improve our understanding of NSCs in more complex organisms.

Type II neuroblasts express the Hes family bHLH-O transcription factor *deadpan* (*dpn*), which is expressed in all self-renewing *Drosophila* neural progenitors (Bier et al., 1992), in a manner comparable to Hes1 and Hes5 expression in mammalian NSCs (Nakamura et al., 2000; Ohtsuka et al., 2001) (**Fig. 1.6A**). The first gene that was identified to be expressed differentially between type I and type II neuroblasts was the pro-neural gene *asense* (*ase*) (Bowman et al., 2008). *ase* is one of four genes that make up the *achaete-scute* complex (AS-C) (González et al., 1989), which is orthologous to the vertebrate gene *achaete-scute family bHLH transcription factor 1* (*ASCL1*, also known as *mammalian achaete-scute homolog 1* (*Mash-1*)) (Johnson et al., 1990). *ase* is absent from type II neuroblasts but is expressed in mature INPs and type I neuroblasts (**Fig. 1.6A**) (Bowman et al., 2008). The expression pattern of *ase* in type II neuroblasts is analogous to that of ASCL1 in mouse NSC lineages (Calof et al., 1998; Gordon et al., 1995; Guillemot et al., 1993; Mumm et al., 1996; Murray et al., 2003; Wu et al., 2003).

In addition to the repression of *ase*, type II neuroblasts also lack expression of the homeodomain gene *prospero* (*pros*) (**Fig. 1.6B**) (Bayraktar et al., 2010). *pros* is homologous to the mammalian gene prospero-related homeobox 1 (*Prox1*) and promotes neuronal differentiation in NSC progeny in a similar manner (Doe et al., 1991; Oliver et al., 1993; Torii et al., 1999). In *Drosophila* type I neuroblasts and INPs, Pros protein is excluded from the nucleus and is distributed to GMCs upon asymmetric cell division (Doe et al., 1991; Knoblich et al., 1995; Spana and Doe, 1995; Vaessin et al., 1991). Therefore, type II neuroblasts lack the expression of two genes (*ase* and *pros*) that are expressed widely throughout the *Drosophila* CNS and promote neuronal fate. However, the repression of *ase* and *pros* is a consequence of type II neuroblast fate rather than an instructive signal (Bayraktar et al., 2010;

Bowman et al., 2008), indicating that additional genes must be required for specifying type II neuroblast fate.

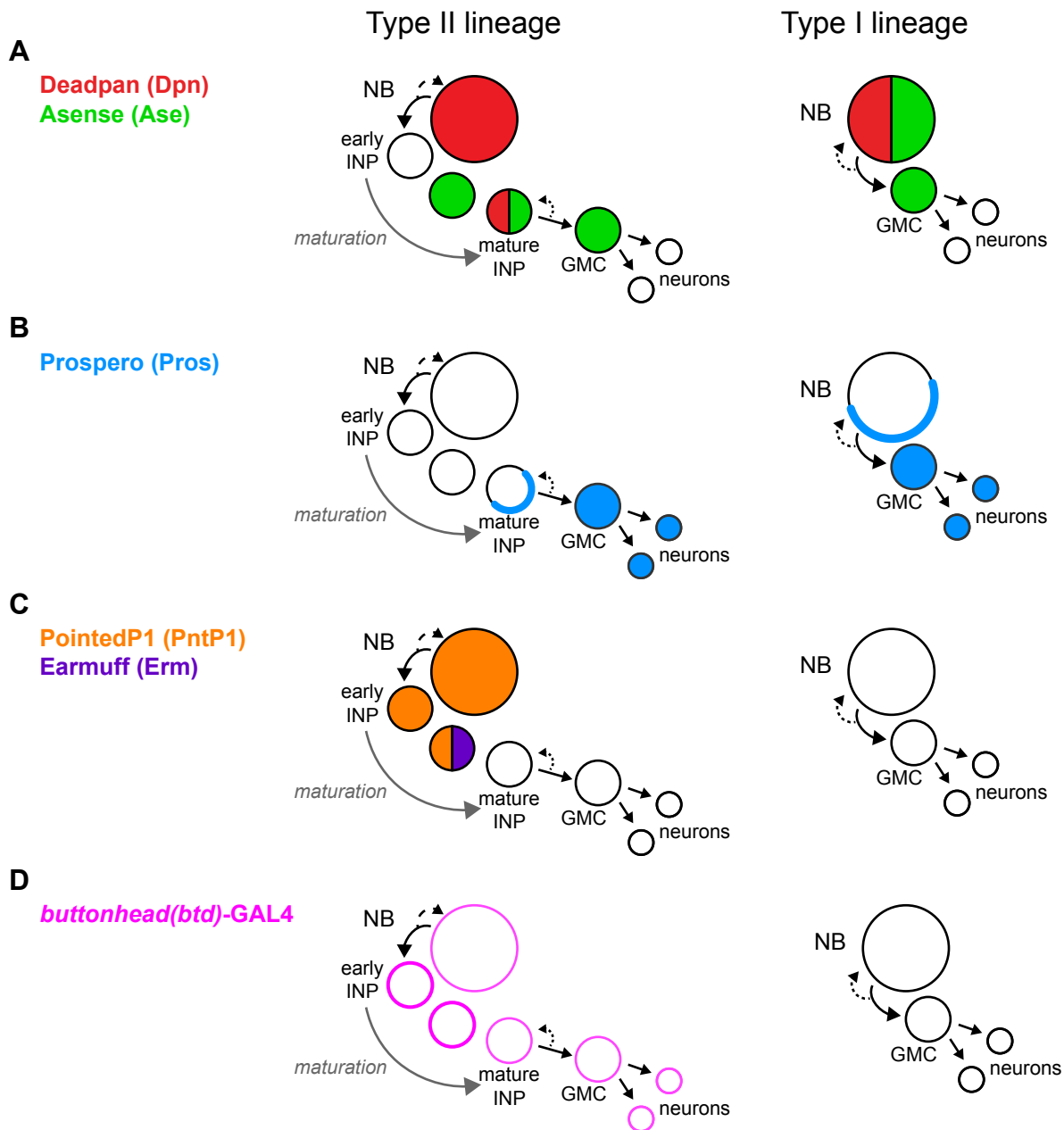


**Figure 1.6: Differential gene expression between type II and type I neuroblast lineages**

Schematics depicting the division modes and lineages of type II and type I neuroblasts.

(A) Type II neuroblasts, mature INPs and type I neuroblasts express the bHLH-O transcription factor Dpn (red). The pro-neural gene Ase (green) is not expressed in type II neuroblasts, but becomes activated during INP maturation. Type I neuroblasts express Ase and GMCs maintain Ase expression.

(B) Pros (blue) is not expressed in type II neuroblasts. Pros is expressed in mature INPs and type I neuroblasts but is excluded from the nucleus and is segregated to GMCs at asymmetric cell division. Pros enters the nucleus of GMCs, where it represses self-renewal and promotes differentiation, and expression is maintained in young neurons.

(C) PntP1 (orange) is expressed in type II neuroblasts and is maintained in early INPs where it promotes the expression of Erm (purple). Erm represses PntP1 expression during INP maturation and promotes lineage progression. PntP1 and Erm are not expressed in type I lineages.

(D) *btd*-GAL4 (pink) is an insertion at the *btd* locus. In type II lineages, *btd*-GAL4 expression begins in the neuroblast but is stronger in immature INPs. *btd*-GAL4 is also expressed in a subset of type I lineages.

One candidate for a gene that promotes type II neuroblast fate is the Ets transcription factor *pointedP1* (*pntP1*). PntP1 is expressed in type II neuroblasts and early-born INPs but is absent from type I lineages (**Fig. 1.6C**) (Zhu et al., 2011). The loss of PntP1 results in the derepression of Ase in type II neuroblasts, but this only affects 60-80 % of type II lineages (Xie et al., 2016; Zhu et al., 2011). In INPs, PntP1 activates expression of the Fezf factor *earmuff* (*erm*), which is required for the acquisition of INP fate (Weng et al., 2010). As such, it seems that PntP1 functions to promote lineage progression rather than specify neuroblast fate (Xie et al., 2016). The Sp8 homologue *buttonhead* (*btd*) is also enriched in type II lineages compared to type I lineages (Komori et al., 2014a; Xie et al., 2014). It has recently been shown that *btd* acts redundantly to specify type II neuroblast fate in embryogenesis and expressing *btd* ectopically is not sufficient to transform type I neuroblasts to type II neuroblasts (Álvarez and Díaz-Benjumea, 2018; Xie et al., 2014). As such, many of the transcription factors that have been identified as type II-specific genes act downstream in the lineage to regulate INP maturation. This suggests that as yet unidentified genes regulate type II neuroblast fate itself.

## **1.5 Project aims**

The aim of this project was to study genetic regulators of NSC fate and how dysregulation of these genes can lead to tumorigenesis. Mammalian TLX is expressed at high levels in aggressive human GBM and can induce NSC expansion *in vivo* (Chavali et al., 2014; Park et al., 2010; Zou et al., 2012). The molecular conservation between mammalian TLX and *Drosophila* Tll suggests that these genes act through conserved mechanisms. The lineage progression of type II neuroblasts is highly comparable to mammalian NSCs and provides a genetically tractable system to study NSC fate *in vivo*. Tll has widespread roles in *Drosophila* CNS development and is a promising candidate for a type II neuroblast regulator.

### **1.5.1 The characterisation of Tll in type II neuroblasts and tumorigenesis**

The majority of the work in this thesis was focussed on the identification of the *Drosophila* gene Tll as a regulator of type II neuroblast fate. I found that:

1. Tll is expressed in type II neuroblasts and is required for neuroblast fate and lineage progression (**Chapter 2**);
2. Targeted DamID of Tll in type II neuroblasts showed that Tll binds to many important type II-specific genes and may regulate their expression directly (**Chapter 3**);
3. Tll must be down-regulated in type II lineages for differentiation to occur. Failure to do so results in INP reversion to neuroblast fate and tumour initiation (**Chapter 4**);

4. Expressing human TLX in INPs also results in tumourigenesis, highlighting the conserved mechanisms of tumour initiation and implicating intermediate progenitors as a cell of origin for TLX-induced tumours (**Chapter 4**).

### **1.5.2 Characterising the early stages of optic lobe neuroepithelium development**

During the study of type II neuroblasts, I observed that many genes that regulate type II lineages are also expressed in the developing optic lobe. For example, *tll* is expressed in the optic lobe neuroepithelium throughout development and is required to maintain neuroepithelial cell fate (Daniel et al., 1999; Guillermin et al., 2015; Pignoni et al., 1990; Rudolph et al., 1997; Younossi-Hartenstein et al., 1997). I identified additional similarities between type II lineages and NSCs in the optic lobe, which prompted the re-examination of NSC behaviour in the early stages of optic lobe development.

The optic lobe generates the visual processing centre of the adult brain and contains two populations of NSCs: (1) symmetrically dividing neuroepithelial cells, which give rise to (2) asymmetrically dividing neuroblasts (**Fig. 1.7**) (Bertet, 2017; Egger et al., 2011). Previously, it was thought that neuroblast generation was limited to the late stages of larval development (Egger et al., 2007; Egger et al., 2010; Yasugi et al., 2010; Yasugi et al., 2008). However, I identified a new marker that is expressed at the neuroepithelial to neuroblast transition, which facilitated the discovery of a new, embryonic phase of neuroblast production from the optic lobe neuroepithelium. This work was carried out in collaboration with Dr Leo Otsuki and is introduced in more detail in **Chapter 5**.

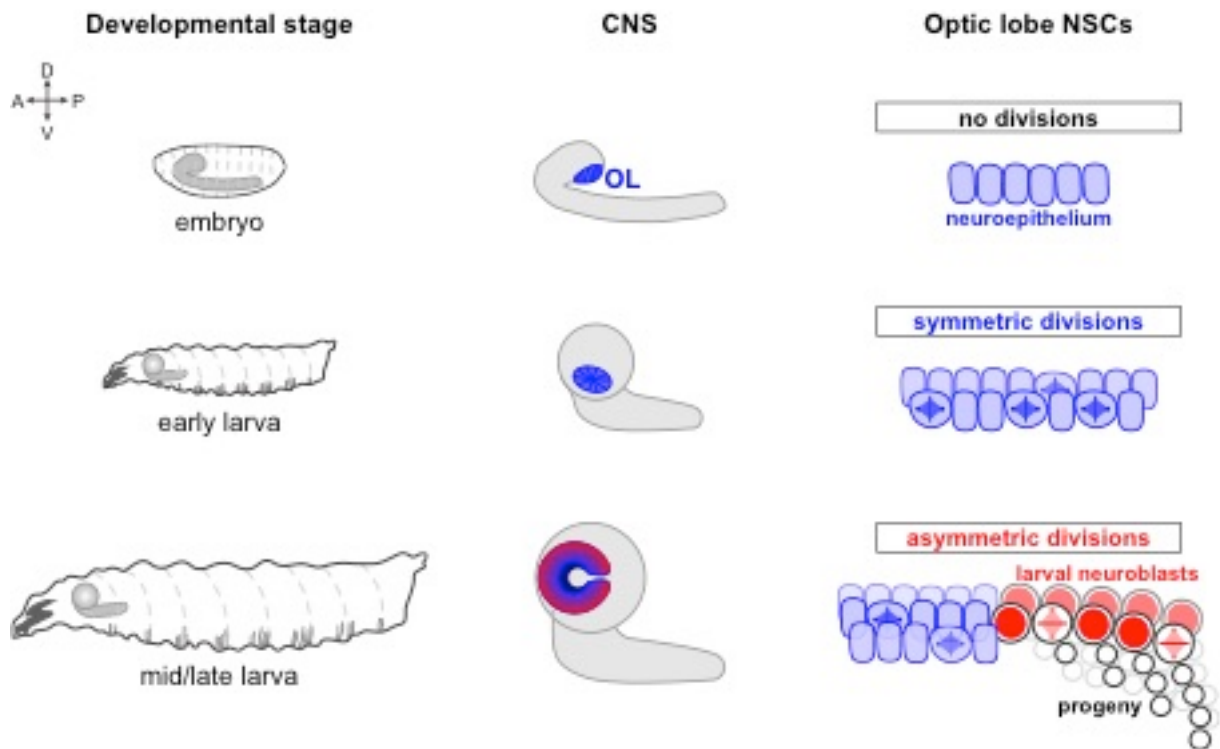


**Figure 1.7: The development of the *Drosophila* optic lobe**

The optic lobe neuroepithelium is specified in the embryo and is found at the posterior-lateral sides of the brain lobes. Neuroepithelial cells have been reported to be quiescent during embryogenesis. In early larval stages, the optic lobe begins symmetric divisions and subsequently generates asymmetrically dividing neuroblasts in mid/late larval stages. The majority of optic lobe neuroblasts undergo type I division mode (the minority divide in a type 0 manner) and generate neurons and glia of the adult visual processing centre.



## Chapter 2

### TLX is required to maintain type II neuroblast and lineage identity

The orphan nuclear receptor TLX is expressed in NSCs during development and in adulthood (Li et al., 2012; Li et al., 2008; Liu et al., 2008; Monaghan et al., 1995; Monaghan et al., 1997; Obernier et al., 2011). Levels of TLX must be maintained in a fine balance throughout life. The loss of TLX results in the reduction of NSC proliferation and neurogenesis and is linked to mood disorders (Davis et al., 2014; Dick et al., 2003; Li et al., 2008; Liu et al., 2008; McQueen et al., 2005; Middleton et al., 2004; Monaghan et al., 1997; O’Leary et al., 2016; Roy et al., 2002; Wong et al., 2010; Young et al., 2002). Conversely, high levels of TLX induce the expansion of NSCs and can lead to gliomagenesis (Liu et al., 2010; Park et al., 2010; Zou et al., 2012). TLX is also required for the self-renewal capacity of glioblastoma stem cells (GSCs) (Cui et al., 2016; Zhu et al., 2014) and high TLX levels in glioblastoma and neuroblastoma correlate with poor patient prognosis (Chavali et al., 2014; Park et al., 2010). As such, determining the molecular mechanisms through which TLX controls NSC behaviour has implications for both normal brain development and cancer.

On a population level, mammalian NSCs show reduced proliferation in the absence of TLX but the effect on NSC fate and lineage progression is not clear (Li et al., 2012; Li et al., 2008; Liu et al., 2008; Niu et al., 2011; Shi et al., 2004). Performing genetic lineage tracing of adult mammalian NSCs *in vivo* is still a relatively recent technical development and the properties of NSCs at the single cell level are not well understood (Bonaguidi et al., 2011; Hippenmeyer, 2013; Zong et al., 2005). In contrast, there are many lineage tracing techniques available to study NSCs in the comparatively simple *Drosophila* CNS, as well as many cell fate markers that allow lineage progression to be followed (for a review, see (del Valle Rodriguez et al., 2011)).

*Drosophila* type II neuroblasts divide in a manner analogous to mammalian NSCs and provide a genetically tractable system to study factors that regulate NSCs. Type II neuroblasts divide asymmetrically to produce transit-amplifying intermediate neural progenitors (INPs), which have a more limited capacity for proliferation. Following maturation, INPs divide asymmetrically to give rise to ganglion mother cells (GMCs), which undergo terminal division to produce two neurons (**Fig. 2.1A**). The division mode of type II neuroblasts is unique within the *Drosophila* brain; the majority of neuroblasts generate GMCs upon

asymmetric division (**Fig. 2.1A**). Therefore, type II neuroblasts represent a *Drosophila* NSC population with an increased self-renewal and neurogenic capacity. Understanding the factors that regulate the ability of type II neuroblasts to produce INPs could have implications for mammalian NSC lineages. Although Tll has been studied extensively in *Drosophila* neural development, no role has been described for this gene in type II neuroblasts (Daniel et al., 1999; Guillermin et al., 2015; Hartmann et al., 2001; Kurusu et al., 2009; Strecker et al., 1988; Younossi-Hartenstein et al., 1997). Identifying a role for *Drosophila* Tll in type II lineages could provide insights into the role of its human counterpart TLX in NSCs in development and disease.

## **2.1 Tll is expressed in type II neuroblasts**

To determine if Tll regulates type II neuroblasts, I assessed if *tll* was expressed in these cells. There are eight type II neuroblasts in each brain lobe of the developing CNS. Type II neuroblasts are located in the dorsoposterior medial region of the brain lobes (**Fig. 2.1B**) and can be identified unambiguously by co-staining for the bHLH-O factor Dpn and the pro-neural gene Ase (type II neuroblasts are the only NSCs that express Dpn but not Ase) (Bello et al., 2008; Boone and Doe, 2008; Bowman et al., 2008).

### **2.1.1 Assessing the expression of *tll***

There are many tools available to examine *tll* expression in *Drosophila*. Tll-EGFP is a protein fusion under the control of an ~20 kb insert containing the *tll* coding sequence (CDS) and surrounding regulatory sequences (Venken et al., 2009). Importantly, this construct can rescue the lethality of homozygous *tll*<sup>l49</sup> mutants ((Guillermin et al., 2015) and verified in this study, *data not shown*). I found that Tll-EGFP was expressed in all type II neuroblasts throughout larval development (**Fig. 2.1C-E**). Tll-EGFP was also detected in the four mushroom body lineages, which generate the olfactory system of the adult, consistent with a previous report of Tll expression in these lineages (Kurusu et al., 2009) (arrow heads in **Fig. 2.1C-E**).

The expression of a second independent genetic reporter of *tll*, *tll-lacZ* (Liaw and Lengyel, 1992), was also assessed. This construct contains 5.9 kb of the 5' regulatory region of *tll* and expresses  $\beta$ -Gal in a comparable manner to endogenous *tll* during embryonic stages (Rudolph et al., 1997). *tll-lacZ* was expressed strongly in all type II neuroblasts and showed weaker expression in their lineages (**Fig. 2.1F**). Interestingly, *tll-lacZ* did not recapitulate endogenous Tll expression entirely in larval stages. Notably, mushroom body lineages lacked expression of *tll-lacZ*, despite high levels of endogenous Tll (Kurusu et al., 2009) (**Fig. 2.1G-G'**). This

indicated that the cis-regulatory region of the *tll-lacZ* reporter does not include all the enhancer elements that regulate native *tll* expression throughout development. However, it does indicate that the sequence required for *tll* activation in type II lineages is found within 5.9 kb upstream of the *tll* transcriptional start site (TSS).

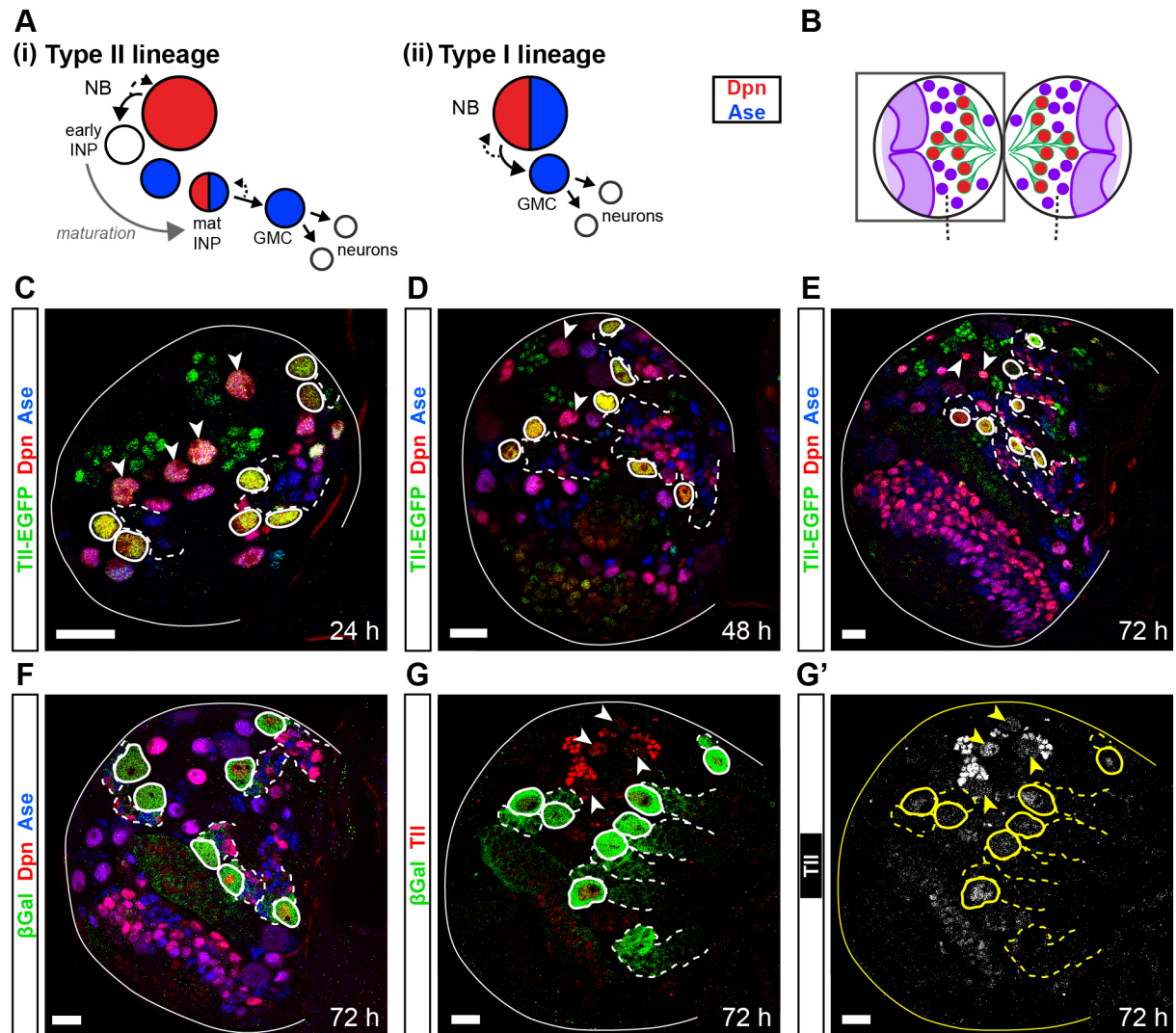


**Figure 2.1: *tll* reporters are expressed in type II neuroblasts**

(A) Schematic showing (i) Type II lineages express Dpn (red) but not Ase (blue) and divide asymmetrically to generate INPs. During maturation, INPs turn on Ase and, later, Dpn before dividing to produce GMCs. (ii) Type I neuroblasts express Dpn and Ase and divide to generate GMCs.

(B) Schematic showing the position of the eight type II neuroblasts (red) per brain lobe and their associated lineages (green). The majority of the other larval neural progenitors are type I neuroblasts (purple). The box corresponds to region shown in panels (C-G').

(C-E) Tll-EGFP (green) (Venken et al., 2009) is expressed in all type II neuroblasts (Dpn<sup>+</sup> Ase<sup>-</sup>, outlined with solid white lines) and down-regulated in progeny (outlined with dotted white lines) at 24 (C), 48 (D), or 72 (E) hours after larval hatching (ALH). *pntPI-GAL4* driving *UAS-myr-mRFP* was used to identify type II lineages. Tll-EGFP expression in mushroom body lineages is indicated by white arrowheads.

(F) *tll-lacZ* (green) (Liaw and Lengyel, 1992) is expressed strongly in type II neuroblasts (outlined with solid white lines) and weakly in lineages (outlined with dotted white lines).

(G-G') Strong *tll-lacZ* expression (green) overlaps with Tll (red in G; white in G') in type II neuroblasts (solid outline). *tll-lacZ* is not expressed in mushroom body lineages (arrowheads), which express Tll protein. Dotted outlines indicate type II lineages.

Note that seven of eight type II lineages are shown in panels C-F (lineage DM1 not visible). Single section confocal images. Scale bars represent 15  $\mu$ m.

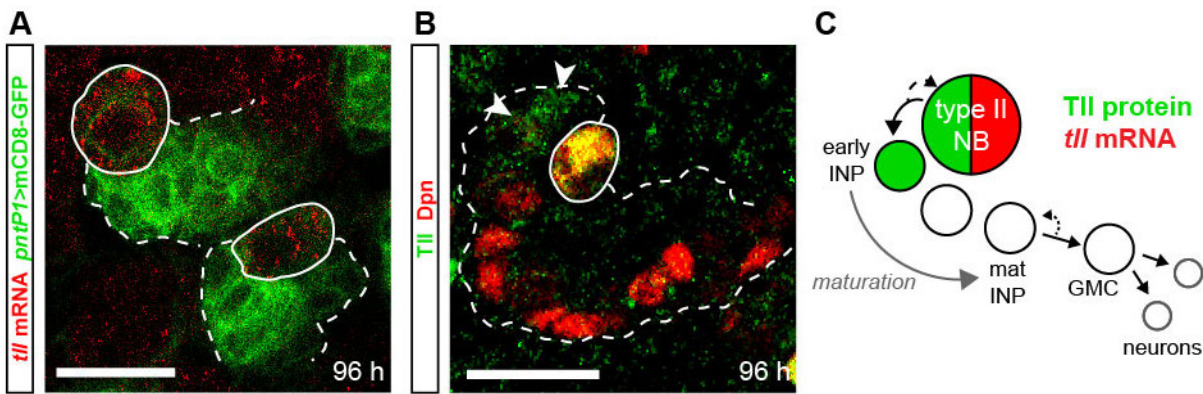


**Figure 2.2: *tll* mRNA and protein is expressed in type II neuroblasts**

(A) RNA FISH against *tll* mRNA (red) shows expression in type II neuroblasts (outlined with solid white line) but not in differentiating cells in the lineage (outlined with dotted white line). *pntP1-GAL4* driving membrane-targeted GFP (green) labels type II lineages.

(B) Immunostaining for Tll (green) shows strong expression in type II neuroblasts (Dpn<sup>+</sup> (red) outlined with solid white line) and weaker expression in immature INPs (arrow heads). *pntP1-GAL4* driving membrane-targeted GFP (represented by white outlines) labels type II lineages.

(C) Summary of *tll* mRNA (red) and Tll protein (green) expression in type II lineages.

Single section confocal images. Scale bars represent 15  $\mu$ m.

To determine the expression pattern of Tll within type II lineages, I examined endogenous *tll* expression. I performed fluorescence *in situ* hybridisation (FISH) against *tll* mRNA, which showed that *tll* mRNA is transcribed in type II neuroblasts but not in other cells of type II lineages (Fig. 2.2A). Staining with an antibody raised against Tll showed that Tll protein is present in type II neuroblasts and at low levels in newly born progeny (immature INPs) (Fig. 2.2B). These data show that *tll* is expressed at high levels in the neuroblast of all type II lineages and that low levels of Tll protein are present in immature INPs but not in other cells of the lineage (Fig. 2.2C).

### 2.1.2 Examining the expression patterns of *tll*-GAL4 lines

Using a combination of genetic tools and staining for endogenous Tll revealed a strong enrichment of *tll* expression in type II neuroblasts. To determine if I could identify new tools to label and manipulate type II lineages, I screened available *tll*-GAL4 lines for type II neuroblast expression (Fig. 2.3A). The Janelia FlyLight (GAL4 lines denoted with a “GMR” identification number) (Jenett et al., 2012; Pfeiffer et al., 2008) and VDRC Vienna Tiles (GAL4 lines denoted with a “VT” identification number) libraries are collections of cis-regulatory DNA fragments ranging from ~2 kb (Vienna Tiles) to ~3 kb (FlyLight) that drive GAL4 expression. Constructs from both libraries are integrated in a single genomic insertion site (*attP2*) allowing for expression comparison between the two collections. There are four *tll* GAL4 lines from the FlyLight collection (GMR39A01, GMR31H09, GMR31F04, and GMR31D09) and seven from the Vienna Tiles collection (VT151, VT152, VT153, VT156,

VT157, VT158, and VT159). To determine expression in the larval CNS, flies carrying each GAL4 line were crossed to flies carrying *UAS-mCD8-GFP* and larval progeny were dissected at wandering third instar stage. GAL4 expression patterns are shown in **Figs. 2.3B-L** and are described in **Table 2.1**. All *tll* fragments showed some level of expression in type II lineages but only GMR31F04-GAL4, VT151-GAL4, VT153-GAL4, and VT159-GAL4 were expressed consistently in all eight lineages.

GMR31F04-GAL4 and VT153-GAL4 share overlapping cis-regulatory sequences and also fall within the 5.9 kb sequence of *tll-lacZ*, allowing a putative type II element to be mapped within the 5' region of *tll* (**Fig. 2.4A** bold red outline). However, upon closer analysis of brains from larvae that carried either GMR31F04-GAL4 (**Fig. 2.4B**) or VT153-GAL4 (**Fig. 2.4C**), I found that the number of type II lineages was altered: the number varied between seven and nine lineages, and often differed between brain lobes of the same animal (*data not shown*). Therefore, although these GAL4 lines had minimal expression outside of type II lineages, they were not appropriate for use in functional experiments. The expression of VT151-GAL4 (**Fig. 2.4D**) in type II lineages was unexpected because this fragment is in a more distal 5' position than *tll-lacZ* (**Fig. 2.4A**). The surrounding, overlapping *tll* fragments do not show comparable expression to VT151-GAL4, which means that it is not possible to map a type II regulatory element to this region with these tools. In addition, VT151-GAL4 is expressed in a few type I neuroblasts near type II lineages making it unsuitable for functional studies of type II lineages. VT159-GAL4 (**Fig. 2.4E**) was the only fragment downstream of the *tll* CDS expressed in all type II lineages. Previous characterisation of *tll* regulatory elements has focussed exclusively on the 5.9 kb upstream of the *tll* transcriptional start site (TSS) (Liaw et al., 1995; Liaw et al., 1993; Liaw and Lengyel, 1992; Rudolph et al., 1997), but the expression of VT159-GAL4 in type II lineages indicates that an additional type II regulatory element could be located downstream of *tll* (**Fig. 2.4A** dotted red outline). Unfortunately, VT159-GAL4 is also expressed in surrounding type I lineages and so was not suitable for functional experiments.

Through a combination of genetic tools and staining for *tll* mRNA and Tll protein, I have shown that *tll* is expressed in all type II lineages. Tll protein and mRNA are enriched in the neuroblasts of these lineages and are downregulated in differentiating progeny. Analysis of available *tll* GAL4 lines made it possible to map putative regulatory elements required for the expression of *tll* in type II lineages.

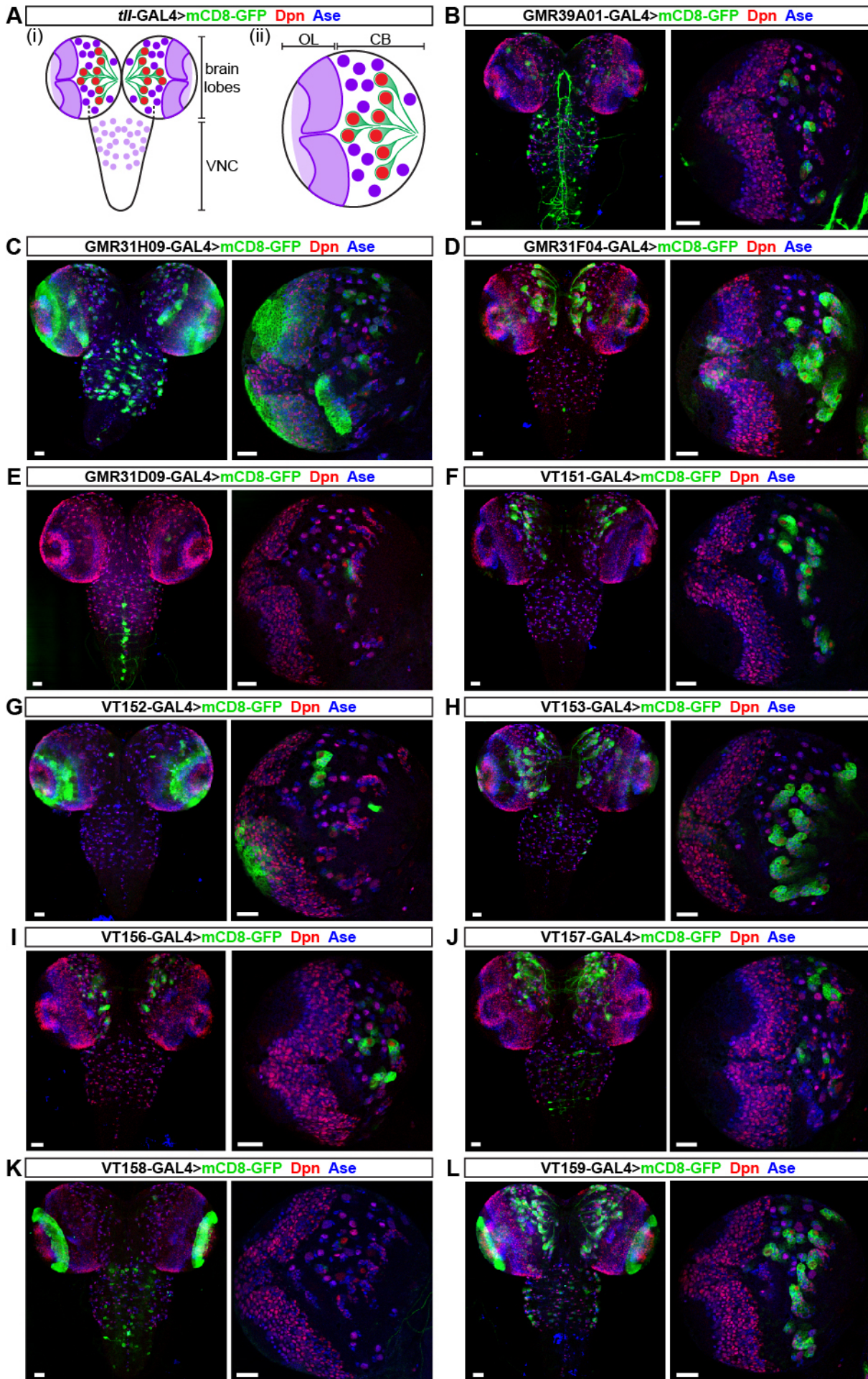


**Figure 2.3: Expression of *tll*-GAL4 drivers in the larval CNS**

(A) Schematic showing idealised expression of a type II-specific GAL4 driver. (i) shows the entire CNS, which consists of the brain lobes and the VNC; (ii) shows a brain lobe, which consists of the optic lobe (OL) and the central brain (CB).

(B-L) Each *tll*-GAL4 was crossed to flies carrying UAS-*mCD8-GFP* (green) and progeny were dissected at wandering third instar stage. A maximum projection in z across the entire brain (left-hand panels) and a single section confocal image showing type II lineages (right-hand panels) are shown for each GAL4 driver line. Type II neuroblasts were identified as Dpn<sup>+</sup> (red) and Ase<sup>-</sup> (blue). Expression patterns are described in Table 1. Scale bars represent 30  $\mu$ m.

| <b>GAL4</b>             | <b>Type II expression</b>                                     | <b>Other brain expression</b>                                |
|-------------------------|---------------------------------------------------------------|--------------------------------------------------------------|
| GMR39A01<br>(Fig. 2.3B) | DL lineages<br>DM4-6                                          | Few central brain type Is<br>Few VNC neurons                 |
| GMR31H09<br>(Fig. 2.3C) | DL lineages<br>DM4 and 5 variable expression                  | Optic lobe<br>Some central brain type Is<br>Many VNC type Is |
| GMR31F04<br>(Fig. 2.3D) | All                                                           | Optic lobe                                                   |
| GMR31D09<br>(Fig. 2.3E) | DM4 and DM5                                                   | Midline neurons of the VNC                                   |
| VT151<br>(Fig. 2.3F)    | All                                                           | Few central brain type Is<br>Optic lobe                      |
| VT152<br>(Fig. 2.3G)    | DL lineages<br>Weak and variable expression in<br>DM lineages | Optic lobe                                                   |
| VT153<br>(Fig. 2.3H)    | All                                                           | Optic lobe                                                   |
| VT156<br>(Fig. 2.3I)    | All except DM3 (occasionally<br>absent from DM2)              | Few central brain type Is                                    |
| VT157<br>(Fig. 2.3J)    | None (occasional weak<br>expression in DM6)                   | Expression in most central brain and<br>some VNC type Is     |
| VT158<br>(Fig. 2.3K)    | Very weak expression in DL1,<br>DM1 and DM4                   | Optic lobe: lamina                                           |
| VT159<br>(Fig. 2.3L)    | All                                                           | Optic lobe: lamina<br>Many central brain and VNC type Is     |

**Table 2.1: Expression patterns of *tll* GAL4 lines.** Description of the brain expression of *tll* GAL4 lines shown in Figure 2.3. Flies carrying each GAL4 driver were crossed to flies carrying UAS-*mCD8-GFP* and progeny were dissected at wandering third instar. DL: dorsolateral; DM: dorsomedial.

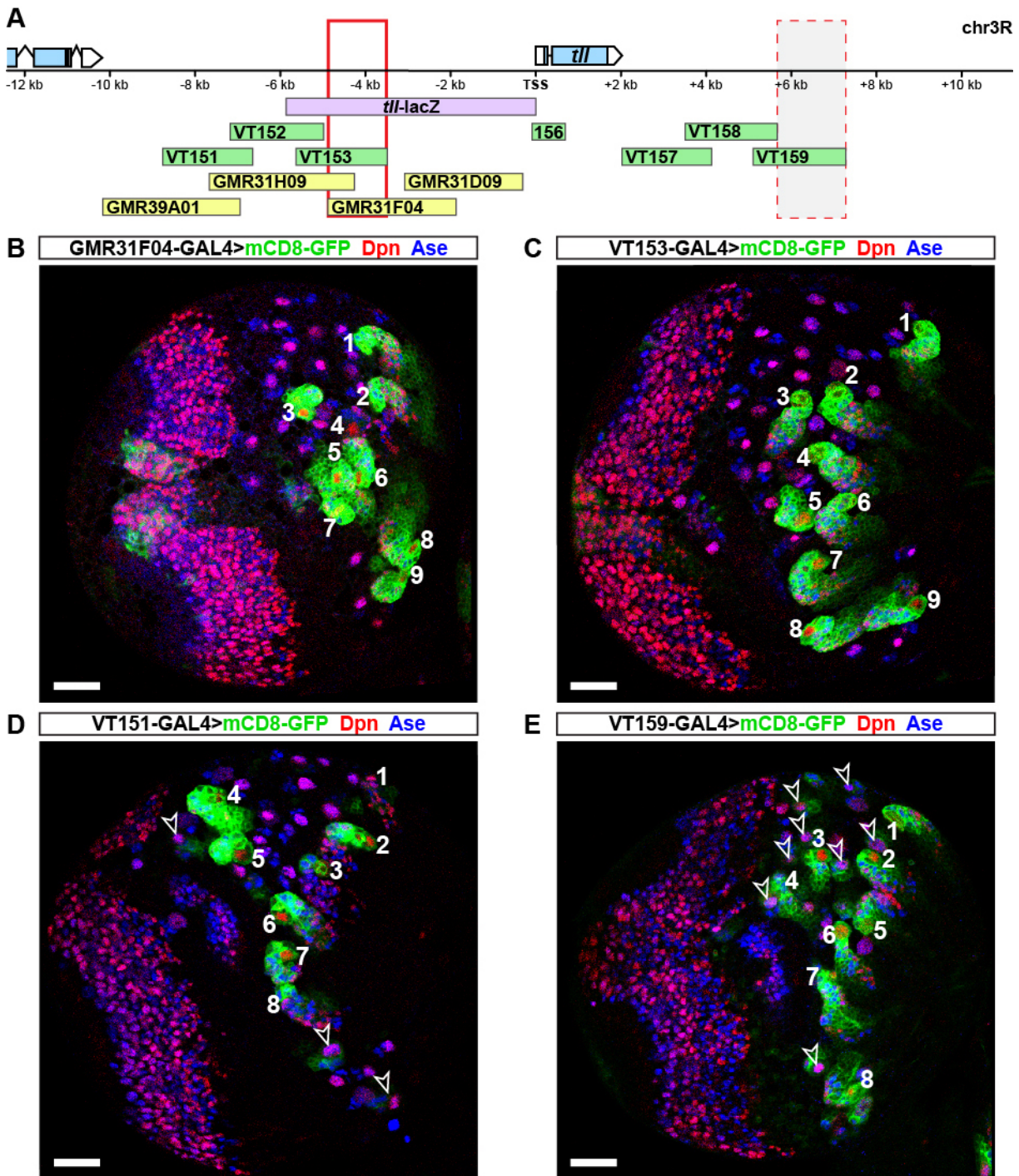


**Figure 2.4: Type II *tll* fragments map to overlapping genomic regions**

(A) Map of the *tll* locus with the regulatory fragment for each *tll* reporter construct shown below. The region in *tll-lacZ* is shown in purple and the genomic fragments for each *tll*-GAL4 are shown in green (VT GAL4 drivers) or yellow (GMR GAL4 drivers). VT and GMR GAL4 constructs are inserted in the *attP2* landing site. Bold red outline highlights the presumptive 5' type II regulatory element; dotted red line highlights the presumptive 3' type II regulatory element.

(B) GMR31F04-GAL4 is expressed strongly in type II neuroblasts (Dpn<sup>+</sup> (red) and Ase<sup>-</sup> (blue)) but brain lobes contain more than eight type II lineages (white numbers).

(C) VT153-GAL4 is expressed strongly in type II neuroblasts (Dpn<sup>+</sup> Ase<sup>-</sup>) but brain lobes contain more than eight type II lineages (white numbers).

(D) VT151-GAL4 is expressed in type II all neuroblasts (Dpn<sup>+</sup> and Ase<sup>-</sup>, and white numbers) and a few nearby type I neuroblasts (arrowheads).

(E) VT159-GAL4 is expressed in type II all neuroblasts (Dpn<sup>+</sup> and Ase<sup>-</sup>, and white numbers) and a few nearby type I neuroblasts (arrowheads).

Single section confocal images. Scale bars represent 30  $\mu$ m.

## **2.2 Determining the role of Tll in type II lineages**

The enrichment of Tll expression in type II neuroblasts suggested a role for Tll in regulating type II neuroblast identity or proliferation. Type II neuroblasts have an increased proliferative capacity compared to type I neuroblasts; asymmetric division of type II neuroblasts generates INPs, which can also self-renew, whereas type I neuroblasts generate GMCs that undergo terminal division. One defining feature of type II neuroblasts is the repression of Ase, which is required to generate INPs (Bowman et al., 2008). Early INPs lack Ase and Dpn expression but turn on Ase and, later, Dpn during maturation (**Fig. 2.5A**). INP fate acquisition can be followed using a genetic reporter for the FezF transcription factor *earmuff* (*erm*), R9D11-*lacZ*. R9D11-*lacZ* comprises a ~4 kb fragment of the *erm* enhancer and becomes expressed during INP maturation (**Fig. 2.5A**) (Haenfler et al., 2012; Weng et al., 2010). In contrast, type I neuroblasts co-express Dpn and Ase and their lineages do not express R9D11-*lacZ*.

### **2.2.1 Tll is required for type II lineage maintenance**

To determine if *tll* has a role in regulating type II neuroblast identity, I knocked down *tll* using two independent RNAi constructs that target different regions of the *tll* CDS (**Fig. 2.5B**). Expression of either *tll* RNAi in neuroblasts during larval development resulted in the loss of all type II neuroblasts in all brains (*i.e.* all neuroblasts expressed Dpn and Ase) (**Figs. 2.5C-D**). To confirm that the RNAi effects were due to the loss of *tll* and were not due to an RNAi off-target, I assessed neuroblast identity in *tll*<sup>l49</sup> mutant type II lineages. *tll*<sup>l49</sup> is a point mutation that creates a stop codon within the DBD (**Fig. 2.5B**), resulting in a null mutation that is embryonic lethal in homozygous animals (Pignoni et al., 1990). In order to study the *tll*<sup>l49</sup> allele in larval type II neuroblasts, I generated MARCM (Mosaic Analysis with a Repressible Cell Marker) clones (Lee and Luo, 1999) during larval stages (**Fig. 2.6A**). I used *wor-GAL4,UAS-mCD8-mCherry* to restrict clone visualisation to neuroblasts and the *erm* reporter R9D11-*lacZ* for the identification of type II lineages. I found that type II lineages were often labelled in wild type clones (**Fig. 2.6B-B'**), demonstrating that MARCM clones could encompass type II neuroblasts. However, I was unable to recover *tll*<sup>l49</sup> mutant type II clones, despite *tll*<sup>l49</sup> clones being visible in other neuroblasts (**Fig. 2.6C**). This suggested that *tll*<sup>l49</sup> type II neuroblasts underwent a cell fate transition that resulted in the loss of type II markers. Intriguingly, quantification of the number of type II lineages in brains with *tll*<sup>l49</sup> clones revealed a reduction in the number of type II lineages. The number of absent type II lineages in brains with *tll*<sup>l49</sup> clones was comparable to the number of type II lineages in wild type clones in control brains (**Fig. 2.6D**). This provided indirect evidence that *tll*<sup>l49</sup> type II

neuroblasts lost their identifying features and that *tll* was required for type II lineage maintenance during development.

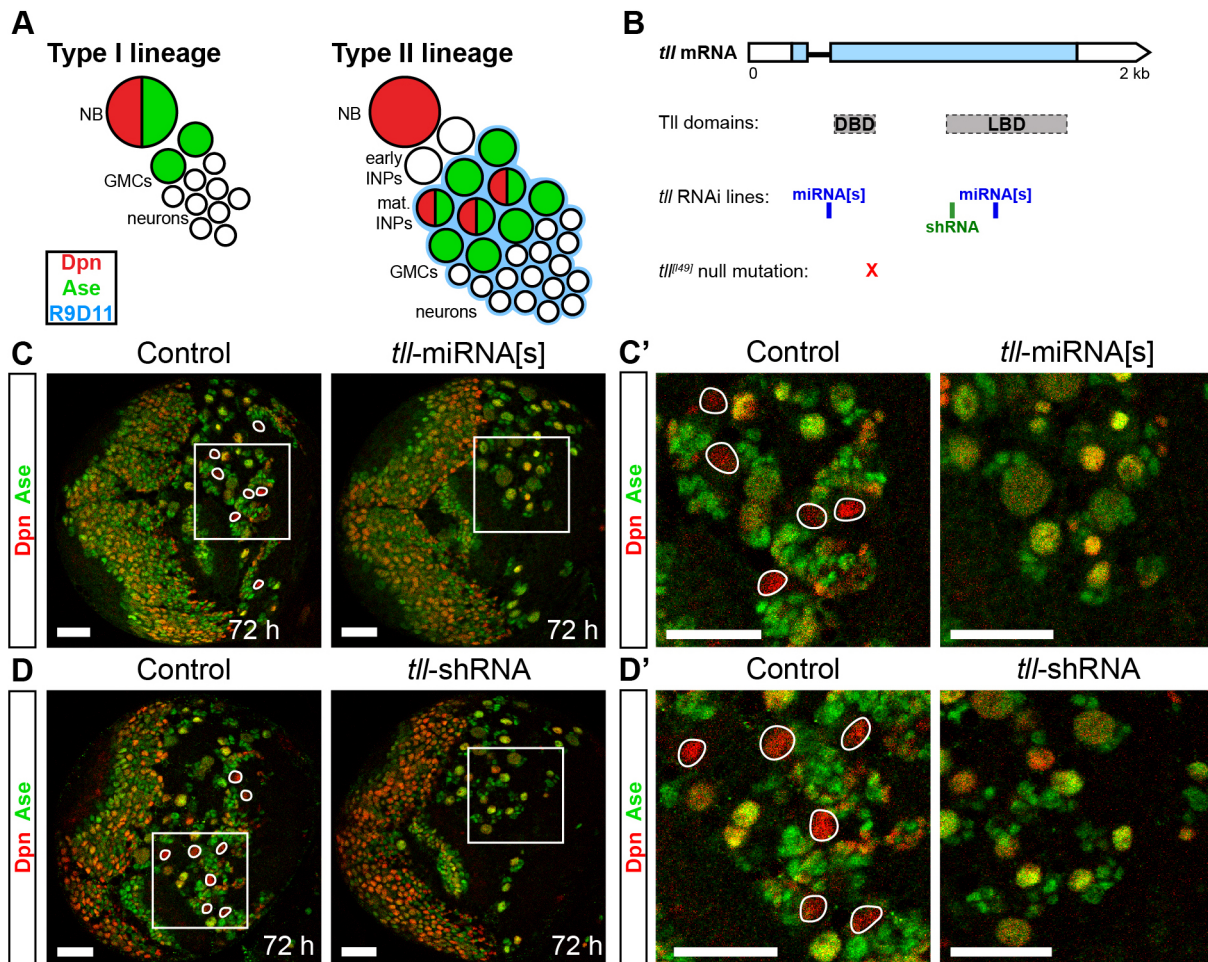


**Figure 2.5: Knockdown to *tll* results in the loss of all type II neuroblasts**

(A) Schematic depicting the expression of Dpn (red), Ase (green) and *erm* reporter R9D11 (blue) in type I and type II lineages.

(B) The *tll* coding sequence (blue regions of *tll* mRNA) includes two protein domains (grey): DBD and LBD. *tll* RNAi lines miRNA[s] (Lin et al., 2009) and shRNA (VDRC) target different regions of *tll* mRNA. *tll*<sup>49</sup> contains a point mutation (x) at the 3' end of the DBD that creates a stop codon, resulting in a null mutant (Diaz et al., 1996; Pignoni et al., 1990).

(C-C') Knockdown of *tll* during larval stages (*wor*-GAL4>*tll*-miRNA[s]) results in the absence of all type II neuroblasts. Control brains contain eight type II neuroblasts (Dpn<sup>+</sup> (red) and Ase<sup>-</sup> (green), white outlines; seven visible in the section shown). In *tll*-miRNA[s] brains, all neuroblasts express Dpn and Ase. (C') is a magnification of the boxed region in (C). *n* = 10 brain lobes for Control; *n* = 11 brain lobes for *tll*-miRNA[s].

(D-D') Using *wor*-GAL4 to drive *tll*-shRNA also results in the loss of all type II neuroblasts (white outlines in Control). (C') is a magnification of the boxed region in (C). *n* = 11 brain lobes for Control and *tll*-shRNA.

Brains dissected 72 hours ALH. Single section confocal images. Scale bars represent 30 μm.

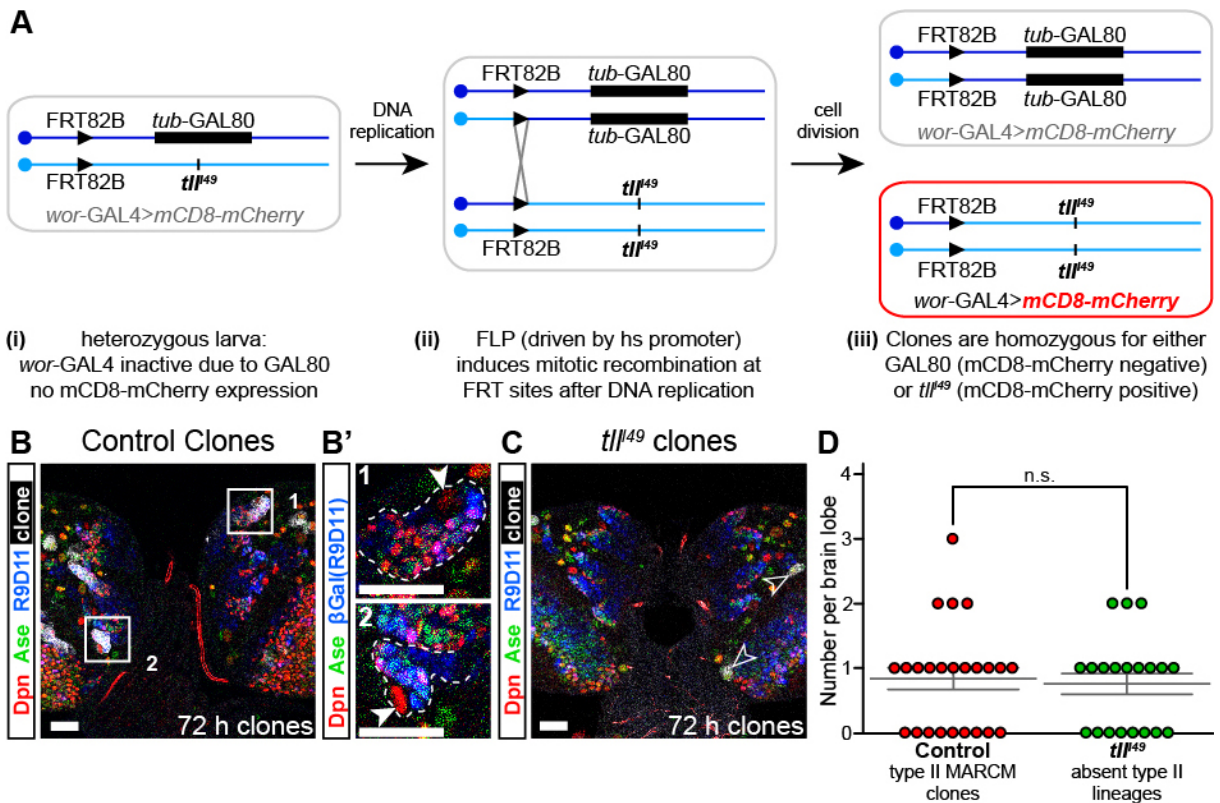


### Figure 2.6: *tll* null type II neuroblast clones cannot be recovered

(A) Schematic showing the genetic components of MARCM (Lee and Luo, 1999). Mitotic recombination can occur in all dividing cells but clone visualisation is restricted to neuroblasts through the use of *wor-GAL4* to drive the expression of *UAS-mCD8-mCherry*. For control clones, a chromosome carrying FRT82B without *tll<sup>49</sup>* was used for recombination with FRT82B,*tub-GAL80*.

(B-B') Type II neuroblasts (*Dpn*<sup>+</sup> (red) and *Ase*<sup>-</sup> (green)) could be encompassed within control MARCM clones at 72 hours after clone induction. *wor-GAL4*>*mCD8-mCherry* (white) identified neuroblast clones and *R9D11-lacZ* (blue) labelled type II lineages. (B') shows magnifications of the boxed regions in (B). Type II neuroblasts (arrowheads) and their lineages marked by clones (dotted white outlines). 20 type II MARCM clones were observed in 24 brain lobes analysed (from 12 brains).

(C) Central brain type I *tll<sup>49</sup>* neuroblasts could be visualised (arrowheads), but no *tll<sup>49</sup>* type II lineage clones could be recovered at 72 hours after clone induction. *n* = 20 brain lobes (from 10 brains).

(D) Quantifications of the number of type II lineages labelled by control MARCM clones (*n* = 20 clones in 24 brain lobes) compared to the number of type II lineages absent in *tll<sup>49</sup>* brains (*n* = 15 absent lineages in 20 brains). Mann-Whitney U test, *P* = n.s. (*P* = 0.849).

Single section confocal images. Scale bars represent 30  $\mu$ m.

### 2.2.2 Creating an immortalised type II-specific GAL4

Initial experiments showed that type II lineages that do not have *tll* are no longer distinguishable from surrounding type I lineages. The next step was to follow the effect of the loss of *tll* on type II lineages in a specific manner. In order to do this, I needed to label specifically and permanently to allow the effect of *tll* loss of function on type II lineages to be determined. In addition, because the frequency of MARCM clones in type II lineages was rather low, I decided to perform further loss of function analysis with an RNAi against *tll* (specifically, *tll*-miRNA[s]) so that *tll* function could be removed from all type II lineages consistently.

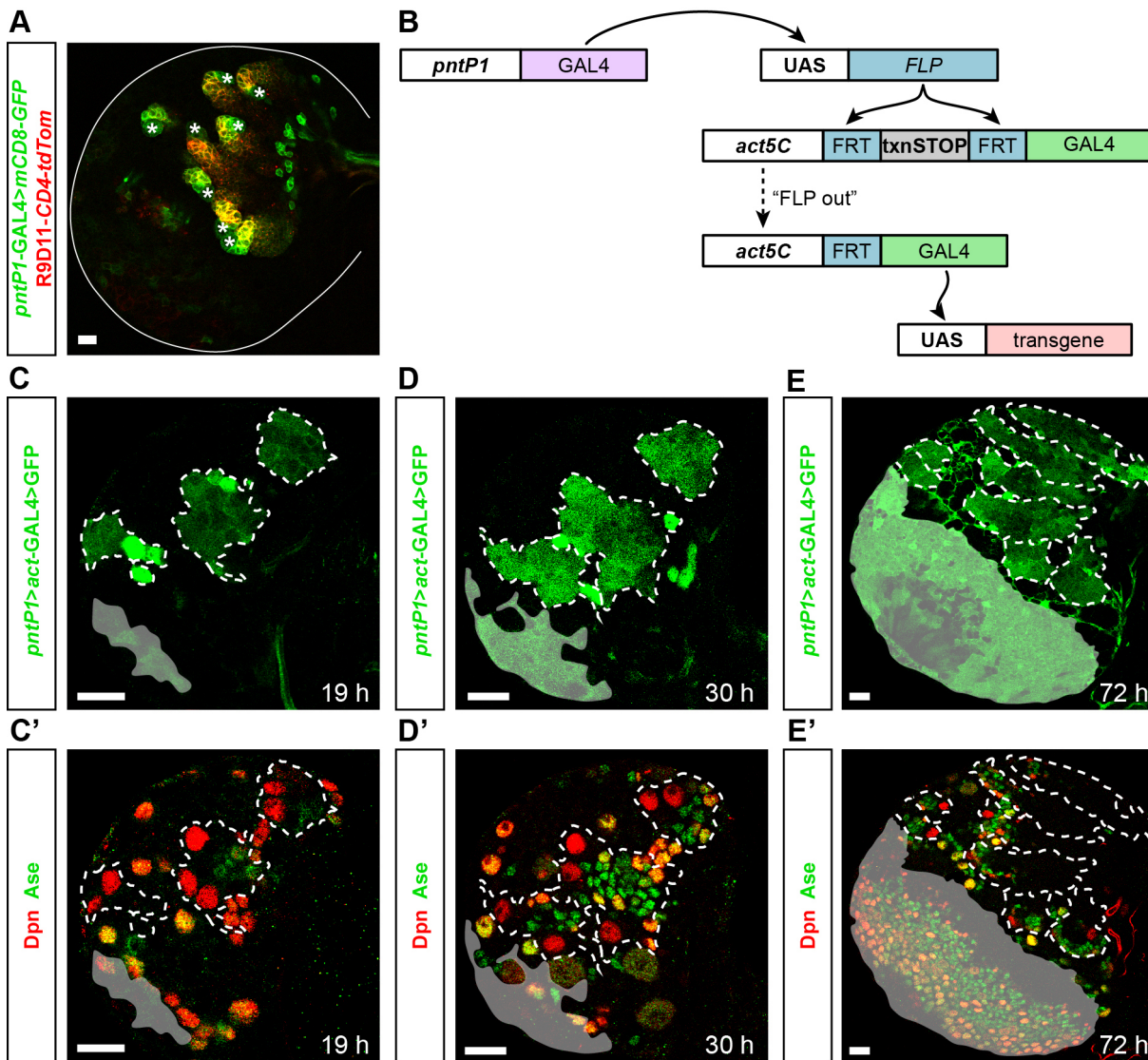


**Figure 2.7: *pntPI>act-GAL4* – an immortalised type II GAL4 driver**

(A) *pntPI-GAL4* drives UAS-*mCD8-GFP* expression (green) in central brain type II lineages but not in type I lineages at wandering third instar. Type II lineages were identified by R9D11-*CD4-tdTomato* (red), which labels type II INPs. Type II neuroblasts are highlighted with asterisks (\*).

(B) Schematic showing the genetic components of *pntPI>act-GAL4*, an immortalised type II GAL4. *pntPI-GAL4* drives the expression of UAS-*FLP*, which excises a transcriptional (txn) stop sequence, resulting in the *act5C* promoter driving GAL4 in type II lineages.

(C-E') *pntPI>act-GAL4* driving UAS-*GFP* labels type II lineages (outlined with white dotted lines) throughout larval development. *pntPI-GAL4* is also expressed at the optic lobe transition zone, resulting in expression of *pntPI>act-GAL4* in optic lobe neuroblasts (shaded regions). Larvae were raised at 29 °C after hatching: (C-C') 19 h corresponds to the start of second instar; (D-D') 30 h corresponds to the start of third instar and (E-E') 72 h corresponds to the end of third instar.

Single section confocal images. Scale bars represent 15 μm.

To generate an immortalised type II driver, I used a GAL4 driver that is expressed specifically in type II neuroblasts (*pntPI-GAL4* (Zhu et al., 2011)) (Fig. 2.7A) and immortalised its expression using a “FLP out” GAL4 cassette (Fig. 2.7B). *pntPI-GAL4* was used to drive the expression of UAS-*FLP*, which catalyses the excision of a transcriptional stop sequence from the “FLP out” cassette (*act5C>FRT-txnSTOP-FRT>GAL4* (Ito et al., 1997)). Subsequently, GAL4 expression is no longer dependent on type II neuroblast fate and *act5C-GAL4* drives

the expression of transgenes under the control of UAS. Immortalised *pntPI*-GAL4 will be referred to as *pntPI>act*-GAL4.

Initial characterisation of *pntPI>act*-GAL4 showed that this line labels all type II lineages throughout larval development (**Figs. 2.7C-E**). During early-to-mid larval stages, expression of *pntPI>act*-GAL4 is restricted almost entirely to type II lineages (**Fig. 2.7C-D**). At late third instar, *pntPI>act*-GAL4 labels type II neuroblasts and progeny but GAL4 expression is widespread throughout the CNS due to the expression of *pnt* at the OL transition zone (Yasugi et al., 2010) and in glial cells (Klaes et al., 1994; Klämbt, 1993) (**Fig. 2.7E**).

### **2.2.3 Type II neuroblasts switch to type I neuroblasts in the absence of *tll***

Generation of *pntPI>act*-GAL4 allowed the effect of *tll* loss of function (lof) on type II neuroblasts to be followed throughout larval development. *tll*-miRNA[s] was used to characterise the *tll* loss of function phenotype in type II neuroblasts as this construct has been shown to recapitulate the *tll* mutant phenotype in the *Drosophila* CNS (Guillermin et al., 2015; Lin et al., 2009). Expressing *tll*-miRNA[s] using *pntPI>act*-GAL4 revealed that Ase was derepressed in all type II neuroblasts in all brains at early larval stages (**Fig. 2.8A**). At mid larval stages, I was able to determine lineage composition. In normal type II lineages, INPs are the progeny in closest proximity to the neuroblasts, whereas GMCs are found in a more distal position (control panels of **Fig. 2.8B**). An important distinction between INPs and GMCs is the differential expression of Pros: GMCs have nuclear Ase and Pros, whereas INPs acquire nuclear Ase during maturation but never nuclear Pros (**Fig. 2.8B**). In the absence of *tll*, all cells next to type II neuroblasts that expressed Ase also had nuclear Pros, indicating cells with GMC fate in place of INPs. In addition, in 60 % of brains, *tll* knockdown type II neuroblasts had Pros crescents (red arrow, **Fig. 2.8B**), which was never observed in control type II neuroblasts (Boone and Doe, 2008). In type I neuroblasts and INPs, however, Pros is localised in crescents at mitosis to distribute Pros to differentiating daughter cells (Doe et al., 1991; Knoblich et al., 1995; Vaessin et al., 1991). Thus, the observation of Pros crescents in *tll* lof type II neuroblasts, and the presence of Pros<sup>+</sup> progeny adjacent to these neuroblasts, suggests that type II neuroblasts segregate Pros to their progeny at division in the absence of *tll*. The expression of Ase and segregation of Pros to differentiating daughter cells are hallmarks of type I neuroblasts and INPs, suggesting that type II neuroblasts are converted to a more restricted progenitor in the absence of *tll*.

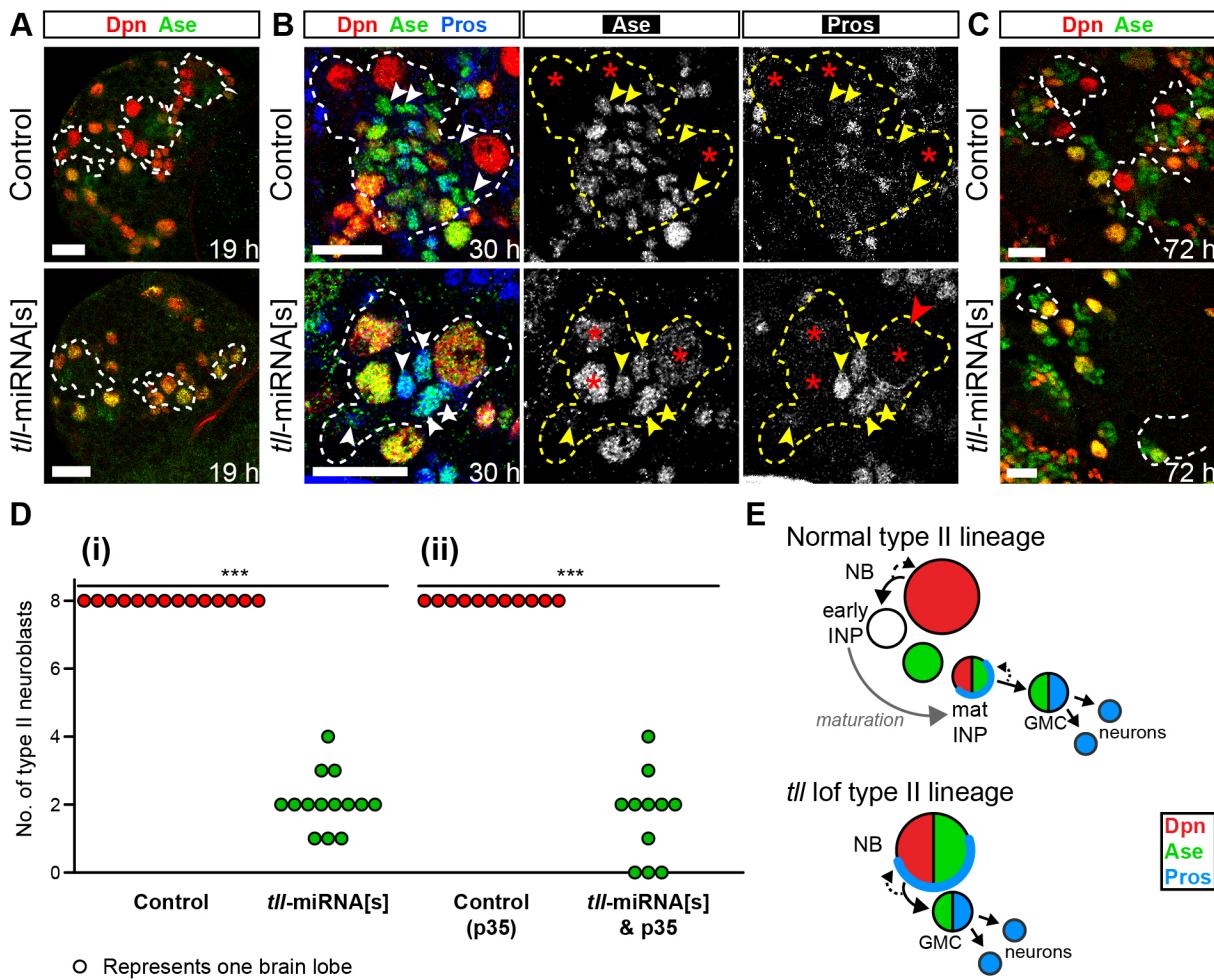


**Figure 2.8: Loss of *tll* causes type II lineages to transform to type I identity**

(A) At 19 h ALH, *pntPI>act-GAL4* driving *tll-miRNA[s]* results in the derepression of Ase (green) in all type II neuroblasts ( $Dpn^+$ , red). Type II lineages are outlined with dotted white lines.  $n = 14$  brains for Control;  $n = 11$  brains for *tll-miRNA[s]*.

(B) At 30 h ALH, type II lineages have INPs (arrowheads in Control,  $Ase^+$  and  $Pros^-$ ) closest to the neuroblast ( $Dpn^+$  and  $Ase^-$ ). *tll-miRNA[s]* results in  $Ase^+$  type II neuroblasts that generate GMCs (arrowheads in *tll-miRNA[s]*,  $Ase^+$  and  $Pros^+$ ). *tll-miRNA[s]* type II neuroblasts also exhibit Pros crescents (red arrowhead). In each panel, dotted lines highlight three type II lineages; red asterisks (\*) indicate neuroblasts in panels without Dpn staining.  $n = 10$  brains for Control and *tll-miRNA[s]*.

(C) *tll-miRNA[s]* type II neuroblasts retain co-expression of Ase (green) and Dpn (red) at late larval stages (72 h ALH).  $n = 14$  brain lobes for Control and *tll-miRNA[s]*.

(D) Quantification of the number of type II lineages. (i) The number of type II lineages is reduced significantly in *tll-miRNA[s]* brains. Kolmogorov-Smirnov test \*\*\*,  $P < 0.001$  ( $P = 1.66E-06$ ).  $n = 14$  brain lobes for Control and *tll-miRNA[s]*. (ii) Co-expressing p35 cannot rescue the disappearance of type II lineages in *tll-miRNA[s]* brains. Kolmogorov-Smirnov test \*\*\*,  $P < 0.001$  ( $P = 0.000033$ ).  $n = 11$  brain lobes for Control and *tll-miRNA[s]*.

(E) Schematic summarising the *tll* loss of function (lof) phenotype in type II neuroblasts. Without *tll*, type II neuroblasts divide in a type I manner.

Single section confocal images. Scale bars represent 15  $\mu m$ .

At late larval stages, *tll* type II lineages maintain their altered identity, as assessed by the co-expression of Dpn and Ase, (**Fig. 2.8C**) but are reduced in number (**Fig. 2.8D**). The loss of type II neuroblasts cannot be rescued by co-expressing the apoptosis inhibitor p35 (**Fig. 2.8D**), suggesting that type II neuroblasts do not undergo programmed cell death upon *tll* knockdown. These data show that in the absence of *tll*, type II neuroblasts derepress Ase and Pros and divide in a type I neuroblast manner (**Fig. 2.8E**). As a result, INPs are no longer present because GMCs are generated from type II neuroblasts directly. Furthermore, the lifespan of type II neuroblasts is reduced.

#### **2.2.4 Removing *tll* prevents *brat* tumour formation**

Mutations in the tumour suppressor *brain tumour* (*brat*) result in ectopic type II neuroblasts at the expense of neuronal progeny (Bello et al., 2006; Bowman et al., 2008; Lee et al., 2006). Tumours arise because type II lineage progression is prevented; in the absence of *brat*, immature INPs revert back to a type II neuroblast fate (Janssens et al., 2014; Komori et al., 2014b) (**Fig. 2.9A**).

Since *tll* is required for type II neuroblast fate and INP generation, I tested if removing *tll* from type II lineages that lacked *brat* was able to prevent tumour formation. Control brain lobes contained eight type II neuroblasts (Dpn<sup>+</sup> Ase<sup>-</sup>, *n* = 10 brain lobes) and showed a lineage progression from neuroblasts (Dpn<sup>+</sup>) to neuronal progeny (Pros<sup>+</sup>) (**Fig. 2.9B**, left-hand panel). Removing *brat* resulted in the generation of large tumours consisting of ectopic type II neuroblasts (brain lobes contained in excess of 1000 Dpn<sup>+</sup> Ase<sup>-</sup> neuroblasts, *n* = 10 brain lobes) at the expense of neurons (**Fig. 2.9B**, middle panel). However, knocking down both *brat* and *tll* prevented the production of ectopic type II neuroblasts (**Fig. 2.9B** right-hand panel). In fact, all neuroblasts expressed Ase (*i.e.* there were no type II neuroblasts, *n* = 10 brain lobes) and neuronal differentiation was restored (**Fig. 2.9B**, right-hand panel). Therefore, because of the requirement of *tll* for INP production, removing *tll* from type II neuroblasts prevents the generation of the tumour-initiating cell (INPs) for *brat* tumours. As a result, type II neuroblast lineages are no longer susceptible to tumours caused by the loss of *brat*.

#### **2.2.5 Repression of *ase* is downstream of *tll***

The repression of *ase* in type II neuroblasts is essential for the maintenance of lineage identity; ectopic expression of Ase in type II neuroblasts is sufficient to prevent the generation of INPs (Bowman et al., 2008). In addition, expressing Ase in type II neuroblasts prevents type II lineages from being susceptible to tumour-inducing *brat* mutations (Bowman

et al., 2008). These data suggest that the loss of *tll* and ectopic expression of *ase* affect type II neuroblasts (and their lineages) in the same way.

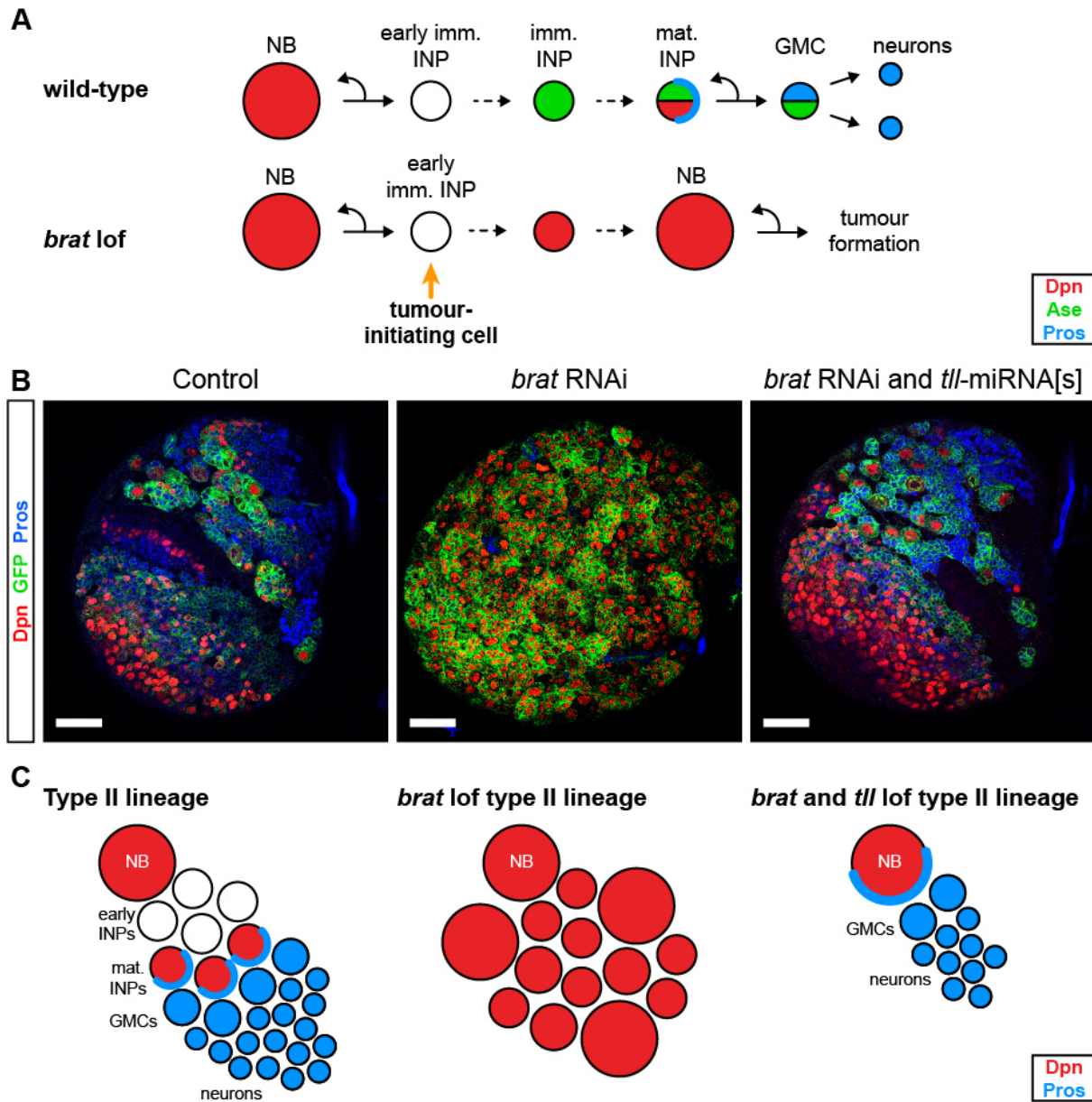


**Figure 2.9: Removing *tll* prevents *brat* tumours**

(A) *brat* mutations result in tumourigenesis by causing early immature INPs to revert to type II neuroblast fate (Janssens et al., 2014).

(B) Control brains contain neural lineages with one neuroblast (Dpn<sup>+</sup>, red) per lineage and multiple Pros<sup>+</sup> (blue) differentiating progeny. *brat* RNAi causes the production of ectopic neuroblasts (Dpn<sup>+</sup>) at the expense of neuronal progeny (Pros<sup>+</sup>). Knockdown of both *brat* and *tll* does not result in tumourigenesis. *n* = 10 brain lobes for all conditions.

(C) Schematics depicting the composition of normal type II lineages (left), *brat* lof type II lineages (middle), and *brat* and *tll* lof type II lineages (right).

Single section confocal images. Scale bars represent 30 μm.

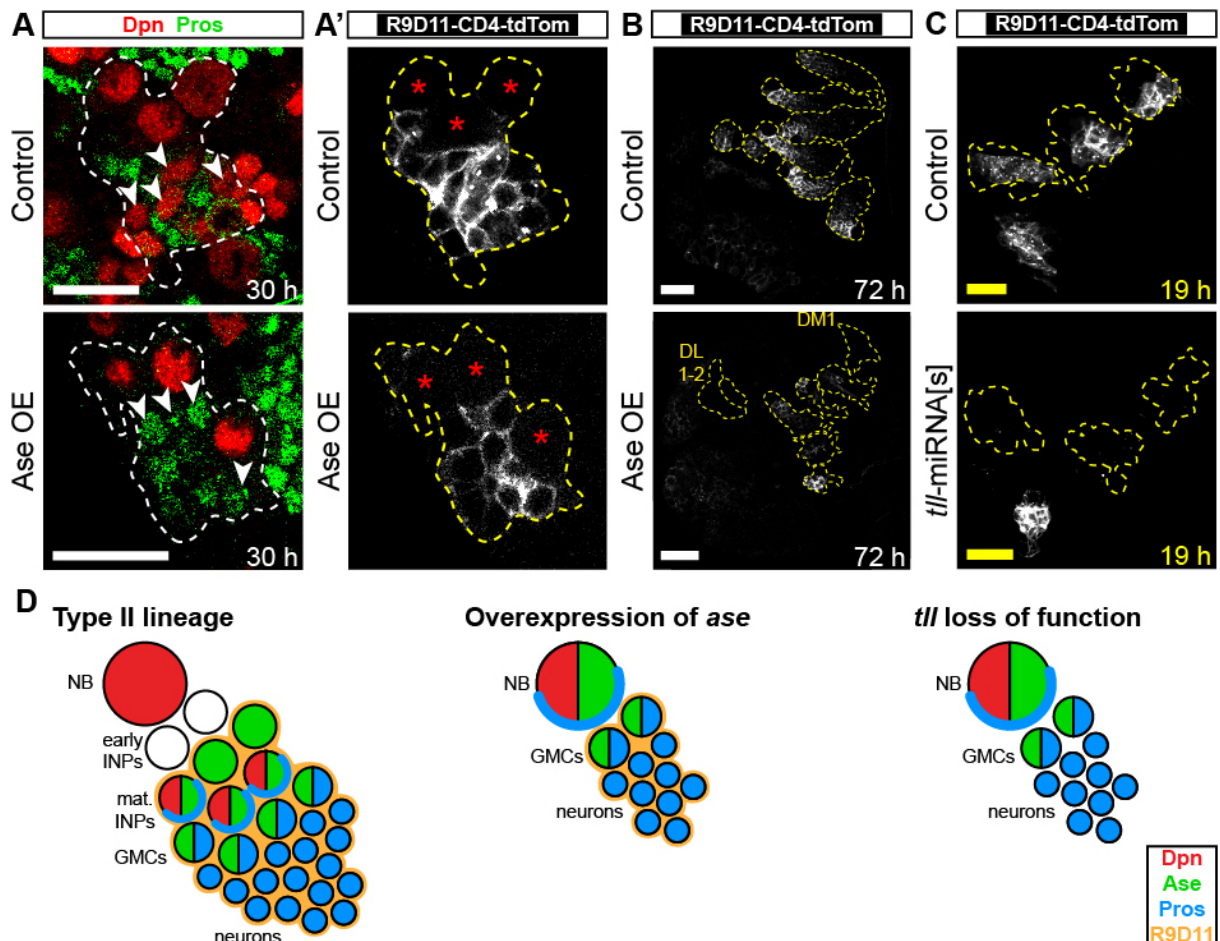


**Figure 2.10: Tll acts upstream of *ase* repression in type II neuroblasts**

(A) *Ase* overexpression (*Ase OE*) in type II neuroblasts (large  $Dpn^+$  (red) cells) results in the loss of INPs (small  $Dpn^+$  cells in Control, arrowheads); instead, type II neuroblasts generate GMCs ( $Pros^+$  (green) arrowheads in *Ase OE*). (A') *R9D11-CD4-tdTom* expression (white) is maintained in type II neuroblast progeny upon *Ase OE*, but remains absent from neuroblasts (\*). Dotted outlines highlight three type II lineages identified by *pntP1>act-GAL4* driving *UAS-GFP*.  $n = 11$  brains for Control and *Ase OE*. Brains dissected 30 hours ALH.

(B) All type II lineages are present at late larval stages in *Ase OE* brains and *R9D11-CD4-tdTom* remains expressed (except in DL1, DL2 and DM1 lineages). Dotted outlines highlight type II lineages, identified by *pntP1>act-GAL4* driving *UAS-GFP*.  $n = 11$  brain lobes for Control and *Ase OE*. Brains dissected 72 hours ALH.

(C) Expressing *tll-miRNA[s]* in type II lineages results in the loss of *R9D11-CD4-tdTom* from type II lineages. Dotted outlines highlight type II lineages, identified by *pntP1>act-GAL4* driving *UAS-GFP*. Control  $n = 14$  brains; *tll-miRNA[s]*  $n = 11$  brains. Brains dissected 19 hours ALH, images are max projections across  $10 \mu m$  in z.

(D) Schematic summarising the effects of *ase* overexpression or *tll* knockdown on type II lineages. Control lineages contain a large  $Dpn^+$  *Ase*<sup>-</sup> neuroblast and an associated lineage with INPs and differentiating progeny. Misexpression of *ase* causes the division mode to change type I, but the type II lineage marker *R9D11* remains. Upon loss of *tll*, type II neuroblasts behave as type I neuroblasts and lineages lose type II identifying features.

Single section confocal images unless specified otherwise. Scale bars represent  $15 \mu m$ .

However, comparison of expressing *tll-miRNA[s]* or *UAS-ase* in type II lineages revealed a key difference. Both genetic manipulations resulted in the failure of type II neuroblasts to produce INPs and GMCs were produced instead (all cells in immediate proximity to type II neuroblasts had nuclear *Pros*) (compare Fig. 2.8B and Fig. 2.10A). However, the INP marker

R9D11-*CD4-tdTom*, which reports *erm* expression, was still expressed in type II neuroblast progeny upon ectopic expression of *Ase* (**Fig. 2.10A**) and remained so even at late larval stages (**Fig. 2.10B**). In contrast, R9D11-*CD4-tdTom* was absent entirely at early larval stages when *tll* was knocked down (**Fig. 2.10C**). Furthermore, expressing *ase* in type II neuroblasts did not effect the survival of type II lineages (eight type II neuroblast lineages were present in all control and UAS-*ase* brains). Therefore, these data confirm the previous observation that the repression of *ase* is a consequence of type II lineage specification (Bowman et al., 2008), strongly suggesting that Tll acts upstream of *ase* repression to instruct type II neuroblast specification (summarised in **Fig. 2.10D**).

### **2.3 Chapter 2 discussion**

I have identified Tll as a new factor that regulates type II neuroblast fate and lineage identity. Throughout larval development, Tll is expressed at high levels in the neuroblast of type II lineages, weakly in immature INPs and not at all in mature INPs or the cells they give rise to. Removing Tll from type II neuroblasts revealed that Tll acts as an instructive signal for type II neuroblast fate. The loss of Tll results in the absence of all identifying features of type II lineages: type II neuroblasts derepress *Ase*, appear to segregate Pros to their progeny and lineages no longer express the INP marker *erm*. In the absence of Tll, type II neuroblasts undergo a cell fate transition to type I neuroblasts, which have a much lower self-renewal capacity and neurogenic potential.

In mice, TLX is expressed in NSCs during embryonic development and in adulthood (Li et al., 2012; Li et al., 2008; Liu et al., 2008; Shi et al., 2004). Embryonic NSCs display defects in proliferation in the absence of TLX (Li et al., 2008) and the loss of TLX in adult mice results in the depletion of the NSC pool and reduction in neurogenesis (Li et al., 2012; Liu et al., 2008; Niu et al., 2011; Shi et al., 2004). As such, TLX has been designated as a cell cycle regulator but the effects of the loss of TLX on NSC fate and lineage progression have not been assessed robustly *in vivo*. The requirement of TLX for maintaining the undifferentiated state and self-renewal capacity of NSCs is consistent with the role of Tll in type II neuroblasts. If TLX and Tll act in a conserved manner, it would be predicted that the loss of TLX would result in NSCs switching to a more differentiated progenitor type that maintains some properties of NSC but with a reduced capacity for self-renewal and neurogenesis.

In addition, the loss of TLX results in abnormal, aggressive behaviour in flies (Davis et al., 2014) and mice (Monaghan et al., 1997; O'Leary et al., 2016; Roy et al., 2002; Young et al.,

2002), and TLX mutations have been linked to hereditary cases of bipolar disorder and schizophrenia in humans (Dick et al., 2003; McQueen et al., 2005; Middleton et al., 2004; Wong et al., 2010). Despite the conserved effect that loss of TLX has on social behaviour, it is not clear if this is due to the regulation of NSCs by TLX or a separate mechanism. Therefore, it is important that we improve our understanding of how TLX controls NSC fate and lineage progression in different regions of the brain and at different stages of development. This could provide important links between mood disorders and genetic variants, which could improve our knowledge of the molecular causes of mental illnesses and facilitate the development of new treatments.



### Chapter 3

#### Targeted DamID reveals the genome-wide binding sites of Tll *in vivo*

Tll is expressed in type II neuroblasts and is required for the maintenance of NSC identity and lineage progression. I showed that in the absence of Tll, type II neuroblasts transform into type I neuroblasts, which have a more limited proliferation capacity and produce fewer neuronal progeny. In a similar manner, the loss of TLX has a negative impact on the proliferative capacity of vertebrate NSCs and results in a reduction in neurogenesis (Liu et al., 2008; Shi et al., 2004; Zhang et al., 2008).

TLX/Tll is an orphan nuclear receptor that acts primarily as a transcriptional repressor. There is no known biological ligand for TLX but its repressive function is mediated by a number of cofactors: Atrophin (Haecker et al., 2007; Wang et al., 2006; Zhang et al., 2006), BCL11 (Estruch et al., 2012), LSD1 (Yokoyama et al., 2008), as well as a number of HDACs (Yokoyama et al., 2008). There are also a small number of genes for which TLX is a transcriptional activator (Chavali et al., 2014; Elmi et al., 2010; Qu et al., 2010). No cofactors that mediate transcriptional activation of target genes by TLX have been identified so far (Corso-Díaz et al., 2016).

Determining the target genes of TLX is essential for understanding how TLX regulates NSC fate. Currently, there is no genome-wide binding data available for TLX or any of its homologues in other species. A number of studies have determined mouse TLX target genes by comparing changes in RNA levels in wild type adult NSCs with TLX null NSCs (Qu et al., 2010; Zhang et al., 2008) or TLX overexpressing NSCs (Liu et al., 2010). However, only a small number of genes whose expression was altered upon TLX manipulation were found to be regulated directly by TLX; candidate targets were confirmed using a combination of gel shift, chromatin immunoprecipitation (ChIP) reverse transcription (RT)-PCR and luciferase reporter assays to show direct binding by TLX (Liu et al., 2008; Liu et al., 2010; Qu et al., 2010). The change in expression of the majority of genes identified was likely due to a secondary effect of other TLX target genes. In addition, many of the targets were identified in cells in culture, meaning that additional *in vivo* validation was required. Profiling the genomic binding sites of TLX/Tll *in vivo* would provide a valuable complementary data set to



very low levels of Dam-fusion being present in the cell-type of interest, but this is sufficient to methylate the DNA at sites of Dam-fusion binding (**Fig. 3.1B**). The control experiment for TaDa is the expression of the Dam protein alone under the same conditions as the Dam-fusion protein (**Fig. 3.1C**) to provide a low level of random DNA methylation, which also reveals open chromatin (Aughey et al., 2018).

### 3.1.1 Creating a type II-specific GAL4 for Targeted DamID

Profiling TII binding sites in type II neuroblasts using TaDa requires a GAL4 driver that is specific to these neuroblasts. Unfortunately, many type II-specific genes are expressed in additional cells in the brain other than type II neuroblasts (such as *pntP1* and *btd*, see **Fig. 3.2**) and so using their regulatory elements to drive GAL4 expression would result in TII-NDam binding in additional cell types.

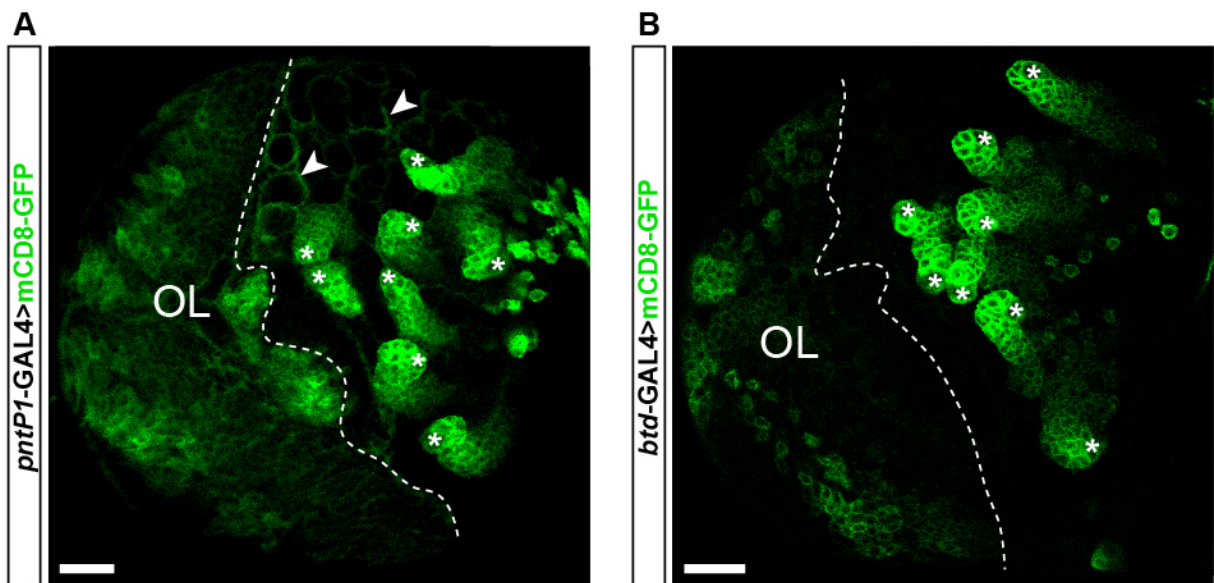


**Figure 3.2: Available type II GAL4s are not suitable for TaDa**

(A) *pntP1*-GAL4 driving UAS-*mCD8-GFP* (green) labels type II lineages (\*) but is also expressed in the optic lobe (OL) and in cortex glia (arrow heads).

(B) *btd*-GAL4 driving UAS-*mCD8-GFP* labels type II lineages (\*) but is also expressed in the OL.

Brains dissected at wandering third instar. Single section confocal images. Scale bars represent 30  $\mu$ m.

In order to target type II neuroblasts alone, I used an intersectional GAL4-based system that was developed by the Lee Lab (Yang et al., 2016). This approach requires multiple genetically encoded elements in order for GAL4 expression to be restricted to type II lineages (**Fig. 3.3A**). GAL4 expression is under the control of a *dpn* fragment. *dpnEE* is a 600 bp genomic fragment from *dpn* that drives expression in all neuroblasts outside of the optic lobes (Awasaki et al., 2014). GAL4 expression is prevented due to a transcriptional stop sequence separating the *dpn* enhancer and *GAL4*. Excision of the transcriptional stop sequence is

catalyzed by a KD recombinase, expression of which is driven by an enhancer of the *stg* gene (*stg14*, a 975 bp sequence located 8.5 kb upstream of the predicted TSS of *stg*) that drives transient expression in embryonic type II neuroblasts (Wang et al., 2014).

I assessed the expression of this system at mid-larval stages and found that *stg14* drives low levels of expression in type I neuroblasts, (as reported in Yang et al., 2016) (**Fig. 3.3B**). To restrict GAL4 expression to type II neuroblasts, I included *asense*-GAL80 (Neumüller et al., 2011) to block GAL4 activity in type I neuroblasts (**Fig. 3.3C**). Assessment of the final genetic set-up showed that I could use this system to restrict GAL4 activity to type II lineages, which meant that it was suitable for performing TII TaDa (**Fig. 3.3D-D'**).

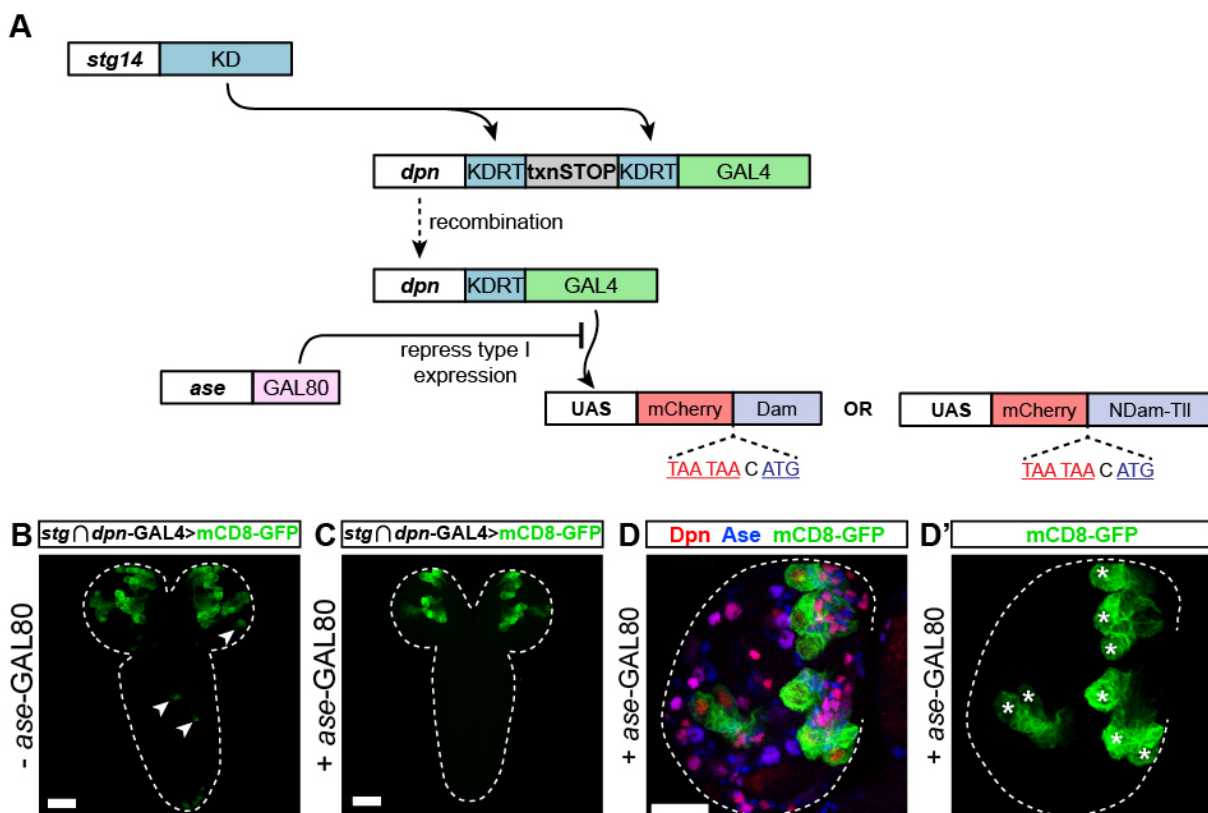


**Figure 3.3: Testing the expression of  $stg \cap dpn-GAL4$**

(A) Schematic showing *stg14*-patterned *dpn*-GAL4. *stg14* drives the expression of KD recombinase, which excises a transcriptional stop resulting in the *dpn<sup>EE</sup>* promoter driving GAL4. *ase*-GAL80 was included to prevent GAL4 activity in type I neuroblasts. This system results in the expression of TaDa constructs (under the control of UAS) in type II neuroblasts specifically.

(B) *stg14*-patterned *dpn*-GAL4 ( $stg \cap dpn-GAL4$ ) driving UAS-*mCD8-GFP* (green) without *ase*-GAL80 is expressed in type II neuroblasts and a small number of type I neuroblasts (arrowheads). Image is a projection over 61  $\mu\text{m}$  in z.

(C) *stg14*-patterned *dpn*-GAL4 ( $stg \cap dpn-GAL4$ ) driving UAS-*mCD8-GFP* (green) with *ase*-GAL80 is expressed in type II neuroblasts ( $GFP^+$ ) and not in type I neuroblasts. Projection over 75  $\mu\text{m}$  in z.

(D-D') *stg14*-patterned *dpn*-GAL4 ( $stg \cap dpn-GAL4$ ) driving UAS-*mCD8-GFP* (green) is expressed exclusively in type II neuroblasts ( $Dpn^+$  (red) and  $Ase^-$  (blue) in D, marked by asterisks (\*) in D'). Image is a projection over 30  $\mu\text{m}$  in z.

Brains dissected 50 hours ALH. Scale bars represent 50  $\mu\text{m}$  in B-C; 30  $\mu\text{m}$  in D-D'.

### **3.2 Profiling Tll binding sites in type II neuroblasts**

TaDa is a robust and reproducible technique that requires no cross-linking or antibodies (Southall et al., 2013; van Steensel and Henikoff, 2000; van Steensel et al., 2001). In addition, TaDa is highly sensitive and has been used to profile small numbers of neurons in the adult *Drosophila* brain (~100 neurons of ~150,00 per brain (Southall et al., 2013)). Type II neuroblasts are the minority progenitor type in the larval brain: there are 16 type II neuroblasts per brain, compared to ~320 type I neuroblasts in the central brain and VNC (Doe, 2008; Ito and Hotta, 1992; Truman and Bate, 1988). Despite the small number of type II neuroblasts in the larval brain, the sensitivity of TaDa allowed me to determine Tll binding *in vivo* by extracting methylated DNA from an average of 45 brains per replicate, which corresponds to ~720 type II neuroblasts per sample.

Performing peak-calling on the binding sites of Tll showed that Tll was bound at 2,495 genes (see **Appendix 2** for full list). Gene Ontology (GO) term analysis of the gene list showed enrichment for genes required for nervous system development and neuron production (**Table 3.1**), demonstrating that Tll binds to genes associated with neural fate during development.

| Term                                    | # genes | p value   |
|-----------------------------------------|---------|-----------|
| <b>nervous system development</b>       | 391     | 2.07e-51  |
| <b>neurogenesis</b>                     | 323     | 1.76e-47  |
| <b>generation of neurons</b>            | 310     | 6.04e-46  |
| <b>regulation of cellular process</b>   | 858     | 1.51e-44  |
| <b>regulation of biological process</b> | 913     | 2.33e-43  |
| <b>biological regulation</b>            | 990     | 8.54e-42  |
| <b>system development</b>               | 565     | 1.54e-40  |
| <b>cell communication</b>               | 503     | 1.31e-37  |
| <b>neuron differentiation</b>           | 268     | 4.107e-37 |
| <b>signalling</b>                       | 494     | 5.51e-37  |

**Table 3.1: GO term analysis of genome-wide Tll protein-coding targets.** The top ten GO terms reveal enrichment for genes required for nervous system development. Analysis performed using GO::TERMFINDER (Boyle et al., 2004).

#### **3.2.1 Tll TaDa shows cell type specific binding**

A small number of genes have been identified as direct transcriptional targets of Tll in the early stages of embryogenesis. Tll binds upstream of *knirps* (*kni*) (Pankratz et al., 1992), *Krüppel* (*Kr*) (Hoch et al., 1992) and *hunchback* (*hb*) (Margolis et al., 1995) and regulates their transcription to define the anterior-posterior axis of the embryo. The fragments bound by Tll within the 5' regulatory regions of *kni*, *Kr*, and *hb* were determined by *in vitro* DNase footprinting assays (Galas and Schmitz, 1978), which also revealed a consensus Tll binding sequence (AAGTCA) (Hoch et al., 1992; Margolis et al., 1995; Pankratz et al., 1992).

I assessed if Tll bound to its embryonic targets in type II neuroblasts. In the Tll TaDa data, Tll binding is observed at the 5' regulatory regions of *kni* (Fig. 3.4A), *Kr* (Fig. 3.4B), and *hb* (Fig. 3.4C). The binding of Tll at these genes is statistically significant and these genes are identified in the list of Tll targets (Appendix 2). However, with the exception of *hb*, the cis-regulatory fragments to which Tll binds in type II neuroblasts do not correspond to the elements defined in the embryo (highlighted in green in Fig. 3.4). This demonstrates that the binding pattern of Tll changes over the course of development and provides initial validation that the binding targets identified by Tll TaDa are specific to type II neuroblasts.

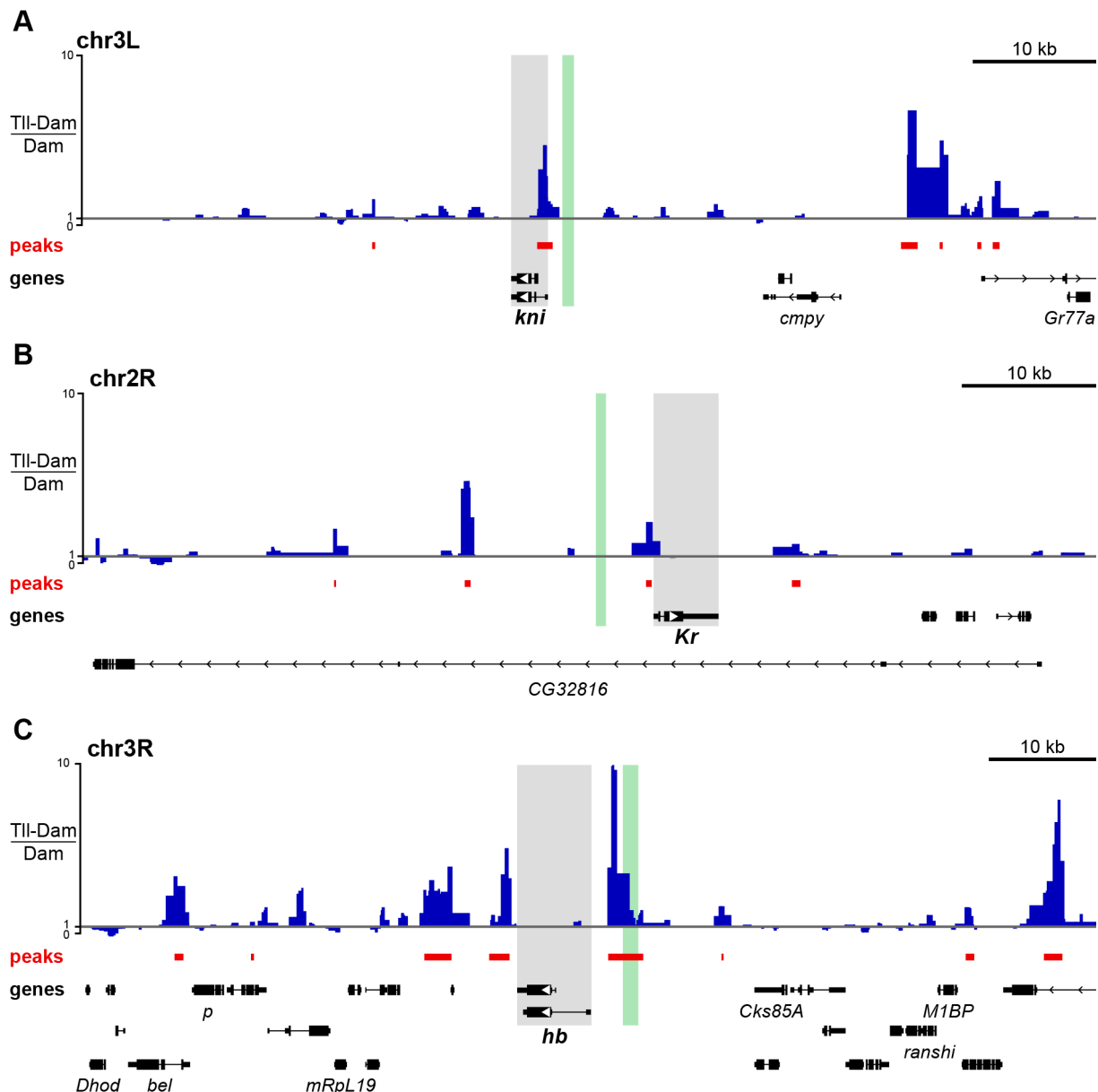


**Figure 3.4: Tll binds to previously determined target genes**

(A) Tll binds at the TSS of *kni* (*kni* shown in grey), with binding (blue peaks) also observed across the first intron of the long isoform. No binding is observed at the previously characterised 5' regulatory element (green) (Pankratz et al., 1992).

(B) Tll binds at the TSS of *Kr* (*Kr* shown in grey). No Tll binding is observed at the previously defined 5' element (green) (Hoch et al., 1992; Hoch et al., 1991).

(C) Tll binds upstream of *hb* and binding overlaps with the embryonic 5' regulatory fragment (green) (Margolis et al., 1995).

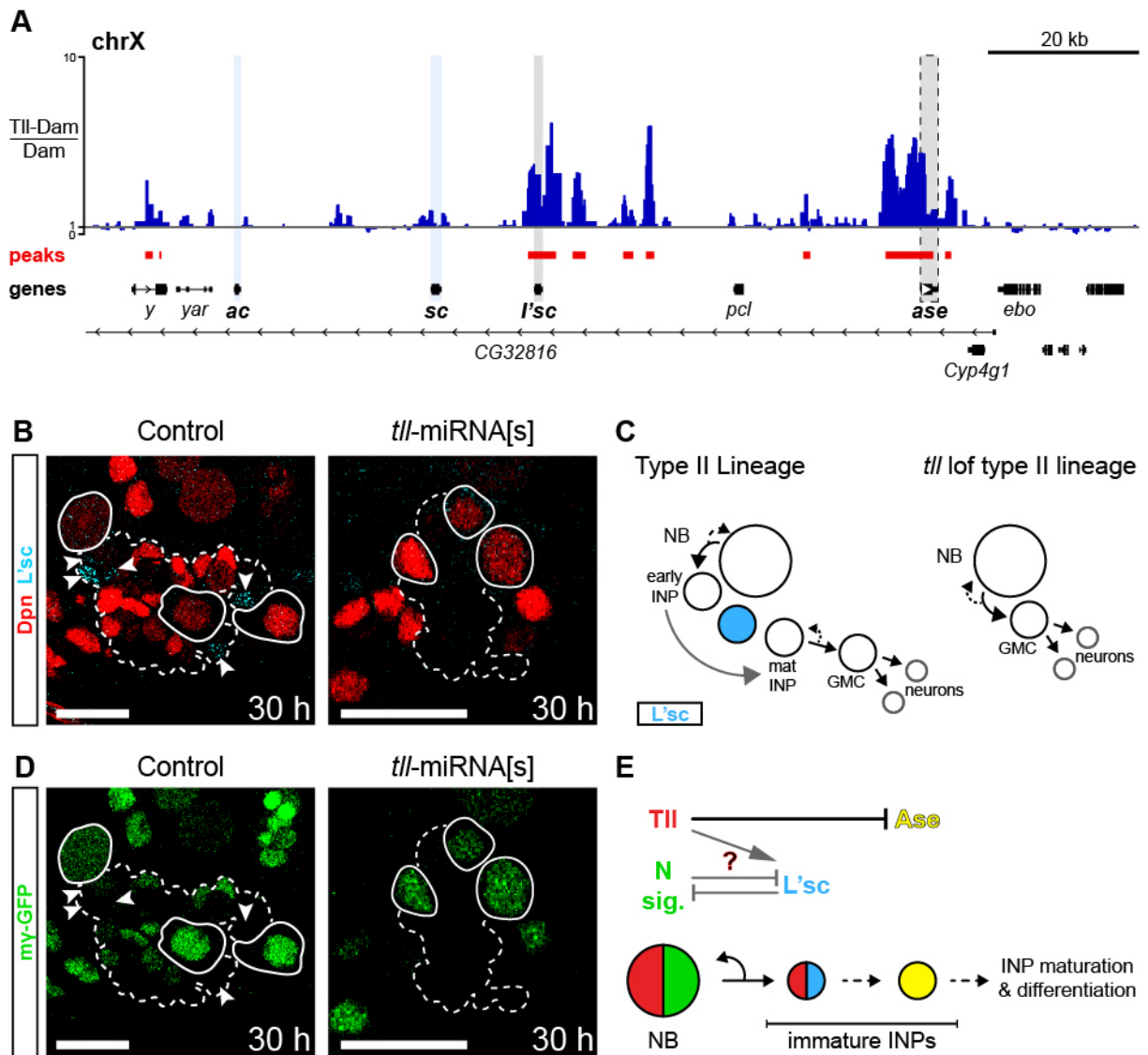


**Figure 3.5: TII binds to *ase* and *l'sc*, two AS-C genes**

(A) The AS-C comprises *ac*, *sc*, *l'sc*, and *ase*. TII binds to *ase* (grey with dotted outline) and *l'sc* (grey) but not to *ac* or *sc* (blue). All genes of the AS-C are transcribed from left to right.

(B) L'sc (cyan) is expressed in immature INPs (arrowheads) but is absent from type II neuroblasts (Dpn<sup>+</sup>, red, and outlined with solid white line). Neither L'sc expression nor INPs are present in *tll*-miRNA[s] lineages. Type II lineages were identified using *pntP1>act-GAL4* and are outlined with white dotted lines. Brains dissected 30 hours ALH. *n* = 13 brains for Control; *n* = 12 brains for *tll*-miRNA[s].

(C) Schematic showing L'sc (cyan) expression in immature INPs. No L'sc expression is detected in type II lineages in the absence of TII.

(D) Notch signalling is active in the neuroblast (outlined with solid white line) of type II lineages, which is unaffected upon *tll* knockdown. Type II lineages were identified with *pntP1>act-GAL4* and are outlined with white dotted lines. Arrowheads indicate immature INPs that express L'sc, which do not display Notch signalling. Brains were dissected 30 hours (h) ALH. *n* = 13 brains for Control; *n* = 12 brains for *tll*-miRNA[s].

(E) Schematic depicting a model of the relationship between TII, AS-C genes, and Notch signalling.

TII expression (red) and Notch signalling (green) are high in type II neuroblasts. TII represses *Ase* expression in the neuroblast. Early born immature INPs lack Notch signalling but maintain low levels of TII expression. L'sc (blue) is also expressed in early immature INPs. TII binds to L'sc and may activate its expression, which is likely repressed by Notch signalling in the neuroblast.

Control panel images are a projection of two 1  $\mu$ m slices; *tll*-miRNA[s] panels single section confocal images. Scale bars represent 15  $\mu$ m.

### **3.2.2 Tll binds to AS-C genes**

Tll is required for type II neuroblast fate, which is dependent on the repression of *asense* (*ase*). In Chapter 2, I showed that *ase* is derepressed in type II neuroblasts when Tll is knocked down suggesting that *ase* repression is downstream of Tll. To determine if *ase* could be a transcriptional target of Tll, I assessed the binding of Tll at the *ase* locus using TaDa. Analysis of the Tll peaks showed that Tll binds strongly at the *ase* locus (**Fig. 3.5A**). Therefore, Tll appears to repress *ase* expression directly in order to promote type II neuroblast fate.

*ase* is part of the *achaete-scute* complex (AS-C) (González et al., 1989). The AS-C comprises four bHLH transcription factors, *achaete* (*ac*), *scute* (*sc*), *lethal of scute* (*l'sc*) and *ase*, that promote neural fate (Skeath and Carroll, 1994). Further analysis of Tll binding peaks across the AS-C showed that, in addition to binding at *ase*, Tll binds at *l'sc* but not at *ac* or *sc* loci (**Fig. 3.5A**). This suggested that *l'sc* could also be a direct transcriptional target of Tll. However no role has been described for *l'sc* in type II lineages. Intriguingly, a previous study showed that *tll* mutant embryos lacked regions of *l'sc* expression, resulting in the absence of neuroblasts, and identified a Tll binding site upstream of *l'sc* (Younossi-Hartenstein et al., 1997). In addition, loss of *tll* in the developing optic lobe resulted in the loss of *l'sc* expression as neuroepithelial cells transition to neuroblasts (Guillermin et al., 2015). These observations suggested that Tll activates *l'sc* expression but provided no binding data to support this claim.

To determine if *l'sc* is expressed in type II lineages, I performed immunostaining with an antibody raised against *l'sc* (Caygill and Brand, 2017). This showed that *l'sc* is expressed transiently in type II lineages: *l'sc* is expressed in newly-born progeny of type II neuroblasts (early INPs) in all lineages but not in other cells of the lineage (Control panels of **Fig. 3.5B**). To determine if Tll binding at *l'sc* has a functional role in type II lineages, I assessed the expression of *l'sc* in *tll* knockdown lineages. *l'sc* expression was abolished upon the loss of *tll* (**Fig. 3.5B**), suggesting that Tll activates *l'sc* expression in type II lineages. Thus, the regulatory relationship between Tll and *l'sc* in type II lineages appears to mirror the role of *tll* in the embryo and optic lobe (Guillermin et al., 2015; Younossi-Hartenstein et al., 1997). However, it is difficult to determine the regulatory relation between Tll and *l'sc* in type II lineages due to the loss of INPs in the absence of *tll* (**Fig. 3.5C**). Assessing the regulatory relationship between Tll and *l'sc* is complicated further by the activity of Notch signalling. Notch signalling represses proneural gene expression (for a review, see Bertrand et al., 2002)

and so the cells in which *L'sc* is expressed show downregulation of Notch signalling (Yasugi et al., 2010 and **Fig. 3.5B-C**). Type II neuroblasts have active Notch signalling, which is not disrupted upon loss of *tll*, and so could explain the absence of *L'sc* in both normal type II neuroblasts and in *tll* knockdown lineages (**Fig. 3.5D**). If this is the case, *L'sc* expression in early INPs could be permitted due to the maintenance of Tll (see Chapter 2) and the lack of Notch signalling in these cells (Knoblich et al., 1995). Since Notch signalling is not affected by the loss of *tll* (**Fig. 3.5D**) it is likely that the Notch pathway and Tll act in parallel pathways to maintain a balance between neuroblast fate and differentiation (**Fig. 3.5E**). It should be noted that *ase* and Notch signalling co-exist in INPs and type I neuroblasts during development (Zacharioudaki et al., 2012), demonstrating that *ase* is not repressed by Notch signalling in the same manner as classical proneural genes (*ac*, *sc* and *l'sc*).

In summary, TaDa showed that Tll binds across the AS-C in type II neuroblasts. Significant binding was found at *ase* (which Tll represses) and *l'sc* (which Tll may activate), demonstrating the complexity of gene regulation by Tll. While *ase* has been much studied in type II neuroblast fate, the role of *l'sc* has not yet been explored. The expression of *l'sc* in early immature INPs suggests it may regulate INP maturation.

### **3.2.3 Tll binds to genes that are expressed differentially in type II lineages: *pros*, *pntP1*, *erm*, *btd*, *Sp1***

Repression of *ase* is central to the ability of *tll* to promote type II neuroblast fate. However, the loss of *ase* is not sufficient to induce type II neuroblast fate in type I neuroblasts (Bowman et al., 2008), demonstrating that additional factors are required to specify type II lineages.

Type I neuroblasts exhibit cortical crescents of Prospero (Pros), a homeodomain protein that promotes neuronal differentiation, at asymmetric division (Choksi et al., 2006). As a result, Pros is segregated to differentiating daughter cells, where it enters the nucleus and both represses neuroblast genes and promotes neuronal fate (Knoblich et al., 1995; Spana and Doe, 1995; Vaessin et al., 1991). In contrast, type II lineages do not express Pros, which is required for the generation of full neuronal lineages (Bayraktar et al., 2010). In Chapter 2, I showed that removing *tll* from type II neuroblasts results in the derepression of Pros in type II neuroblasts and that Pros was segregated asymmetrically upon neuroblast division into differentiating progeny. To determine if Tll represses *pros* directly, I assessed Tll binding at the *pros* locus in type II neuroblasts. TaDa revealed that Tll was bound within the *pros* coding sequence (in the first exon of the longer isoforms, which also corresponds to the TSS of the

shorter isoforms) (**Fig. 3.6A**), suggesting that Tll represses the expression of this pro-differentiation gene directly.

In contrast to Ase and Pros, which are repressed selectively in type II neuroblasts, the ETS transcription factor PointedP1 (PntP1) is expressed in type II but not type I neuroblasts. PntP1 expression promotes both type II neuroblast fate and INP specification (Xie et al., 2016; Zhu et al., 2011). TaDa revealed that Tll bound across the *pnt* locus, with the majority of binding observed at the region immediately upstream of the shorter *pntP1* isoform (**Fig. 3.7A**). The longer *pnt* isoform, *pntP2*, is not expressed in type II lineages (Zhu et al., 2011) and so the selective binding of Tll observed at the promoter of *pntP2* suggests that Tll may promote the differential expression of *pntP1* and *pntP2* in type II neuroblasts.

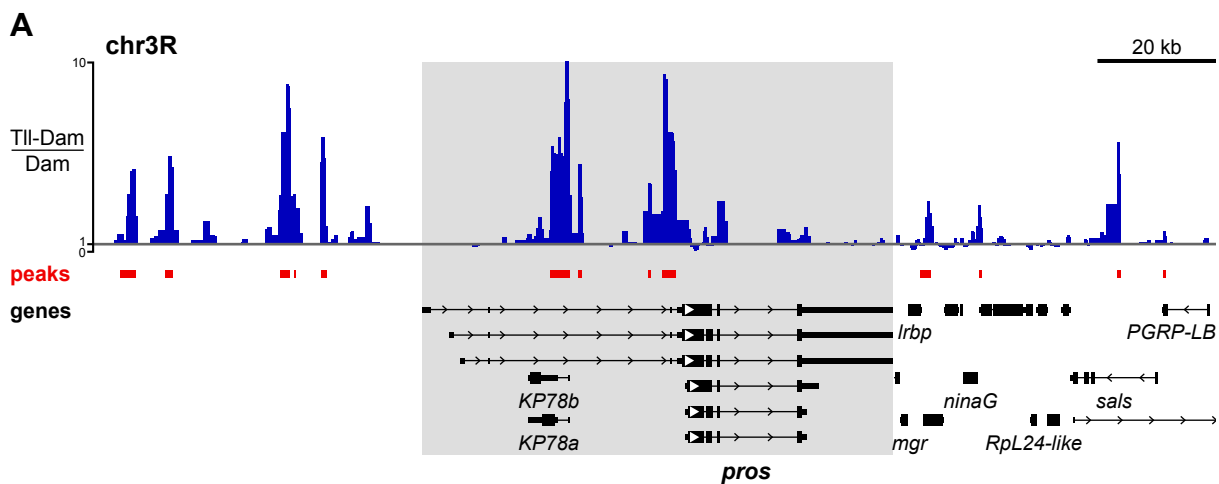


**Figure 3.6: Tll binds at the *pros* locus**

(A) Tll binds within the coding sequence of *pros*, with binding enriched at the 5' region of the shorter isoforms.

To determine if loss of *tll* affects PntP1 expression, I compared PntP1 expression in control type II lineages and in the absence of *tll*. PntP1 is expressed in the neuroblast and early INPs in type II lineages (Zhu et al., 2011). However, loss of *tll* results in the absence of PntP1 in all cells of type II lineages (**Fig. 3.7B**), demonstrating that Tll is required for PntP1 expression in type II neuroblasts (**Fig. 3.7C**).

PntP1 expression in type II neuroblasts is required to promote INP specification (Zhu et al., 2011) via a feedback loop with *earmuff* (*erm*) and Notch signalling (Li et al., 2017; Li et al., 2016; Xie et al., 2016). In maturing INPs, PntP1 activates *erm* expression to prevent INP reversion to neuroblast fate and Erm represses *pntP1* to ensure lineage progression. I showed

in Chapter 2 that type II lineages that lack *tll* lose *erm* reporter (*R9D11-CD4-tdTomato*) expression, suggesting that Tll could also be involved in this regulatory loop.

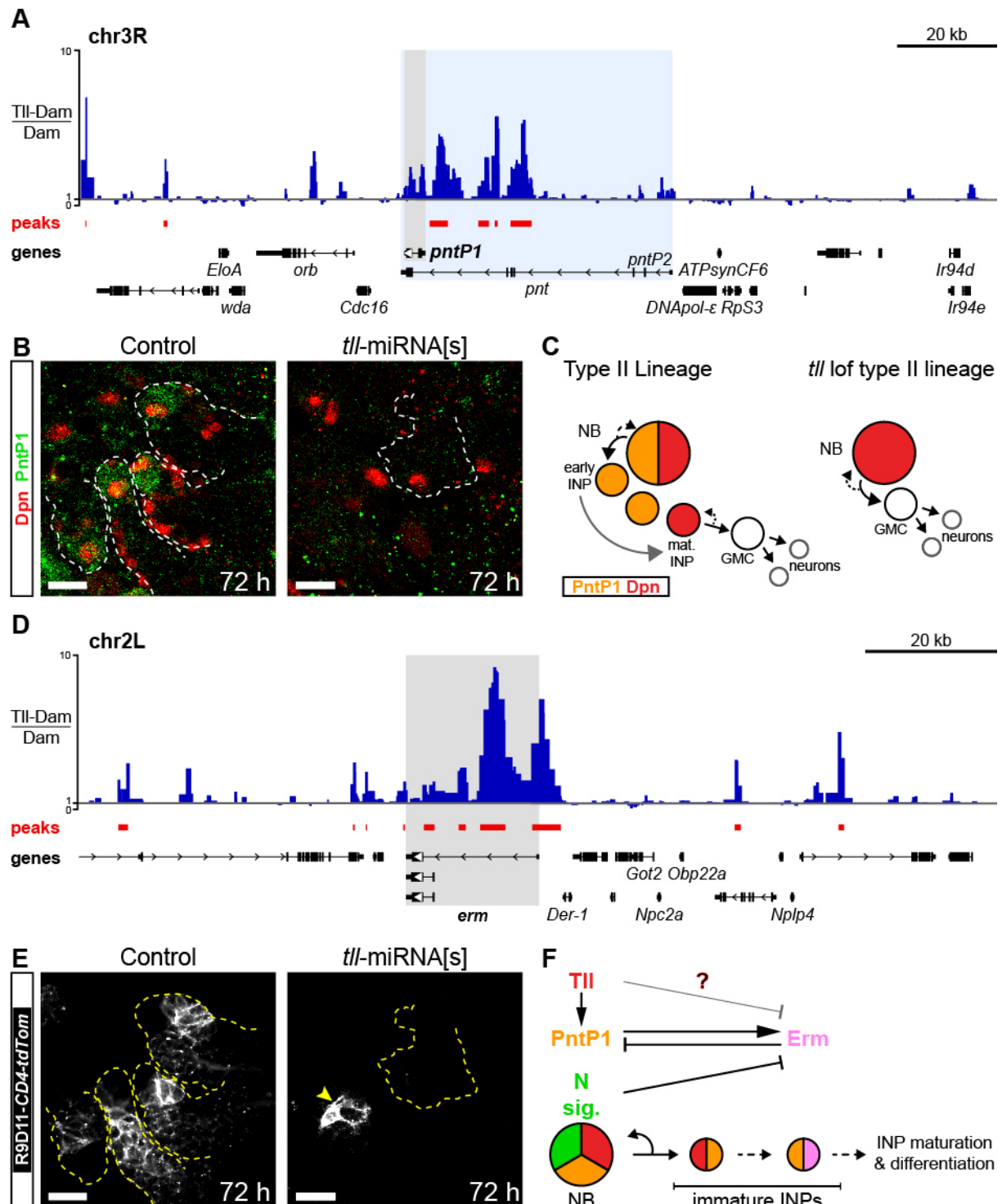


**Figure 3.7: Tll binds to genes required for INP specification**

(A) Tll binding at the *pnt* locus is enriched at the shorter *pntP1* isoform (grey), which is expressed in type II neuroblasts. The longer isoform *pntP2* (blue) is not expressed in type II lineages and does not have significant Tll binding near its promoter.

(B) PntP1 (green) expression in type II neuroblasts ( $Dpn^+$ , red) is lost when *tll* is knocked down. Type II lineages were identified using *pntP1>act-GAL4* driving *UAS-GFP* (white dotted lines).

(C) PntP1 (orange) expression in type II neuroblasts ( $Dpn^+$ , red) and immature INPs is lost in the absence of *tll*.

(Figure legend continues on next page)

(D) Tll binds across the *erm* locus (grey), with binding enriched at the 5' region of the gene body.  
 (E) Expression of the *erm* reporter R9D11-*CD4-tdTomato* (white) in INPs is lost when *tll* is knocked down. Type II lineages were identified using *pntP1>act-GAL4* driving UAS-*GFP* (white dotted lines).  
 (F) PntP1 promotes INP maturation by activating *erm* expression, which in turn represses *pntP1*. Notch signalling represses *erm* to maintain type II neuroblast fate. Tll is required for neuroblast fate and PntP1 expression, but the regulatory relationship between Tll and *erm* is uncertain.  
 Brains were dissected 72 hours ALH.  $n = 10$  brain lobes for Control and *tll*-miRNA[s]. Single section confocal images. Scale bars represent 15  $\mu$ m.

Analysis of the TaDa peaks showed Tll binding across the *erm* locus, with enrichment at the 5' region of all isoforms, suggesting that Tll could regulate *erm* expression directly (Fig. 3.7D). Type II lineages that lack *tll* do not express PntP1 nor do they express *erm* (Fig. 3.7B and Fig. 3.7E) and so Tll could be involved in this regulatory network. Due to the overlap in expression of Tll and PntP1 in type II neuroblasts, Tll likely regulates the expression of *pntP1* in a positive manner. Determining the regulatory relationship between Tll and *erm* is difficult due to the switch in lineage type. It is possible that Tll represses *erm* expression in type II neuroblasts as, unlike PntP1 and Erm, Tll and Erm are not expressed in the same cell type during lineage progression. However, the loss of *erm* in *tll* lof type II lineages could be explained due to the loss of PntP1 (which activates *erm* (Xie et al., 2016)) and the persistence of Notch signalling (which represses *erm* (Li et al., 2016)). This suggests that Tll acts as an upstream factor that is necessary for initiating the regulatory network between PntP1, Erm and Notch signalling (Fig. 3.7F).

Tll binding is also observed at *buttonhead* (*btd*) and *Sp1* loci (Fig. 3.8A). The expression of these genes is enriched in type II neuroblasts compared to other lineages (Carney et al., 2012). *btd* and *Sp1* act redundantly to specify type II neuroblast fate in the embryo (Álvarez and Díaz-Benjumea, 2018) and, later in development, *btd* is also required for INP fate acquisition. Tll binding at these genes suggests that these genes may act downstream of Tll both during the early stages of type II fate specification and in mature type II lineages.

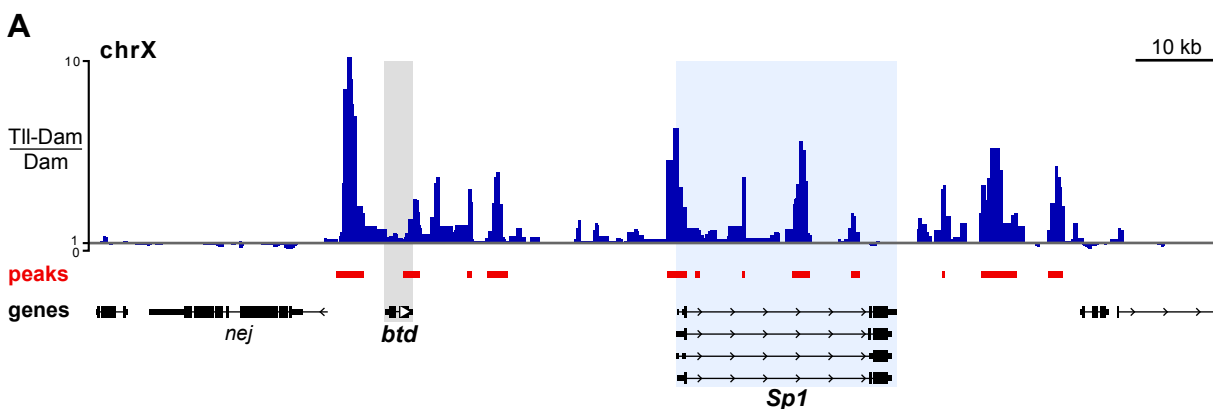


**Figure 3.8: Tll binds to *btd* and *Sp1***

(A) Tll binds at the *btd* (grey) and *Sp1* (blue) loci. *btd* and *Sp1* are required for type II neuroblast fate specification in the embryo (Álvarez and Díaz-Benjumea, 2018).

### 3.2.4 Tll binds to canonical NSC genes

In addition to binding to genes that are regulated in a type II-specific manner, Tll binding was also observed at pan-neuroblast genes. The bHLH-O Hes-like transcription factor *deadpan* (*dpn*) is expressed in all neuroblasts (as well as mature INPs) and promotes the self-renewal capacity of progenitors (San-Juán and Baonza, 2011; Wallace et al., 2000; Zacharioudaki et al., 2012; Zhu et al., 2012). Ectopic expression of Dpn is sufficient to produce large tumours that consist of neuroblasts (San-Juán and Baonza, 2011; Wallace et al., 2000; Zhu et al., 2012). Tll binding is observed upstream of the TSS of *dpn* and also within an intron of *dpn*, suggesting that this region could contain regulatory elements.

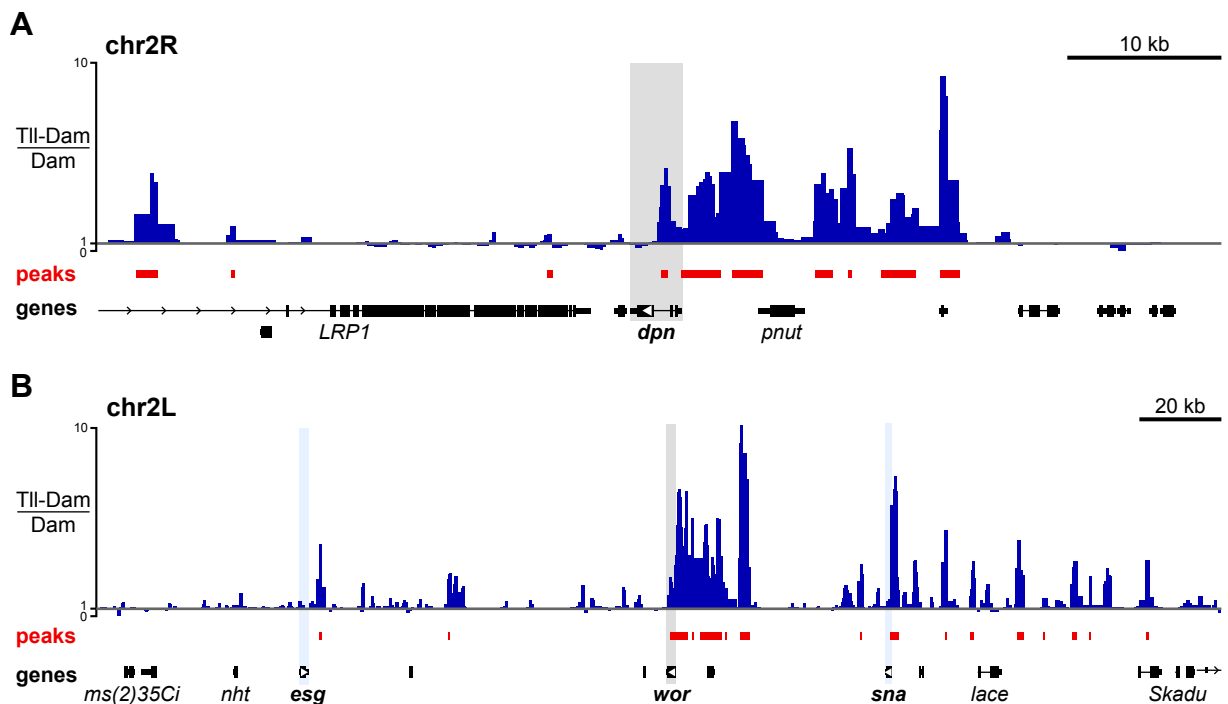


**Figure 3.9: Tll binds to canonical NSC genes**

(A) Tll binds upstream of *dpn* (grey), a bHLH-O transcription factor that promotes the self-renewal of neuroblasts.

(B) Tll binds to a large region upstream of *wor* (grey), a Snail family transcription factor that prevents premature differentiation of neuroblasts. The other Snail family members, *esg* and *sna* (blue), are found in the same genomic region as *wor*. Tll does not bind to sequences upstream of *esg*, but does bind near *sna*.

The Snail family zinc finger transcription factors *worniu* (*wor*), *escargot* (*esg*) and *snail* (*sna*) are required in embryogenesis to promote neuroblast delamination (Ashraf et al., 1999). However, *wor* is the only member that remains expressed in neuroblasts throughout development (Ashraf et al., 2004) and is required to promote cell-cycle progression and maintain the stem cell state of neuroblasts (Lai et al., 2012). Many Tll peaks are found immediately upstream of *wor*, suggesting that Tll could promote the expression of *wor* in type II neuroblasts.

Therefore, it seems likely that Tll regulates other transcription factors that positively regulate general properties of NSC fate, such as self-renewal, active cell cycle progression, and inhibition of differentiation. This provides a more complex view of Tll as a regulator of NSC fate. Studies in mammalian NSCs have suggested that TLX regulates cell cycle factors directly (Li et al., 2008; Zhang et al., 2008), but cell cycle stalling alone does not necessarily induce neural differentiation from NSCs. Overall, Tll binds to many genes that must be coordinated to maintain type II neuroblast fate during development.

### **3.3 Tll binds to a subset of TLX orthologues**

*Drosophila* Tll and mammalian TLX are highly conserved genes; their amino acid sequences show a high degree of similarity, they are regulated by conserved cofactors, and they can bind to the same DNA consensus sequence. One of the aims of performing Tll TaDa in *Drosophila* type II neuroblasts was to identify conserved target genes that are also regulated by vertebrate TLX. I identified 2945 Tll targets using TaDa and validated a small number of these in type II neuroblast lineages.

To determine if Tll bound any of the previously identified TLX targets, I compiled a list of the known mouse TLX target genes and determined the orthologous *Drosophila* genes. I used DIOPT (*Drosophila* RNAi Screening Center Integrative Ortholog Prediction Tool) (Hu et al., 2011) to predict orthologous gene pairs, which does so by comparing sixteen published databases (updated from the nine reported in Hu et al., 2011). A ‘DIOPT score’ (the number of databases out of sixteen that identify the match) and a ‘DIOPT rank’ (based on the DIOPT score and if the orthologue prediction occurs both ways) are generated for each pair prediction, which provides a simple way to filter potential orthologues. The full list of TLX target genes and their *Drosophila* orthologues is provided as **Table 3.2**. I compared the *Drosophila* orthologue list with the Tll TaDa gene list (**Appendix 2**) and found that Tll bound to six of the ten TLX target genes orthologues in type II neuroblasts (**Table 3.2**). Most notable was the binding of TLX to *ASCL1* (Elmi et al., 2010), which is orthologous to genes of the AS-C (*ac*, *sc*, *l’sc* and *ase*). As shown above, Tll binding was observed at *l’sc* and *ase* in type II neuroblasts. Interestingly, TLX has been reported to show the opposite regulatory relationship with *ASCL1* (TLX activates *ASCL1* expression in rat adult hippocampal-derived progenitors (Elmi et al., 2010)) compared to Tll and *ase* (Tll represses *ase* to maintain type II neuroblast fate). However, Tll could activate *l’sc* expression and *l’sc* shows the highest conservation with *ASCL1* of the genes of the AS-C (**Table 3.2**). This strongly suggests that the regulation of proneural genes is a conserved function of Tll/TLX from flies to mammals.

Intriguingly, TII binding was not observed at the cell cycle regulators (*Tctp/p21* and *Pten*) (Table 3.2). This was surprising because the regulation by TLX has been shown in multiple cell types and these orthologues showed high conservation between mice and flies (the orthologues had DIOPT scores of 13 or 16) (Sun et al., 2010; Sun et al., 2007; Yokoyama et al., 2008; Zhang et al., 2006). The other TLX targets that did not show TII binding were the orthologues of *Sirt1* and *VEGF* (Table 3.2). However, TLX regulation of *Sirt1* and *VEGF* was determined in HEK293 (a kidney-derived cell line) and in neuroblastoma cell lines under hypoxic stress, respectively, suggesting that these regulatory relationships may not occur during development (Iwahara et al., 2009; Zeng et al., 2012).

| <b>TLX target</b> | <b>Activated or Repressed</b> | <b>Drosophila orthologue</b> | <b>DIOPT score</b> | <b>DIOPT rank</b> | <b>TII binding?</b> |
|-------------------|-------------------------------|------------------------------|--------------------|-------------------|---------------------|
| <i>ASCL1</i>      | <i>activated</i>              | <i>ac</i>                    | 7                  | moderate          | n                   |
|                   |                               | <i>sc</i>                    | 6                  | moderate          | n                   |
|                   |                               | <i>l'sc</i>                  | 8                  | high              | y                   |
|                   |                               | <i>ase</i>                   | 5                  | moderate          | y                   |
| <i>MMP-2</i>      | <i>activated</i>              | <i>mmp2</i>                  | 3                  | moderate          | y                   |
|                   |                               | <i>mmp1</i>                  | 2                  | low               | n                   |
| <i>Oct-4</i>      | <i>repressed</i>              | <i>vvl</i>                   | 3                  | moderate          | y                   |
|                   |                               | <i>nub</i>                   | 2                  | low               | y                   |
|                   |                               | <i>pdm2</i>                  | 2                  | low               | y                   |
| <i>p21</i>        | <i>repressed</i>              | <i>Tctp</i>                  | 13                 | high              | n                   |
| <i>Pax2</i>       | <i>repressed</i>              | <i>sv</i>                    | 6                  | moderate          | y                   |
|                   |                               | <i>poxn</i>                  | 2                  | low               | y                   |
| <i>Pou5f1</i>     | <i>activated</i>              | <i>vvl</i>                   | 3                  | moderate          | y                   |
|                   |                               | <i>nub</i>                   | 2                  | low               | y                   |
|                   |                               | <i>pdm2</i>                  | 2                  | low               | y                   |
| <i>PTEN</i>       | <i>repressed</i>              | <i>pten</i>                  | 13                 | high              | n                   |
| <i>Sirt1</i>      | <i>activated</i>              | <i>sirt1</i>                 | 10                 | high              | n                   |
|                   |                               | <i>sirt2</i>                 | 2                  | low               | n                   |
| <i>VEGF</i>       | <i>activated</i>              | <i>pvf1</i>                  | 2                  | low               | n                   |
| <i>Wnt7a</i>      | <i>activated</i>              | <i>wnt2</i>                  | 12                 | moderate          | y                   |
|                   |                               | <i>wnt10</i>                 | 3                  | low               | n                   |
|                   |                               | <i>wnt4</i>                  | 2                  | low               | y                   |
|                   |                               | <i>wnt5</i>                  | 2                  | low               | n                   |
|                   |                               | <i>wg</i>                    | 2                  | low               | y                   |
|                   |                               | <i>wnt6</i>                  | 2                  | low               | n                   |

**Table 3.2: TII binds to a subset of TLX targets.** *Drosophila* orthologues of TLX target genes were determined using DIOPT (Hu et al., 2011). Orthologues that are bound by TII in type II neuroblasts are highlighted in blue. The DIOPT score indicates the number of databases that identify the orthologue pair (the maximum DIOPT score is 16). DIOPT ranks are high (DIOPT score  $\geq 2$  and best score both ways), moderate (DIOPT score  $\geq 2$  with similar scores both ways or DIOPT score  $\geq 4$ ), or low (all others).

Therefore, Tll binds to a subset of TLX target orthologues in type II neuroblasts (**Table 3.2**). The absence of Tll binding from *PTEN* (*phosphatase and tensin homolog*) and *p21* suggests that Tll may have a more prominent role in regulating NSCs fate rather than cell cycle progression in a developmental context. Identifying potential TLX target genes based on the Tll TaDa gene list will require functional validation of more Tll targets.

### **3.4 Chapter 3 discussion**

Overall, TaDa has revealed that Tll binds to many genes that are required for type II neuroblast fate (*ase*, *pros*, *pntP1*, *btd* and *Sp1*) as well as genes that promote lineage progression (such as *erm*). Tll also binds to transcription factors that are expressed in all cycling neuroblasts, such as *dpn* and *wor*, suggesting that Tll may also have a more general role in maintaining neuroblast identity and self-renewal.

Tll TaDa led to the discovery that the proneural gene *L'sc* is expressed in immature INPs. Immature INPs are a transient state within type II lineages, which can mean that genes expressed in the early stages of INP maturation are difficult to profile. TaDa showed that Tll binds at the *l'sc* locus, indicating that Tll could regulate *l'sc* expression in type II lineages. However, it has not been possible to determine the regulatory relationship between Tll and *l'sc* since the loss of Tll affects the progression of the entire lineage. Further experiments are required to assess if Tll promotes *l'sc* expression, as has been observed during early embryo development and in the optic lobe (Guillermin et al., 2015; Younossi-Hartenstein et al., 1997), and also to investigate if *l'sc* has a functional role in INP maturation.

#### **3.4.1 Tll binds to many genes throughout the genome**

TaDa showed that Tll binds widely across the genome with around 2,500 target genes. Tll binds to DNA through the recognition of the consensus sequence (AAGTCA) (Pankratz et al., 1992), which is found at a high frequency throughout the *Drosophila* genome (*data not shown*). Vertebrate TLX can also bind to the Tll binding sequence due to the high conservation of the DBDs (Monaghan et al., 1995; Yu et al., 1994). However, while the consensus binding sequence is required to recruit Tll to its target genes, the repressive activity of Tll/TLX is mediated by a number of cofactors. In vertebrates, TLX has a number of co-repressors but the only one for which a *Drosophila* counterpart is known so far is Atrophin (Zhang et al., 2002). *Drosophila* Atrophin and mammalian Atrophin-2 have highly similar molecular structures and both proteins interact with the LBD of Tll/TLX via their C-terminal domains (Wang et al., 2006; Zhi et al., 2015). Atrophin is expressed widely throughout the

*Drosophila* CNS (*data not shown*), which would allow it to act as a co-repressor for different transcriptional regulators, in particular Tll. It is also possible that there are unidentified cofactors of Tll (such as orthologues of the vertebrate cofactors BCL11A (CG9650, dCTIP), LSD1 (Su(var)3-3) or certain HDACs) that could bind to Tll and mediate its repressive function. The functional role of Atrophin and additional co-repressor candidates in type II neuroblasts should be evaluated (*e.g.* by RNAi or assessing mutants) as an initial step.

Due to the high number of Tll target genes, and the likely role of cofactors in coordinating gene expression control, it is difficult to determine the biological significance of Tll binding at every target gene identified in this TaDa experiment. One approach that may help to identify repressive targets would be to determine the binding sites of Tll co-repressors in type II neuroblasts. For example, profiling the binding sites of Atrophin with TaDa would provide complementary data that could be used to identify common binding sites. However, performing separate TaDa experiments would not show that two proteins bind at the same loci at the same time. Split DamID (SpDamID) is an adaptation of DamID that can be used to determine the recruitment of cofactors to common target genes (Hass et al., 2015). In SpDamID, the N-terminal D half is fused to one interacting partner (*e.g.* Tll) and the C-terminal AM half is fused to the other (*e.g.* Atrophin). As a result, the Dam protein is reconstituted only when the two interacting partners come together and so GATC fragment methylation occurs at shared target genes. In this way, genes repressed by Tll-Atrophin complexes could be determined *in vivo*, and a similar approach could be used to characterise other potential Tll cofactors.

### **3.4.2 Implications for vertebrate TLX**

Tll TaDa performed here has provided the first genome wide binding data for Tll/TLX in any species. In addition, the binding data was generated *in vivo* and in a cell-type-specific manner. The binding of Tll at AS-C genes was of particular interest for studies of TLX, as TLX has been shown to bind the *ASCLI* promoter in adult rat hippocampus-derived progenitors (Elmi et al., 2010). Tll bound to two members of the AS-C – *ase* and *l'sc* – and likely has opposite effects on the transcription of these genes, which highlights the complex regulatory roles of Tll in the nervous system.

Comparing the known TLX targets with the Tll TaDa gene list showed that Tll binds to a subset of TLX targets. However, generating binding data for Tll provides an opportunity to determine new transcriptional targets of TLX. A number of studies have assessed gene

expression changes upon the manipulation of TLX (through overexpression or loss of function) in NSCs using RNA sequencing. It would be interesting to perform a more detailed comparison of the putative TLX targets identified in those studies and the *Drosophila* Tll targets identified by TaDa here (Liu et al., 2010; Qu et al., 2010; Zhang et al., 2008). In addition, the Brand Lab has recently published Mammalian Targeted DamID (MaTaDa), which can be used to profile transcription factors in cells in culture (Cheetham et al., 2018), and this system is being developed for *in vivo* profiling of DNA binding proteins (van den Aamele et al., in preparation). It would be interesting to perform *in vivo* TaDa with mouse TLX during brain development and compare the binding targets with the Tll TaDa gene list from *Drosophila* type II neuroblasts. Furthermore, MaTaDa could be used to profile human TLX binding in glioblastoma stem cells (GSCs) to identify if the transcriptional targets identified during development are conserved in cancer. As such, Tll TaDa has provided an insight into the role of Tll in type II neuroblasts and there are many avenues that could extend this knowledge to NSCs in other species.

## Chapter 4

### TII/TLX initiates tumourigenesis from intermediate neural progenitors

TLX promotes the self-renewal and proliferation of neural stem cells (NSCs) during development and into adulthood (Li et al., 2012; Li et al., 2008; Liu et al., 2008; Monaghan et al., 1995; Monaghan et al., 1997; Obernier et al., 2011). High TLX expression has also been identified in human brain tumours, in particular aggressive glioblastoma and neuroblastoma tumours, and TLX expression correlates with poor patient survival (Chavali et al., 2014; Park et al., 2010; Zou et al., 2012). Intriguingly, a subset of glioblastoma samples showed an increase in the copy number of TLX and studies in mice have demonstrated that the number of NSCs correlates with TLX copy number (Liu et al., 2010).

The life expectancy of patients with aggressive brain tumours has not improved since the 1980s (Bondy et al., 2008). One reason for this is a population of NSC-like cells, known as cancer stem cells, that are resistant to treatment and are capable of reinitiating tumours following therapy (Reya et al., 2001; Singh et al., 2003). As such, being able to target cancer stem cells is essential for improving the survival from tumours affecting the central nervous system (CNS). It is likely that cancer stem cells hijack normal developmental programmes that are active in NSCs. Interestingly, TLX is expressed in glioblastoma stem cells (GSCs) and is required for their self-renewal capacity (Zhu et al., 2014). Removing TLX from GSCs inhibits tumourigenicity and prevents tumour reinitiation upon GSC transplantation (Cui et al., 2016; Zhu et al., 2014). As such, TLX is a promising therapeutic target for treating aggressive glioblastomas. It is important that we understand the molecular mechanisms through which TLX regulates stem cells in normal development and in tumourigenesis so that we can realise the therapeutic potential of TLX.

*In vivo* mouse models have shown that high levels of TLX expression in NSCs are sufficient to expand the NSC pool and can lead to glioblastoma when combined with additional mutations (Liu et al., 2010; Park et al., 2010; Zhu et al., 2014; Zou et al., 2012). Although this implicates NSC lineages as the origin of TLX-induced tumours, the cell type of origin within the lineage is not known. The cell of origin likely differs between different driver mutations and so identifying the cell type of origin of TLX-induced glioblastoma is an important step in developing targeted therapies. However, following cell fate and lineage progression of specific mammalian NSCs *in vivo* is technically challenging. The high conservation between

mammalian TLX and *Drosophila* Tll, combined with the extensive genetic tools available in *Drosophila*, means that the fly brain provides an excellent system in which to study the role of TLX/Tll in NSCs. I showed that Tll is expressed in type II neuroblasts to maintain their division mode. Type II neuroblasts show many parallels with mammalian NSCs and provide a simple system in which to study NSCs and tumour initiation.

#### 4.1 Assessing the tumourigenic capacity of Tll in *Drosophila* type II lineages

During development, Tll is expressed in the neuroblast of type II lineages but is downregulated concomitantly with differentiation. Tll is required for type II neuroblast fate and regulates key type II genes directly (Chapters 2 and 3). Given that high levels of TLX results in ectopic NSCs (Liu et al., 2010; Park et al., 2010; Zhu et al., 2014; Zou et al., 2012), the first step was to investigate if expressing high levels of Tll was sufficient to prevent differentiation of type II lineages and lead to tumourigenesis in *Drosophila*.

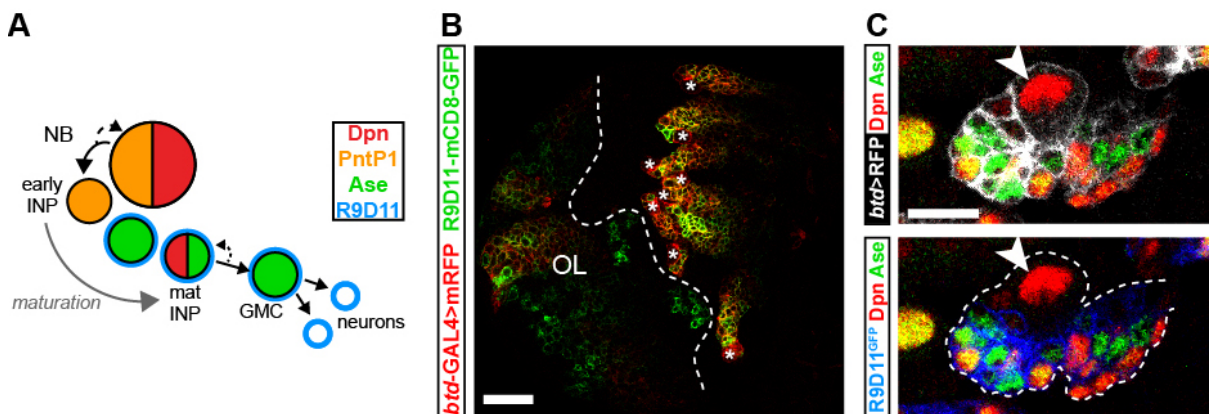


**Figure 4.1: Molecular markers for following type II lineage progression**

(A) Schematic showing markers for different cell fates in type II lineages. Type II neuroblasts are Dpn<sup>+</sup> (red), PntP1<sup>+</sup> (orange) and Ase<sup>-</sup> (green). R9D11 (blue) is a fragment of the 5' regulatory region of *erm*, which is expressed in maturing INPs (Pfeiffer et al., 2008; Weng et al., 2010). R9D11 can be used to drive the expression of GAL4 or fluorescent reporters.

(B) *btd-GAL4>myr-mRFP* (red) labels all type II lineages (asterisks, \*) at wandering third instar (Xie et al., 2014). Type II lineages express *R9D11-mCD8-GFP* (green). *btd-GAL4* and *R9D11-mCD8-GFP* are also both expressed in the optic lobe (OL).

(C) *btd-GAL4>myr-mRFP* (white, and indicated by dotted outline) is expressed in the neuroblast (arrowhead) of type II lineages and is maintained in INPs (Dpn<sup>+</sup> Ase<sup>+</sup>). *R9D11-mCD8-GFP* (blue) is absent from type II neuroblasts (arrowhead) but is expressed in INPs coincident with Ase expression. Single section confocal images. Scale bars represent 30  $\mu$ m in B; 10  $\mu$ m in C.

There are many molecular markers that can be used to follow cell fate transitions in type II lineages (Fig. 4.1A). Type II neuroblasts express the bHLH-O factor Deadpan (Dpn) and the Ets transcription factor PointedP1 (PntP1) but are negative for pro-neural factor Asence (Ase) (Bowman et al., 2008; Zhu et al., 2011). Their immediate progeny, immature intermediate neural progenitors (INPs), maintain PntP1 but not Dpn. During maturation, INPs turn off PntP1 as they begin to express the FezF transcription factor Earmuff (Erm) and later turn on

Ase (Janssens et al., 2014, Li et al., 2016). Mature INPs express Dpn and Ase and divide asymmetrically to generate Ase<sup>+</sup> GMCs, which in turn divide to produce neurons.

#### 4.1.1 High levels of Tll in type II lineages results in tumours

To express Tll at high levels throughout type II lineages, I used *buttonhead* (*btd*)-GAL4 to drive UAS-*tll*. *btd*-GAL4 is a GAL4 enhancer trap line inserted 753 bp upstream of the transcription start site of *btd* (Estella et al., 2003). *btd*-GAL4 is expressed in all type II neuroblasts (Fig. 4.1B) and expression is maintained throughout INP maturation (Xie et al., 2014) (Fig. 4.1C). Expressing UAS-*tll* with *btd*-GAL4 resulted in a large expansion in type II neuroblasts (Fig. 4.2A): control brain lobes always had 8 Dpn<sup>+</sup> Ase<sup>-</sup> type II neuroblasts ( $n = 8$ ) whereas Tll overexpression (Tll OE) brain lobes had at least 250 ( $n = 12$ ). These ectopic type II neuroblasts were generated at the expense of neurons (as assessed by Elav (Embryonic lethal abnormal vision) staining Fig. 4.2B). This shows that preventing the downregulation of Tll in type II lineages is sufficient to induce ectopic neuroblasts and tumourigenesis.

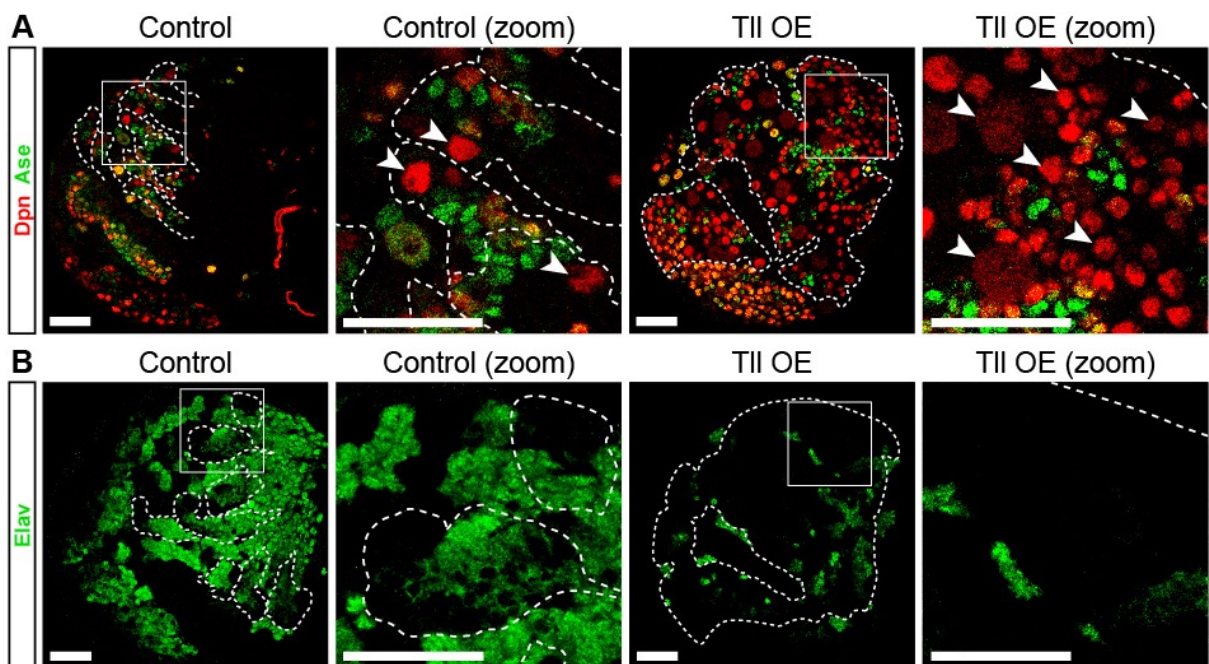


**Figure 4.2: High levels of Tll cause tumours in type II lineages**

(A) Overexpressing *tll* with *btd*-GAL4 (Tll OE) results in the expansion of type II neuroblasts (Dpn<sup>+</sup> (red) and Ase<sup>-</sup> (green)). Dotted white lines indicate *btd*-GAL4>*myr-RFP* expression in type II lineages. Arrowheads indicate type II neuroblasts.  $n = 8$  brain lobes for Control;  $n = 6$  brain lobes for Tll OE. (B) Tll OE with *btd*-GAL4 results in the loss of neurons (Elav, green). Dotted white lines indicate type II lineages identified by *btd*-GAL4>*myr-RFP*.  $n = 10$  brain lobes for Control and Tll OE. Single section confocal images. Scale bars represent 30  $\mu$ m.

#### 4.1.2 Tll can generate type II neuroblasts from INPs

It has been observed previously that the asymmetric division of neuroblasts is not affected by high levels of Tll; neuroblasts that expressed high levels of Tll exhibited normal cortical

localisation of aPKC, Pins, Brat, and Mira (Kurusu et al., 2009). This indicates that TII tumours do not arise from disruptions to the asymmetric division of type II neuroblasts and suggests that the tumour-initiating cell is not the type II neuroblast itself. As such, this implicates the dedifferentiation of a more committed cell type as the route to tumourigenesis.

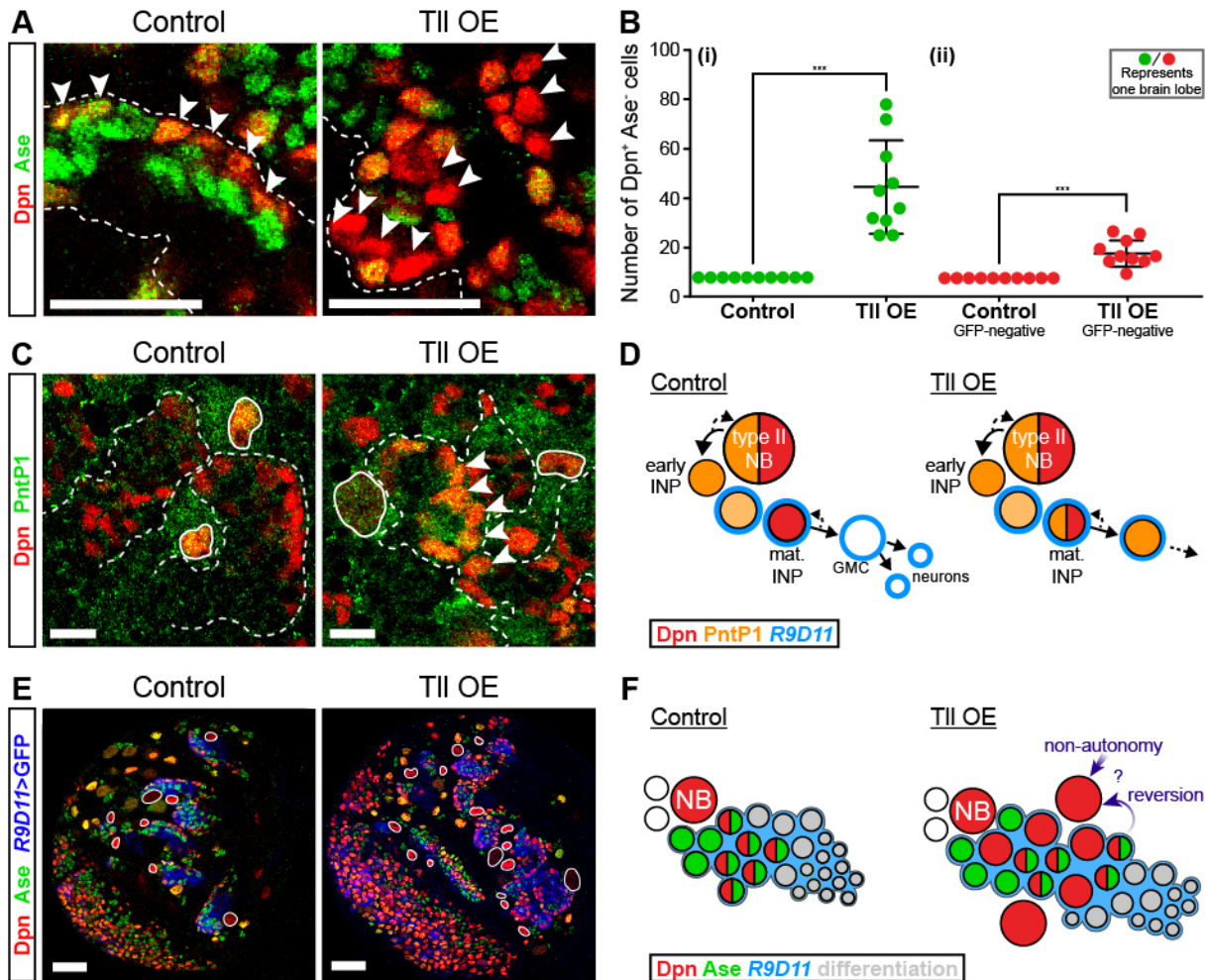


**Figure 4.3: TII is sufficient to induce type II neuroblast fate from INPs**

(A) In Control, all  $Dpn^+$  cells within  $R9D11-GAL4 > mCD8-GFP$  express Ase (arrowheads). TII OE in INPs results in  $Dpn^+$  cells that lack Ase (arrowheads). Dotted white lines indicate  $R9D11-GAL4 > mCD8-GFP$ .  $n = 10$  brain lobes for Control and TII OE.

(B) Quantification of the number of type II neuroblasts (i) Total number of  $Dpn^+ Ase^-$  cells; (ii) GFP-negative  $Dpn^+ Ase^-$  cells. Kolmogorov-Smirnov test \*\*\*,  $P < 0.001$  ( $P = 0.000091$ ).

(C) In Control lineages, PntP1 (green) is expressed in neuroblasts (solid white outlines) and immature INPs. TII OE results in  $Dpn^+$  INPs activating PntP1 (arrowheads in TII OE). Dotted white lines indicate  $R9D11-GAL4 > mCD8-GFP$ .  $n = 10$  brain lobes for Control and TII OE.

(D) Schematic showing the effect of TII OE in INPs (using  $R9D11-GAL4$ , blue) on PntP1 expression. In Control lineages, PntP1 (orange) and Dpn (red) overlap only in the neuroblast, but INPs maintain PntP1 expression in TII OE lineages.

(E) TII OE with  $R9D11-GAL4 > mCD8-GFP$  (blue) results in ectopic type II neuroblasts ( $Dpn^+ Ase^-$ , white outlines) outside of the GAL4 domain.  $n = 10$  brain lobes for Control and TII OE.

(F) Schematic showing the effect of expressing TII in INPs on type II lineages. Ectopic type II neuroblasts that do not express  $R9D11-GAL4$  could arise from INP reversion to neuroblast fate or from a cell non-autonomous effect.

Single section confocal images. Scale bars represent  $10 \mu m$  in A, C;  $30 \mu m$  in E.

To investigate if Tll is able to cause de-differentiation of INPs, I expressed UAS-*tll* in INPs and assessed the effect on lineage progression. To target UAS-*tll* to INPs, I used the R9D11 fragment to drive GAL4 expression. R9D11 is a regulatory region of *erm*, a gene that is expressed in maturing INPs but is absent from type II neuroblasts (See Fig. 4.1) (Pfeiffer et al., 2008; Weng et al., 2010). Expressing Tll in INPs resulted in ectopic type II neuroblasts (Fig. 4.3A); the total number of Dpn<sup>+</sup> Ase<sup>-</sup> cells increased from 8 (in control) to 44.5±5.97 (in Tll OE) per brain lobe (Fig. 4.3Bi). Furthermore, ectopic expression of Tll in INPs also resulted in the reinitiation of PntP1 expression in Dpn<sup>+</sup> INPs (Fig. 4.3C), whereas PntP1 is restricted to type II neuroblasts and Dpn<sup>-</sup> INPs in control lineages (Fig. 4.3D).

Although Tll was able to generate neuroblasts from INPs, the number of ectopic type II neuroblasts induced from INPs was much lower than that produced by expressing Tll throughout the lineage with *btd*-GAL4 (*btd*-GAL4 Tll OE >250 type II neuroblasts; R9D11-GAL4 Tll OE ~44.5 type II neuroblasts). However, upon closer analysis, I observed an important difference between the ectopic neuroblasts generated in each experiment. When UAS-*tll* was expressed throughout the lineage with *btd*-GAL4, all ectopic neuroblasts expressed *btd*-GAL4 (Fig. 4.2A). In contrast, I found that many of the ectopic type II neuroblasts that resulted from expressing UAS-*tll* in INPs were found outside of the GAL4 expression domain (*i.e.* they were negative for R9D11-GAL4>*mCD8-GFP*) (Fig. 4.3Bii). In control brain lobes, the eight type II neuroblasts were negative for R9D11-GAL4, but in Tll OE brains there was an average of 17.6±1.694 type II neuroblasts that did not express R9D11-GAL4 (Fig. 4.3E). To determine the origin of these R9D11-GAL4-negative type II neuroblasts in Tll OE brains, I used lineage tracing techniques to follow the effect of Tll on INPs.

## **4.2 Tll/TLX causes INPs to revert to type II neuroblast fate**

I found that expressing Tll in type II INPs resulted in ectopic type II neuroblasts. Tll caused R9D11-GAL4<sup>+</sup> INPs to acquire characteristics of type II neuroblasts (Dpn<sup>+</sup> INPs repressed Ase and expressed PntP1), indicating that INPs were de-differentiating to neuroblast fate. However, there was also a significant proportion of ectopic type II neuroblasts that did not express R9D11-GAL4 in Tll OE brains. I considered two explanations for the origin of R9D11-GAL4-negative type II neuroblasts: (1) Tll caused INPs to revert fully to neuroblast fate (which would include lack of expression of the INP marker R9D11) or (2) that these cells arose from a non-autonomous effect and never expressed R9D11-GAL4 (Fig. 4.3F).

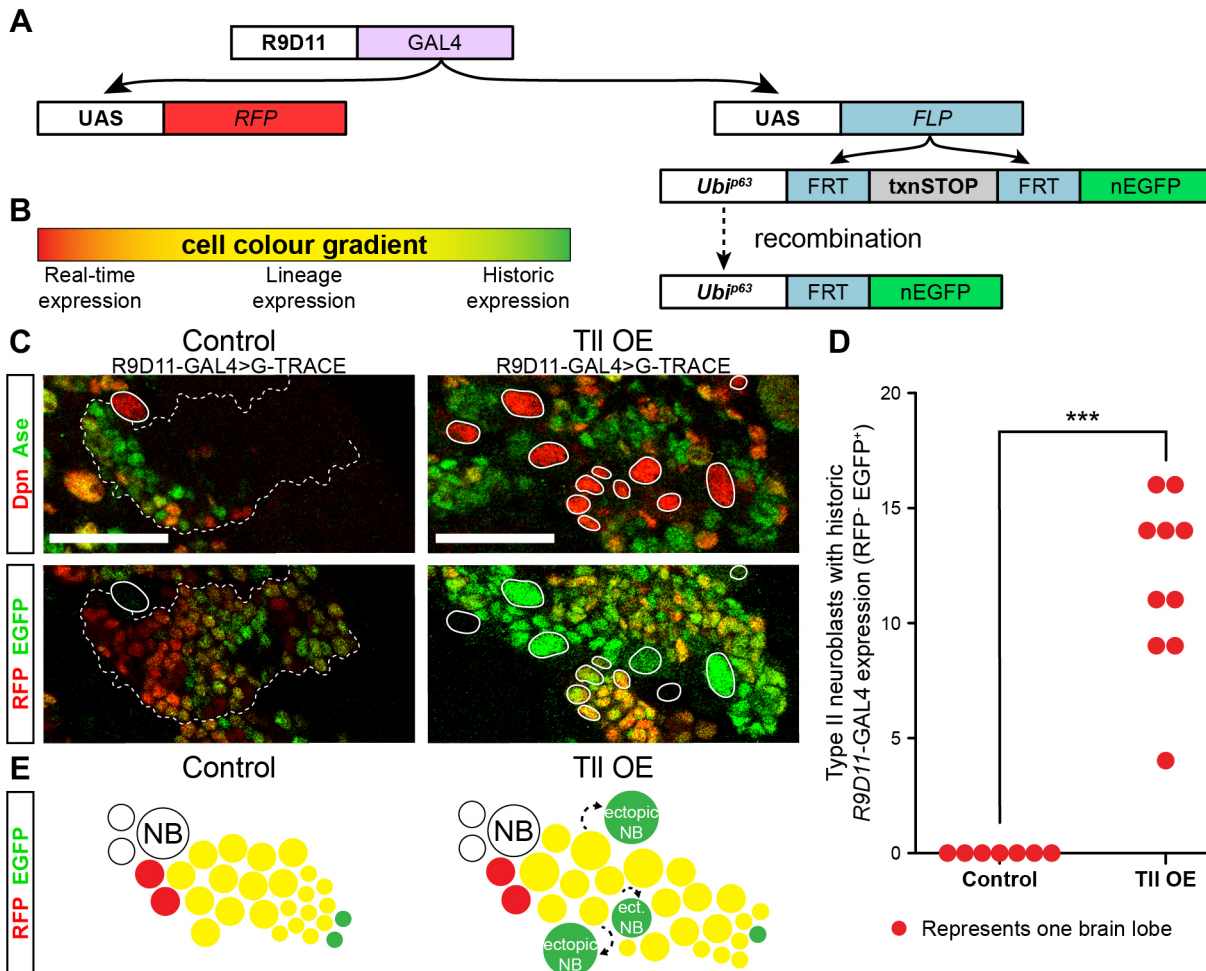


**Figure 4.4: G-TRACE reveals that INPs revert to type II neuroblast fate in response to Tll**

(A) Schematic showing the genetic components of the G-TRACE system.

(B) Schematic showing the cell colour of lineages when G-TRACE is expressed.

(C) In Control lineages, type II neuroblasts (Dpn<sup>+</sup> Ase<sup>-</sup>, solid outlines) are negative for both components of G-TRACE (bottom panels) and lineages show a transition from current (RFP) to historic (GFP) expression. In Tll OE brains, a subset of ectopic type II neuroblasts (Dpn<sup>+</sup> Ase<sup>-</sup>) express the historic (GFP) component of the G-TRACE only.  $n = 8$  brain lobes for Control;  $n = 10$  brain lobes for Tll OE.

(D) Quantification of type II neuroblasts expressing G-TRACE memory only. Kolmogorov-Smirnov test \*\*\*,  $P < 0.001$  ( $P = 0.000103$ ).  $n = 7$  brain lobes for Control;  $n = 10$  brain lobes for Tll OE.

(E) Schematic showing G-TRACE labelling of Control type II lineages compared to Tll OE. The neuroblast (NB) and early progeny do not express R9D11-GAL4 and so are not labelled.

Single section confocal sections. Scale bars represent 15  $\mu\text{m}$ .

#### 4.2.1 G-TRACE shows that Tll causes INPs to revert to neuroblasts

I investigated if Tll caused INPs to revert back to neuroblast fate and turn off R9D11-GAL4 expression as a consequence of this fate change. To do this required a GAL4 memory cassette. I used the GAL4 technique for real-time and clonal expression (G-TRACE) (Evans et al., 2009), which reports current and historic expression of any GAL4. When the G-TRACE cassette is expressed, GAL4 drives the expression of (1) UAS-*RFP* (real-time expression) and (2) UAS-*FLP*, which excises a transcriptional stop sequence to allow a *Ubi* promoter to drive EGFP expression (historic expression) (Fig. 4.4A). In other words, the current to historic

GAL4 expression is reported by an RFP-only (real-time), to RFP and EGFP co-expression (lineage), to EGFP-only (historic) transition (**Fig. 4.4B**).

When G-TRACE was expressed using R9D11-GAL4, the eight type II neuroblasts in control brain lobes were negative for both real-time and historic G-TRACE components because they had never expressed R9D11-GAL4 (**Fig. 4.4C**). Control type II lineages showed a transition from RFP to EGFP as differentiation progressed; INPs expressed the GAL4 in real-time GAL4 (RFP) and differentiated cells, such as neurons, showed historic expression (EGFP) (Control panels of **Fig. 4.4C**). However, type II lineages in Tll OE brains no longer showed a clear progression from RFP to EGFP expression; lineages consisted mostly of cells that expressed both components of the G-TRACE cassette (Tll OE panels of **Fig. 4.4C**). Importantly, there were type II neuroblasts that showed historic expression of R9D11-GAL4 but did not express it currently (**Fig. 4.4C-D**). In addition, many of these INP-derived type II neuroblasts had lineages associated with them that showed current R9D11-GAL4 expression, indicating that the ectopic neuroblasts were able to generate new INPs. Overall, these data show that expressing Tll in mature INPs reactivates type II neuroblast fate, which includes the inactivation of an INP-specific marker (R9D11-GAL4) (summarised in **Fig. 4.4E**).

#### **4.2.2 GAL4 immortalisation reveals tumourigenic capacity of Tll from INPs**

Expressing high levels of Tll resulted in INPs acquiring type II neuroblast characteristics (such as the repression of *Ase*). The G-TRACE cassette showed that the dedifferentiation of INPs includes the inactivation of R9D11-GAL4, which is active in INPs but is not expressed in type II neuroblasts (Weng et al., 2010). This indicates that, while Tll is able to induce type II neuroblast fate from INPs, the true tumourigenic capacity of Tll may be limited due to fluctuations in GAL4 level caused by cell fate changes.

To ensure that GAL4 expression remains constant in INPs, I combined R9D11-GAL4 with a “FLP-out” cassette to immortalise GAL4 expression (**Fig. 4.5A**). In this system, R9D11-GAL4 was used to drive the expression of UAS-*FLP*, which catalyses the excision of a transcriptional stop sequence from the “FLP-out” cassette (*act5C>FRT-txnSTOP-FRT>GAL4* (Ito et al., 1997)). Subsequently, *act5C-GAL4* drives the expression of transgenes under the control of UAS and the expression of GAL4 is no longer dependent on cell fate. Immortalised R9D11-GAL4 will be referred to as R9D11>*act-GAL4*. Using R9D11>*act-GAL4* to manipulate type II lineages will prevent changes in GAL4 expression as UAS-*tll* levels increase in INPs (**Fig. 4.5B**).

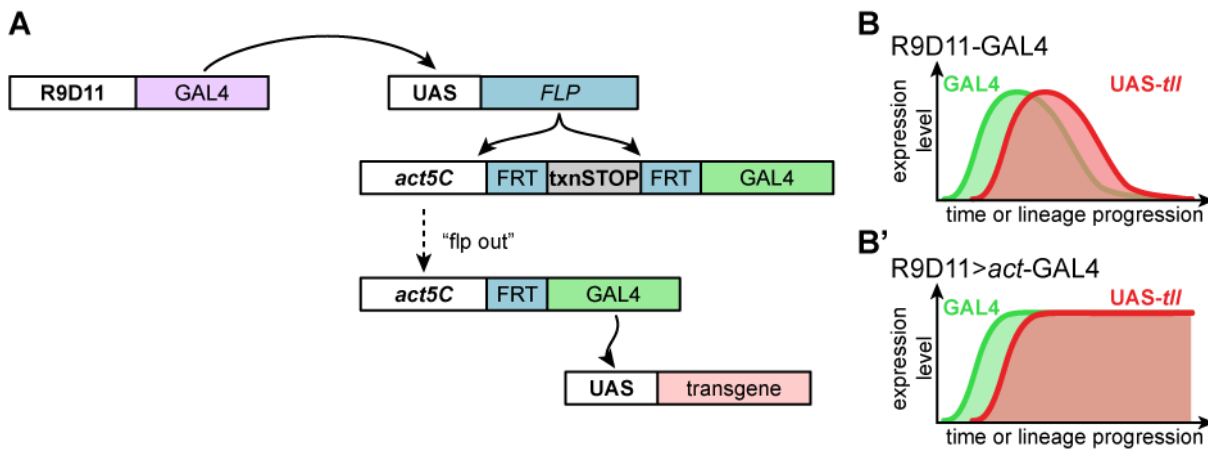


**Figure 4.5: R9D11>act-GAL4 is an immortalised INP driver**

(A) Schematic showing the genetic components of R9D11>act-GAL4, an immortalised INP GAL4. (B-B') Theoretical representation of GAL4 levels (green) and the effect on UAS-*tll* expression (red) with (B) R9D11-GAL4 or immortalised (B') R9D11>act-GAL4.

In control brain lobes, the eight type II neuroblasts ( $Dpn^+ Ase^-$ ) were negative for R9D11>act-GAL4 (Fig. 4.6A-B). However, expressing UAS-*tll* with R9D11>act-GAL4 resulted in a large expansion of type II neuroblasts; there were  $109 \pm 12.12$  type II neuroblasts per brain lobe ( $n = 10$  brain lobes) (Fig. 4.6A-B). In addition, Tll OE lineages exhibited a reduction in differentiated progeny such as ganglion mother cells (GMCs) (as assessed by Pros) (Fig. 4.6C) and neurons (as assessed by Elav) (Fig. 4.6D). As such, high levels of Tll in INPs induced type II neuroblast fate and inhibited neuronal differentiation (Fig. 4.6E). Furthermore, the number of type II neuroblasts resulting from R9D11>act-GAL4 driving UAS-*tll* ( $109 \pm 12.12$ ) was much higher than when UAS-*tll* was expressed by R9D11-GAL4 alone ( $44.5 \pm 5.97$ ). This provides supporting evidence that fluctuating GAL4 levels were restricting the ability of *tll* to induce type II neuroblast fate from INPs. Thus, ectopic expression of Tll is sufficient to repress the differentiation programme of INPs and causes reversion to type II neuroblast fate (Fig. 4.6F).

### 4.2.3 Non-autonomous contribution to tumorigenesis

Two independent genetic techniques (G-TRACE and R9D11>act-GAL4) showed that INPs respond to high levels of Tll directly and revert to type II neuroblast fate. However, both methods also revealed a small contribution of cell non-autonomy to the generation of ectopic type II neuroblasts. The original eight type II neuroblasts are not labelled using either technique, as was observed in control brain lobes. However, in Tll OE G-TRACE brain lobes, I observed a very small number of unlabelled (negative for RFP and EGFP) type II neuroblasts in addition to the endogenous eight ( $0.3 \pm 0.15$  extra G-TRACE-negative neuroblasts, *i.e.* 3 of 10 brain lobes contained 9 unlabelled neuroblasts in total). Similarly, in R9D11>act-GAL4 Tll OE brains there was a small number of additional unlabelled type II

neuroblasts ( $1.5 \pm 0.48$  extra GFP-negative type II neuroblasts per brain lobe, *i.e.* 7 of 10 brain lobes contained between 9 and 13 unlabelled type II neuroblasts in total). The origin of these non-INP-derived type IIs is unknown but suggests a role for a density or distance-dependent signalling molecule that specifies type II neuroblast fate. Although the contribution of non-autonomy compared to direct INP reversion is very low, this observation has implications for the potential of Tll/TLX to initiate tumourigenesis in a non-autonomous manner.

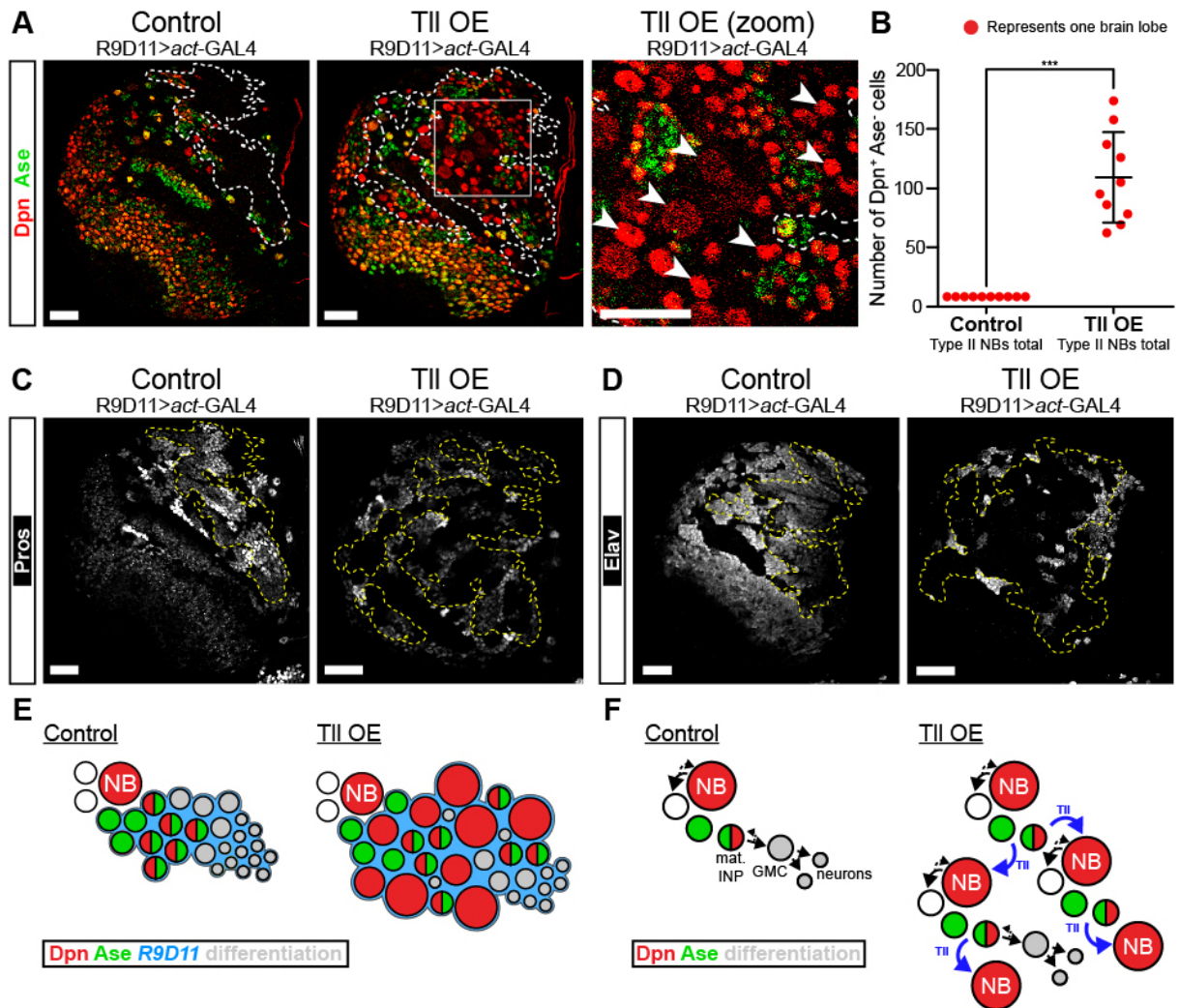


**Figure 4.6: Immortalised INP GAL4 results in large Tll OE tumours**

(A) Tll OE with R9D11>act-GAL4 results in a large expansion of type II neuroblasts, as identified by Dpn<sup>+</sup> (red) and Ase<sup>-</sup> (green). Arrowheads in Tll OE (zoom) highlight ectopic type II neuroblasts. Dotted white lines indicate R9D11>act-GAL4 expression.  $n = 10$  brain lobes for Control and Tll OE.

(B) Quantification of the number of type II (Dpn<sup>+</sup> Ase<sup>-</sup>) neuroblasts in Control or Tll OE brains. (i) Total number of type II neuroblasts ( $P=0.000091$ ); (ii) type II neuroblasts within R9D11>act-GAL4 expression domain ( $P=0.000091$ ). Kolmogorov-Smirnov test \*\*\*,  $P<0.001$ .  $n = 10$  brain lobes for Control and Tll OE.

(C) Using R9D11>act-GAL4 to express high levels of Tll results in the loss of differentiating progeny compared to Control, as assessed by Pros staining (white).  $n = 10$  brain lobes for Control and Tll OE.

(D) High levels of Tll reduces the production of neurons, as assessed by staining for Elav (white).  $n = 13$  brain lobes for Control;  $n = 12$  brain lobes for Tll OE.

(E) Schematic showing the effect on type II lineages of expressing Tll with R9D11>act-GAL4.

(F) A model for the effect of expressing Tll in INPs. Tll prevents differentiation and causes INPs to revert to type II neuroblast fate, thereby initiating tumour formation.

Single section confocal images. Scale bars represent 30  $\mu\text{m}$ .

#### 4.2.4 Human TLX can induce tumours from *Drosophila* INPs

*Drosophila* Tll and human TLX are highly conserved genes: (1) their amino acid sequences are extremely similar (81 % identity in the DBD and 40 % in the LBD) (Jackson et al., 1998), (2) they can bind to the same consensus DNA motif (Yu et al., 1994), and (3) they can be regulated by conserved cofactors (such as Atrophin (Zhi et al., 2015)). TLX is expressed in NSCs and intermediate progenitors in the adult mouse brain, which is highly comparable to the pattern of Tll expression I found in type II lineages (compare **Figs. 4.7A-B**). Expressing high levels of TLX in the adult mouse brain causes the expansion of NSCs (Liu et al., 2010; Park et al., 2010; Zhu et al., 2014; Zou et al., 2012), which mirrors the effect of overexpressing Tll in type II lineages. I investigated if human TLX could also induce dedifferentiation and tumourigenesis from *Drosophila* INPs, given the high molecular conservation of TLX and Tll.

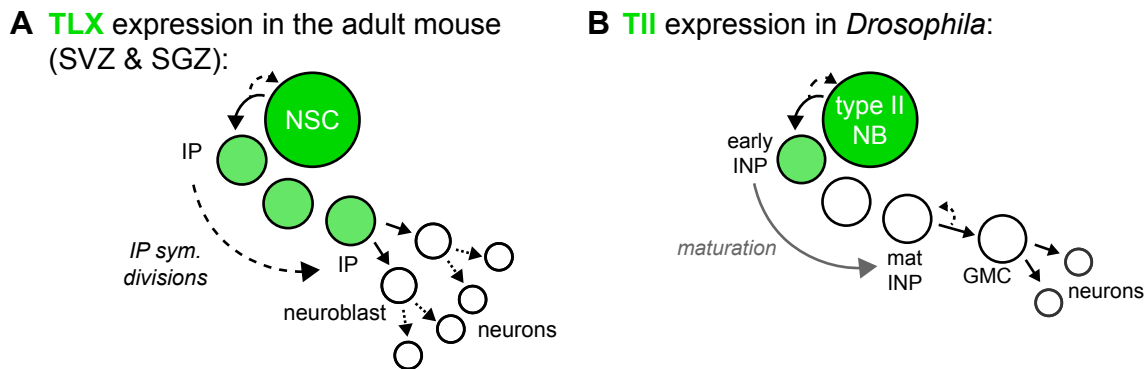


**Figure 4.7: Tll and TLX show comparable expression in NSC lineages**

(A) TLX is expressed in NSCs and intermediate progenitors (IP) in the adult mouse brain (based on previously published data (Li et al., 2012; Liu et al., 2008)).

(B) *Drosophila* Tll is expressed in type II neuroblasts and early immature INPs (this study).

Expressing UAS-*TLX* in *Drosophila* INPs with R9D11-GAL4 resulted in a large expansion of type II neuroblasts; TLX OE resulted in the generation of many ectopic neuroblasts ( $Dpn^+$ ) that did not express *Ase* (**Fig. 4.8A**) but were positive for  $PntP1^+$  (**Fig. 4.8B**). In addition, a large number of these ectopic type II neuroblasts were found outside of the R9D11-GAL4 expression domain (**Fig. 4.8A' and B'**). To determine the lineage relationship between INPs and the ectopic type II neuroblasts, I expressed TLX in combination with the G-TRACE cassette. This showed that many of the ectopic  $Dpn^+ Ase^-$  cells induced by expressing TLX in INPs were positive for historic R9D11-GAL4 expression but no longer expressed it currently (**Figs. 4.9A-B**). These results showed that Tll and TLX are conserved in tumourigenic capacity and likely act through conserved molecular mechanisms.

I have shown that Tll is required for type II neuroblast and lineage fate; in the absence of Tll, type II neuroblasts switch to type I identity and INPs are no longer generated. During development, Tll expression is downregulated concomitant with differentiation. However, tumours arise if Tll is expressed at high levels within type II lineages. I found that this is due to the reversion of INPs to neuroblast fate and the inhibition of differentiation. Furthermore, the ectopic expression of TLX causes type II INPs to revert to neuroblast fate, resulting in tumours. However, one notable difference is that the tumourigenic capacity of TLX appears to be more severe than Tll as TLX generates much larger tumours from INPs. Overall, this indicates that INPs are the tumour cell of origin for Tll/TLX-induced tumours in type II neuroblast lineages. This finding has implications for the cell of origin of TLX-induced tumours from neural lineages and suggests that mammalian intermediate progenitors could show a similar fate transition in response to high levels of TLX, leading to tumour initiation.

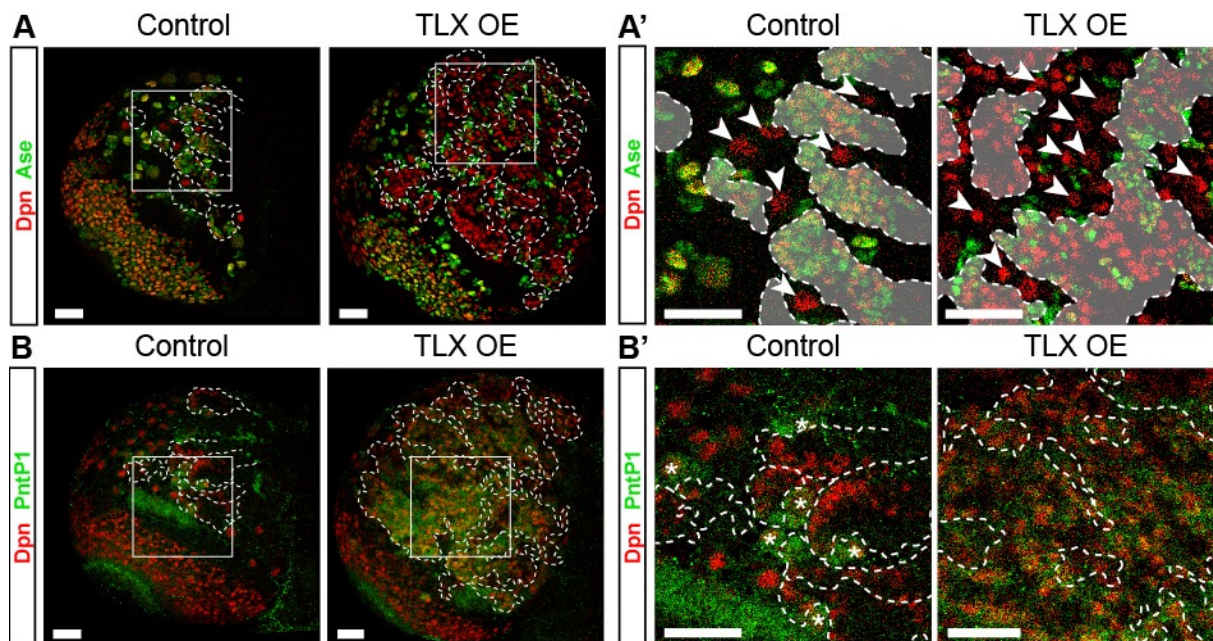


**Figure 4.8: Human TLX initiates tumourigenesis from type II INPs**

(A) TLX overexpression (TLX OE) in INPs with R9D11-GAL4 results in large tumours consisting of neuroblasts that are Dpn<sup>+</sup> (red) and Ase<sup>-</sup> (green). Dotted white lines indicate R9D11-GAL4>mCD8-GFP. *n* = 10 brain lobes for Control and TLX OE.

(A') Many ectopic type II neuroblasts in TLX OE brains do not express R9D11-GAL4 (arrowheads). R9D11-GAL4>mCD8-GFP expression is represented by dotted white lines and white shading. Images are magnifications of the boxed regions highlighted in (A).

(B) Neuroblast tumours generated by TLX OE also express PntP1<sup>+</sup> (green) in Dpn<sup>+</sup> cells. Dotted white lines indicate R9D11-GAL4>mCD8-GFP. *n* = 10 brain lobes for Control and TLX OE.

(B') Type II lineages express PntP1 (green) in the neuroblast (Dpn<sup>+</sup>, asterisk). Ectopic neuroblasts generated by TLX OE express PntP1. Dotted white lines indicate R9D11-GAL4>mCD8-GFP. Images are magnifications of the boxed regions highlighted in (B).

Single section confocal images. Scale bars represent 30  $\mu$ m.

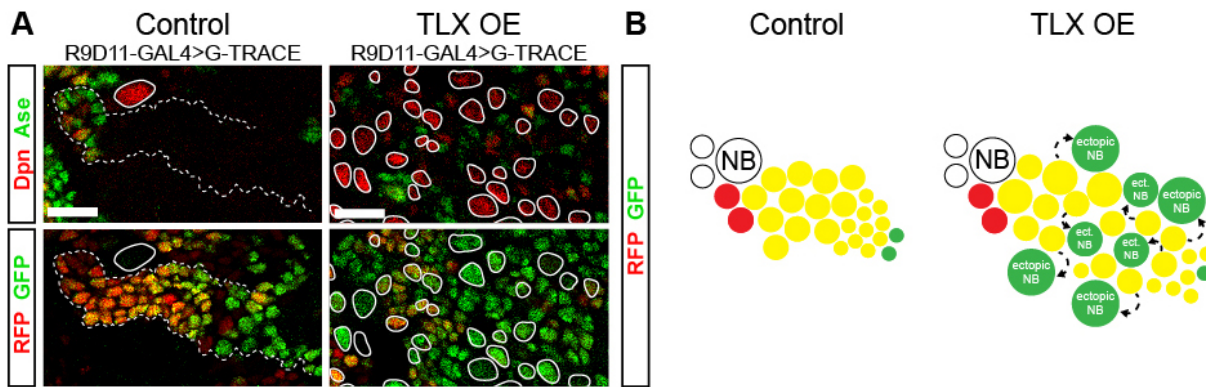


**Figure 4.9: Type II INPs revert to neuroblast fate in response to human TLX**

(A) G-TRACE reveals TLX causes INP reversion to neuroblast fate. In Control lineages, type II neuroblasts ( $Dpn^+ Ase^-$ , solid outline) are negative for both components of G-TRACE (bottom panel) and lineages show transition from current (RFP) to historic (GFP) expression. In TLX OE brains, many ectopic type II neuroblasts (solid outlines) express the historic (GFP) component of the G-TRACE only.  $n = 10$  brain lobes for Control and TLX OE.

(B) Schematic depicting G-TRACE expression in Control type II lineages compared to TLX OE. Single section confocal images. Scale bars represent  $15 \mu m$ .

### **4.3 Assessing the tumourigenic capacity of Tll in other *Drosophila* neural progenitors**

The majority of the neural progenitors in the *Drosophila* larval brain are type I neuroblasts (Fig. 4.10A). Type I neuroblasts divide in the same manner as type II INPs and express many of the same molecular markers; both progenitors express Dpn and Ase and segregate Pros into their daughter cells (GMCs) upon asymmetric division (Fig. 4.10B). Expressing high levels of Tll/TLX in type II INPs was sufficient to induce type II neuroblast fate, and subsequent tumourigenesis. Given the similarities between type II INPs and type I neuroblasts, I tested if Tll/TLX could initiate tumours from type I neuroblasts in a similar manner.

#### **4.3.1 Tll and TLX induce type II neuroblast fate from type I neuroblasts**

As an initial step, I expressed UAS-*tll* in neuroblasts throughout the CNS. This resulted in ectopic neuroblasts that persisted into adulthood at the expense of neuronal progeny (Fig. 4.10C). Tll OE adult flies died within one day of eclosion, demonstrating that expressing Tll in larval neuroblasts resulted in lethal brain tumours. Analysis of Tll tumours during larval stages showed that these tumours affected neuroblasts in the majority of the CNS (as assessed by Dpn staining, Fig. 4.10D). Of particular interest was the presence of large  $Dpn^+$  tumours in the ventral nerve cord (VNC) as this region consists entirely of type I neuroblasts. To investigate Tll induced tumours from type I VNC neuroblasts by inducing type II neuroblast fate, in a similar manner to tumour initiation from INPs, I assessed Ase expression. Ase is repressed in type II neuroblasts (Bowman et al., 2008) and I found that the ectopic neuroblasts in Tll OE VNCs were negative for Ase almost entirely (Fig. 4.11A). Type II neuroblasts also lack Pros expression (Bayraktar et al., 2010) and Tll-induced tumours exhibited

downregulation of Pros (**Fig. 4.11A**). This indicated that Tll induced type II neuroblast tumours from type I neuroblast through a similar mechanism as from type II INPs, suggesting that Tll is an instructive signal for type II neuroblast fate.

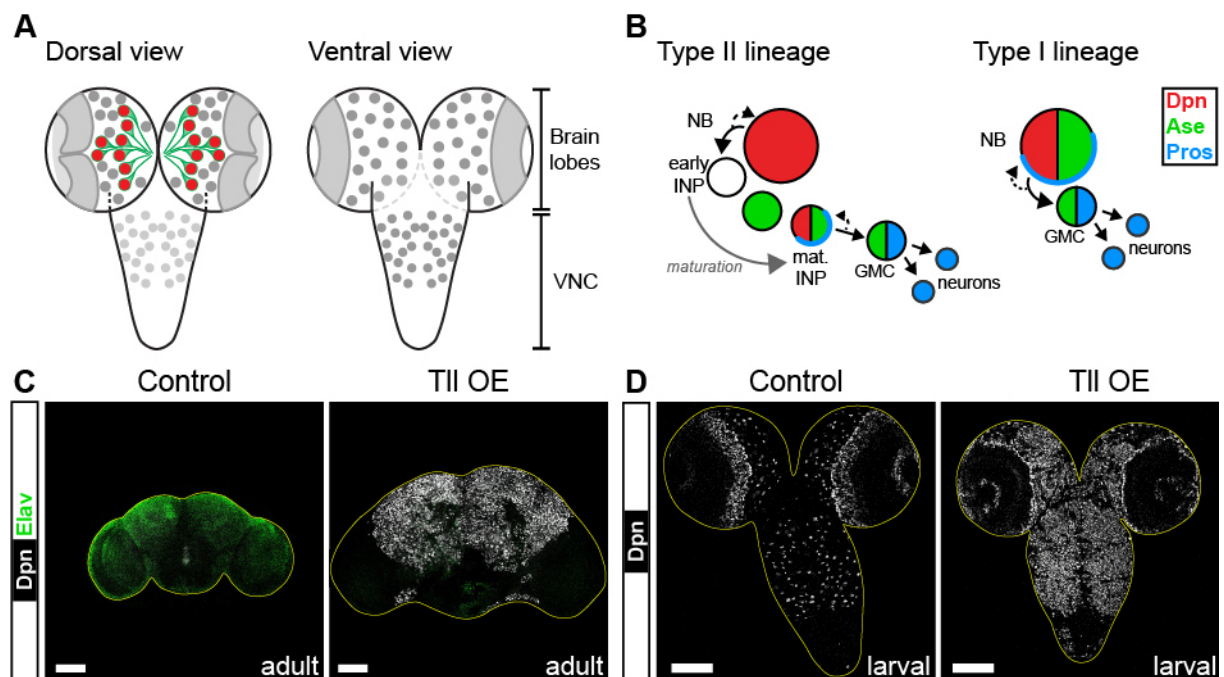


**Figure 4.10: Tll can induce tumours outside of type II lineages**

(A) Schematic of a third instar larval brain when mounted dorsal-side up (right) or ventral-side up (left) for imaging. Type II neuroblasts (red) and their lineages (green) are visible in brain lobes in the dorsal view. Type I neuroblasts are shown in grey. VNC: ventral nerve cord.

(B) Type II vs type I lineage comparison. Type II neuroblasts express Dpn but lack Ase. INPs and type I neuroblasts divide in the same manner both express Dpn and Ase and segregate Pros to their progeny (GMCs).

(C) Control adult brains do not contain neuroblasts ( $Dpn^+$ , white) and consist mostly of neurons ( $Elav^+$ , green). Tll overexpression (Tll OE) brains contain large tumours consisting of neuroblasts ( $Dpn^+$ ) and very few neurons ( $Elav^+$ ). Tumours induced at mid third instar stage.  $n = 7$  for Control and Tll OE.

(D) Tll OE in neuroblasts throughout larval development results in neuroblast tumours ( $Dpn^+$ ) that affect the larval VNC and brain lobes.  $n = 10$  VNCs for Control and Tll OE.

Single section confocal images. Scale bars represent 100  $\mu m$  in C; 30  $\mu m$  in D.

### 4.3.2 Co-operativity with *btd* is required for *tll* to induce tumours

Expressing Tll in VNC type I neuroblasts caused a large expansion of  $Dpn^+$  cells, the majority of which were negative for Ase. However,  $Ase^+$  neuroblasts and  $Pros^+$  cells could still be observed when Tll was expressed throughout the developing CNS (**Fig. 4.11A-A''**). This indicated that some type I lineages may be unresponsive to Tll-induced tumorigenesis and remained able to generate differentiated progeny. In addition, the regions of ectopic  $Dpn^+ Ase^-$  cells were found often with regular organisation and  $Pros^+$  cells were found at the edges of the tumours (**Fig. 4.11A-A''**). This suggested that not all type I neuroblasts in the VNC were competent to respond to high levels of Tll.

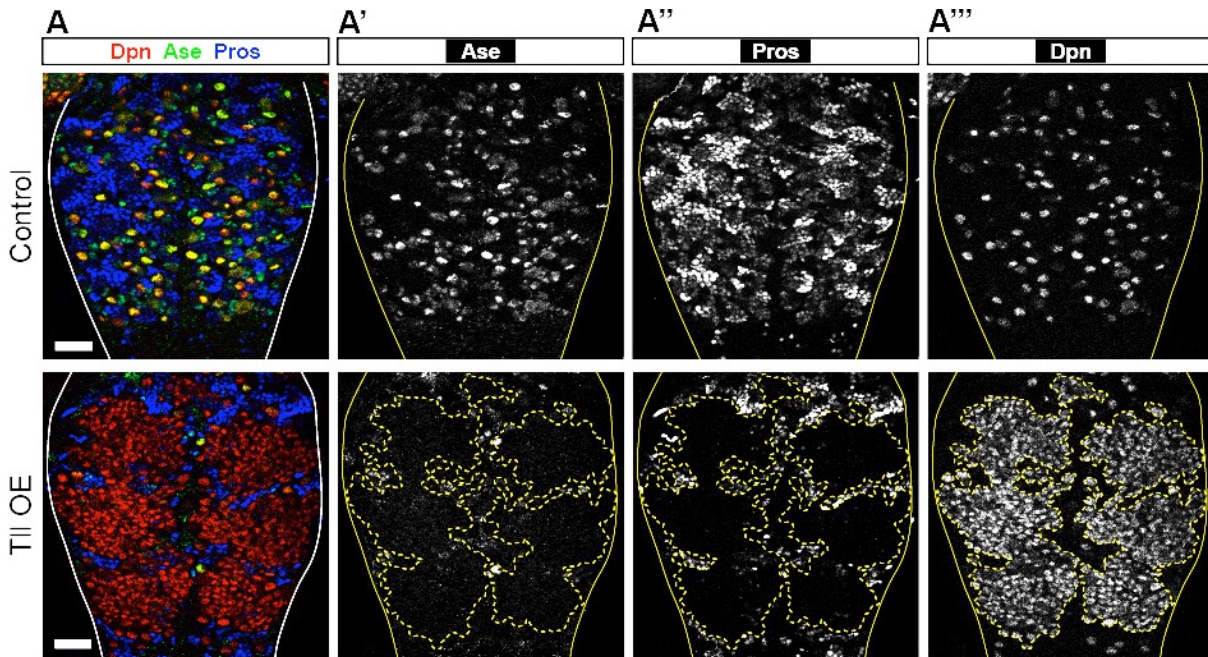


**Figure 4.11: Tll tumours lack Ase and Pros**

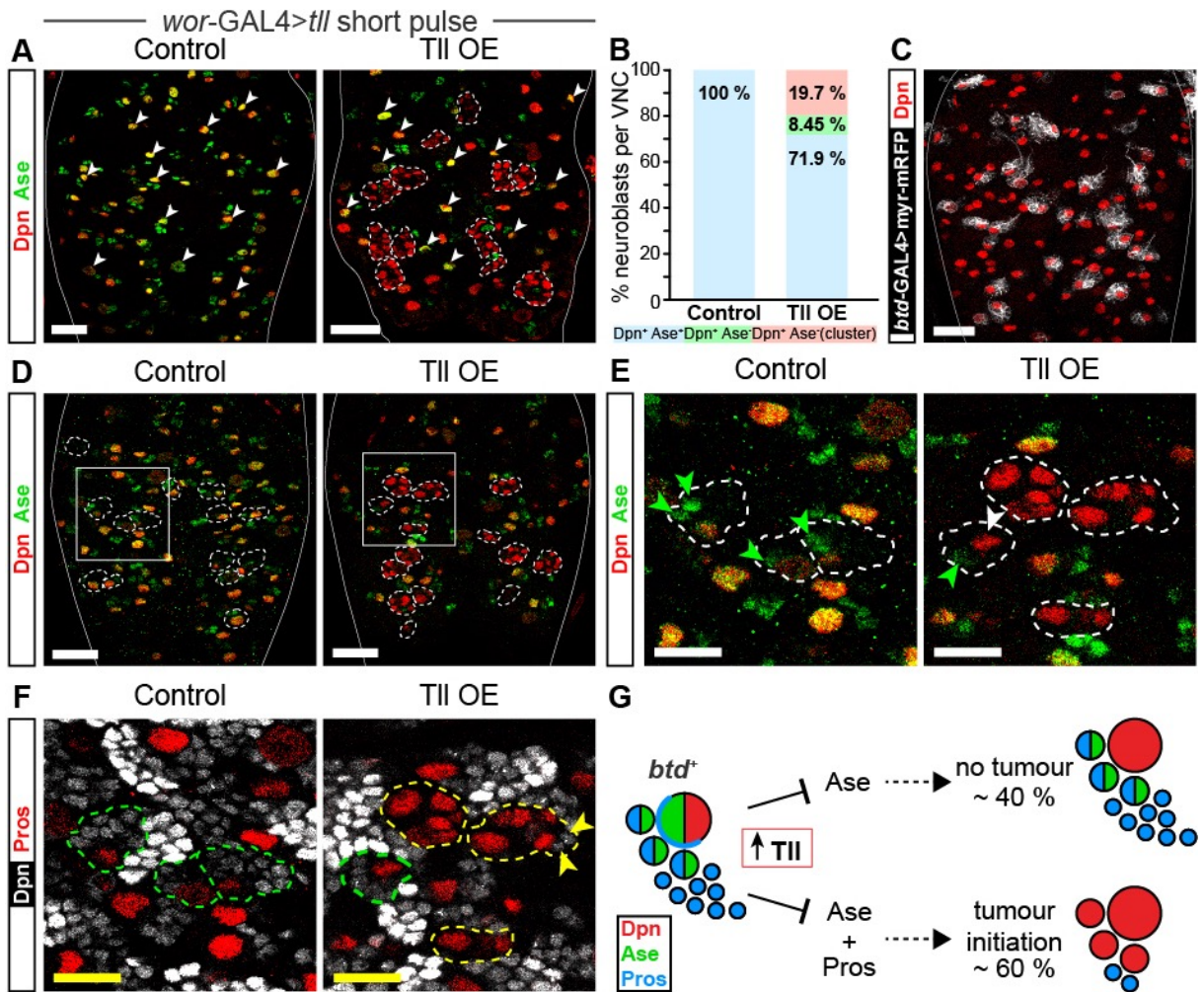
(A-A''') Larval neuroblast tumours ( $Dpn^+$ , red) induced by expressing UAS-tll throughout the VNC with wor-GAL4 show downregulation of the Ase (green) and Pros (blue).

Differentiation, as assessed by Ase (A') and Pros (A'''), can be observed at the edges of  $Dpn^+$  tumours (A''').  $n = 10$  VNCs for Control and Tll OE.

Single section confocal images. Scale bars represent 30  $\mu m$ .

To assess how individual type I lineages responded to ectopic Tll in the early stages of tumour initiation, I expressed UAS-*tll* throughout the VNC for a short period (24 hours) of time. This showed that Tll-induced tumours began as small clusters of  $Dpn^+$  Ase $^-$  cells (Fig. 4.12A). However, this also showed that the majority of neuroblasts retained Ase expression and did not produce ectopic neuroblasts (Fig. 4.12A-B). There was also a small number of lineages that repressed Ase but did not generate ectopic neuroblasts (Fig. 4.12B). Together, this suggested that an additional factor was required to mediate Tll-induced tumourigenesis from type I neuroblast lineages.

One candidate gene for a Tll competency factor was the Sp8 transcription factor *btd*, which is expressed in a subset VNC type I neuroblasts (Xie et al., 2014). Importantly, *btd* is expressed in type II lineages, where it promotes type II neuroblast specification in the embryo (Álvarez and Díaz-Benjumea, 2018). The role of *btd* in type II neuroblasts and its restricted expression in type I lineages suggested that *btd* could mediate Tll-induced tumourigenesis.



I assessed the expression of *btd*-GAL4 and found that it was expressed in  $38 \pm 1.5$  ( $n = 8$  VNCs) VNC type I neuroblasts (in contrast to 31 that had been reported previously (Xie et al., 2014)) (**Fig. 4.12C**). To determine the competency of *btd*<sup>+</sup> lineages to generate tumours, I expressed UAS-*tll* with *btd*-GAL4 for a short pulse. This resulted in the repression of Ase in all *btd*-positive neuroblasts (**Fig. 4.12D**). However, only  $60.5 \pm 3.1$  % of Tll OE *btd* lineages ( $n = 348$  *btd*<sup>+</sup> Tll OE lineages) contained clusters of Dpn<sup>+</sup> cells, which were also negative for Ase. Despite the repression of Ase, the remaining ~40 % of *btd* lineages contained only one Dpn<sup>+</sup> cell (**Fig. 4.12E**). Surprisingly, *btd*<sup>+</sup> lineages with only one neuroblast had small Ase<sup>+</sup> cells adjacent to the neuroblast (**Fig. 4.12E**) and these Ase<sup>+</sup> progeny also expressed Pros<sup>+</sup> (**Fig. 4.12F**), suggesting that differentiation was not perturbed. In contrast, lineages with ectopic Dpn<sup>+</sup> Ase<sup>-</sup> cells lacked Ase<sup>+</sup> Pros<sup>+</sup> progeny, indicating that differentiation was inhibited (**Fig. 4.12F**).

This showed that Tll is sufficient to repress *ase* in all *btd*<sup>+</sup> neuroblasts. However, only the subset of *btd*<sup>+</sup> neuroblasts in which *pros* is also repressed generate ectopic neuroblasts and initiate tumourigenesis (**Fig. 4.12G**). These data suggest that *tll* requires cooperation with *btd* to repress *ase* but that an additional, unknown factor is required to repress *pros* and initiate tumourigenesis. In addition, these data also suggest that the expression of Ase in neuroblast progeny (GMCs) is downstream of differentiation, since Ase<sup>+</sup> progeny can be generated from Ase<sup>-</sup> neuroblasts. This is consistent with the observation that the repression of *ase* alone does not inhibit differentiation and is not sufficient to induce type II neuroblast fate or tumourigenesis (Bowman et al., 2008) (confirmed in this study, **Figs. 4.13A-B**).

To follow the tumourigenic capacity of Tll in *btd*<sup>+</sup> lineages, I drove UAS-*tll* with *btd*-GAL4 throughout larval development. Tll OE VNCs contained large Dpn<sup>+</sup> tumours (**Fig. 4.14A**) that were almost entirely negative for Ase and Pros (**Fig. 4.14A'**). These late-stage tumours also showed a large reduction of neurons (as assessed by Elav **Fig. 4.14B**), consistent with the repression of differentiation observed in early tumours. I attempted to follow these tumours in the adult but all *btd*-GAL4 Tll OE animals failed to complete pupariation (both when Tll expression was driven throughout larval development or only for a short pulse at late larva stage), which was likely due to the effect of *btd*-GAL4 expression in other tissues (Estella et al., 2003).

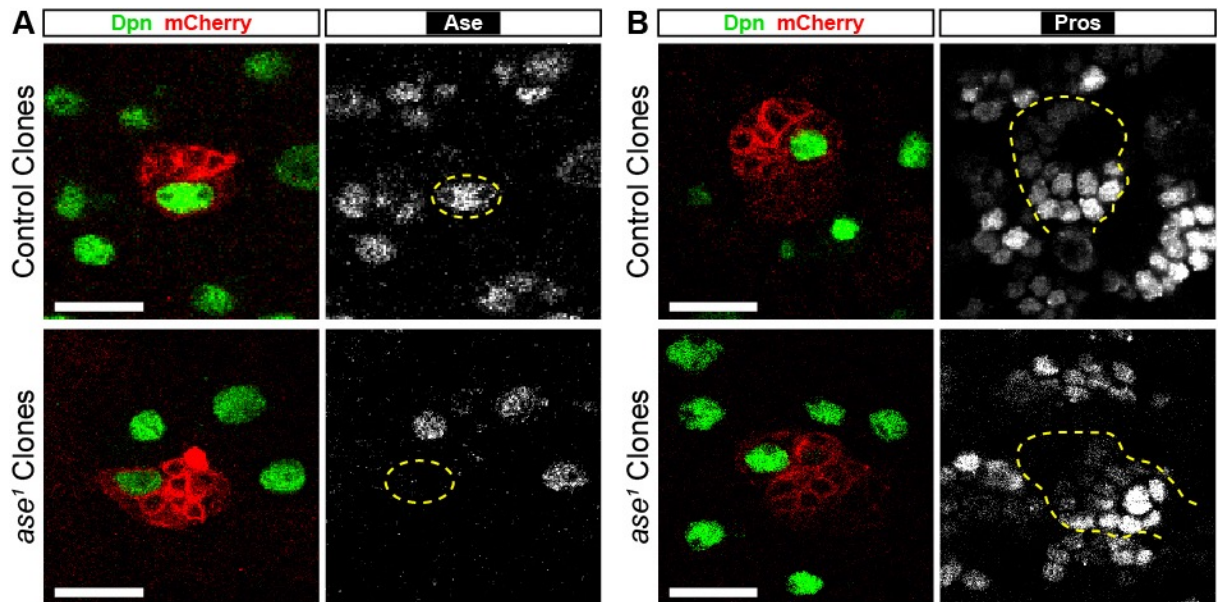


**Figure 4.13: Loss of *ase* from type I lineages is not sufficient to induce type II fate**

(A) Control MARCM clones (mCherry<sup>+</sup>, red) contain one Dpn<sup>+</sup> (green) Ase<sup>+</sup> (white) type I neuroblast. *ase*<sup>1</sup> clones contain one Dpn<sup>+</sup> cell, despite the loss of Ase. Dotted yellow outline indicates a type I neuroblast encompassed within a MARCM clone. *n* = 13 wild type clones; *n* = 20 *ase*<sup>1</sup> clones.

(B) Control MARCM clones (mCherry<sup>+</sup>) contain one Dpn<sup>+</sup> cell (green) and Pros (white) is expressed in the differentiating cells of the lineage. Pros expression is not affected in *ase*<sup>1</sup> clones and no defects in differentiation are observed. Dotted yellow outline indicates a type I lineage encompassed within a MARCM clone. *n* = 29 wild type clones; *n* = 52 *ase*<sup>1</sup> clones.

Single section confocal images. Scale bars 15 μm.

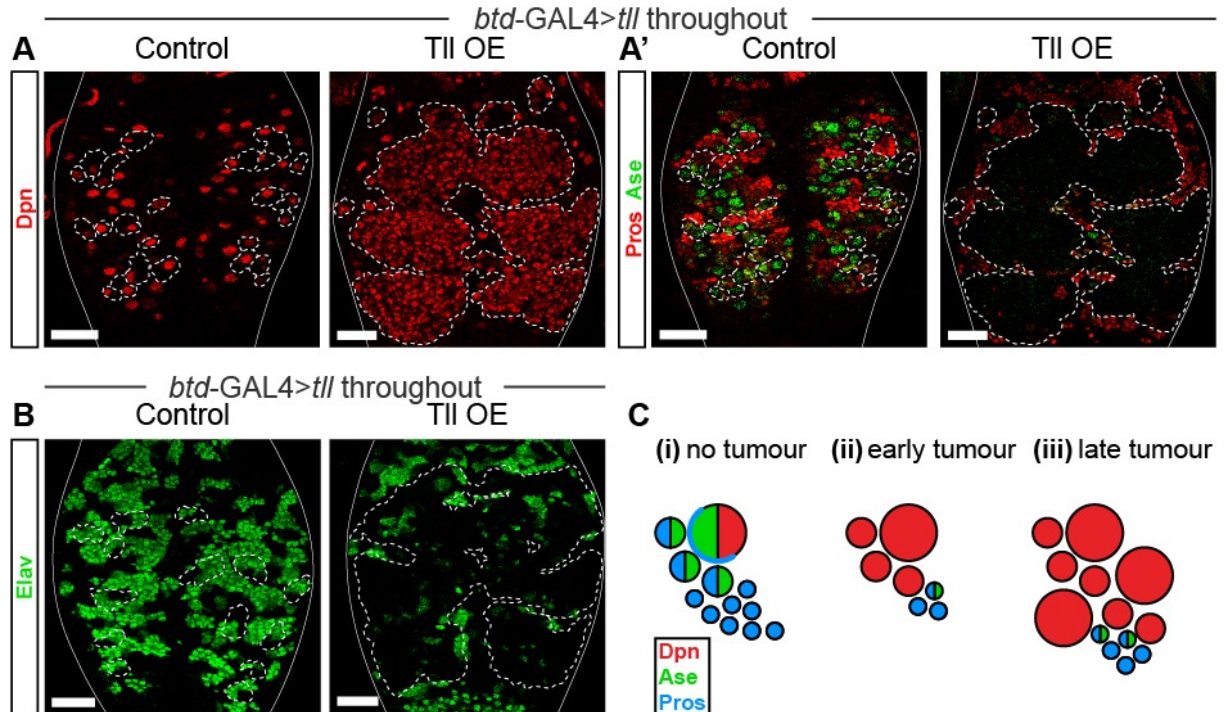


**Figure 4.14: TII OE in *btd*<sup>1</sup> type I neuroblasts generates large type II neuroblast tumours**

(A-A') *btd*-GAL4 driving UAS-*tll* throughout larval development results in large tumours that consist of Dpn<sup>+</sup> (red in A) cells that do not express Ase (green in A') or Pros (red in A').

(B) Ectopic neuroblasts resulting from TII OE are generated at the expense of neurons (Elav, green).

(C) Schematic showing the stages of tumour progression cause by TII OE in *btd*<sup>1</sup> lineages.

Single section confocal images. Scale bars 30 μm.

Overall, these experiments indicate that *btd* mediates the ability of Tll to induce type II neuroblast fate and tumourigenesis. The generation of ectopic neuroblasts occurs at the expense of differentiation (notably, through the inactivation of *ase*, *pros* and *elav*) (**Fig. 4.14C**). During normal development, *btd*<sup>+</sup> type I neuroblasts are Ase<sup>+</sup> and produce Pros<sup>+</sup> progeny. When Tll is expressed in *btd*<sup>+</sup> lineages, *ase* is repressed in all neuroblasts and a subset also represses *pros*, which results in tumour initiation. If these tumours are allowed to progress, they grow into large expansions of Dpn<sup>+</sup> Ase<sup>-</sup> cells.

#### **4.4 Tll-induced tumours are prevented by promoting differentiation**

The repression of *ase* is central to the mechanism through which Tll regulates type II neuroblast fate during development and tumour initiation. This suggests that developmental NSC programmes become reactivated during tumour initiation and highlights the importance of studying NSC factors in tumourigenesis. TLX is expressed at high levels in aggressive brain tumours in humans and is required for the self-renewal capacity of GSCs, the treatment-resistant cells that can re-initiate tumourigenesis (Cui et al., 2016; Zhu et al., 2014). Excitingly, a recent study has also identified that a subset of GSCs show downregulation of *ASCL1* (the mammalian homologue of *ase* (Guillemot and Joyner, 1993; Johnson et al., 1990)) (Park et al., 2017). This study found that the self-renewal capacity of GSCs could be attenuated if *ASCL1* expression was induced in GSCs (Park et al., 2017). Intriguingly, *ASCL1* restricts tumour growth by promoting neuronal differentiation (Park et al., 2017). So far, no link has been made between *TLX* and *ASCL1* in glioblastoma tumours or GSCs but it is an attractive hypothesis that GSCs with high *TLX* correspond to those with low *ASCL1*, in a parallel manner to Tll-induced type II tumours.

##### **4.4.1 Ase can rescue Tll tumours**

Ectopic expression of *ASCL1* in GSCs can prevent tumour growth by inducing neuronal differentiation (Park et al., 2017). *ASCL1* is orthologous to members of the *achaete-scute* complex, which includes *ase*. To assess if expressing *ase* could restrict the growth of Tll-induced tumours, I co-expressed Tll and Ase in neuroblasts. I found that ectopic expression of Ase prevented the formation of ectopic clusters of Dpn<sup>+</sup> cells and VNC lineages resumed type I identity (**Fig. 4.15A**). In addition, neuronal differentiation was restored (**Fig. 4.15B**), which occurred despite Tll protein remaining present at high levels, indicating that Tll cannot override neuronal differentiation induced by Ase (**Fig. 4.15C**). Therefore, ectopic expression of Ase rescued Tll tumours by promoting neuronal differentiation in a comparable manner to *ASCL1* in GSCs (**Fig. 4.15D**).

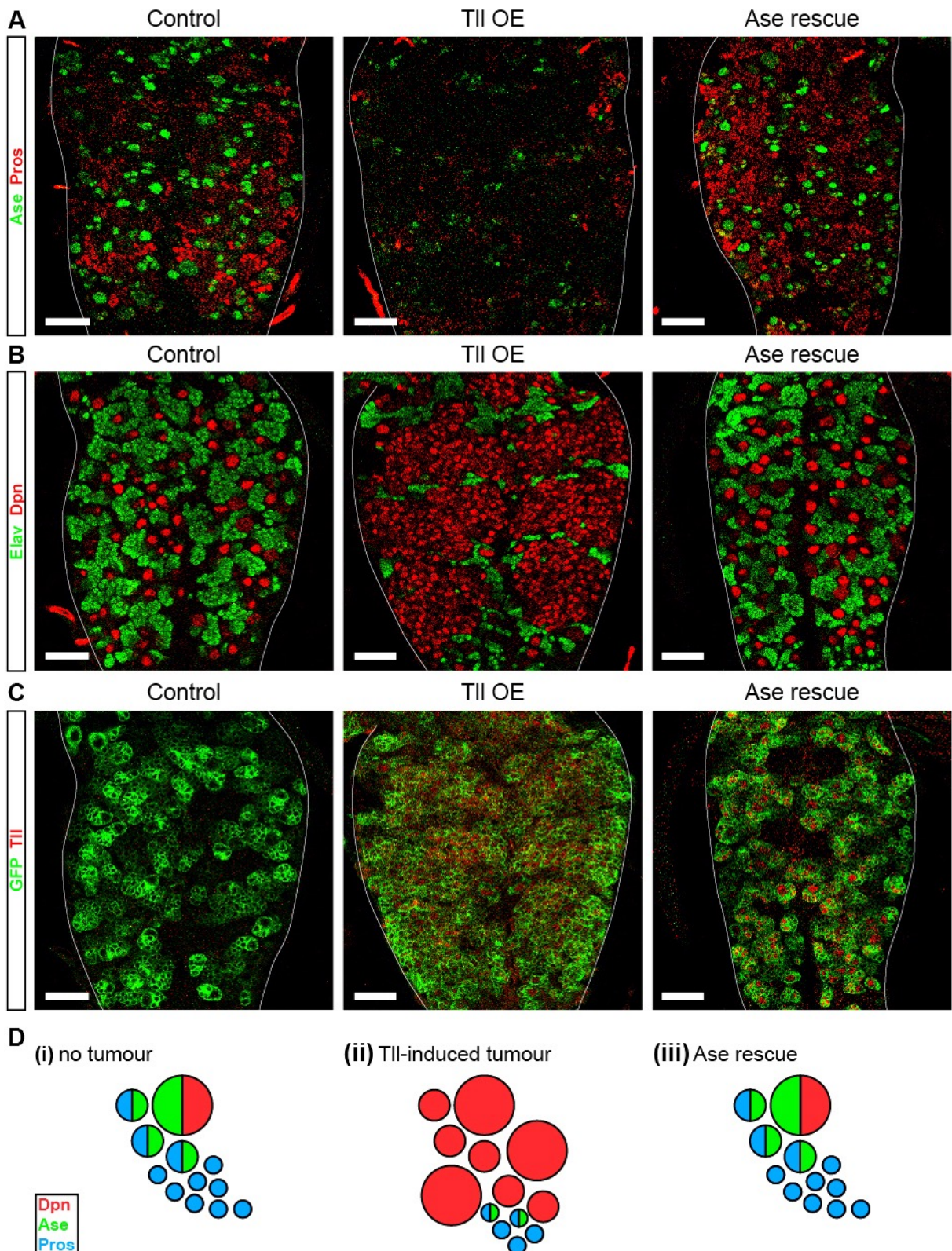


**Figure 4.15: Expressing Ase in Tll tumours prevents tumour formation**

(A) Ase rescues Tll tumours by promoting differentiation (Pros, green).  $n = 9$  brains for Control;  $n = 10$  brains for Tll OE and Ase rescue.

(B) Expressing Ase in Tll tumours is sufficient to restore the production of neurons (Elav, green) from type I neuroblasts ( $Dpn^+$ , red).  $n = 10$  brains for all conditions.

(C) Tll expression is maintained when Ase is co-expressed.  $n = 10$  brains for all conditions.

(D) Schematic showing the lineage progression of normal development, Tll tumours, and in tumours that have high levels of Ase.

Single section confocal images. Scale bars represent  $30 \mu\text{m}$ .

#### 4.4.2 Differentiating cells are resistant to Tll-induced tumourigenesis

Tll tumours induced in type I neuroblasts could be prevented by reinstating differentiation by ectopically expressing Ase. During normal lineage progression, type I neuroblasts divide asymmetrically to generate GMCs, which express Ase and Pros. GMCs undergo terminal division to generate post-mitotic neurons. Given that inducing differentiation via ectopic Ase expression blocked Tll-induced tumours, I investigated if the differentiation state acquired during development also conferred resistance to Tll-induced tumourigenesis.

To target UAS-*tll* to GMCs I used GMR71C09-GAL4, a GAL4 driver that is expressed in GMCs but not in type I neuroblasts in the VNC (Li et al., 2014). Strikingly, expressing high levels of Tll in GMCs did not generate ectopic Dpn<sup>+</sup> cells and type I lineage progression was not disrupted (**Fig. 4.16A**). Therefore, despite the ability of GMCs to divide, this cell type can not respond to high levels of Tll. To restrict UAS-*tll* to neurons I used *vGlut*<sup>OK371</sup>-GAL4, a GAL4 enhancer trap inserted ~9 kb upstream of the *VGlut* gene that is expressed in glutamatergic neurons (Mahr and Aberle, 2006)). I found that expressing Tll in neurons also did not result in ectopic neuroblasts (**Fig. 4.16B**). These results demonstrate that cells that are committed to neuronal identity are resistant to Tll-induced tumourigenesis (**Fig. 4.16C**).

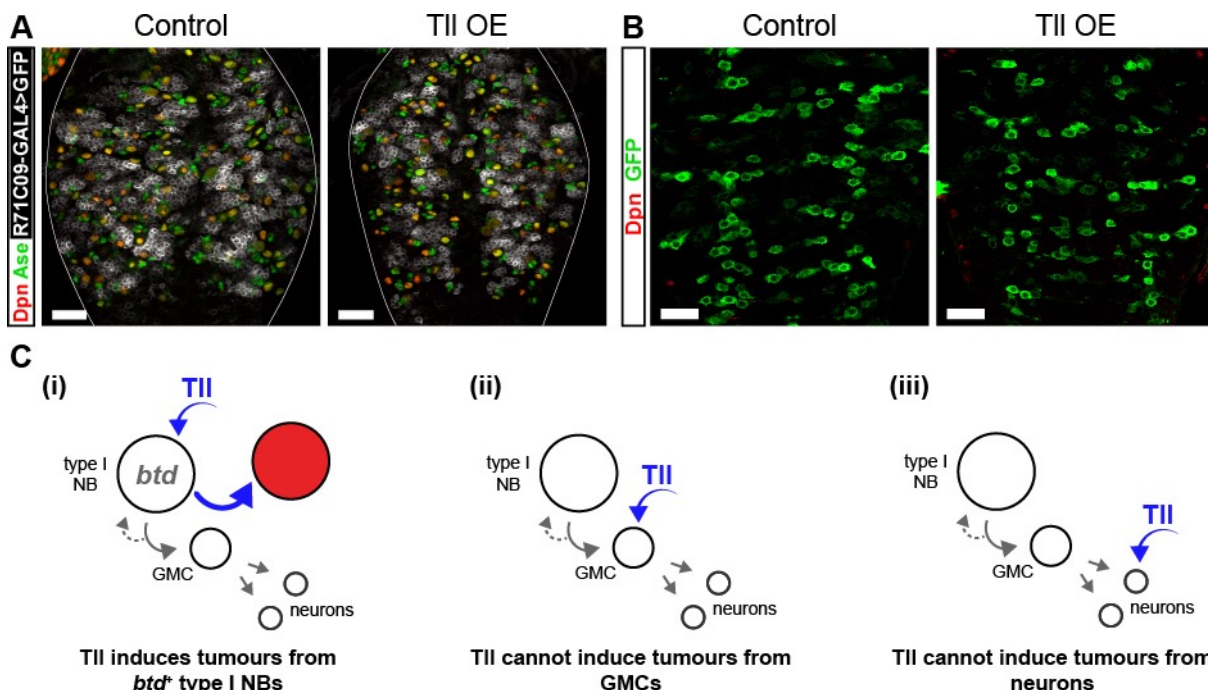


**Figure 4.16: Differentiating cells do not generate tumours in response to high levels of Tll**

(A) Expressing Tll in GMCs (GFP, white) does not result in ectopic neuroblasts. All neuroblasts in the VNC express Dpn (red) and Ase (green).  $n = 10$  brains for Control;  $n = 12$  brains for Tll OE.

(B) Expressing Tll in neurons with *vGlut*<sup>OK371</sup>-GAL4>*mCD8-GFP* (green), does not result in ectopic neuroblasts (Dpn, red).  $n = 4$  brains for Control and Tll OE.

(C) Schematics summarising the tumourigenic capacity of Tll in type I lineages. (i) Tll can induce tumours from type I neuroblasts; (ii) Tll cannot induce tumours from GMCs; (iii) nor can Tll induce tumours from neurons.

Single section confocal images. Scale bars represent 30  $\mu$ m.

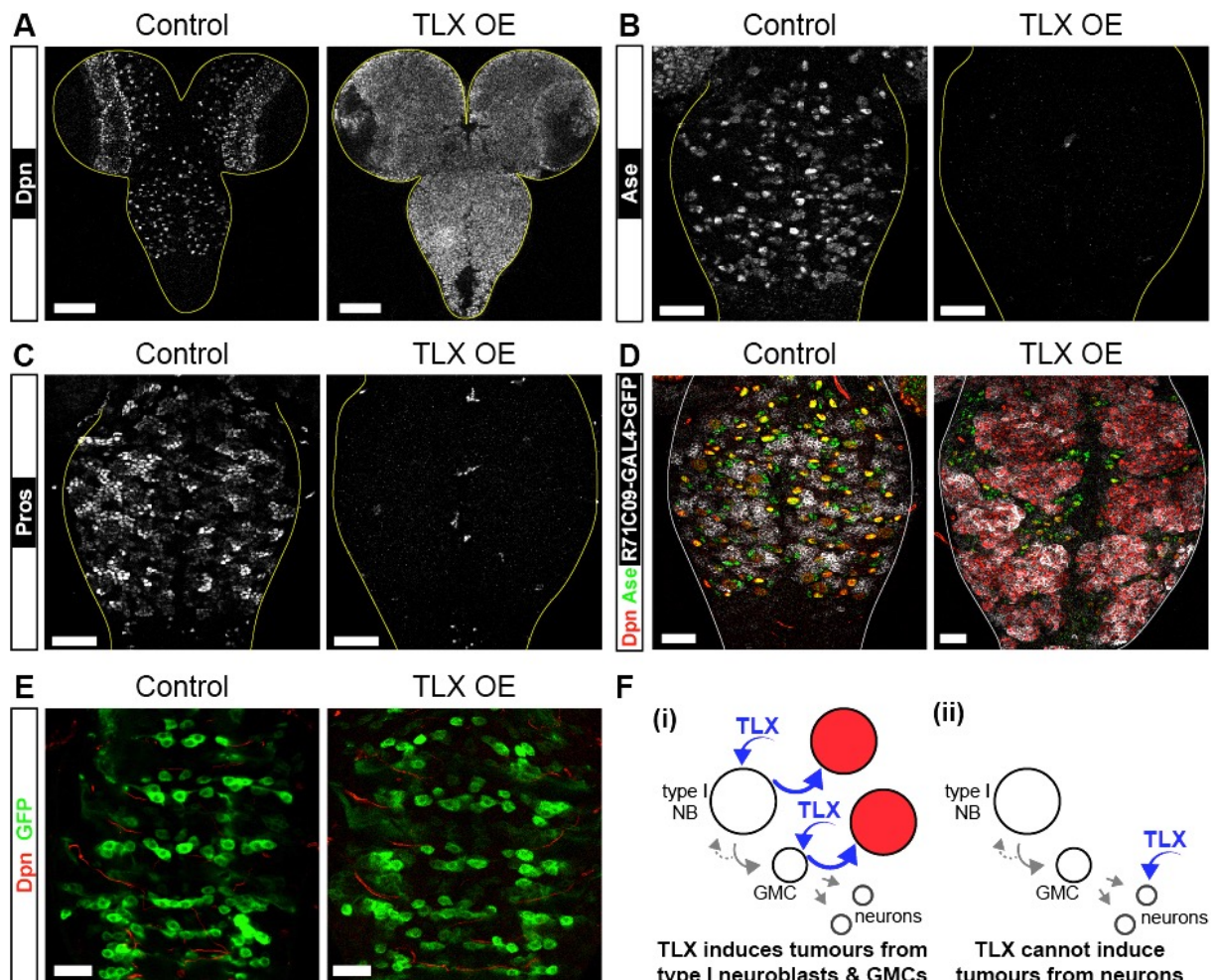


**Figure 4.17: TLX induces tumours from type I neuroblasts and GMCs but not from neurons**

(A) TLX overexpression (OE) in neuroblasts throughout larval development results in neuroblast tumours (Dpn<sup>+</sup>, white) that affect the entire CNS.  $n = 10$  brains for Control and TII OE.

(B) TLX tumours induced in type I neuroblasts are negative for the proneural gene Ase (white).  $n = 10$  brains for Control and TII OE.

(C) Differentiation, as assessed Pros (white), is prevented in TLX tumours.  $n = 10$  brains for Control and TII OE.

(D) Expressing TLX in GMCs causes direct conversion to type II neuroblast fate.  $n = 10$  brains for Control and TII OE.

(E) Expressing TLX in neurons with *vGlut<sup>OK371</sup>-GAL4>mCD8-GFP* (green), does not result in ectopic neuroblasts (Dpn, red).  $n = 8$  brains for Control and TII OE.

(F) Schematics summarising the tumourigenic capacity of TLX in type I lineages. (i) TLX can induce tumours from type I neuroblasts and GMCs; (ii) TLX cannot induce tumours from neurons.

Single section confocal images. Scale bars represent 30  $\mu$ m.

#### 4.5 TLX has a stronger tumourigenic capacity than Tll

Expressing *Drosophila* Tll or human TLX in type II INPs resulted in the same transition of INPs to neuroblast fate, indicating that Tll and TLX initiate tumourigenesis through a conserved mechanism. However, expressing TLX in INPs resulted in a more severe tumourigenic phenotype, with more ectopic type II neuroblasts generated compared to expressing *Drosophila* Tll under the same conditions. To investigate the tumourigenic capacity of human TLX in other *Drosophila* lineages, I expressed human TLX throughout the developing CNS. Expressing UAS-*TLX* with *wor*-GAL4 caused almost the entire CNS to

consist of  $Dpn^+$  neuroblasts (**Fig. 4.17A**). Furthermore, all ectopic  $Dpn^+$  cells in the VNC (where all neuroblasts are normally type I and express *Ase*) were negative for *Ase* (**Fig. 4.17B**). Tumours induced by TLX also occurred at the expense of differentiation, as assessed by *Pros* staining (**Fig. 4.17C**). Therefore, TLX can also induce type II neuroblast tumours from type I neuroblasts in a similar manner to Tll. However, the tumourigenic capacity of TLX does not appear to be restricted to certain type I lineages, as was the case for Tll.

Intriguingly, I found that expressing TLX in GMCs resulted in large tumours that consisted of type II neuroblasts ( $Dpn^+ Ase^-$ ) (**Fig. 4.17D**). This appeared to be a direct conversion of GMCs to type II fate as type I neuroblasts were still present and  $Dpn^+ Ase^-$  cells were found in place of GMCs (**Fig. 4.17D**). However, TLX was unable to induce tumours from neurons, showing that post-mitotic cells cannot reinitiate the NSC programme in response to TLX (**Figs. 4.17E**). Taken together, these results indicate that, while TLX and Tll appear to act through conserved molecular mechanisms to induce tumourigenesis, TLX has an increased capacity to induce tumourigenesis (**Fig. 4.17F**). Importantly, post-mitotic neurons are resilient to tumour initiation by high levels of Tll or TLX suggesting that promoting neuronal differentiation could be an effective treatment for brain tumours with high TLX expression.

#### **4.6 Chapter 4 discussion**

Tll and TLX are important regulators of NSCs that must be kept in a fine balance to ensure that sufficient neuronal progeny are generated but that tumours do not arise. I found that Tll is expressed in type II neuroblasts to maintain neuroblast fate but is downregulated as the lineage progresses. Preventing Tll downregulation in type II lineages resulted in tumour initiation through the reversion of type II INPs to neuroblast fate. This has significant importance for the role of TLX in tumour initiation. Overexpression of TLX in the mouse brain causes expansion of the NSC population and can lead to glioblastoma (GBM) when combined with additional mutations (Park et al., 2010). However, how TLX affects lineage progression is not clear and so the tumour cell of origin has not been identified.

Both Tll and TLX can induce tumours from type II INPs and appear to act through conserved molecular mechanisms: both genes repress *ase* and *pros* to induce tumours that consist of type II neuroblasts. This shows that INPs present a genetic weak point during lineage progression; they maintain some aspects of NSC behaviour and so can re-initiate NCS gene pathways in response to Tll/TLX. The similarity of type II lineage progression with mammalian NSC lineages and the ability of Tll/TLX to promote tumours from INPs implicates intermediate

progenitors as a potential cell of origin for TLX-induced tumours in mammals. It would be interesting to investigate if TLX induces gliomas from intermediate progenitors in mammalian NSC lineages and if this occurs via reversion to NSC fate. Identifying the cell of origin for different tumour subtypes is crucial for developing therapies that can be targeted to specific cell-types.

Although Tll and TLX induce tumours through conserved molecular mechanisms, TLX has a higher tumourigenic capacity. Tll-induced tumours are restricted to type II lineages and type I lineages that express *btd*. However, TLX appears to induce tumours from type II INPs, all type I neuroblasts and GMCs. The reason for the differences in cell types in which Tll/TLX can initiate tumours is not known. One possible explanation could be the lower conservation of the LBD between TLX and Tll (LBDs share 40 % identical amino acids; DBDs share 81 % identity). Although TLX and Tll are regulated by conserved co-repressors (such as Atrophin, (Zhi et al., 2015)) the binding affinity for their cofactors differs between species (Wang et al., 2006). As such, it is possible that the differences in the LBDs between human TLX and *Drosophila* Tll are sufficient to result in different transcriptional regulation by these genes.

The repression of *ase* was central to the ability of Tll/TLX to induce tumourigenesis. *ase* promotes neurogenesis in a comparable manner to its homologue ASCL1 (Guillemot et al., 1993; Torii et al., 1999). I found that ectopic expression of Ase was able to block the formation of Tll-induced tumours, which could provide an important link between two aspects of glioblastoma genetics. Firstly, TLX is expressed in a subset of aggressive GBM tumours and correlates with poor patient prognosis (Park et al., 2010; Zou et al., 2012). Of particular significance is the requirement of TLX for the self-renewal capacity of GSCs (Cui et al., 2016; Zhu et al., 2014). Secondly, an independent study found that ASCL1 is downregulated in a subset of GSCs, which resulted in failure to respond to differentiation signals (Park et al., 2017). However, introducing ASCL1 to these GSCs was sufficient to induce neuronal differentiation, which restricted GSC self-renewal and prevented tumour growth (Park et al., 2017). Therefore, in light of my results, it would be interesting to investigate if GSCs with low ASCL1 also exhibit high TLX expression and vice versa. If this is the case, this could implicate differentiation therapy as a treatment for aggressive GBM with high TLX expression.



## Chapter 5

### The optic lobe generates a newly discovered neural stem cell population during embryogenesis

#### Statement on collaboration:

The majority of the work in this chapter was carried out in collaboration with Dr Leo Otsuki, a former member of the Brand Lab. Together, we discovered embryonic optic neuroblasts (EONs). This work has been published in *Development* (the paper is attached as **Appendix 4** for reference). We are co-first authors on this paper; we designed the experiments and analysed the data together. Figure panels in this thesis provided by Dr Leo Otsuki (LO) are indicated under each figure; those provided by me are denoted AEH.

During development, NSC divisions must be regulated precisely to generate a functioning nervous system. Symmetric NSC divisions increase the number of NSCs, whereas asymmetric NSC divisions generate post-mitotic progeny. Disruption to the mode of NSC divisions can result in insufficient progeny or overgrowth and tumorigenesis. Understanding how NSCs are regulated during normal development is of key importance for improving our knowledge of how disorders and diseases affecting the CNS arise.

During the early stages of brain development symmetrically dividing neuroepithelial cells expand the NSC pool in the mammalian cerebral cortex and the *Drosophila* visual system (Egger et al., 2007; Noctor et al., 2004). Neuroepithelial cells later transform into asymmetrically dividing NSCs (called neuroblasts in *Drosophila*) that generate neurons and glia (Brand and Livesey, 2011; Egger et al., 2011; Noctor et al., 2004). The developing *Drosophila* visual system has proved to be a valuable system for investigating the fundamental mechanisms of NSC regulation (Bertet, 2017).

#### **5.1 The optic lobe and type II neuroblasts are regulated by common factors**

During development, the optic lobe neuroepithelium gives rise to neuroblasts that produce the neurons and glia of the medulla, the largest ganglion of the adult visual processing system (Dillard et al., 2018; Egger et al., 2007; Egger et al., 2010; Kawamori et al., 2011; Reddy et al., 2010; Yasugi et al., 2008; Yasugi et al., 2010). Neuroepithelial cells are converted to neuroblasts at mid larval stages (~48 hours ALH) through the progression of a proneural wave (Yasugi et al., 2008) (**Fig. 5.1A**).

The transition from neuroepithelial cells to neuroblasts shares many parallels with lineage progression from type II neuroblasts. In both systems, NSCs (neuroepithelial cells or type II

neuroblasts) undergo a transition that results in progenitors with a more restricted self-renewal capacity (type I optic lobe neuroblasts or type II INPs) (**Fig. 5.1A-B**). In addition, there are many molecular similarities between the optic lobe and type II neuroblasts that regulate parallel fate transitions in both systems. For example, *tll* is expressed in the optic lobe neuroepithelium throughout development, where it is required for neuroepithelial cell survival (Daniel et al., 1999; Guillermin et al., 2015). In Chapters 2-4, I showed that *tll* is expressed in type II neuroblasts and promotes neuroblast fate and lineage identity. Looking for additional similarities between these systems could enhance our understanding of the genes that regulate the NSCs in the optic lobe and type II lineages in *Drosophila* as well as NSCs in other species.

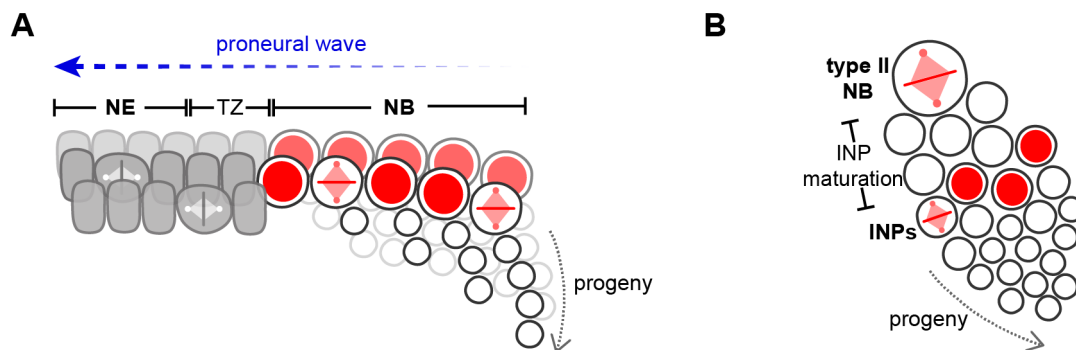


**Figure 5.1: Division modes of stem cells in the optic lobe and type II neuroblasts**

(A) During larval development, symmetric divisions expand the optic lobe neuroepithelium (NE, grey). The proneural wave (blue arrow) converts neuroepithelial cells to neuroblasts (NB, red) at the transition zone (TZ). Neuroblasts divide asymmetrically to generate post-mitotic progeny.

(B) In type II lineages, the neuroblast (NB) divides asymmetrically to generate immature INPs. Following maturation, INPs (red, small) divide asymmetrically to generate post-mitotic progeny.

All panels provided by AEH.

### **5.1.1 Earmuff is an optic lobe transition zone marker**

The transition from neuroepithelial cells to optic lobe neuroblasts is defined by the expression of *lethal of scute* (*l'sc*); timely expression of *l'sc* is required for the generation of medulla neuroblasts (Yasugi et al., 2008). I discovered that optic lobe transition zone marker *L'sc* is also expressed in type II INPs during maturation (see Chapter 3). This suggested that INP maturation could be considered as a “transition zone” in type II lineages whereby INP fate is acquired. In addition to *L'sc*, immature INPs express the *Fezf* transcription factor Earmuff (*Erm*) (**Fig. 5.2A**), which is required for INP maturation (Janssens et al., 2014; Weng et al., 2010). I assessed the overlap between *L'sc* and *Erm* in immature INPs and I found that these genes were co-expressed in immature INPs (**Fig. 5.2A'-A''**). *erm* expression can also be followed using the genetic reporter R9D11-mCD8-GFP, which was activated after *Erm/L'sc* in type II INPs (**Fig. 5.2A-A''**).

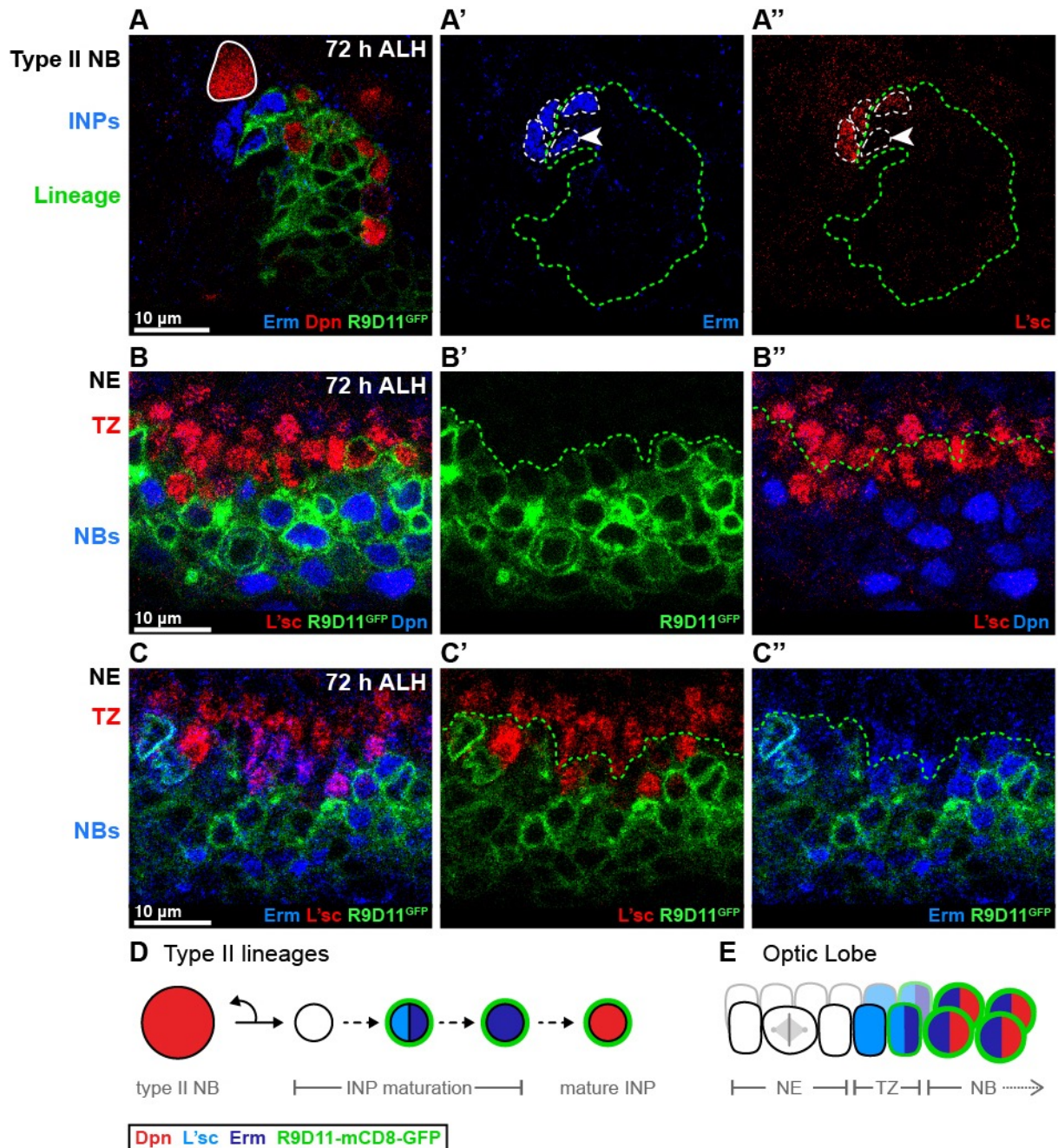


**Figure 5.2: Maturing type II INPs and the optic lobe transition zone express Erm and L'sc**

(A-A'') Type II neuroblasts ( $Dpn^+$ , red, solid white outline) generate immature INPs that express Erm (blue, dotted white outlines) (Weng et al., 2010). Younger  $Erm^+$  INPs also express L'sc (red) but older  $Erm^+$  INPs do not (arrowhead). Type II lineages express R9D11-mCD8-GFP ( $R9D11^{GFP}$ , green, dotted green outlines), which comes on after Erm and L'sc.

(B-B'') The transition from neuroepithelial cells (NE) to neuroblasts (NB,  $Dpn^+$ , blue) in the optic lobe is marked by the expression of L'sc (red) (Yasugi et al., 2008).  $R9D11^{GFP}$  (green) is expressed at the transition zone (TZ) after the initiation of L'sc expression.

(C-C'') Erm (blue) is also expressed at the optic lobe TZ, after the initiation of L'sc expression and is maintained in neuroblasts.

(D-E) Schematics summarising type II INP maturation and the optic lobe neuroepithelium to neuroblast transition. L'sc and Erm are coexpressed in both systems. L'sc has a more limited expression window compared to Erm, which is maintained in maturing INPs and optic lobe neuroblasts ( $Dpn^+$ ).  $R9D11^{GFP}$  is expressed during the cell fate transition in both systems.

Single section confocal images. Brains dissected 72 hours ALH. All panels provided by AEH.

Given the overlap of *Erm* and *L'sc* in type II lineages, I investigated whether these factors were also co-expressed in the optic lobe. Indeed, the *erm* reporter R9D11-mCD8-GFP was expressed at the transition zone (**Fig. 5.2B**) and overlapped with *L'sc* expression (**Fig. 5.2B'-B''**). Staining with an antibody raised against *Erm* showed that the protein was present at the transition zone (**Fig. 5.2C**) and was maintained in optic lobe neuroblasts (**Fig. 5.2C'-C''**). This showed that *Erm* overlapped with *L'sc* at the optic lobe transition zone and during INP maturation in type II lineages (**Fig. 5.2D-E**). The expression of the *erm* reporter R9D11-mCD8-GFP in the optic lobe provided an easily identifiable marker for the neuroepithelial to neuroblast transition. As such, R9D11-mCD8-GFP could be used to follow the generation of neuroblasts from the neuroepithelium during the early stages of optic lobe development.

## **5.2 The optic lobe neuroepithelium divides in the embryo**

The optic lobe neuroepithelium is specified in the embryo, initially as a patch of dense cells in the head ectoderm of stage 11 embryos (Hartenstein and Campos-Ortega, 1984; Poulson, 1950; Turner and Mahowald, 1979). These cells undergo four cell divisions before invaginating from the ectoderm as a neuroepithelial sheet and attaching to the lateral surface of the brain between embryonic stages 12 and 13 (**Fig. 5.3A**) (Green et al., 1993). After this stage, the neuroepithelium has been reported to be dormant until symmetric divisions begin during the first larval instar (12-15 hours ALH) (Datta, 1995; Ebens et al., 1993; Hofbauer and Campos-Ortega, 1990; Prokop and Technau, 1994; White and Kankel, 1978), following which the proneural wave converts neuroepithelial cells to neuroblasts (Yasugi et al., 2008) (**Fig. 5.3B**).

### **5.2.1 Neuroepithelial cells divides throughout embryogenesis**

Neuroepithelial cells can be identified in the embryo by their expression of Fasciclin II (FasII), the orthologue of neural cell adhesion molecule (N-CAM) (Grenningloh et al., 1991; Younossi-Hartenstein et al., 1997). To determine the proliferation pattern of neuroepithelial cells during embryogenesis, we co-stained for FasII and the cell division marker phospho-histone H3 (pH3). We found pH3<sup>+</sup> neuroepithelial cells at all developmental stages between optic primordium invagination and the end of embryogenesis (**Fig. 5.4Ai-iii, quantified in Fig. 5.4B**). Thus, the neuroepithelium divides throughout embryogenesis, in contrast to a previous suggestion that the optic primordium is dormant in the embryo (Green et al., 1993).

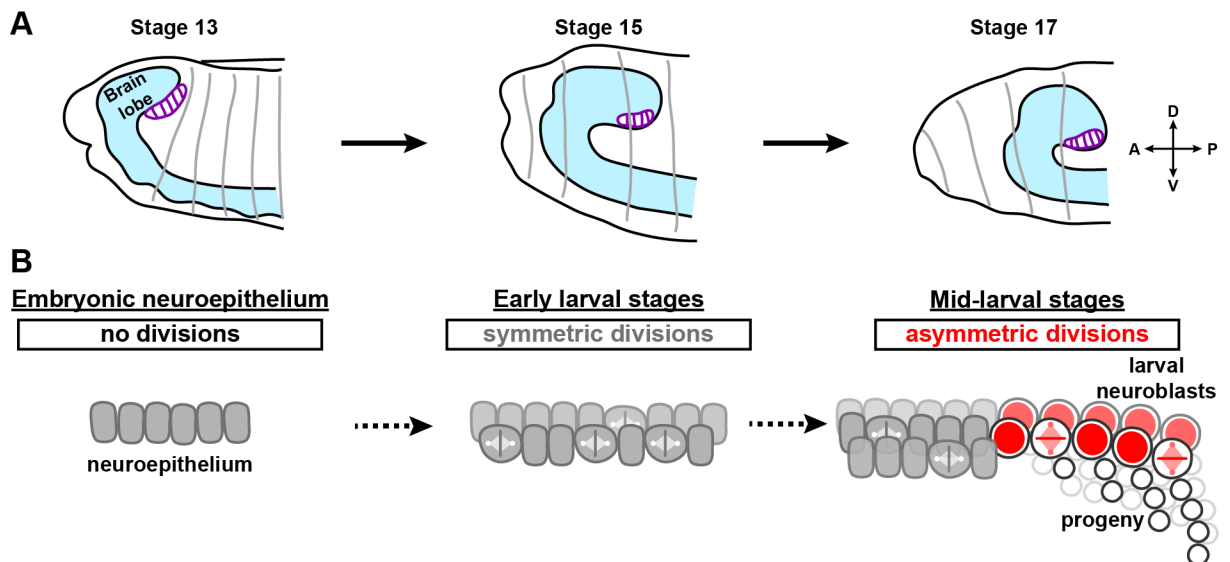


**Figure 5.3: Existing model of neuroepithelium dynamics**

(A) Schematic showing the position of neuroepithelium (purple) after invagination from the head ectoderm. The neuroepithelium attaches to the lateral posterior sides of the brain lobe (CNS shown in blue). A: anterior; P: posterior; D: dorsal; V: ventral.

(B) Previous studies inferred that no cell divisions occurred in the neuroepithelium (grey) during embryogenesis. Symmetric divisions began during early larval stages, to expand the neuroepithelium, and the generation of neuroblasts (red) was restricted to mid-late larval stages. The asymmetric division of neuroblasts resulted in the generation of post-mitotic progeny.

Panel (A) provided by LO; panel (B) provided by AEH.

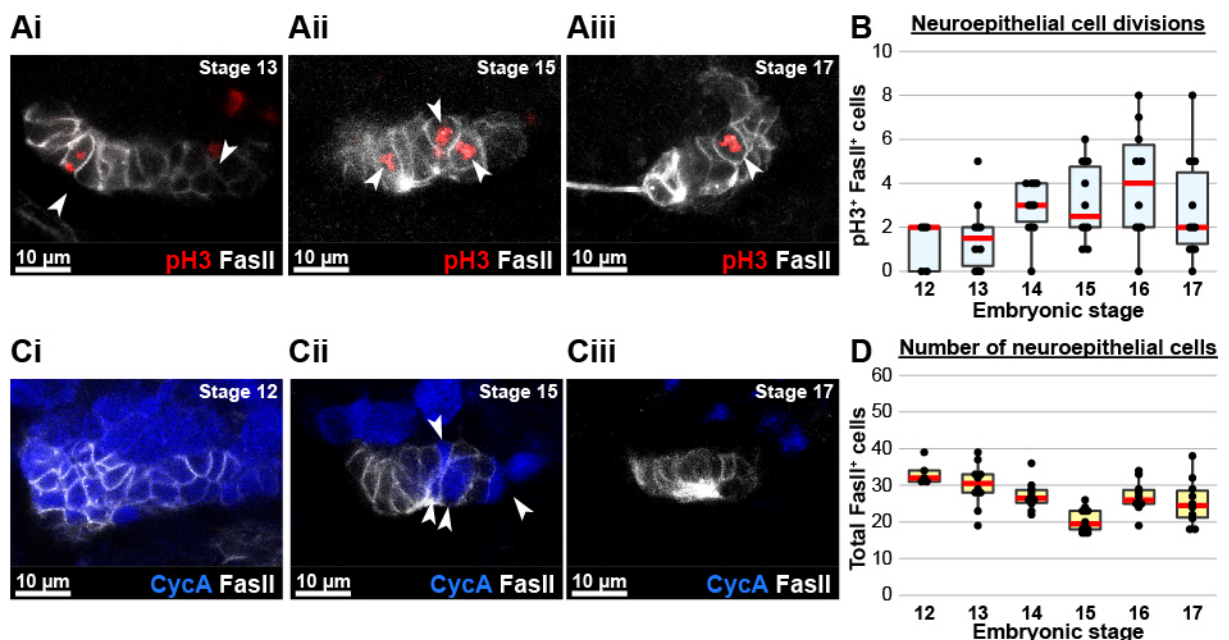


**Figure 5.4: The neuroepithelium divides throughout embryogenesis**

(Ai-iii) The optic lobe neuroepithelium ( $\text{FasII}^+$ , white) divides throughout embryogenesis, as assessed by staining for pH3 (red). Dividing neuroepithelial cells are indicated by arrowheads.

(B) Quantification of the number of neuroepithelial cell divisions ( $\text{pH3}^+ \text{FasII}^+$ ) per brain lobe between embryonic stages 12 and 17.  $n = 10$  embryos per stage, except stage 12 for which  $n = 5$ . Red lines indicate medians.

(Ci-iii) All embryonic neuroepithelial cells ( $\text{FasII}^+$ ) express the G2 cyclin (Cyclin A, blue) soon after invagination (Stage 12). The neuroepithelium loses Cyclin A expression over time.

(D) Quantification of the number of neuroepithelial ( $\text{FasII}^+$ ) cells per brain lobe between embryonic stages 12 and 17.  $n = 10$  embryos per stage, except stage 12 for which  $n = 5$ . Red lines indicate medians.

All panels provided by LO.

Previous studies used BrdU incorporation assays to follow cell divisions of the neuroepithelium (Green et al., 1993). BrdU is a synthetic thymidine analogue that can be used to label cells as they complete S phase of the cell cycle. As such, it would be possible for neuroepithelial cells to divide without incorporating BrdU if they arrested in G<sub>2</sub> phase as they invaginated from the ectoderm (*i.e.* had already completed S phase). To determine the cell cycle phase of neuroepithelial cells, we stained for Cyclin A (CycA), a G<sub>2</sub> phase cyclin and found that neuroepithelial cells were all CycA<sup>+</sup> as they underwent invagination (**Fig. 5.4Ci**). Neuroepithelial cells lost CycA expression over time, concomitant with cell divisions (**Fig. 5.4Cii**), until all were CycA<sup>-</sup> at the end of embryogenesis (**Fig. 5.4Ciii**). Our results show that neuroepithelial cells invaginate in G<sub>2</sub> and subsequently undergo mitosis. This is consistent with previous observations (Green et al., 1993) and, furthermore, we infer that neuroepithelial cells divide once each as they do not undergo S phase in the embryo after invagination (Green et al., 1993).

### **5.2.2 The embryonic neuroepithelium generates neuroblasts**

We next assessed the role of neuroepithelial cell divisions in the embryo. We found no significant increase in the number of neuroepithelial cells over time (**Fig. 5.4D**), indicating that the role of these cell divisions is not to increase the size of the neuroepithelium. We therefore tested whether the embryonic neuroepithelium produces neuroblasts, in a similar manner to the neuroepithelium in larval development.

We found neuroblasts (Dpn<sup>+</sup> cells) in close association with the neuroepithelium beginning at embryonic stage 12 (**Fig. 5.5A**). These neuroblasts expressed the transition zone marker R9D11-mCD8-GFP (**Fig. 5.5B**), suggesting that they were produced by the neuroepithelium. To test if the neuroblasts were derived from the neuroepithelium, we expressed red fluorescent protein (RFP) in the neuroepithelium and assessed whether the Dpn<sup>+</sup> cells inherited RFP. Interestingly, we found that GAL4 lines that label the larval neuroepithelium (GAL4<sup>c855a</sup> (Egger et al., 2007) and *ogre*-GAL4 (Dillard et al., 2018)) were not expressed in the embryonic neuroepithelium (*data not shown*). However, we found that a GAL4 driver under the control of a regulatory region of *tll*, GMR31H09-GAL4 (identified in Chapter 2, referred to as R31H09-GAL4 here) labelled the embryonic neuroepithelium (**Fig. 5.5B'**). When we expressed RFP using R31H09-GAL4, we found that the Dpn<sup>+</sup> cells inherited RFP (**Fig. 5.5B'**). In addition, R9D11-mCD8-GFP<sup>+</sup> cells initially express Eya (**Fig. 5.5C**), which is a robust marker of the embryonic neuroepithelium (Erclik et al., 2008). Therefore, we

conclude that the embryonic neuroepithelium produces neuroblasts and refer to these neuroblasts as EONs (embryonic optic neuroblasts).

EONs were produced continuously from invagination (stage 12) until the end of embryogenesis and we found a final number of  $8.6 \pm 0.7$  EONs per brain lobe (Fig. 5.5D). EONs were initially visible in the neuroepithelial plane and then extruded medially towards the interior of the brain, upon which they downregulated FasII expression (Fig. 5.5Ei-iii). Importantly, our results demonstrate that neuroepithelial cells produce neuroblasts much earlier (~60 hours earlier) than described previously (Fig. 5.5F).

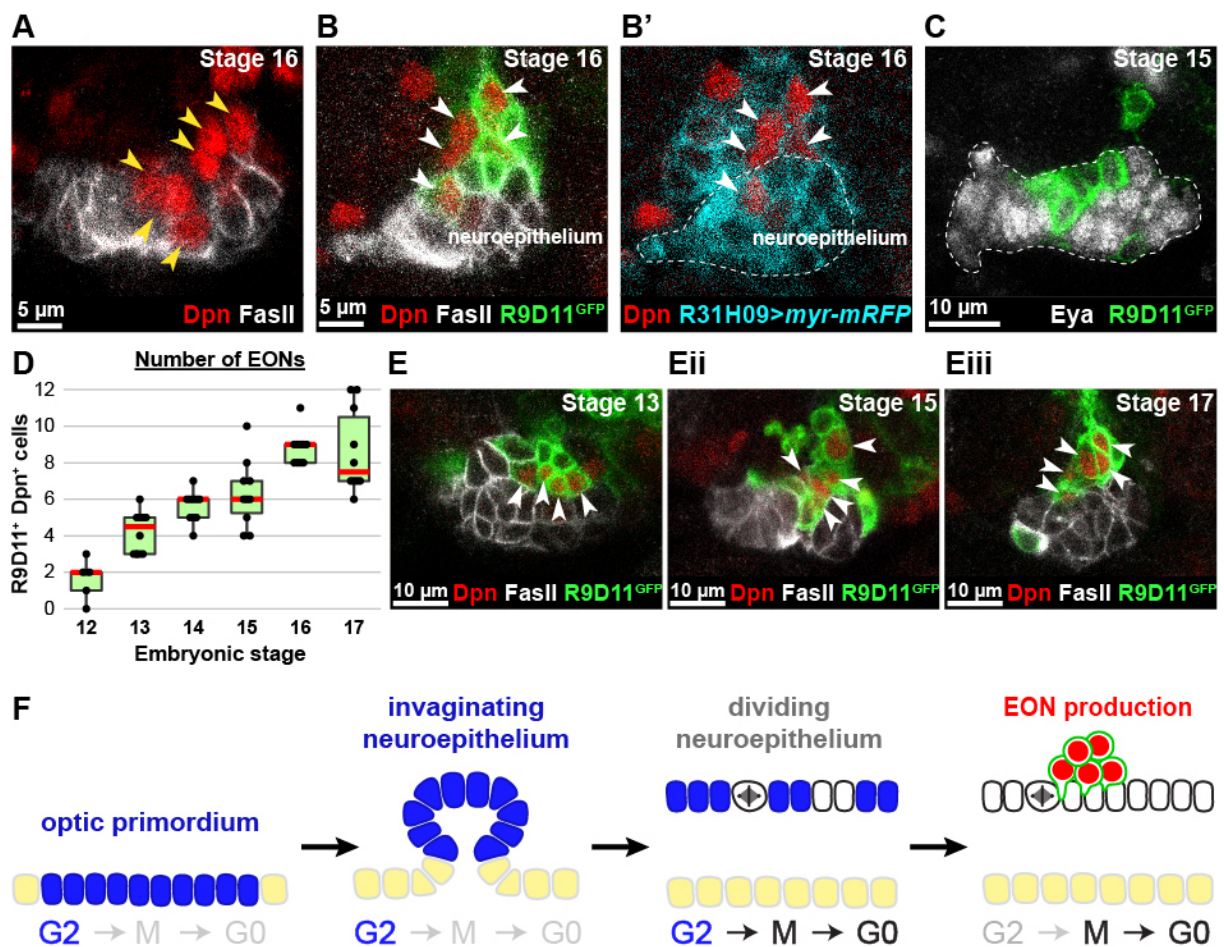


**Figure 5.5: The embryonic neuroepithelium divides to give rise to EONs**

(A) Neuroblasts ( $Dpn^+$ , red, yellow arrowheads) are found in close proximity to the neuroepithelium ( $FasII^+$ , white) in the embryo.

(B-B') Neuroblasts in close association with the neuroepithelium (white arrowheads) express the transition zone marker R9D11-mCD8-GFP (green) and inherit *myr-mRFP* (cyan) expressed in the neuroepithelium (R31H09-GAL4>*myr-mRFP*).

(C) EONs ( $R9D11\text{-mCD8-GFP}^+$ ) initially express *Eya* (white), which is expressed in the neuroepithelium (Erlik et al., 2008).

(D) Quantification of the number of EONs between embryonic stages 12 and 17.  $n = 10$  embryos/stage, except stage 12 for which  $n = 5$ . Red lines indicate medians.

(Ei-iii) EONs ( $Dpn^+$ ,  $R9D11\text{-mCD8-GFP}^+$ ) are generated throughout embryogenesis and remain in close contact with the neuroepithelium ( $FasII^+$ ).

(F) Schematic depicting the early stages of neuroepithelium development and the generation of EONs. Single section confocal images. All panels provided by LO (except C and F, provided by AEH).

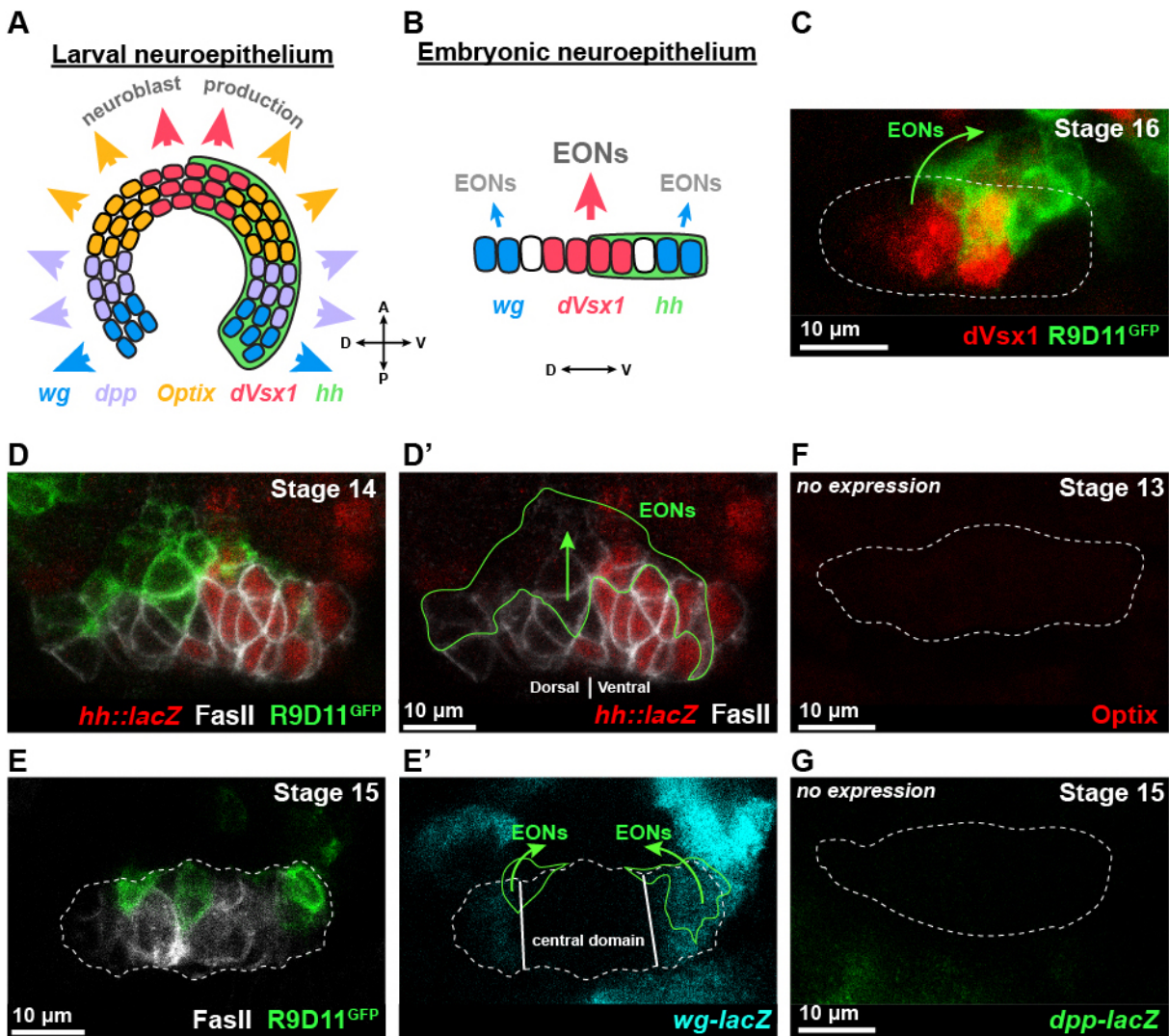


**Figure 5.6: The *dVsx1* and *wg* domains of the embryonic neuroepithelium produce EONs**

(A) The larval neuroepithelium is spatially patterned along the A-P axis by the expression of *dVsx1*, *Optix*, *dpp*, and *wg*. The ventral but not dorsal half of the neuroepithelium expresses *hh*. A: anterior; P: posterior; D: dorsal; V: ventral.

(B) The *wg*, *dVsx1* and *hh* domains are present in the embryonic neuroepithelium but the *Optix* and *dpp* domains are not yet established. D: dorsal; V: ventral.

(C) The majority of EONs (R9D11-mCD8-GFP<sup>+</sup>, green) arise from the *dVsx1*<sup>+</sup> (red) domain of the neuroepithelium.

(D-D') EON production (R9D11-mCD8-GFP) spans the dorsal-ventral boundary of the neuroepithelium (FasII<sup>+</sup>), as defined by *hh::lacZ* expression.

(E-E') A small proportion of EONs (R9D11-mCD8-GFP) are generated by the *wg* domains of the neuroepithelium (FasII<sup>+</sup>), as assessed by *wg-lacZ*.

(F) *Optix* is not expressed in the embryonic neuroepithelium as assessed by immunostaining with an antibody raised against *Optix*.

(G) *dpp* is not expressed in the embryonic neuroepithelium, as assessed by *dpp-lacZ* expression.

Single section confocal images. Panels (A, B, E, E') provided by AEH; panels (C, D, D', F, G) provided by LO.

### **5.3 Characterising EON production**

#### **5.3.1 EONs derive from two spatial domains of the neuroepithelium**

The larval neuroepithelium is patterned into distinct spatial domains: *dVsx1*, *Optix*, *decapentaplegic (dpp)* and *wingless (wg)* are expressed in discrete regions to pattern the neuroepithelium along the anterior-posterior axis (**Fig. 5.6A**) ((Erclik et al., 2008; Gold and Brand, 2014; Kaphingst and Kunes, 1994); reviewed by (Bertet, 2017)) and the ventral (but not dorsal) half of the neuroepithelium expresses *hedgehog (hh)* (**Fig. 5.6A**) (Chen et al., 2016; Evans et al., 2009). All spatial domains of the neuroepithelium generate neuroblasts during the progression of the proneural wave in mid-late larval stages. However, we observed EON production from distinct regions of the embryonic neuroepithelium. This suggested that only a subset of the neuroepithelial spatial domains gave rise to EONs (**Fig. 5.6B**).

We found that almost all EONs originated from the central region, which corresponds to the *dVsx1*<sup>+</sup> domain (**Fig. 5.6C**). The central domain of EONs also overlapped the dorsal-ventral boundary, as defined by *hh* expression (**Fig. 5.6D**). We observed that the *wg*<sup>+</sup> tips of the neuroepithelium were also competent to produce EONs, albeit fewer than the central domain (**Fig. 5.6E-E'**). We could not detect expression of *Optix* (**Fig. 5.6F**) or *dpp* (**Fig. 5.6G**) in the embryonic neuroepithelium, suggesting that the patterning of these domains occurs later in development. Therefore, we conclude that the central domain, and to a lesser extent the tips, of the embryonic neuroepithelium produce neuroblasts.

#### **5.3.2 The embryonic neuroepithelium expresses transition zone markers**

The transformation of neuroepithelial cells to neuroblasts occurs at a transition zone in larvae. Cells at the transition zone express R9D11-mCD8-GFP (this study, see **Fig. 5.2**), *l'sc* (Yasugi et al., 2008), and the microRNA *miR-7* (Caygill and Brand, 2017) (**Fig. 5.7A**). In addition, the transition is regulated by epidermal growth factor receptor (EGFR) and Notch signalling (**Fig. 5.7A**) (Egger et al., 2010; Yasugi et al., 2010). As in larval stages, we found that R9D11-mCD8-GFP expression coincided with *L'sc* (**Fig. 5.7B**). Furthermore, these *L'sc*<sup>+</sup> cells exhibited many features of the larval transition zone: they were positive for EGFR signalling (**Fig. 5.7C-C'**), expressed *miR-7* (**Fig. 5.7D**) and downregulated Notch signalling (**Fig. 5.7E-E'**). This suggests that common molecular mechanisms regulate the generation of neuroblasts from the neuroepithelium during embryogenesis and larval development.

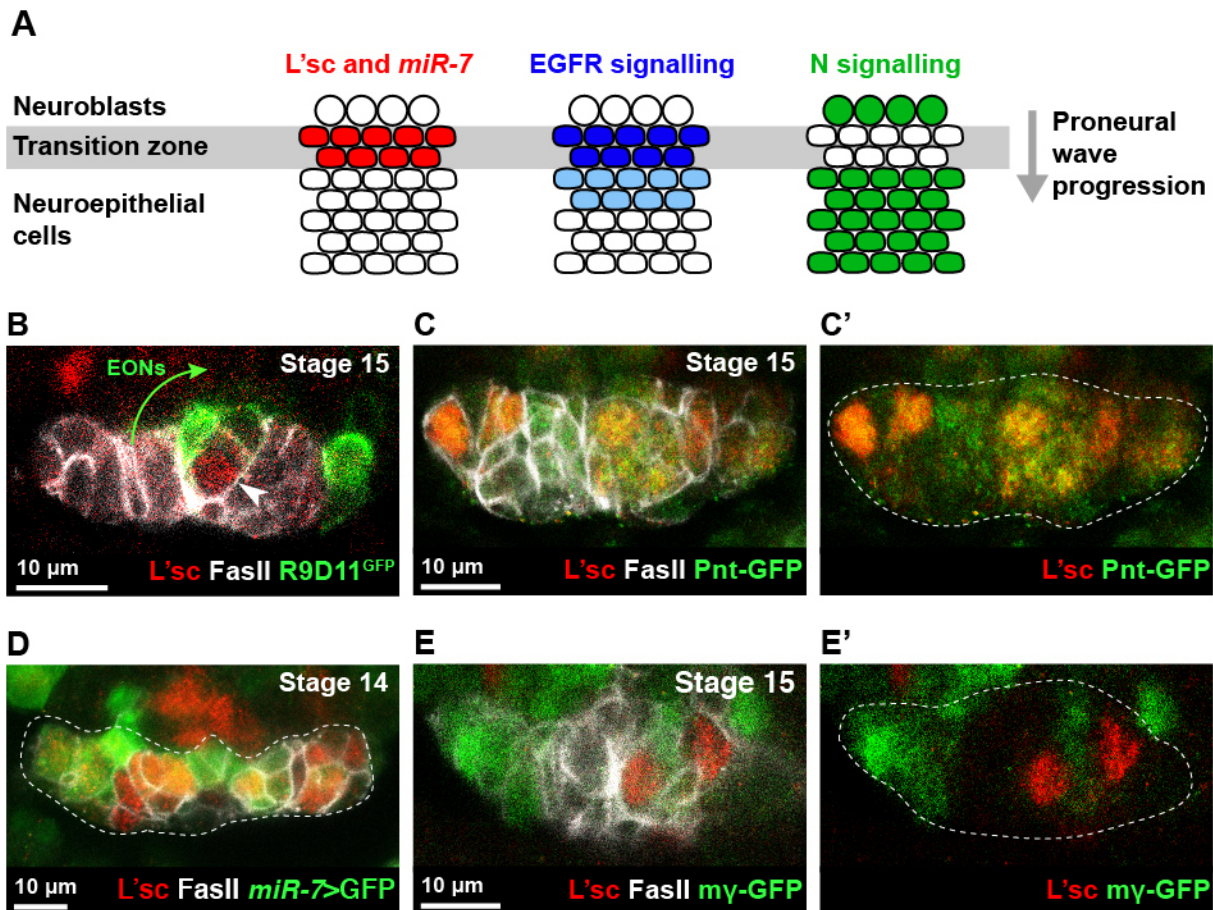


**Figure 5.7: Transition zone markers are expressed in the embryonic neuroepithelium at sites of EON production**

(A) The progression of the proneural wave (grey arrow) converts neuroepithelial cells to neuroblasts at the transition zone (highlighted in grey). The transition zone is characterised by the expression of L'sc and *miR-7* (red), active EGFR signalling (blue) and low Notch signalling (green).

(B) L'sc (red) is expressed in the neuroepithelium (FasII<sup>+</sup>, white) at the regions of R9D11-mCD8-GFP (green) expression.

(C-C') L'sc<sup>+</sup> cells in the neuroepithelium (FasII<sup>+</sup>) are active for EGFR signalling (green), as assessed by Pnt-GFP (a downstream effector of the EGFR pathway).

(D) The transition zone marker microRNA *miR-7* (green) is expressed in L'sc<sup>+</sup> cells in the neuroepithelium (FasII<sup>+</sup>).

(E-E') Notch signalling is downregulated, as assessed by *my*-GFP (green), in neuroepithelial cells (FasII<sup>+</sup>) that express L'sc.

Single section confocal images. Panel (A) provided by AEH; panels (B-E') provided by LO.

### 5.3.3 EONs generate neurons and glia

We showed that EONs are produced from the neuroepithelium in a similar manner to larval optic lobe neuroblasts. In larval stages, asymmetric divisions of optic lobe neuroblasts generate GMCs, which undergo a terminal division to produce neurons and glia. We tested if EONs divided to generate progeny in the embryo. We found that EONs divided and that R9D11-mCD8-GFP encompassed Dpn<sup>+</sup> cells (EONs) and Dpn<sup>-</sup> cells (progeny) (Fig. 5.8A). Furthermore, EONs exhibited asymmetric localisation of Pros and Mira, which is a hallmark of neuroblast neurogenic divisions (Ikeshima-Kataoka et al., 1997) (Fig. 5.8B). We found that the R9D11-mCD8-GFP<sup>+</sup> Dpn<sup>-</sup> cells included GMCs (identified by nuclear Pros, Fig. 5.8C-C'),

neurons (identified by Elav, **Fig. 5.8D-D'**) and glia (identified by Repo, **Fig. 5.8E**). Taken together, these findings indicate that EONs divide in the embryo to generate neurons and glia (**Fig. 5.8F**) ( $16.1 \pm 1.7$  neurons and  $3.7 \pm 1.4$  glia per brain lobe at the end of embryogenesis, ( $n = 10$  brain lobes).

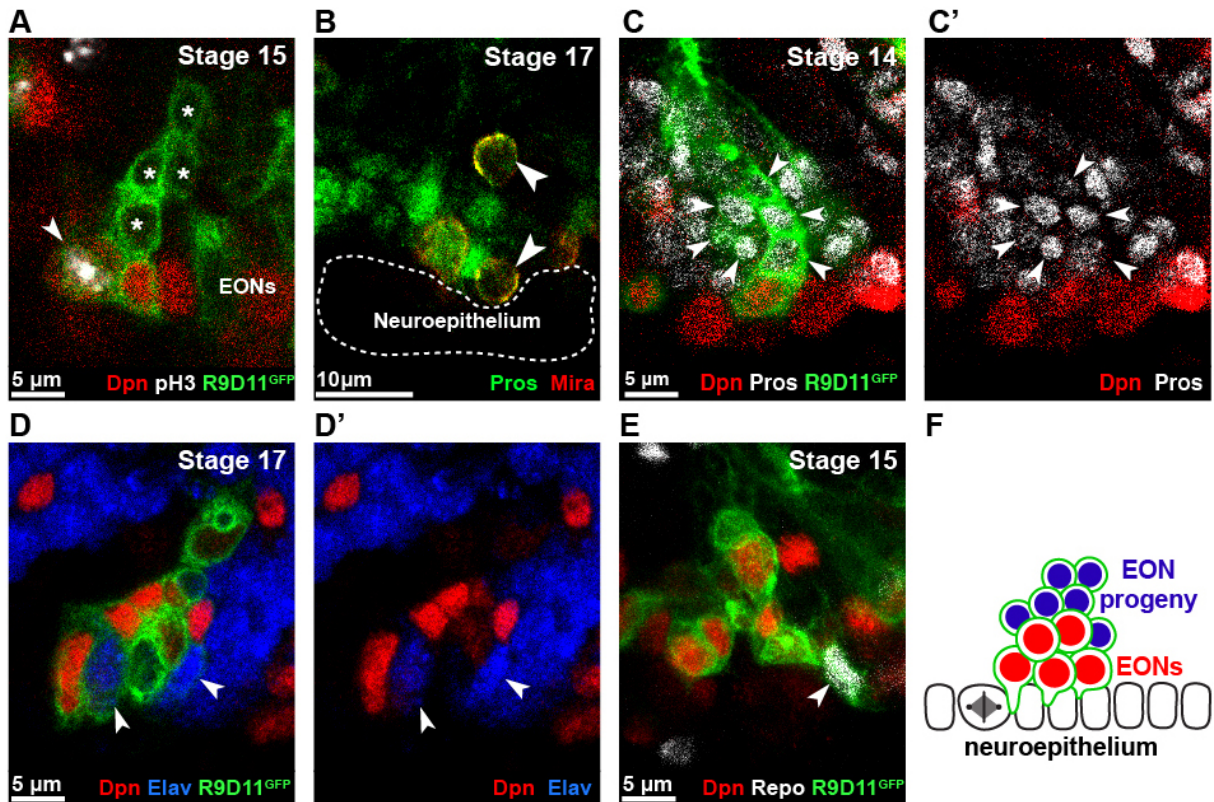


**Figure 5.8: EONs generate neurons and glia**

(A-A') EONs (Dpn<sup>+</sup>, red, R9D11-mCD8-GFP<sup>+</sup>, green) divide, as assessed by immunostaining for p3H3 (white). Dpn<sup>-</sup> R9D11-mCD8-GFP<sup>+</sup> progeny (asterisks) are in close association with EONs.

(B-B') EONs show asymmetric localisation of Pros (green) and Mira (red), which is characteristic of neurogenic neuroblast divisions.

(C-C') Many small, Pros<sup>+</sup> (white) cells lie in close contact with EONs (Dpn<sup>+</sup>, red) and retain R9D11-mCD8-GFP (green) expression.

(D-D') EONs (Dpn<sup>+</sup>, red, R9D11-mCD8-GFP<sup>+</sup>, green) give rise to neurons (Elav<sup>+</sup>, blue) that maintain R9D11-mCD8-GFP expression.

(E-E') Repo<sup>+</sup> cells that also express R9D11-mCD8-GFP (green) and are in close proximity to EONs (Dpn<sup>+</sup>, red, R9D11-mCD8-GFP<sup>+</sup>), indicating that EONs give rise to glia.

(F) Schematic depicting the generation of EONs (red) from the embryonic neuroepithelium. EONs divide to generate progeny (blue) that retain R9D11-mCD8-GFP (green) expression.

Single section confocal images. Panels A-E provided by LO; panel F provided by AEH.

We confirmed the lineage relationship between EONs and neurons using flip-out LexA amplification (FLEXAMP), a memory cassette tool (**Fig. 5.9A**) (Bertet et al., 2014; Yagi et al., 2010). FLEXAMP combines the GAL4 and LexA systems, which are independent binary transcriptional systems, to allow lineage tracing; GAL4 activates the expression of genes under the control of UAS whereas LexA activates genes under the control of lexAop (referred to as lexO). The use of FLEXAMP for lineage tracing requires a specific GAL4 for the cells

of interest. GAL4 activates the expression of UAS-*FLP*, which excises a transcriptional stop sequence between an *act* promoter and LHV<sub>2</sub>. LHV<sub>2</sub> is a GAL80-insuppressible LexA transcriptional activator (Yagi et al., 2010) that binds to lexO and activates transcription, in this case of *mCD8-GFP* (Fig. 5.9A). Using GAL80<sup>ts</sup> to restrict GAL4 expression to the desired temporal window allows lineage tracing to be initiated at specific developmental stages.

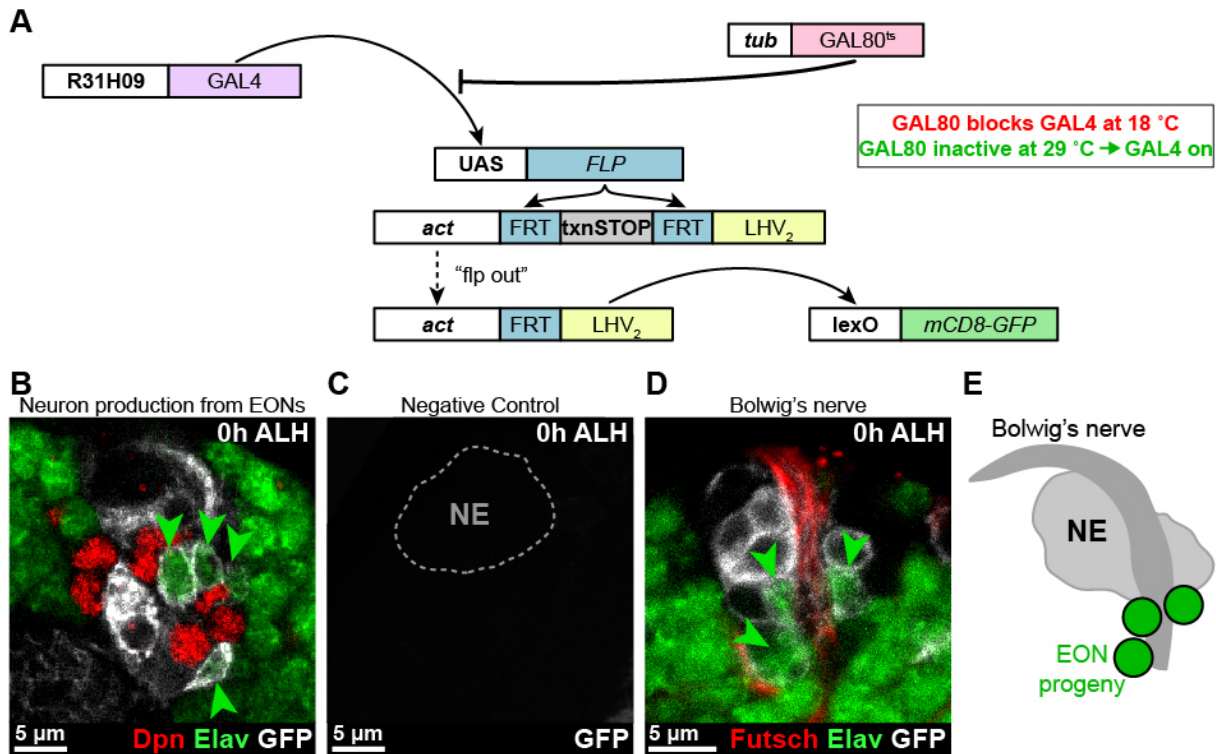


**Figure 5.9: Lineage tracing confirms that EONs generate neuronal progeny that lie in close contact with the larval visual system**

(A) Schematic showing the genetic components of FLEXAMP. At the restrictive temperature for *tub-GAL80<sup>ts</sup>*, R31H09-GAL4 drives the expression of UAS-*FLP* in the neuroepithelium, which catalyses the excision of a transcriptional stop sequence from the “flp-out” cassette. This results in the *act* promoter driving the expression of LHV<sub>2</sub> (a GAL80-insuppressible LexA transcriptional activator) that binds to and activates transcription from lexO sequences, such as *mCD8-GFP* for lineage tracing.

(B) Green arrowheads indicate neurons (Elav<sup>+</sup>, green) produced by EONs (Dpn<sup>+</sup>, red) that are labelled using FLEXAMP (white) at larval hatching. Image is a single section confocal image.

(C) In the negative control for FLEXAMP, no cells are labelled by GFP at larval hatching. Embryos were kept at 18 °C to maintain GAL80<sup>ts</sup> activity. Image is a projection over 14 µm in z.

(D) Green arrowheads indicate neurons (Elav<sup>+</sup>) produced by EONs labelled using FLEXAMP (white), which lie in close contact with Bolwig’s nerve (Futsch<sup>+</sup>, red). Image is a projection over 1 µm in z.

(E) Schematic depicting the spatial relationship between the neuroepithelium (NE), Bolwig’s nerve and EON progeny (green) at larval hatching.

All panels provided by AEH.

Unfortunately, we have been unable to identify a GAL4 driver that labels EONs specifically and so we were limited to neuroepithelial GAL4 driver lines to perform lineage tracing in early developmental time points. Expressing FLEXAMP in the embryonic neuroepithelium allowed us to recover labelled neurons (**Fig. 5.9B-C**) and revealed that a large number of the neuronal progeny were in close proximity to Bolwig's nerve (**Fig. 5.9D**). Bolwig's nerve is part of the larval visual system (Larderet et al., 2017; Schmucker et al., 1997; Schmucker et al., 1992; Tix et al., 1989), the development of which is not well understood, suggesting that neurons generated by EONs contribute to the larval visual processing system (**Fig. 5.9E**). We conclude that, like canonical neuroblasts, EONs undergo neurogenic divisions and generate differentiated progeny.

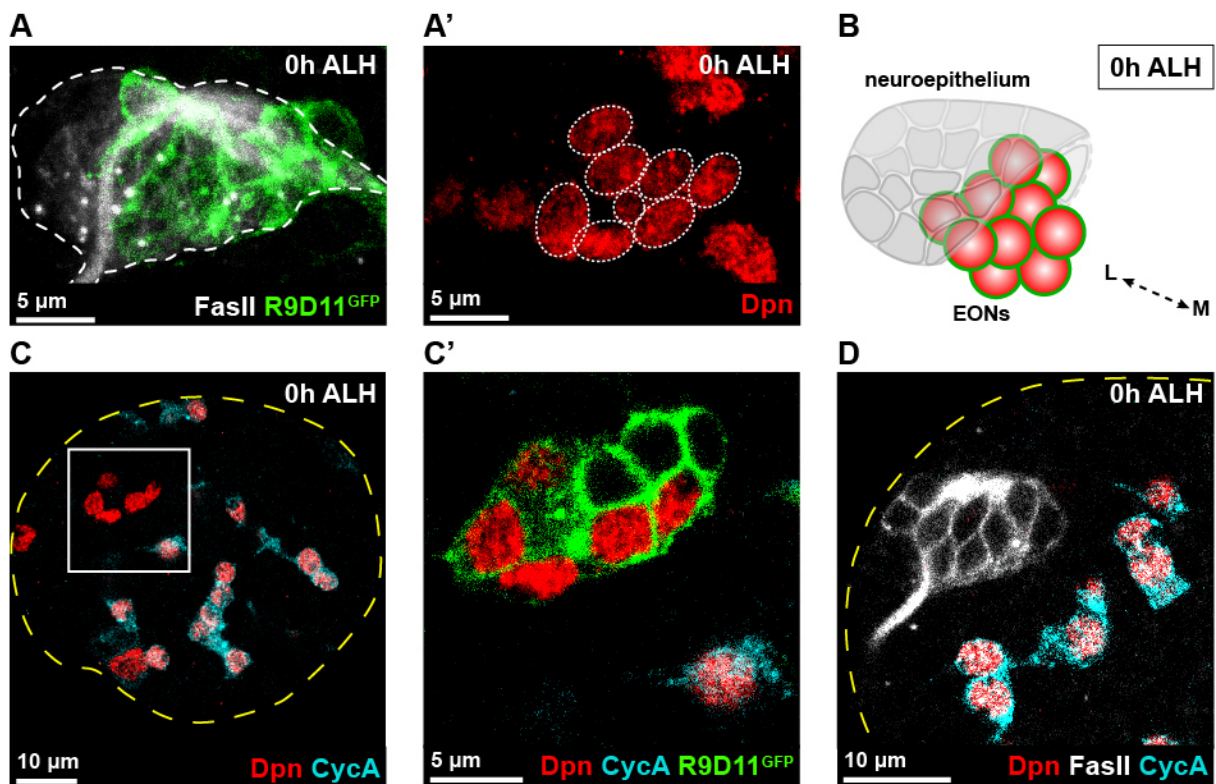


**Figure 5.10: EONs persist in the larval brain in  $G_0$  quiescence**

(A-A') EONs ( $Dpn^+$ , red,  $R9D11-mCD8-GFP^+$ , green) are found in the larval brain in close association with the neuroepithelium ( $FasII^+$ , white). Images are a single frame from a 3D projection.

(B) Schematic depicting the spatial relationship between EONs (red with green outline) and the neuroepithelium at 0 hours ALH. EONs are found medially, towards the centre of the brain, with respect to the neuroepithelium. L: lateral; M: medial.

(C-C') EONs ( $Dpn^+$  and  $R9D11-mCD8-GFP^+$ ) do not express the  $G_2$  cyclin ( $CycA$ , cyan) at larval hatching, demonstrating that EONs are quiescent in  $G_0$  phase of the cell cycle.  $G_0$  quiescence is rare in comparison to  $G_2$  quiescence ( $CycA^+$ ,  $Dpn^+$ ) in the larval CNS. (C') is a magnification of the boxed region highlighted in (C).

(D) The neuroepithelium ( $FasII^+$ ) also undergoes  $G_0$  quiescence. The neuroepithelium does not express  $CycA$  (cyan) at larval hatching, in contrast to the majority of NSCs in the central brain ( $Dpn^+$ ,  $CycA^+$ ). Single section confocal images, unless indicated otherwise. All panels provided by AEH.

## **5.4 EONs in the post-embryonic brain**

### **5.4.1 EONs undergo G<sub>0</sub> quiescence and persist into the larval brain**

The majority of the neuroblasts in the CNS enter mitotic quiescence or undergo apoptosis at the end of the embryogenesis (Maurange and Gould, 2005; Truman and Bate, 1988; White et al., 1994). Quiescent neuroblasts are maintained in the larval brain and re-enter the cell cycle in a nutrition-dependent manner to resume neurogenesis (Britton and Edgar, 1998; Chell and Brand, 2010; Otsuki and Brand, 2018; Sousa-Nunes et al., 2011; Spéder and Brand, 2014; Truman and Bate, 1988). We investigated whether EONs are maintained in the larval brain.

We found that EONs are present in brains from newly hatched larvae. EONs could be identified as a cluster of Dpn<sup>+</sup> R9D11-mCD8-GFP<sup>+</sup> cells in close association with the neuroepithelium (EONs were located medially to the neuroepithelium, as in the embryo) (**Fig. 5.10A-B**). We observed 10.4±0.6 EONs per brain lobe at 0 hours ALH ( $n = 31$  brain lobes), which is comparable to the number found at the end of embryogenesis. Previous studies showed that the only neuroblasts that continue to proliferate at larval hatching are the mushroom body and lateral neuroblasts (Ito and Hotta, 1992; Prokop and Technau, 1991; Truman and Bate, 1988), indicating that EONs are quiescent at this stage.

The Brand Lab discovered recently that neuroblasts can reside in two types of quiescence (Otsuki and Brand, 2018); the majority of quiescent neuroblasts arrest in the G<sub>2</sub> phase of the cell cycle, and the minority in G<sub>0</sub>. The type of quiescence has functional significance because G<sub>2</sub> neuroblasts re-enter the cell cycle faster than G<sub>0</sub> neuroblasts in response to nutritional inputs (Otsuki and Brand, 2018). We found that all EONs undergo G<sub>0</sub> quiescence, as they did not express the G<sub>2</sub> marker CycA at 0 hours ALH (**Fig. 5.10C-C'**). In addition, we found that neuroepithelial cells also become G<sub>0</sub> quiescent (**Fig. 5.10D**) demonstrating that all NSCs in the developing visual system undergo G<sub>0</sub> quiescence, which is otherwise uncommon in the *Drosophila* brain.

### **5.4.2 EONs turn off R9D11-mCD8-GFP before they re-enter the cell cycle**

At hatching, EONs were identifiable as Dpn<sup>+</sup> R9D11-mCD8-GFP<sup>+</sup> CycA<sup>-</sup> cells adjacent to the neuroepithelium (**Fig. 5.10**). The absence of CycA provided a useful marker to follow EONs during early larval development before neuroblasts re-enter the cell cycle. At 6 hours ALH, the neuroepithelium and EONs remained associated closely (**Fig. 5.11A**) and both NSC populations were quiescent and negative for CycA (**Fig. 5.11A'**). At this stage, EONs retained R9D11-mCD8-GFP expression but at a lower level (**Fig. 5.11A''**).

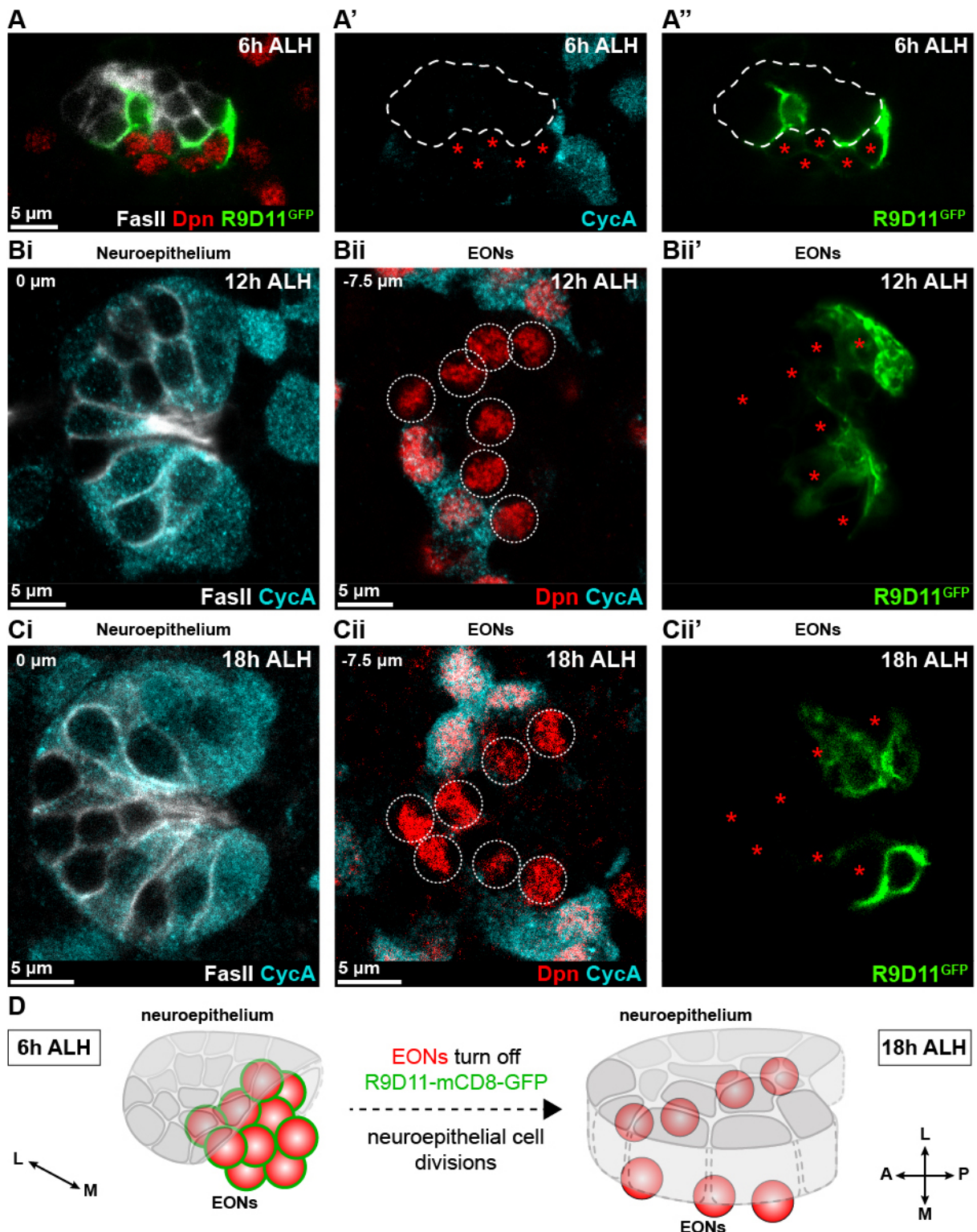


**Figure 5.11: EONs turn off R9D11-mCD8-GFP before re-entering the cell cycle**

(A-A'') At 6 hours ALH, neuroepithelial cells ( $\text{FasII}^+$ , white) and EONs ( $\text{Dpn}^+$ , red) remain quiescent ( $\text{CycA}^-$ , cyan). EONs (red asterisks in A' and A'') are in close association with neuroepithelium (dotted white outline in A' and A'') and begin to downregulate R9D11-mCD8-GFP (green).

(Bi-Bii') At 12 hours ALH, the neuroepithelium has re-entered the cell cycle ( $\text{FasII}^+ \text{CycA}^+$ ). EONs remain quiescent ( $\text{Dpn}^+ \text{CycA}^-$ ) and many show no/extremely weak R9D11-mCD8-GFP expression.

(Ci-Cii) At 18 hours ALH, neuroepithelial cells ( $\text{FasII}^+$ ) continue to express CycA but EONs ( $\text{Dpn}^+$ ) do not. EONs (red asterisks) no longer express R9D11-mCD8-GFP at this time point.

(D) EONs are closely associated with the neuroepithelium in the first few hours ALH. Once the neuroepithelium has re-entered the cell cycle, EONs are found medial the neuroepithelium and lose R9D11-mCD8-GFP expression over time. L: lateral; M: medial; A: anterior; P: posterior.

Single section confocal images. All panels provided by AEH.

Neuroepithelial cells begin symmetric, expansive divisions between 12 and 15 hours ALH (Datta, 1995; Ebens et al., 1993; Hofbauer and Campos-Ortega, 1990; Prokop and Technau, 1994; White and Kankel, 1978). As a consequence, neuroepithelial cells expressed CycA at 12 hours ALH (**Fig. 5.11Bi**). In contrast, quiescent neuroblasts remained dormant (Ito and Hotta, 1992; Prokop and Technau, 1991; Truman and Bate, 1988) and, accordingly, EONs remained CycA negative at 12 hours ALH (**Fig. 5.11Bii**). Furthermore, the majority of EONs exhibited very weak R9D11-mCD8-GFP expression (**Fig. 5.11Bii'**), but could be identified by their lack of CycA expression and medial position to the neuroepithelium. At 18 hours ALH, the dividing neuroepithelium continued to express CycA (**Fig. 5.11Ci**) whereas EONs remained quiescent (small, CycA<sup>-</sup>) (**Fig. 5.11Cii**). At this stage, R9D11-mCD8-GFP expression in EONs was extremely weak or absent entirely and reliable identification of EONs was only possible based on their position relative to the neuroepithelium and the lack of CycA (**Fig. 5.11D**). At 24 hours ALH, an average of  $4.3 \pm 0.5$  Dpn<sup>+</sup> weak R9D11-mCD8-GFP<sup>+</sup> CycA<sup>-</sup> cells ( $n = 11$  brain lobes) were present in a medial position to the neuroepithelium, suggesting that most EONs had reactivated at this time point. This indicates that EONs are amongst the last neuroblasts to reactivate in the brain, consistent with the Brand Lab's previous finding that G<sub>0</sub> neuroblasts reactivate after G<sub>2</sub> neuroblasts (Otsuki and Brand, 2018).

#### **5.4.3 The fate of EONs after reactivation is unclear**

We found that R9D11-mCD8-GFP labels EONs during embryogenesis and soon after larval hatching, but this label is turned over during early larval development and so cannot be used for long term tracking of EONs or their progeny. We tried to label EONs permanently using genetic tools, but all methods tried have proved unsuccessful. R9D11-GAL4 driving UAS-*mCD8-GFP* labels EONs at larval hatching, albeit very weakly (**Fig. 5.12A**) but when R9D11-GAL4 is used for lineage tracing, for example using a “flp-out” cassette, EONs are not labelled (**Fig. 5.12B-B'**). Permanent labelling techniques that do label EONs are expressed in the neuroepithelium from embryonic stages, which results in all epithelial progeny being labelled, and so cannot be used to follow EONs once the neuroepithelium resumes cell divisions in larval stages (**Fig. 5.12C**).

While we have been unable to follow the fate of EONs into later stages of larval development, it is likely that they reactivate. This is supported by the observation that all neuroblasts surrounding the neuroepithelium have re-entered the cell cycle at 30 hours ALH (**Fig. 5.13Ai-**

Aii). Therefore, we have identified a new, embryonic phase of neuroepithelium division that generates a small population of neuroblasts that persist in the larval brain (Fig. 5.13B).

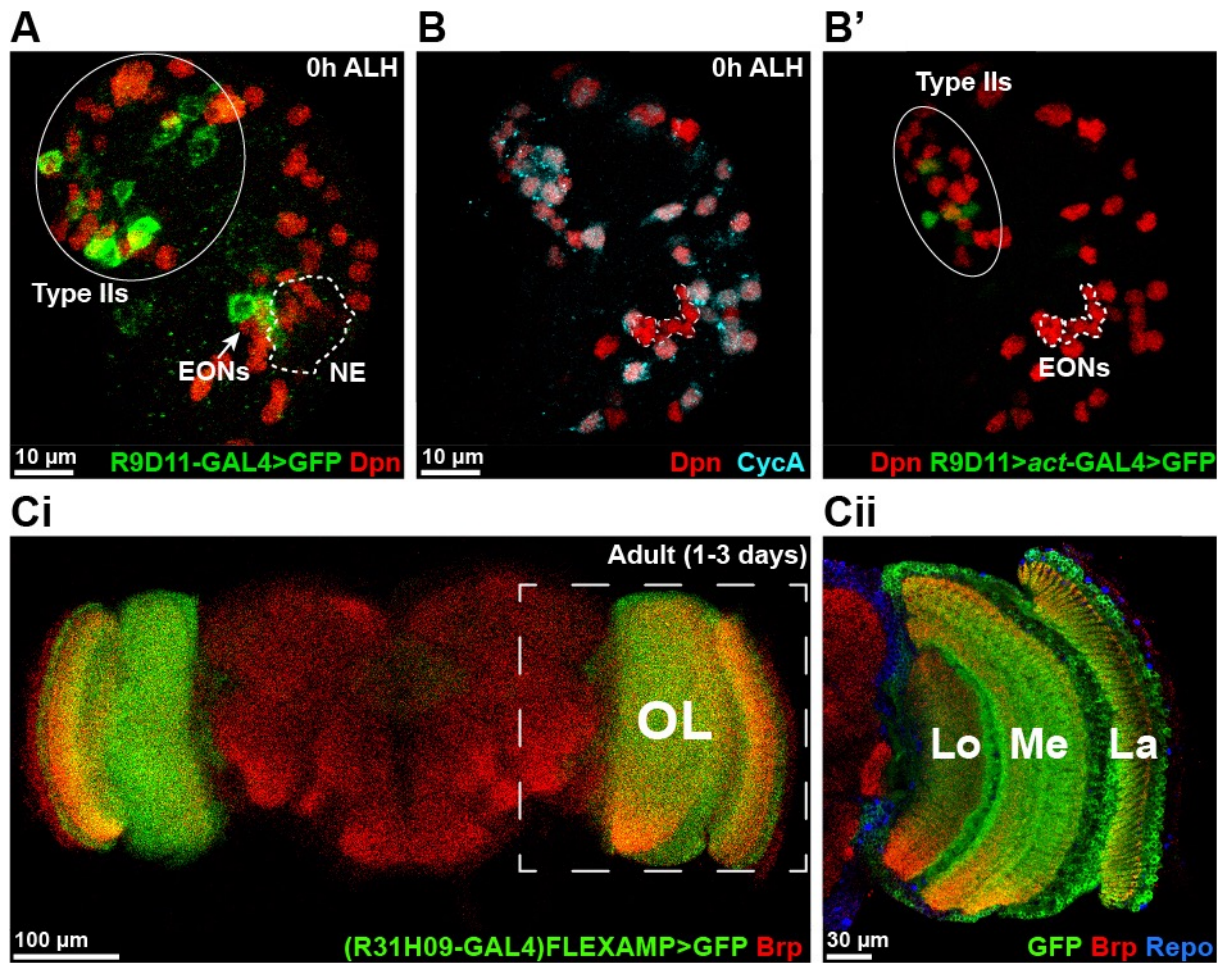


**Figure 5.12: Tracing the fate of EONs and their progeny is not possible with the tools available**  
 (A) At 0 hours ALH, R9D11-GAL4>mCD8-GFP (green) is expressed in only a few Dpn<sup>+</sup> cells next to the neuroepithelium (NE, white dotted outline), *i.e.* EONs. Strong expression is observed consistently in type II lineages (circled). Image is a projection over 13.6  $\mu\text{m}$  in z.  
 (B-B') At 0h ALH, EONs can be identified by the lack of CycA expression (cyan in B) and their location in the brain. R9D11-GAL4 driving the expression of an immortalisation cassette (*act5C*>FRT-txnSTOP-FRT>GAL4) does not label any EONs (white dotted outline) but does label type II lineages (circled). Image is a projection over 12  $\mu\text{m}$  in z.  
 (Ci-Cii) Performing FLEXAMP with R31H09-GAL4 (which labels EONs at hatching, see Fig. 5.9) results in labelling of the entire optic lobe (OL) in the adult brain, despite inactivation of the GAL4 after larval hatching (see Chapter 7 for experimental details). All neurons (Brp, red) and glia (Repo, blue) in the lobula (LO), medulla (Me) and lamina (La) appear to be labelled. The boxed region in Ci highlights the OL, which is shown in Cii. Single section confocal images. All panels provided by AEH.

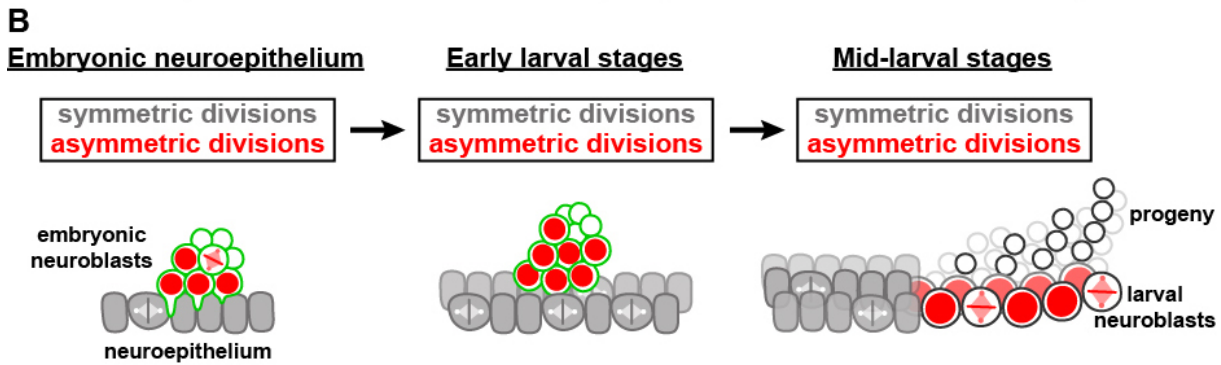
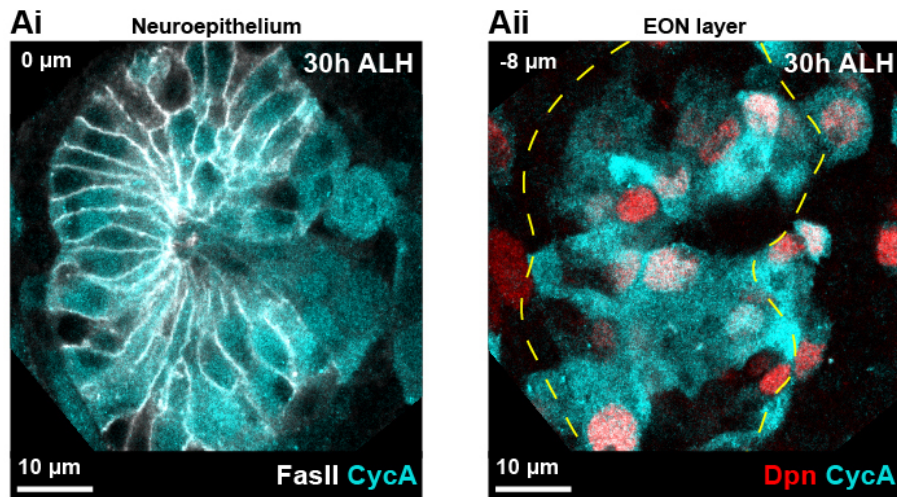


**Figure 5.13: All neuroblasts surrounding the neuroepithelium re-enter the cell cycle**  
 (Ai-Aii) At 30 hours ALH, neuroepithelial cells ( $FasII^+$ , white) continue to express CycA (cyan) as they undergo symmetric divisions to expand the neuroepithelium. All neuroblasts found medially to the neuroepithelium (*i.e.* in the EON layer) express CycA at this time, indicating that EONs resume cell divisions. Dashed yellow line indicates periphery of the neuroepithelium.  
 (B) Schematic showing a revised model in the developing visual system. In the embryo, neuroepithelial cells (grey) divide and generate neuroblasts (red). These neuroblasts are maintained in the larval brain and remain in close association with the neuroepithelium as symmetric neuroepithelial cell divisions begin. At mid-late larval stages, the proneural wave converts neuroepithelial cells to neuroblasts, which generate neurons and glial of the adult visual system.  
 All panels provided by AEH.

### 5.5 Early larval neuroblast transition

In the process of following EONs in early larval stages, which downregulate R9D11-mCD8-GFP, I observed strong R9D11-mCD8-GFP expression at the edges of the neuroepithelium. While EONs are found medially (“under”) the neuroepithelium, the strongly R9D11-mCD8-GFP<sup>+</sup> cells were in the plane of the neuroepithelium. Expression of R9D11-mCD8-GFP in this manner could be observed from 12 hours ALH (*i.e.* neuroepithelium reactivation) onwards (Fig. 5.14A).

As R9D11-mCD8-GFP is a marker of the neuroepithelial to neuroblast transition, I assessed if the early expression of R9D11-mCD8-GFP corresponded to neuroblast generation. At 12 hours ALH, no Dpn<sup>+</sup> cells were found within strong R9D11-mCD8-GFP<sup>+</sup> cells (Fig. 5.14A’).



### 5.5.1 Early larval optic lobe neuroblasts come from the *wg* domains

Dpn<sup>+</sup> R9D11-mCD8-GFP<sup>+</sup> cells were observed at the posterior tips of the neuroepithelium, which corresponded spatially to the *wg*<sup>+</sup> domains. Assessing *wg* expression showed that, indeed, strong R9D11-mCD8-GFP<sup>+</sup> cells in the plane of the neuroepithelium co-expressed *wg* or were in close association with cells that did (Fig. 5.15A-C). This indicated that the *wg*<sup>+</sup> domains of the neuroepithelium generate a small number of neuroblasts during early larval development, approximately 24 hours before the initiation of the proneural wave (which begins ~48 hours ALH).

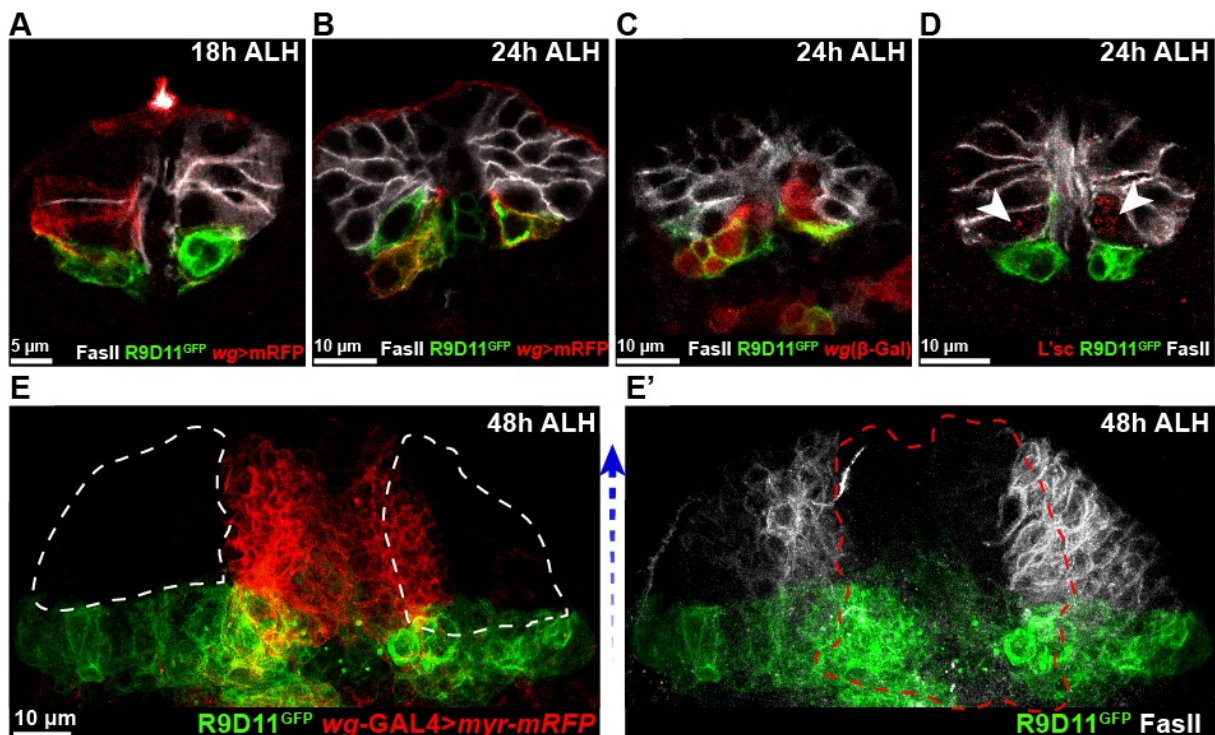


**Figure 5.15: The *wg* domain expresses the transition zone marker R9D11-mCD8-GFP during early larval development**

(A) R9D11-mCD8-GFP expression (green) overlaps with *wg*-GAL4>*myr-mRFP* (red) in the neuroepithelium (FasII<sup>+</sup>) at 18 hours ALH. Image is a projection over 2.5  $\mu$ m in z.

(B-C) R9D11-mCD8-GFP expression remains restricted to the *wg*<sup>+</sup> domain of the neuroepithelium (FasII<sup>+</sup>) at 24 hours ALH, as assessed by *wg*-GAL4>*myr-mRFP* (B) and *wg-lacZ* (C).

(D) Weak L'sc expression (arrowheads) is observed in the neuroepithelial cells immediately next to R9D11-mCD8-GFP<sup>+</sup> cells at 24 hours ALH.

(E-E') At 48 hours ALH, R9D11-mCD8-GFP expression overlaps with *wg*-GAL4>*myr-mRFP* (red and indicated by red dotted lines) in addition to other domains of the neuroepithelium (FasII<sup>+</sup> and indicate by white dotted lines). The direction of the proneural wave is indicated by the blue dotted arrow (between panels E and E'). Images are single frames taken from a 3D projection

Single section confocal images unless indicated otherwise. All panels provided by AEH.

The mechanisms that regulate this early phase of larval optic lobe neuroblast generation are not known. However, preliminary assessment of L'sc showed that a small number of cells (1 or 2) at the posterior tips of the neuroepithelium express low levels of L'sc (Fig. 5.15D). The co-expression of L'sc and R9D11-mCD8-GFP in early larval development is consistent with

the transition zones found in the embryo and later in larval development (**Fig. 5.15E-E'**).

The preliminary observation of neuroblast generation from the optic lobe neuroepithelium during early larval development is extremely intriguing. It suggests that the neuroepithelium is competent to produce neuroblasts throughout development, in contrast to the view that symmetric divisions precede neuroblast generation. Additional support for this observation comes from other studies that have identified expression of transition zone markers (L'sc and PntP1) at the edges of the neuroepithelium at late second instar stage, before the initiation of the proneural wave (Dillard et al., 2018; Sato et al., 2016).

However, due to the fluctuation of R9D11-mCD8-GFP throughout optic lobe development, additional genetic tools must be used to profile the generation of early larval optic lobe neuroblasts more carefully. This could be achieved by performing lineage tracing during early larval stages before the proneural wave is initiated. Lineage tracing could also be used to identify the role of these neuroblasts and their progeny. Overall, the re-examination of the early development of the neuroepithelium led to the identification of two new phases of neuroblast production: an embryonic phase and an early larval phase. This challenges the dogma that neuroblast production from neuroepithelial cells is restricted to late larval stages and demonstrates that the division mode of the optic lobe neuroepithelium is more dynamic than thought previously.

## **5.6 Chapter 5 discussion**

Type II neuroblasts and the optic lobe neuroepithelium are unique NSCs in the developing *Drosophila* brain that share parallel lineage transitions. R9D11-mCD8-GFP is a reporter of *erm* expression that has been used extensively to follow type II lineage progression (Janssens et al., 2014; Weng et al., 2010). I found that this reporter is expressed as neuroepithelial cells become neuroblasts, which facilitated the careful re-examination of the division mode and neuroblast generation from the neuroepithelium throughout development. This observation also suggests that *erm* could regulate the optic lobe transition zone, but this has not yet been explored.

Together with Dr Leo Otsuki, I have discovered that the neuroepithelium generates neuroblasts in the embryo and in the early stages of larval development before the initiation of the proneural wave (**Fig. 5.16**). We found that the neuroepithelium divides in the embryo and generates EONs. EONs divide in the embryo to generate neurons and glia, but the role of

these progeny is not known. However, we found that the neurons generated in the embryo lie in close contact with Bolwig's nerve, which is part of the larval visual system (Tix et al., 1989). The neuroepithelium generates the adult visual processing system during larval stages and so it is an attractive hypothesis that the neuroepithelium divides in the embryo to produce the larval visual system.

The discovery of a new phase of neuroblast production from the optic lobe neuroepithelium also raises questions about how the neuroepithelial to neuroblast transition is regulated throughout development. The proneural wave results in the conversion of neuroepithelial cells to neuroblasts, such that there are no neuroepithelial cells remaining at the end of larval development. This is not the case for the earlier stages of neuroblast generation, which occur in parallel with expansive symmetric neuroepithelial divisions. It will be an interesting topic for future study to investigate the mechanisms that regulate the early transition zones such that neuroepithelial cells are preserved for neuroblast production later in development.

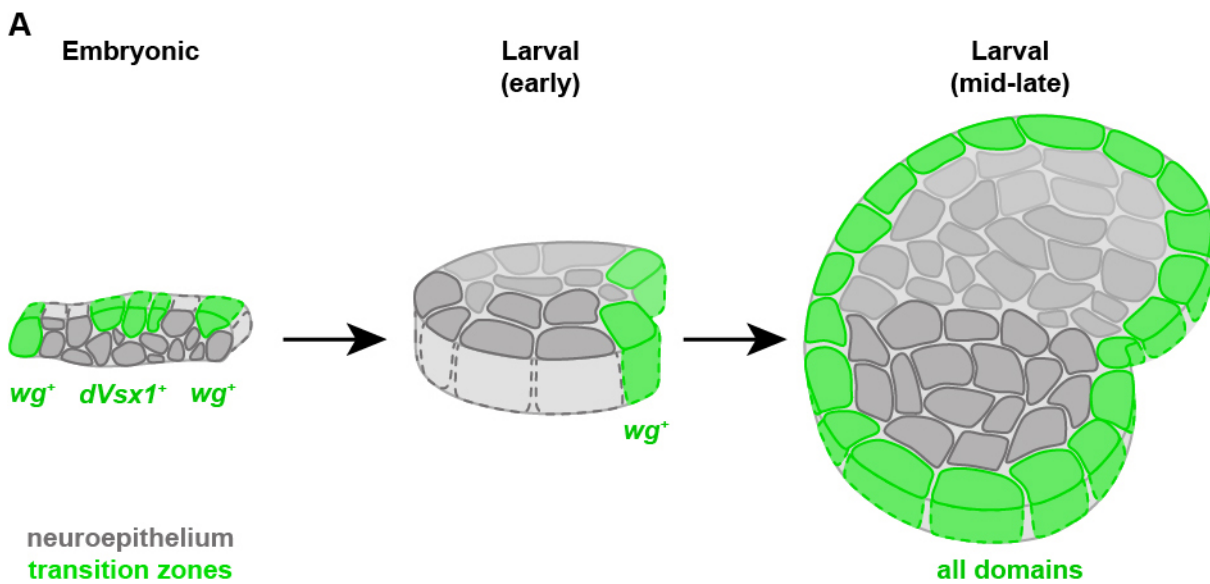


**Figure 5.16: Summary of transition zones in the neuroepithelium throughout development**

(A) The embryonic neuroepithelium (grey) generates neuroblasts from spatially distinct transition zones (green) in the *wg* and *dVsx1* domains. During early larval development, the *wg* domains show expression of transition zone markers and a small number of neuroblasts are generated. Later in larval development, transition zone markers are expressed in all spatial domains as the proneural wave converts neuroepithelial cells to neuroblasts. Previous models of neuroepithelium division did not include the embryonic or early larval phases of neuroblast generation.

All panels provided by AEH.

## Chapter 6

### Discussion

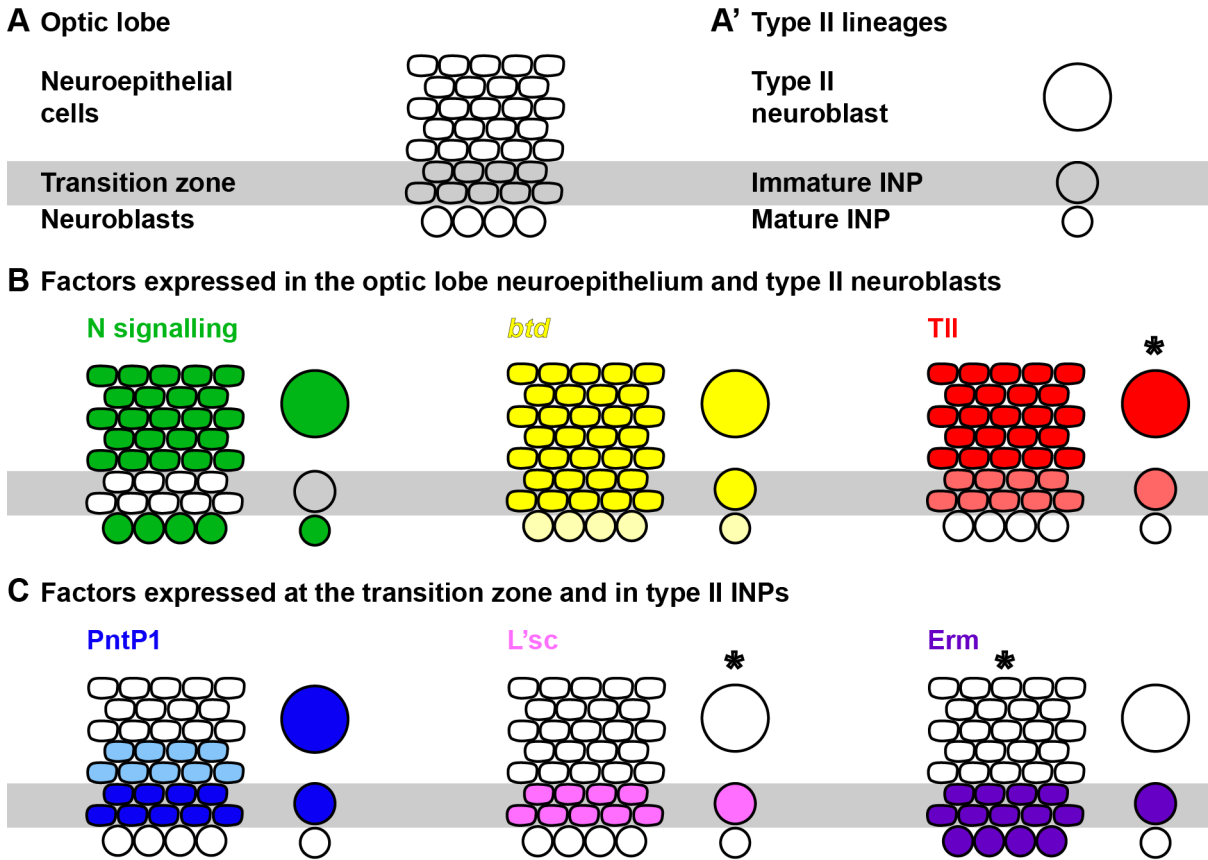
The maintenance of neural stem cells (NSCs) is essential for generating the correct number of neurons and glia during brain development. However, tumours can arise from NSC lineages if the division mode of NSCs is disrupted or if differentiation is prevented. Understanding the genetic programmes that regulate different NSC populations is central for understanding normal development and the diverse causes of tumourigenesis.

The *Drosophila* central nervous system (CNS) consists of many different types of NSCs that work together to create a functioning brain (for a review see (Doe, 2017)). Importantly, *Drosophila* NSCs share many similarities with their mammalian counterparts. For example, type II neuroblasts divide in a manner analogous to mammalian NSCs; they divide asymmetrically to generate INPs, which maintain the ability to self-renew but which have a restricted proliferation capacity (Bello et al., 2008; Boone and Doe, 2008; Bowman et al., 2008). Similarities also exist between the developing optic lobe and the mammalian cerebral cortex, in which symmetrically dividing neuroepithelial cells give rise to asymmetrically dividing NSCs (Brand and Livesey, 2011; Egger et al., 2011; Noctor et al., 2004). Intriguingly, there is considerable overlap in the molecular mechanisms that regulate different NSC lineage transitions in the *Drosophila* CNS and many of these genes have conserved mammalian counterparts.

#### **6.1 Common genetic mechanisms regulate different NSC populations**

The identification of common genetic networks that control distinct populations of NSCs within the *Drosophila* brain suggests that the fundamental mechanisms of NSC regulation could be conserved in other species. Investigating how conserved genes act in different developmental contexts in *Drosophila* provides an elegant system to improve our understanding of how diverse NSC division modes are regulated throughout development. Many transcription factors are expressed in NSCs of both the optic lobe and in type II lineages (**Fig. 6.1A-A'**). For example, expression of the Sp8 factor *btd* and active Notch signalling are common features of neuroepithelial cells and type II neuroblasts (**Fig. 6.1B**) (Egger et al., 2010; Komori et al., 2014a; Li et al., 2016; Xie et al., 2014; Younossi-Hartenstein et al., 1997). *tll* is also expressed in the optic lobe neuroepithelium, where it

maintains neuroepithelial cell fate (Daniel et al., 1999; Guillermin et al., 2015) and I found that *tll* is required in type II neuroblasts to promote NSC and lineage identity (Fig. 6.1B).



Gene expression identified in this study indicated by (\*)

**Figure 6.1: Common molecular mechanisms regulate NSC transitions in the developing optic lobe and type II neuroblast lineages**

(A) Optic lobe (OL) neuroepithelial cells transform into type I neuroblasts at the transition zone (grey). (A') In type II lineages, neuroblasts give rise to immature INPs (grey) that undergo maturation before dividing asymmetrically. There are multiple stages in INP maturation that are represented as a single state in this schematic for simplicity.

(B) Many genes are expressed in OL neuroepithelial cells and in type II neuroblasts. Notch (N) signalling (green) is absent from transition zone (Egger et al., 2010; Yasugi et al., 2010) and immature INPs (Bowman et al., 2008) but is active in other NSCs; *btd*-GAL4 (yellow) is expressed in both systems (Komori et al., 2014a; Xie et al., 2014; Younossi-Hartenstein et al., 1997); Tll (red) is expressed in the neuroepithelium (Guillermin et al., 2015; Younossi-Hartenstein et al., 1997) and in type II neuroblasts (this study), but is downregulated as the lineage progress.

(C) Genes that are expressed at the OL transition zone are also expressed in maturing INPs. PntP1 (blue) is expressed at the transition zone (Yasugi et al., 2010) and in type II neuroblasts and immature INPs (Zhu et al., 2011); L'sc (pink) marks the transition zone (Yasugi et al., 2008) and INP maturation (this study); Erm (purple) is a transition zone gene that remains expressed in OL neuroblasts (this study) and is also expressed in maturing INPs (Janssens et al., 2014; Weng et al., 2010).

Intriguingly, there is a number of genes that label both the optic lobe transition zone and maturing INPs in type II lineages (Fig. 6.1C): L'sc marks the front of the proneural wave (Yasugi et al., 2008) and I discovered that this gene is also expressed in immature INPs; PntP1 is expressed at the optic lobe transition zone as a downstream effector of EGFR

signalling and is also required for INP maturation (Yasugi et al., 2010; Zhu et al., 2011). However, the most informative discovery was that Erm, which is expressed in immature INPs (Weng et al., 2010), is expressed at the optic lobe transition zone (**Fig. 6.1C**). Using an *erm* reporter to follow the neuroepithelial to neuroblast transition led to the discovery of a small number of neuroblasts that are generated from the optic lobe during embryogenesis (EONs) and in the early stages of larval development. The optic lobe has been studied for many years, but the identification of new neuroblasts demonstrates that its development is still not fully understood.

The *Drosophila* optic lobe is considered to develop in a manner parallel to the mammalian cerebral cortex (Brand and Livesey, 2011) and so the discovery of EONs challenges the current dogma that neuroepithelial cells undergo sequential modes of cell division: an initial phase of symmetric, proliferative divisions that is followed by asymmetric, neurogenic cell divisions. Conserved molecular mechanisms regulate the transition from symmetric to asymmetric NSC divisions in *Drosophila* and mammals, suggesting that the mammalian neuroepithelium may also undergo as yet undiscovered neurogenic divisions during early developmental stages.

Understanding how different populations of NSCs are regulated throughout development is essential for improving our understanding of disorders that affect the nervous system and also the cellular events that can give rise to cancer. Interestingly, the most frequent human cancers arise from epithelial tissues (such as skin, colon, breast and lung) (Ferlay et al., 2010) and so the dynamics of the neuroepithelium are particularly relevant for tumour studies. However, the cancer cell of origin is likely to differ between tumour types found within the same tissue (reviewed in (Blanpain, 2013; Pisapia, 2017)). For example, neuroepithelial cells give rise to neuroblasts that generate post-mitotic neurons; symmetrically dividing neuroepithelial cells are the tumour cells of origin in *lethal(3)malignant brain tumour (l(3)mbt)* mutants (Richter et al., 2011) whereas *longitudinals lacking (lola)* mutations affect the lineages of asymmetrically dividing neuroblasts (Southall et al., 2014). Therefore, we must continue to explore how NSCs are regulated during development and the molecular mechanisms involved.

## **6.2 TLX: implications for brain disorders and tumour initiation**

The orphan nuclear receptor TLX is expressed at high levels in aggressive glioblastoma multiforme (GBMs) and correlates with poor patient survival (Park et al., 2010; Zou et al., 2012). Furthermore, TLX is expressed in glioblastoma stem cells (GSCs), which are thought

to be resistant to conventional therapies and reinitiate tumour growth (Cui et al., 2016). High levels of TLX can also induce NSC expansion *in vivo*, and generate malignant gliomas when combined with additional mutations, suggesting a role for TLX in glioma initiation (Liu et al., 2010; Park et al., 2010; Zou et al., 2012). TLX is also expressed in endogenous NSCs during development and adulthood and is required for NSC self-renewal and proper neurogenesis (Li et al., 2008; Liu et al., 2008; Monaghan et al., 1995; Shi et al., 2004; Yu et al., 1994). In addition, mice that lack TLX display aggressive behaviour (Monaghan et al., 1997; O’Leary et al., 2016; Roy et al., 2002; Young et al., 2002) and TLX is associated with hereditary cases of bipolar disorder and schizophrenia in humans (Dick et al., 2003; McQueen et al., 2005; Middleton et al., 2004; Wong et al., 2010). However, despite the developmental and clinical importance of TLX, the molecular mechanisms through which it controls NSC fate are not clear.

Much of the work in this thesis was focussed on investigating the role of Tll, the *Drosophila* counterpart of TLX, in type II neuroblast lineages. I found that Tll is expressed in type II neuroblasts and is downregulated as differentiation occurs, which is analogous to the expression of TLX in mammalian NSCs (Li et al., 2012; Liu et al., 2008). I followed the expression of cell fate markers to show that in the absence of *tll*, type II neuroblasts transform into type I neuroblasts, which have a more restricted self-renewal capacity. As a consequence, transit amplifying INPs are no longer generated and the resulting lineages have a lower neurogenic potential. Removing INPs from NSC lineages also has implications for cancer; mutation in *brat* or *erm* results in tumours arising from INPs, but type I lineages are not affected (Bowman et al., 2008; Weng et al., 2010).

In addition to behavioural disorders, TLX mutations are associated with microcephaly (Kumar et al., 2007b; Kumar et al., 2007a). However, the cell fate and lineage changes that occur when TLX function is disrupted in mammalian NSCs are not known. In light of the role of Tll in type II neuroblasts, mammalian NSCs with impaired TLX function could transition to a more restricted progenitor type that is unable to generate the full cohort of neurons and glia required for proper brain growth. It may also be the case that NSCs in different regions of the brain respond differently to the loss of TLX, as is the case in *Drosophila*, and so it would be interesting to perform lineage tracing on different populations of mammalian NSCs.

### **6.2.1 A conserved route to tumourigenesis**

I made use of the extensive genetic toolkit available in *Drosophila* to investigate the cellular and molecular mechanisms through which Tll/TLX contributes to tumour initiation from NSC lineages. I used the GAL4 system to express Tll at high levels in different cells within NSC lineages, which revealed that Tll tumours originated from type II INPs. High levels of Tll were sufficient to cause INPs to revert to neuroblast fate, prevent differentiation, and create tumours that consisted of type II neuroblasts. Importantly, this highlights the relevance of developmental genetic programmes in tumour initiation since Tll promotes type II neuroblast fate during development and in tumourigenesis.

*Drosophila* Tll and human TLX are highly conserved genes and so likely act through conserved molecular mechanisms (Jackson et al., 1998). I found that human TLX could also induce type II neuroblast tumours from *Drosophila* INPs, which indicates that Tll and TLX regulate common target genes and may recruit conserved cofactors in order to do so. These findings implicate NSC-derived intermediate progenitors as one possible cell of origin for TLX-induced tumours. Intriguingly, intermediate progenitors have been implicated in glioma initiation previously. Oligodendrocyte progenitor cells give rise to gliomas even when tumour suppressor mutations are present in the parent NSCs (Liu et al., 2011). It seems that intermediate progenitors present a genetic weak point in NSC lineages because they maintain many properties of NSCs and are susceptible to aberrant reactivation of the NSC genetic programme. I showed that TLX is an example of an oncogene that can initiate tumours from intermediate progenitors and this route to tumourigenesis should be investigated in mammalian glioblastoma models.

High levels of TLX are not only sufficient to induce glioma tumours from NSC lineages but high TLX expression has also been identified in glioblastoma stem cells (GSCs) (Cui et al., 2016; Liu et al., 2010; Park et al., 2010; Zhu et al., 2014). The relationship between NSCs and GSCs is still being explored and it is not clear if TLX regulates common genes in both cell types. One of my most intriguing findings was the regulatory relationship between TLX/Tll and *ase*. I found that Tll represses *ase* in type II neuroblasts during development and that tumours induced by Tll or TLX consisted of NSCs that lacked *ase* expression. This suggested that the repression of *ase* is central to the mechanism through which Tll/TLX controls NSC fate and tumour initiation. *Drosophila ase* is closely related to mammalian gene *ASCL1* and both genes are expressed in neural precursors to promote differentiation (Guillemot and Joyner, 1993; Johnson et al., 1990; Torii et al., 1999).

Intriguingly, a recent study identified that a subtype of GSCs isolated from patient GBM tumours showed downregulation of *ASCL1*, which influenced the survival of GSCs (Park et al., 2017). GSCs with high *ASCL1* expression were stimulated to produce neurons when Notch signalling was inhibited, but those with low *ASCL1* expression were not and continued to undergo self-renewal (Park et al., 2017). However, GSCs with low endogenous *ASCL1* expression could be stimulated to produce neurons if *ASCL1* was induced ectopically, which inhibited the self-renewal capacity of GSCs and attenuated tumourigenicity (**Fig. 6.2**) (Park et al., 2017). Given the relationship between Tll/TLX and *ase* in *Drosophila* NSC tumours, it is tempting to speculate that GSCs with low levels of *ASCL1* correspond to those with high *TLX* expression and that introducing *ASCL1* could restrict the growth of these GSCs. In support of this, I found that expressing *ase* ectopically in Tll-induced tumours could prevent tumour initiation and restore differentiation. It would be interesting to investigate if ectopic expression of *ase* prevents TLX-induced tumours in a similar manner, which would allow this regulatory relationship to be studied *in vivo*.

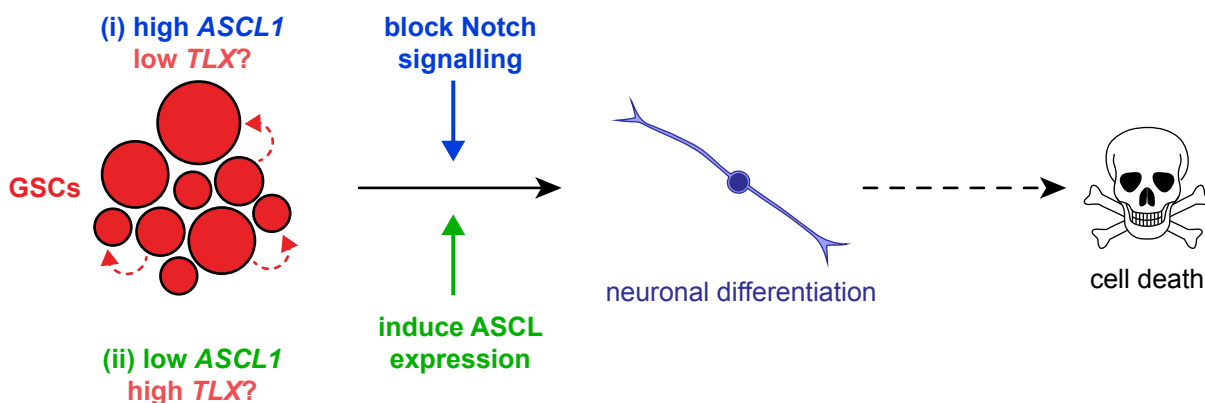


**Fig. 6.2: Targeting GSCs with differentiation therapy**

Glioblastoma stem cells (GSCs) were found to have (i) high or (ii) low *ASCL1* expression. GSCs with high *ASCL1* differentiated to neuronal fate when Notch signalling was blocked, but this did not occur in *ASCL1* low GSCs. Ectopic expression of *ASCL1* was required to induce neuronal fate from low *ASCL1* GSCs. Promoting neuronal differentiation inhibited GSC self-renewal and cultures reduced in size. Ectopic neurons are predicted to die *in vivo* due to the lack of synaptic partners. Based on data from (Park et al., 2017).

The ability of *ASCL1*-mediated neurogenesis to attenuate GSC self-renewal suggests that differentiation therapy could be an effective means of targeting GSCs. GSCs are thought to be one of the main sources of tumour regrowth following surgery and so targeting these tumour reinitiating cells will be an important therapeutic advance. However, the success of using neuronal differentiation as a means to remove GSCs is reliant on the resulting neurons being resistant to tumourigenic transformation. Promisingly, I found that neither TLX nor Tll were able to induce NSC fate or tumours from neurons, indicating that post-mitotic cells are not

competent to respond to ectopic expression of these genes. If differentiation therapy was implemented *in vivo*, it is proposed that the ectopic neurons generated would not form functional synapses and so would undergo apoptosis. In this way, GSCs could be removed from tumours *in vivo* by stimulating them to differentiate into neurons, which are resistant to tumourigenesis.

### **6.2.2 TLX as a therapeutic target**

TLX is an attractive therapeutic target for brain disorders and cancer. However, the lack of understanding surrounding the molecular mechanism of TLX has inhibited the translational applications of this gene. For example, TLX mutations are linked to microcephaly and bipolar disorder but treating these conditions with ectopic TLX expression carries the risk of inducing tumours. In order to realise the full potential of TLX as a therapeutic target for both developmental disorders and tumourigenesis, we must learn more about how TLX regulates NSCs *in vivo*.

I used targeted DamID (TaDa) to profile the genome wide binding sites of Tll in type II neuroblasts *in vivo*. These data complemented the genetic experiments and showed that Tll could regulate many type II-specific genes directly to promote type II neuroblast fate. However, TaDa also revealed that Tll has many target genes throughout the genome (2495, see **Appendix 2**). This is perhaps not surprising given that the transcriptional regulation by Tll and TLX is known to be mediated through the recognition of a relatively short consensus binding sequence (AAGTCA) and through the recruitment of a number of cofactors (reviewed in (Wang and Xiong, 2016)). Performing TaDa with Atrophin, a conserved cofactor of Tll and TLX (Wang et al., 2006; Zhi et al., 2015), could reveal common binding sites of Tll and Atrophin and so identify coregulated target genes. Furthermore, a bioinformatic approach could be used to analyse the sequences within Tll binding regions so as to identify putative cofactor binding sites. This approach has been used previously by the Brand Lab to identify novel cofactors of the homeodomain transcription factor Prospero (Southall et al., 2014).

As such, the Tll TaDa data provide an excellent starting point for improving our understanding of Tll/TLX function in NSCs. The Tll binding targets could be compared with gene expression changes in NSCs resulting from TLX manipulation (Liu et al., 2010; Qu et al., 2010; Zhang et al., 2008). In addition, the Brand Lab has recently developed mammalian targeted DamID (MaTaDa) to profile transcription factor binding in mammalian cells in culture (Cheetham et al., 2018) and has adapted this system to work *in vivo* (van den Aamele

et al., in preparation). Profiling TLX binding using MaTaDa in embryonic NSCs and in malignant GSCs would allow the identification of conserved target genes regulated by Tll and TLX during brain development and in tumourigenesis.

### **6.2.3 *Drosophila* as a drug screening system**

The diversity of glioblastoma tumours, both between patients and within individual tumours, makes developing effective treatments for these cancers extremely challenging. Creating simple screening systems to identify drugs, or drug combinations, that target different subtypes of GBMs could produce early leads on new therapies. TLX is expressed at high levels in a subset of GSCs and expression in these tumours correlates with poor patient prognosis (Cui et al., 2016; Liu et al., 2010; Park et al., 2010; Zhu et al., 2014). In this way, TLX is a useful diagnostic marker but also a therapeutic target for tumours that have high TLX expression. Human TLX can generate large brain tumours from *Drosophila* NSCs and so could provide a novel system to test drugs that target TLX *in vivo*. Drug screening in *Drosophila* has been used previously to identify novel drug combinations that target difficult-to-treat cancers, such as thyroid and lung cancer (Bangi et al., 2016; Das and Cagan, 2013; Das et al., 2013; Levine and Cagan, 2016; Sonoshita and Cagan, 2017). While no physiological ligand has been identified that regulates the activity of TLX, three small molecules have been identified that bind to TLX and modulate its ability to bind to DNA *in vitro* (Benod et al., 2014). This indicates that TLX may be druggable *in vivo* and suggests that further screening could identify additional compounds that bind to and mediate the function of TLX or its cofactors in brain tumours.

### **6.3 Concluding remarks**

This study has identified a novel regulator of type II neuroblasts (Tll) and discovered a new population of NSCs (EONs). These findings demonstrate the importance of *Drosophila* as a model system for studying the fundamental mechanisms of NSC regulation and neurogenesis. The identification of Tll as a regulator of type II neuroblast fate provides a simple, *in vivo* system in which to investigate the molecular mechanism of Tll and its vertebrate counterpart TLX. The genetic tools available in *Drosophila* allowed me to follow cell fate changes during normal development and upon manipulation of Tll. I found that in the absence of Tll type II neuroblasts switch to a more restricted progenitor and, conversely, high levels of Tll initiate tumours from intermediate progenitors. The cell fate changes that resulted in tumourigenesis were conserved with human TLX and suggest that intermediate progenitors could be one possible cell of origin for TLX-induced tumours.

## Chapter 7

### Materials and methods

**Statement on collaboration:** Embryo and larval immunostaining protocols for the data presented in Chapter 5 were performed in collaboration with Dr Leo Otsuki (contribution to each figure in Chapter 5 is indicated in the figure legends). Thanks go to Dr Robert Krautz for the bioinformatic analysis of the TII Targeted DamID sequencing data using his unpublished “DamPy” pipeline (section 7.4.2).

#### **7.1 Fly stocks and husbandry**

*Drosophila melanogaster* were reared in cages at 25 °C. Embryos were collected on yeasted apple juice plates and stages according to (Campos-Ortega and Hartenstein, 1985). For larval experiments, larvae were picked within one hour of hatching and dissected (designated 0 hours after larval hatching (ALH) or transferred to yeasted food plates and reared at 25 °C to the desired stage before dissection. Animals for RNAi experiments were transferred to 29 °C ALH to improve the efficacy of RNAi. For experiments involving GAL80<sup>ts</sup>, embryos were kept at 18 °C until hatching (or the time point specified) and then transferred to 29 °C before dissection. Full details of the genotypes and temperature conditions for each experiment are given in **Appendix 3**.

##### **7.1.1 GAL4 driver lines**

The following GAL4 lines were used: *Ay*-GAL4 (BL3953), *Ay*-GAL4,UAS-*GFP* (BL4411), *Ay*-GAL4,UAS-*lacZ* (BL4410), *btd*-GAL4(Xie et al., 2014), *GAL4*<sup>c855a</sup> (Manseau et al., 1997), GMR9D11-GAL4 (Pfeiffer et al., 2008; Weng et al., 2010) (BL40731), GMR29C07-GAL4 (BL49340), GMR31D09-GAL4 (BL49676), GMR39A01-GAL4 (BL45667), GMR31F04-GAL4 (BL46187), GMR31H09-GAL4 (BL49694), GMR71C09-GAL4 (BL39575), *pntP1*<sup>14-94</sup>-GAL4 (Zhu et al., 2011), *VGlut*<sup>OK371</sup>-GAL4 (BL26160), VT151-GAL4 (VDRC 206052) VT152-GAL4 (VDRC 207542), VT153-GAL4 (VDRC 212933), VT156-GAL4 (VDRC 208104), VT157-GAL4 (VDRC 207543), VT158-GAL4 (VDRC 213852), VT159-GAL4 (VDRC 205796), *wg*[ND382]-GAL4 (Gerlitz and Basler, 2002), *wor*-GAL4 (BL56553). *tub*-GAL80<sup>ts</sup> (BL7018) was used to restrict GAL4 activity to larval stages as indicated.

##### **7.1.2 UAS-driven transgenes**

The following UAS-transgenes were used: UAS-*ase* (Brand et al., 1993), UAS-*brat*-RNAi (BL34646), UAS-*FLP* (BL4539 and BL4540), G-TRACE (BL28280), UAS-*lacZ* ( $\beta$ g4-1-2)

(Brand and Perrimon, 1993), UAS-*mCD8-GFP* (BL5130 and BL5137), UAS-*mCD8-mCherry* (BL27391), UAS-*myr-mRFP* (BL7118 and BL7119), UAS-LT3-NDam (Southall et al., 2013), UAS-LT3-NDam-*tll* (this study), UAS-*tll*-miRNA[s] (Lin et al., 2009), UAS-*tll*-shRNA (VDRC 330031), UAS-*tll* (Kurusu et al., 2009) Kyoto Stock Center 109-680), UAS-*TLX* (this study). *w*<sup>1118</sup>; +; + was used as a reference stock.

### **7.1.3 Reporter lines**

The following genetic reporter lines were used: 9D11-*lacZ* (Haenfler et al., 2012), *dpp-lacZ*<sup>Exel.2</sup> (BL8411), *hh::lacZ* (*hh*<sup>P30</sup>) (Lee et al., 1992), *my-GFP* (Almeida and Bray, 2005), (*miR-7*)*E*>GFP (Li et al., 2009), *pnt-GFP* (BL42680), R9D11-*mCD8-GFP* (Zhu et al., 2011), R9D11-*CD4-tdTomato* (Han et al., 2011), *tll-lacZ* (Liaw and Lengyel, 1992), *tll*-EGFP (Venken et al., 2009) (BL30874), and *wg-lacZ* (1-*en*-11) (Kassis et al., 1992).

### **7.1.4 MARCM clones**

For *tll*<sup>49</sup> mutant clones, virgin female flies carrying *hsFLP*<sup>122</sup>; *wor*-GAL4,UAS-*mCD8-mCherry*/(*CyOact*-GFP); FRT82B,*tub*-GAL80 were crossed to male flies carrying *w*; 9D11-*lacZ*; FRT82B or *w*; 9D11-*lacZ*; FRT82B, *tll*<sup>49</sup>/TM6B. For *ase*<sup>1</sup> mutant clones, male flies carrying FRT19A,*tub*-GAL80,*hsFLP*<sup>1</sup>; *wor*-GAL4,UAS-*mCD8-mCherry*, R9D11-*mCD8-GFP*/(*CyO act*-GFP); + were crossed to virgin female flies carrying FRT19A; +; + or FRT19A, *ase*<sup>1</sup>/(*FM7Dfd*-YFP); +; +. Embryos were collected on apple juice plates at 25 °C and newly hatched larvae were transferred to yeasted food plates and raised at 25 °C. Clones were induced by a heat shock in a water bath (5 minutes 37 °C, 5 minutes rest at room temperature, 1 hour 37 °C) at 24 hours ALH and larvae were dissected 72 hours later.

### **7.1.5 FLEXAMP lineage tracing**

To perform lineage tracing using FLEXAMP, virgin female flies carrying *yw*; *tub*-GAL80<sup>ts</sup>,UAS-*FLP*; *act* >*y*+> LHv2-86Fb,DeltaRFP/(SM5^TM6B) were crossed to male flies carrying *w*; 13XLexAop2-*mCD8-GFP*, *tub*-GAL80<sup>ts</sup>/*CyO act*-GFP; GMR31H09-GAL4. To label EONs at hatching, embryos were collected on apple juice plates at room temperature (~20 °C), transferred to 29 °C and larvae were dissected 0-2 hours after hatching. Embryos were collected on apple juice plates at room temperature (~20 °C) and transferred to 29 °C until larval hatching. New hatched larvae were transferred to yeasted food plates and reared at 18 °C until eclosion (adult flies dissected 1-3 days after eclosion). *yw*; *tub*-GAL80<sup>ts</sup>,UAS-*FLP*; *act* >*y*+> LHv2-86Fb,DeltaRFP/(SM5^TM6B) flies (Bertet et al., 2014; Yagi et al., 2010) were provided by Ryota Yagi. Additional fly lines were obtained from Bloomington

*Drosophila* Stock Centre: 13XLexAop2-*mCD8-GFP* (BL32205), *tub-GAL80<sup>ts</sup>* (BL7019), and GMR31H09-GAL4 (BL49694).

## **7.2 Protocols for imaging techniques**

### **7.2.1 Embryo fixation and immunostaining**

Embryos were transferred from apple juice plates into a nitex basket by washing with distilled H<sub>2</sub>O (dH<sub>2</sub>O). Embryos were dechorionated in 50 % bleach/dH<sub>2</sub>O for three minutes, rinsed with dH<sub>2</sub>O, and then fixed on a rolling shaker for 20 minutes in a 6ml glass bottle containing 3ml of 4 % formaldehyde/phosphate-buffered saline (PBS) and 3ml heptane. After fixation, the lower (formaldehyde/PBS) phase of the fixing solution was removed and replaced with 3 ml methanol. Embryos were shaken vigorously and sunken embryos were transferred to clear 1.5 ml Eppendorf tubes. Embryos were washed three times with 1 ml methanol and could be stored in methanol at -20 °C before proceeding to immunostaining protocol.

Fixed embryos were re-hydrated in PBS with 0.3 % Triton X-100 (PBTx) (three five minute washes at room temperature) and blocked on a shaker for at least 15 minutes in 10 % normal goat serum/PBTx. Embryos were incubated overnight at 4 °C with primary antibodies diluted in 0.3 % PBTx. See **Table 7.1** for details of primary antibodies used. Embryos were washed well with PBTx, then incubated overnight at 4 °C with secondary antibodies diluted in PBTx.

Secondary antibodies conjugated to Alexa Fluor 405, Alexa Fluor 488, Alexa Fluor 568, Alexa Fluor Plus 647 (all 1 in 500, from Invitrogen) or DyLight-405 (1 in 100) Jackson Laboratories were used. Samples were washed with PBTx (three five minute washes) to remove excess secondary antibodies and then mounted in 50 % glycerol/PBS.

### **7.2.2 Larval brain fixation and immunostaining**

Brains were dissected in PBS, fixed in 4 % formaldehyde/PBS for 20 minutes at room temperature and washed with PBTx for three five minute washes. Samples were blocked with 10 % normal goat serum/PBTx for at least 15 minutes before overnight incubation with primary antibodies diluted in PBTx. See **Table 7.1** for details of primary antibodies used. The next day, samples were washed with PBTx (three 15 minute washes) at room temperature before overnight incubation with secondary antibodies diluted in PBTx. Secondary antibodies conjugated to Alexa Fluor 405, Alexa Fluor 488, Alexa Fluor 546, Alexa Fluor 568, Alexa Fluor 633 (all 1 in 500, from Invitrogen) or DyLight-405 (1 in 200) Jackson Laboratories were used. Samples were washed with PBTx (three five minute washes) to remove excess

secondary antibodies and mounted in Vectashield (Vector Laboratories).

### 7.2.3 Adult brain fixation and immunostaining

Brains were dissected from 1-3 day old adult flies. Adult flies were anaesthetised with CO<sub>2</sub> and then placed in 100 % ethanol for 1 minute before dissecting brains in PBS. The fixation and staining protocol was performed as for larval brains (Section 7.2.2).

| Antibody name | Host species | Dilution    | Reference/Source                                                                       |
|---------------|--------------|-------------|----------------------------------------------------------------------------------------|
| anti-Ase      | Rabbit       | 1 in 2,000  | Brand et al., 1993                                                                     |
| anti-Dpn      | Guinea pig   | 1 in 5,000  | Caygill and Brand, 2017                                                                |
| anti-Elav     | Rat          | 1 in 100    | DSHB (7E8A10 conc.)                                                                    |
| anti-GFP      | Chicken      | 1 in 2,000  | abcam (ab13970)                                                                        |
| anti-Pros     | Mouse        | 1 in 30     | DSHB (MR1A conc.)                                                                      |
| anti-Tll      | Rabbit       | 1 in 300    | Asian distribution centre for segmentation antibodies (Kosman et al., 1998)            |
| anti-Erm      | Rabbit       | 1 in 50     | Janssens et al., 2014                                                                  |
| anti-L'sc     | Guinea Pig   | 1 in 1,000  | Hakes, Otsuki and Brand, 2018                                                          |
| anti-L'sc     | Rat          |             | Caygill and Brand, 2017                                                                |
| anti-pH3      | Rabbit       | 1 in 100    | Merck Millipore (06-570)                                                               |
| anti-pH3      | Rat          | 1 in 200    | abcam (ab10543)                                                                        |
| anti-FasII    | Mouse        | 1 in 20     | DSHB (1D4 conc.)                                                                       |
| anti-CycA     | Rabbit       | 1 in 100    | Whitfield et al., 1990 (rb270)<br>Kind gift of Yuu Kimata, University of Cambridge, UK |
| anti-RFP      | Rabbit       | 1 in 1000   | abcam (ab62341)                                                                        |
| anti-Eya      | Mouse        | 1 in 75     | DSHB (10H6)                                                                            |
| anti-dVsx1    | Guinea pig   | 1 in 1,000  | Erclik et al., 2008                                                                    |
| anti-βGal     | Chicken      | 1 in 1,000  | abcam (ab9361)                                                                         |
| anti-βGal     | Rabbit       | 1 in 10,000 | MP Biomedicals (55976)                                                                 |
| anti-Optix    | Rabbit       | 1 in 500    | Kenyon et al., 2005                                                                    |
| anti-Mira     | Rat          | 1 in 500    | Kind gift of Chris Q. Doe, University of Oregon, USA                                   |
| anti-Repo     | Rabbit       | 1 in 10,000 | Kind gift of Benjamin Altenhein, University of Cologne, Germany                        |
| anti-Futsch   | Mouse        | 1 in 50     | DSHB (22C10)                                                                           |
| anti-Brp      | Mouse        | 1 in 10     | DSHB (nc82)                                                                            |
| anti-PntP1    | Rabbit       | 1 in 500    | Alvarez et al., 2003                                                                   |

**Table 7.1: Primary antibodies used for immunostaining.**

### 7.2.4 *tll* RNA FISH

A set of 38 Stellaris FISH probes was designed against the *tll* coding sequence and labeled with Quasar 570. Third instar larval brains were fixed in 4 % formaldehyde/PBS for 45 minutes at room temperature and then permeabilized in 70 % ethanol/PBS for 6 hours at 4 °C.

Brains were washed with Wash Buffer (10 % formamide, 2 x nuclease free saline-sodium citrate (SSC)) for 5 minutes before being incubated with probes (125 nM) in Hybridisation Buffer (100 mg/mL dextran sulfate, 10 % formamide, 2 x SSC) overnight at 45 °C. Brains were washed with Wash Buffer and mounted in Vectashield (Vector Laboratories).

### **7.2.5 Image acquisition and processing**

Fluorescent images were acquired using a Leica SP8 confocal microscope. Images were analysed using Fiji (Schindelin et al., 2012), which was also used to adjust brightness and contrast in images. Adobe Illustrator was used to compile figures.

### **7.2.6 Quantification and statistical analysis**

GraphPad Prism version 7.00 for Mac OS X was used for statistical analysis. The Kolmogorov-Smirnov test was used to compare samples with unequal variance and the Mann-Whitney *U*-test was used to compare samples with equal variance. Statistical analysis of data in Chapter 5 by Dr Leo Otsuki (indicated in figure legends) was performed using R. No data were excluded.

## **7.3 Drosophila transgenesis**

### **7.3.1 Generation of UAS-TLX**

The coding sequence of human *TLX* (Jackson et al., 1998) was amplified from human cDNA prepared from H9 ESCs (kindly provided by Dr Tomoki Otani, Livesey Lab) using the primers Forward: 5'-agatgaattcATGAGCAAGCCAGCCGG-3' and Reverse: 5'-atgactcgagTTAGATATCACTGGATTTGTACATATCTGAAAGCAGTC-3'. PCR amplification was performed using the Q5 High-Fidelity DNA Polymerase PCR kit (New England BioLabs, NEB), as described below:

| <u>PCR reaction mix</u> |        | <u>PCR programme</u> |            |
|-------------------------|--------|----------------------|------------|
| Q5 Buffer (5X)          | 5 µl   | Heated lid 105 °C    |            |
| dNTPs (10 mM)           | 0.5 µl | 98 °C for 5 min      |            |
| Primers (10 µM mix)     | 1 µl   | 98 °C for 15 s       | <b>40X</b> |
| Q5 DNA Polymerase       | 0.5 µl | 60 °C for 30 s       |            |
| cDNA                    | 4 µl   | 72 °C for 2 min 15 s |            |
| DEPC H <sub>2</sub> O   | 15 µl  | 72 °C 15 min         |            |
|                         | 25 µl  |                      |            |

PCR products were visualised using gel electrophoresis on a 1 % agarose gel and the band corresponding to human TLX was extracted using a QIAquick Gel Extraction Kit (Qiagen). The PCR product was cut with restriction enzymes EcoR1 and XhoI, purified using a QIAquick PCR Purification Kit (Qiagen), and ligated into cut pUAST-attB vector {Bischof:2007cb} with a T4 Ligase Kit (NEB). Transgenic flies carrying this construct were generated by germline injection of pUAST-attB-humanTLX into embryos carrying *y,v, nos-phiC integrase; attP40; +* (BL25709) (Ringrose, 2009).

### **7.3.2 Generation of UAS-LT3-NDam-*tll***

The coding sequence of *tll* was amplified from an embryonic cDNA library using the primers Forward: 5'-cagaaactcatctctgaagaggatctgcgagatctaATGCAGTCGTCGGAGG-3' and Reverse: 5' acagaagtaaggttccttcacaaagatcctctagaTCAGATCTTGCGCTGACT 3'. PCR amplification was performed using the Phusion High-Fidelity PCR kit (NEB).

| <u>PCR reaction mix</u> |             | <u>PCR programme</u> |            |
|-------------------------|-------------|----------------------|------------|
| Phusion HF Buffer (5x)  | 10 µl       | Heated lid 110 °C    |            |
| dNTPs (10 mM)           | 1 µl        | 90 °C for 30 s       |            |
| Primers (10 µM mix)     | 2 µl        | 98 °C for 10 s       | <b>35X</b> |
| Phusion Polymerase      | 1 µl        | 60 °C for 30s        |            |
| cDNA                    | 5 µl        | 72 °C for 2 min 15 s |            |
| DEPC H <sub>2</sub> O   | 31 µl       | 72 °C 10 min         |            |
|                         | <hr/> 50 µl |                      |            |

The amplified product was treated with Antarctic Phosphatase (NEB) at 37 °C for 1 hour, followed by heat inactivation at 70 °C for 5 minutes, and purified using a QIAquick PCR Purification Kit (Qiagen). pUASTattB-LT3-NDam (Southall et al., 2013) vector was cut with BglII and XbaI and then purified using a QIAquick Gel Extraction Kit (Qiagen). Ligation of the amplified *tll* coding sequence into cut pUASTattB-LT3-NDam was performed using Gibson Assembly Master Mix (NEB), as per manufacturer's instructions. Transgenic flies carrying this construct were generated by germline injection of pUASTattB-LT3-NDam-*tll* into embryos carrying *y,v, nos-phiC integrase; attP40; +* (BL25709) (Ringrose, 2009).

## **7.4 Targeted DamID**

### **7.4.1 *Drosophila* genetics for Targeted DamID**

Virgin female flies carrying *dpn>KDRTs-stop-KDRTs>GAL4*; *ase-GAL80/CyOact-GFP*; + were crossed to male flies carrying *w*; *UAS-LT3-NDam-tll*; *stg14-kd* or *w*; *UAS-LT3-NDam*; *stg14-kd* males. Embryos were collected on yeasted apple juice plates at 25 °C and larvae were transferred to yeasted food plates within an hour of hatching. Larvae were reared at 25°C and dissected 50 hours ALH (to match conditions from (Yang et al., 2016)). *dpn>KDRTs-stop-KDRTs>GAL4* and *stg14-kd* flies (Yang et al., 2016) were provided by Tzumin Lee and *ase-GAL80* flies (Neumüller et al., 2011) by Jurgen Knoblich .

### **7.4.2 Targeted DamID protocol**

An average of 45 larval brains were dissected for each Targeted DamID replicate and stored at -80 °C. The protocol for Targeted DamID for use with next-generation sequencing (NGS) was performed as described in (Marshall et al., 2016). Genomic DNA was extracted from dissected brains using the QIAamp DNA Micro Kit (Qiagen) and eluted in 50 µl AE buffer. 43.5 µl of genomic DNA was incubated 5 µl CutSmart Buffer (NEB) and 1.5 µl DpnI enzyme (NEB) overnight at 37 °C to cut methylated GATC sites. DNA was purified using a QIAquick PCR Purification Kit (Qiagen) and eluted in 32 µl DEPC H<sub>2</sub>O. 15 µl of DNA was incubated with 4 µl Adaptor Ligation Buffer (0.8 µl adaptors (50 µM); 2 µl T4 Ligase Buffer (NEB), 1.2 µl DEPC H<sub>2</sub>O) and 1 µl T4 DNA Ligase (NEB) at 16 °C for 2 hours, followed by heat inactivation at 65 °C for 10 minutes. Samples were incubated with 19 µl DpnII Buffer (NEB) and 1 µl DpnII enzyme (NEB) at 37 °C for 2 hours to cut unmethylated GATC sites, followed by heat inactivation at 65 °C for 20 minutes. DNA was purified using Sera-Mag SpeedBeads (Fisher Scientific) as per manufacturer's instructions and eluted in 30 µl DEPC H<sub>2</sub>O. 18.5 µl MyTaq Master Mix (10 µl 5X MyTaq Reaction Buffer (Bioline); 2.5 µl 50 µM DamID-PCR primers; 6 µl DEPC H<sub>2</sub>O) and 1.5 µl MyTaq HS DNA Polymerase (Bioline) was added to each 30 µl sample and the following PCR programme was run.

#### **DamID PCR Programme**

Heated lid 110 °C

72 °C for 10 min

95 °C for 30 s

65 °C for 5 min

72 °C for 15 min

--

|                  |  |            |
|------------------|--|------------|
| 95 °C for 30 s   |  | <b>3X</b>  |
| 65 °C for 1 min  |  |            |
| 72 °C for 10 min |  |            |
| --               |  |            |
| 95 °C for 30 s   |  | <b>17X</b> |
| 65 °C for 1 min  |  |            |
| 72 °C for 2 min  |  |            |
| --               |  |            |
| 72 °C for 5 min  |  |            |

Amplified DNA was purified using a QIAquick PCR Purification Kit (Qiagen) and eluted in 32 µl of DEPC H<sub>2</sub>O. 2 µg of DNA was added to 10 µl CutSmart Buffer (NEB) and made up to 100 µl total volume with DEPC H<sub>2</sub>O. Samples were sonicated using a Bioruptor (Diagenode) on high power for 8 cycles (30 s on; 30 s off) to achieve an average fragment size of ~300 bp and then incubated with 1 µl of AwaII enzyme overnight at 37 °C to cleave off DamID adaptors.

To begin library preparation, DNA was purified using Sera-Mag SpeedBeads (Fisher Scientific) as per manufacturer's instructions and eluted in 25 µl Resuspension Buffer (10 mM Tris-HCl, pH 8; 0.1 mM EDTA). 200 ng DNA (in 20 µl Resuspension Buffer) was incubated with 7.5 µl End Repair Buffer (3 µl 10X T4 Ligase Buffer (NEB); 1.2 µl 10 mM dNTPs; 3.3 µl DEPC H<sub>2</sub>O) and 2.5 µl End Repair Enzymes (1.14 µl T4 DNA Polymerase (NEB); 0.23 µl Klenow Fragment (NEB); 1.14 µl T4 Polynucleotide Kinase (NEB)) at 30 °C for 30 minutes, followed by heat inactivation at 75 °C for 20 minutes. Samples were incubated with 0.75 µl Klenow 3'-5' exo-enzyme (NEB) at 37 °C for 30 minutes and then incubated with 2.5 µl of the relevant sequencing adaptor and 2.5 µl Quick Ligase enzyme (NEB) at 30 °C for 10 minutes before the addition of 5 µl Stop Buffer (0.5 M EDTA). DNA was purified using Sera-Mag SpeedBeads (Fisher Scientific) as per manufacturer's instructions and eluted in 50 µl Resuspension Buffer, followed by a second Sera-Mag SpeedBeads purification with sample elution in 22.5 µl Resuspension Buffer. DNA fragments were enriched by a final PCR step; 20 µl of sample was added to 5 µl PCR Primer Cocktail (25 µl 100 µM PCR1 primer; 25 µl 100 µM PCR2 primer; 50 µl DEPC H<sub>2</sub>O) and 25 µl NEBNext High-Fidelity 2X PCR Master Mix (NEB) and the follow PCR programme was run.

### Fragment enrichment PCR programme

|                 |           |
|-----------------|-----------|
| 98 °C for 30 s  |           |
| 98 °C for 10 s  |           |
| 60 °C for 30 s  |           |
| 72 °C for 30 s  |           |
| 72 °C for 5 min | <b>6X</b> |

Amplified fragments were purified using Sera-Mag SpeedBeads (Fisher Scientific) as per manufacturer's instructions and eluted in 30 µl Resuspension Buffer before multiplexing libraries for NGS sequencing. DNA sequencing was performed by the Gurdon Institute NGS Core using an Illumina HiSeq 1500.

### **7.4.3 Targeted DamID analysis**

Tll-Dam read counts were normalized to Dam-only read counts to generate Tll binding profiles; bioinformatic analysis was performed by Dr Robert Krautz (using the "DamPy" pipeline, Krautz and Brand, in preparation). The Integrative Genomics Viewer (IGV, version 2.3.68) was used to visualise binding tracks aligned to release 6 of the *Drosophila* genome. Figures were compiled in Adobe Illustrator, in which Tll binding (Tll-Dam/Dam) was represented as scores in GATC fragments on an untransformed scale ( $y$ -axis). DamID peaks were identified using customized scripts based on MACS2 by Dr Robert Krautz. Peaks were determined at a threshold  $q$ -value ( $q = 1/10^{50}$ ) and were only considered if they occurred in more than half of all replicates. Peaks were represented as maximum coordinates of the overlapping peaks across replicates and were associated with the 'nearest neighbour'-genes via bedtools to determine Tll target genes (the full gene list is provided as **Appendix 2**).

Gene Ontology (GO) analysis was conducted using GO::TERMFINDER (Boyle et al., 2004) and the top ten GO terms are shown in **Table 3.1**. *Drosophila* orthologues of mouse TLX target genes were identified using DIOPT (*Drosophila* RNAi Screening Center Integrative Ortholog Prediction Tool) (Hu et al., 2011). Orthologues bound by Tll in type II neuroblasts are shown in **Table 3.2**. GO and DIOPT analysis was performed by me.







## Appendix 2:

### Tll target genes in type II neuroblasts identified by Targeted DamID

|             |          |             |            |
|-------------|----------|-------------|------------|
| 2mit        | amn      | aub         | boi        |
| 5-HT1B      | amon     | aurB        | bon        |
| 5-HT2B      | Amun     | aust        | bor        |
| 5-HT7       | Amy-p    | Awh         | bou        |
| a5          | Ance-5   | B4          | br         |
| Aats-arg    | Andorra  | bab1        | brat       |
| Aats-his    | Ank2     | bab2        | Brd        |
| ab          | Antp     | babos       | brk        |
| abd-A       | AnxB10   | Bacc        | brp        |
| Abl         | AnxB11   | Baldspot    | bru-3      |
| abo         | aop      | bap         | brv1       |
| abs         | aos      | baz         | bsh        |
| Ac76E       | AOX3     | bbg         | btd        |
| AcCoAS      | AOX4     | BCL7-like   | Btk29A     |
| Acf1        | ap       | bdg         | bun        |
| Acp36DE     | Apc      | be          | bur        |
| Acp62F      | APC10    | beat-Ib     | Bx         |
| Acp76A      | APC4     | beat-IIa    | C15        |
| Act5C       | ApepP    | beat-IIIa   | C3G        |
| Actn        | aPKC     | beat-Va     | C901       |
| ACXC        | app      | beat-Vc     | Ca-alpha1T |
| Acyp        | Aps      | beat-VI     | Ca-beta    |
| Ada         | apt      | beat-VII    | cact       |
| AdamTS-A    | ara      | bel         | Cad74A     |
| Adhr        | aralar1  | Best1       | Cad87A     |
| Ady43A      | Argk     | Best4       | CadN       |
| Aef1        | arr      | Bet5        | CadN2      |
| Afti        | Art9     | beta-Spec   | Caf1-105   |
| Ag5r        | Asator   | betaNACtes3 | Caf1-180   |
| AGBE        | ase      | betaNACtes4 | Calx       |
| ago         | ash2     | betaTub60D  | calypso    |
| AGO1        | asp      | betaTub97EF | Cam        |
| Ahcy89E     | ASPP     | Bgb         | CaMKII     |
| al          | AstA     | bi          | can        |
| Aldh        | AstA-R1  | bib         | CAP        |
| Aldh-III    | AstA-R2  | bif         | Capr       |
| Alh         | Atg1     | bigmax      | capu       |
| alpha-Cat   | Atg10    | Bin1        | cas        |
| alpha-Man-I | Atg17    | bin3        | CCHa1-R    |
| alpha4GT1   | Atg5     | bip1        | CCKLR-17D3 |
| alphaKap4   | Atg8b    | bl          | Ccn        |
| alphaSnap   | atl      | Blimp-1     | Ccp84Ab    |
| almr        | Atpalpha | Blos3       | Cct1       |
| aly         | ATPCL    | blot        | Cct5       |
| Ama         | Atu      | bnl         | Cdep       |

|         |         |         |         |
|---------|---------|---------|---------|
| cdi     | CG10993 | CG11929 | CG1271  |
| CdsA    | CG11000 | CG11964 | CG12721 |
| CecC    | CG11041 | CG11982 | CG12730 |
| CenG1A  | CG11106 | CG11997 | CG12746 |
| Cenp-C  | CG11122 | CG12007 | CG12768 |
| Cerk    | CG11123 | CG12027 | CG12780 |
| cert    | CG11138 | CG12054 | CG12822 |
| cerv    | CG11145 | CG12061 | CG12831 |
| Cf2     | CG11148 | CG12065 | CG12858 |
| CG10011 | CG11192 | CG12107 | CG12863 |
| CG10055 | CG11210 | CG12112 | CG12869 |
| CG10089 | CG11251 | CG12123 | CG12877 |
| CG10096 | CG11286 | CG12147 | CG12898 |
| CG10097 | CG11298 | CG12241 | CG12910 |
| CG10116 | CG11313 | CG12333 | CG12963 |
| CG10126 | CG11317 | CG12347 | CG12964 |
| CG10131 | CG11319 | CG1239  | CG12984 |
| CG10147 | CG11337 | CG12391 | CG12985 |
| CG10164 | CG11340 | CG12395 | CG1299  |
| CG10176 | CG11356 | CG12413 | CG13002 |
| CG10184 | CG11360 | CG12426 | CG13031 |
| CG10195 | CG11362 | CG12438 | CG13055 |
| CG10202 | CG1137  | CG12446 | CG13062 |
| CG10222 | CG11381 | CG12448 | CG13110 |
| CG10226 | CG11396 | CG12480 | CG13123 |
| CG10280 | CG11403 | CG12483 | CG13133 |
| CG10283 | CG11404 | CG12484 | CG13135 |
| CG10395 | CG11447 | CG12496 | CG13168 |
| CG10440 | CG11449 | CG12506 | CG1317  |
| CG10462 | CG11453 | CG12507 | CG13171 |
| CG10465 | CG11456 | CG12516 | CG13185 |
| CG10477 | CG11486 | CG12520 | CG13186 |
| CG10512 | CG11523 | CG12521 | CG13193 |
| CG10550 | CG11576 | CG12535 | CG13197 |
| CG10570 | CG11588 | CG12594 | CG13230 |
| CG10646 | CG11630 | CG12607 | CG1324  |
| CG10651 | CG11663 | CG12609 | CG13244 |
| CG10734 | CG11665 | CG12617 | CG13247 |
| CG10750 | CG11666 | CG12637 | CG13251 |
| CG10752 | CG11686 | CG1265  | CG13252 |
| CG10827 | CG11726 | CG12680 | CG13287 |
| CG10869 | CG11737 | CG12681 | CG13296 |
| CG10881 | CG11791 | CG12682 | CG13297 |
| CG10903 | CG11811 | CG12684 | CG13305 |
| CG10918 | CG11825 | CG12689 | CG13315 |
| CG10943 | CG11828 | CG12691 | CG13321 |
| CG10950 | CG11873 | CG12693 | CG13323 |
| CG10959 | CG11913 | CG12699 | CG13325 |

|         |         |         |         |
|---------|---------|---------|---------|
| CG13332 | CG14182 | CG14756 | CG1550  |
| CG13334 | CG14184 | CG14810 | CG15544 |
| CG13366 | CG14190 | CG14826 | CG15548 |
| CG13405 | CG14200 | CG14830 | CG15549 |
| CG13408 | CG14234 | CG14837 | CG15550 |
| CG13454 | CG14245 | CG14853 | CG15553 |
| CG13482 | CG14252 | CG14882 | CG15564 |
| CG13539 | CG14265 | CG14891 | CG15570 |
| CG1354  | CG14280 | CG14926 | CG15578 |
| CG13558 | CG14282 | CG14937 | CG15594 |
| CG13577 | CG14297 | CG14945 | CG15599 |
| CG13579 | CG14298 | CG14985 | CG15601 |
| CG13616 | CG14299 | CG14990 | CG15630 |
| CG13624 | CG14310 | CG1504  | CG15631 |
| CG13699 | CG14330 | CG15040 | CG15646 |
| CG13700 | CG14354 | CG15080 | CG15711 |
| CG13711 | CG14362 | CG15115 | CG15754 |
| CG13716 | CG14372 | CG15116 | CG15771 |
| CG13737 | CG14401 | CG15136 | CG15822 |
| CG13766 | CG14416 | CG15142 | CG15878 |
| CG13784 | CG14424 | CG15143 | CG15882 |
| CG13786 | CG14427 | CG15145 | CG15890 |
| CG13810 | CG14431 | CG1516  | CG15925 |
| CG13830 | CG14438 | CG15185 | CG1598  |
| CG13865 | CG14441 | CG15186 | CG1636  |
| CG13872 | CG14454 | CG15198 | CG16704 |
| CG13891 | CG14455 | CG15200 | CG16721 |
| CG13898 | CG14457 | CG15225 | CG16732 |
| CG13905 | CG14459 | CG15233 | CG16762 |
| CG13912 | CG14478 | CG15239 | CG1677  |
| CG13931 | CG14491 | CG15254 | CG16779 |
| CG1394  | CG14502 | CG15258 | CG16791 |
| CG13954 | CG14506 | CG15270 | CG16798 |
| CG13983 | CG14508 | CG15283 | CG16799 |
| CG13989 | CG14567 | CG1529  | CG16800 |
| CG1399  | CG14598 | CG15296 | CG16837 |
| CG13994 | CG14634 | CG15333 | CG16857 |
| CG13995 | CG14657 | CG15343 | CG16879 |
| CG14011 | CG14658 | CG15357 | CG1688  |
| CG14050 | CG14661 | CG15394 | CG16898 |
| CG14062 | CG14671 | CG15403 | CG16903 |
| CG14069 | CG14691 | CG15408 | CG16935 |
| CG14075 | CG14693 | CG15429 | CG16989 |
| CG14111 | CG14715 | CG1544  | CG17003 |
| CG14115 | CG14718 | CG15450 | CG1701  |
| CG14120 | CG14721 | CG15452 | CG17010 |
| CG14128 | CG14731 | CG15473 | CG17030 |
| CG1416  | CG14744 | CG15485 | CG17048 |

|         |         |         |         |
|---------|---------|---------|---------|
| CG17110 | CG18508 | CG30411 | CG31709 |
| CG17122 | CG18563 | CG30413 | CG31743 |
| CG17134 | CG18605 | CG30419 | CG31750 |
| CG17207 | CG18765 | CG30429 | CG31760 |
| CG17230 | CG18769 | CG30430 | CG31769 |
| CG17242 | CG18870 | CG30460 | CG31773 |
| CG17244 | CG1888  | CG30466 | CG31797 |
| CG17265 | CG1894  | CG30467 | CG31812 |
| CG17298 | CG1902  | CG30479 | CG31813 |
| CG1732  | CG1958  | CG30480 | CG31819 |
| CG17323 | CG1986  | CG30497 | CG31820 |
| CG17324 | CG1999  | CG3085  | CG31909 |
| CG17325 | CG2003  | CG3092  | CG31913 |
| CG17333 | CG2017  | CG31010 | CG31918 |
| CG17341 | CG2053  | CG31050 | CG31921 |
| CG17344 | CG2113  | CG3107  | CG31928 |
| CG17349 | CG2118  | CG31086 | CG31988 |
| CG17350 | CG2121  | CG31122 | CG3199  |
| CG17364 | CG2201  | CG31128 | CG31997 |
| CG17378 | CG2211  | CG31156 | CG32017 |
| CG1746  | CG2217  | CG31191 | CG32066 |
| CG17493 | CG2267  | CG31226 | CG32087 |
| CG17508 | CG2336  | CG31235 | CG32103 |
| CG17514 | CG2371  | CG31262 | CG3214  |
| CG17564 | CG2611  | CG31275 | CG32147 |
| CG17570 | CG2616  | CG31294 | CG32148 |
| CG17580 | CG2811  | CG31296 | CG32182 |
| CG17648 | CG2846  | CG31320 | CG32188 |
| CG17669 | CG2854  | CG31337 | CG32189 |
| CG17683 | CG2909  | CG31357 | CG32204 |
| CG17684 | CG30015 | CG31437 | CG32235 |
| CG17724 | CG30022 | CG31441 | CG32237 |
| CG17744 | CG30049 | CG31446 | CG32264 |
| CG17746 | CG3008  | CG31459 | CG32305 |
| CG17816 | CG30080 | CG31517 | CG32333 |
| CG17839 | CG30089 | CG31522 | CG32396 |
| CG17974 | CG3011  | CG31559 | CG32432 |
| CG17977 | CG30110 | CG3160  | CG32447 |
| CG17994 | CG30114 | CG31612 | CG32450 |
| CG17999 | CG30120 | CG31619 | CG32454 |
| CG18067 | CG30152 | CG31639 | CG32479 |
| CG18109 | CG30158 | CG3164  | CG32488 |
| CG18136 | CG30159 | CG31646 | CG32521 |
| CG1814  | CG30203 | CG31663 | CG32588 |
| CG18208 | CG30338 | CG31677 | CG32683 |
| CG18265 | CG30350 | CG31689 | CG32718 |
| CG1835  | CG30389 | CG31690 | CG32719 |
| CG18480 | CG30401 | CG31702 | CG32720 |

|         |         |         |         |
|---------|---------|---------|---------|
| CG32758 | CG33970 | CG3568  | CG42323 |
| CG32795 | CG34029 | CG3610  | CG42329 |
| CG32806 | CG34045 | CG3625  | CG42336 |
| CG32816 | CG34057 | CG3638  | CG42339 |
| CG32832 | CG3408  | CG3645  | CG42343 |
| CG32834 | CG3409  | CG3650  | CG42368 |
| CG32846 | CG34106 | CG3651  | CG42369 |
| CG32983 | CG34109 | CG3655  | CG4238  |
| CG32984 | CG34113 | CG3663  | CG42382 |
| CG32986 | CG34114 | CG3679  | CG42389 |
| CG32988 | CG34161 | CG3714  | CG42402 |
| CG33054 | CG34171 | CG3764  | CG42458 |
| CG33056 | CG34172 | CG3775  | CG42492 |
| CG33062 | CG34173 | CG3777  | CG42502 |
| CG33080 | CG34184 | CG3795  | CG42507 |
| CG33158 | CG34200 | CG3847  | CG42521 |
| CG33259 | CG34217 | CG3942  | CG42523 |
| CG33262 | CG34222 | CG4000  | CG42524 |
| CG33275 | CG34236 | CG40178 | CG42534 |
| CG3328  | CG34253 | CG4019  | CG42541 |
| CG33296 | CG34278 | CG40191 | CG42596 |
| CG33298 | CG34283 | CG4021  | CG42598 |
| CG33299 | CG34307 | CG40498 | CG42613 |
| CG33309 | CG34308 | CG4066  | CG42637 |
| CG33322 | CG34313 | CG4073  | CG42662 |
| CG33346 | CG34314 | CG4080  | CG42663 |
| CG3339  | CG34353 | CG41099 | CG42668 |
| CG33463 | CG34356 | CG41128 | CG4267  |
| CG33467 | CG34362 | CG4116  | CG42672 |
| CG3347  | CG3437  | CG41242 | CG42673 |
| CG33474 | CG34371 | CG41378 | CG42674 |
| CG33475 | CG34376 | CG41423 | CG42675 |
| CG3348  | CG34377 | CG41520 | CG42678 |
| CG33490 | CG34384 | CG4159  | CG42680 |
| CG33557 | CG34391 | CG4161  | CG42682 |
| CG3358  | CG34393 | CG4168  | CG42684 |
| CG33640 | CG34398 | CG4218  | CG42692 |
| CG33648 | CG34402 | CG4221  | CG42710 |
| CG33667 | CG34425 | CG42232 | CG42732 |
| CG33673 | CG34436 | CG42235 | CG42740 |
| CG33695 | CG34449 | CG42238 | CG42747 |
| CG33752 | CG34460 | CG42240 | CG42751 |
| CG3376  | CG3473  | CG42261 | CG42758 |
| CG33766 | CG3483  | CG42284 | CG4278  |
| CG33795 | CG3523  | CG4229  | CG42784 |
| CG33912 | CG3526  | CG42299 | CG42790 |
| CG33919 | CG3552  | CG42305 | CG42795 |
| CG33927 | CG3556  | CG42321 | CG42807 |

|         |         |         |        |
|---------|---------|---------|--------|
| CG42808 | CG43441 | CG4467  | CG4984 |
| CG42830 | CG43448 | CG4477  | CG4988 |
| CG42837 | CG43658 | CG4480  | CG5002 |
| CG42852 | CG43666 | CG44815 | CG5004 |
| CG42878 | CG43675 | CG4483  | CG5050 |
| CG4293  | CG43689 | CG44954 | CG5087 |
| CG43049 | CG43702 | CG44956 | CG5103 |
| CG43055 | CG43729 | CG4496  | CG5149 |
| CG43058 | CG43731 | CG45002 | CG5189 |
| CG43064 | CG43732 | CG45011 | CG5204 |
| CG43068 | CG43736 | CG45049 | CG5254 |
| CG43077 | CG43737 | CG45050 | CG5270 |
| CG43078 | CG43742 | CG45062 | CG5273 |
| CG43082 | CG4375  | CG45075 | CG5346 |
| CG43098 | CG43750 | CG45080 | CG5397 |
| CG43106 | CG43759 | CG45092 | CG5455 |
| CG43111 | CG43783 | CG45093 | CG5493 |
| CG43116 | CG43795 | CG45186 | CG5525 |
| CG43131 | CG43800 | CG4520  | CG5548 |
| CG43143 | CG4382  | CG45263 | CG5550 |
| CG43149 | CG43844 | CG45307 | CG5569 |
| CG43163 | CG43867 | CG45413 | CG5608 |
| CG43169 | CG4390  | CG45545 | CG5621 |
| CG43172 | CG43901 | CG45546 | CG5642 |
| CG43175 | CG43919 | CG45603 | CG5662 |
| CG43188 | CG43954 | CG4563  | CG5674 |
| CG43189 | CG43968 | CG45781 | CG5705 |
| CG43192 | CG43980 | CG45783 | CG5724 |
| CG43194 | CG44014 | CG45784 | CG5768 |
| CG43198 | CG44037 | CG4629  | CG5773 |
| CG43207 | CG44038 | CG4631  | CG5804 |
| CG43210 | CG44044 | CG4702  | CG5835 |
| CG43230 | CG44090 | CG4704  | CG5853 |
| CG43236 | CG44195 | CG4725  | CG5866 |
| CG43237 | CG44227 | CG4729  | CG5890 |
| CG43245 | CG44242 | CG4763  | CG5910 |
| CG43273 | CG44243 | CG4766  | CG5934 |
| CG43312 | CG44250 | CG4788  | CG5938 |
| CG43335 | CG44251 | CG4810  | CG5953 |
| CG43336 | CG44259 | CG4839  | CG6005 |
| CG43337 | CG44335 | CG4849  | CG6094 |
| CG43340 | CG44355 | CG4866  | CG6123 |
| CG4335  | CG44362 | CG4882  | CG6125 |
| CG43350 | CG4438  | CG4891  | CG6126 |
| CG43355 | CG44422 | CG4907  | CG6138 |
| CG43402 | CG44438 | CG4908  | CG6142 |
| CG43403 | CG44439 | CG4970  | CG6145 |
| CG43438 | CG44476 | CG4975  | CG6149 |

|        |        |        |              |
|--------|--------|--------|--------------|
| CG6154 | CG7054 | CG8177 | CG9582       |
| CG6163 | CG7079 | CG8180 | CG9596       |
| CG6178 | CG7137 | CG8202 | CG9624       |
| CG6216 | CG7140 | CG8204 | CG9650       |
| CG6220 | CG7214 | CG8281 | CG9657       |
| CG6231 | CG7231 | CG8289 | CG9692       |
| CG6244 | CG7255 | CG8303 | CG9698       |
| CG6280 | CG7294 | CG8353 | CG9701       |
| CG6282 | CG7304 | CG8360 | CG9747       |
| CG6287 | CG7320 | CG8369 | CG9757       |
| CG6308 | CG7337 | CG8370 | CG9759       |
| CG6310 | CG7362 | CG8372 | CG9801       |
| CG6330 | CG7372 | CG8397 | CG9837       |
| CG6332 | CG7407 | CG8399 | CG9839       |
| CG6345 | CG7548 | CG8405 | CG9863       |
| CG6353 | CG7560 | CG8460 | CG9864       |
| CG6404 | CG7568 | CG8475 | CG9899       |
| CG6414 | CG7603 | CG8476 | CG9932       |
| CG6424 | CG7606 | CG8483 | CG9934       |
| CG6481 | CG7653 | CG8578 | CG9970       |
| CG6488 | CG7692 | CG8641 | CG9986       |
| CG6497 | CG7694 | CG8654 | CG9989       |
| CG6508 | CG7707 | CG8679 | CG9993       |
| CG6509 | CG7708 | CG8712 | Cha          |
| CG6527 | CG7720 | CG8735 | Chd64        |
| CG6574 | CG7724 | CG8777 | CheA75a      |
| CG6614 | CG7742 | CG8786 | CheA84a      |
| CG6628 | CG7759 | CG8920 | CheB42b      |
| CG6629 | CG7766 | CG8927 | CheB74a      |
| CG6656 | CG7791 | CG8952 | CheB93b      |
| CG6660 | CG7837 | CG9005 | cher         |
| CG6664 | CG7845 | CG9101 | CHES-1-like  |
| CG6685 | CG7856 | CG9166 | chic         |
| CG6726 | CG7872 | CG9171 | chinmo       |
| CG6739 | CG7882 | CG9222 | CHIP         |
| CG6767 | CG7884 | CG9231 | chn          |
| CG6770 | CG7900 | CG9235 | Cht3         |
| CG6785 | CG7912 | CG9281 | Cib2         |
| CG6812 | CG7956 | CG9308 | cic          |
| CG6836 | CG7991 | CG9330 | cindr        |
| CG6845 | CG8034 | CG9380 | Cip4         |
| CG6891 | CG8036 | CG9410 | Ckl1alpha    |
| CG6893 | CG8078 | CG9411 | Ckl1alpha-i1 |
| CG6908 | CG8100 | CG9426 | Clk          |
| CG6914 | CG8112 | CG9465 | CLS          |
| CG6950 | CG8119 | CG9483 | clumsy       |
| CG6966 | CG8128 | CG9492 | cnc          |
| CG6983 | CG8141 | CG9570 | CngA         |

|         |          |            |                  |
|---------|----------|------------|------------------|
| Cngl    | cv-c     | Dic3       | Dys              |
| cni     | cwo      | Dic61B     | E(spl)m2-BFM     |
| cnk     | cyc      | Diedel2    | E(spl)m5-HLH     |
| CNMaR   | CycA     | Diedel3    | E(spl)m7-HLH     |
| cno     | CycB     | DIP2       | E(spl)m8-HLH     |
| Cnx14D  | CycB3    | disco      | E(spl)malpha-BFM |
| Cnx99A  | CycE     | disco-r    | E(spl)mbeta-HLH  |
| coil    | CycG     | DI         | E(spl)mdelta-HLH |
| comm    | Cyp12e1  | Dlc90F     | E(spl)mgamma-HLH |
| comm2   | Cyp28a5  | dlg1       | e(y)2b           |
| Con     | Cyp309a2 | Dll        | E23              |
| Coop    | Cyp310a1 | dlp        | E2f1             |
| Corin   | Cyp312a1 | dm         | Eaat1            |
| coro    | Cyp49a1  | dmpd       | Eaat2            |
| Corp    | Cyp4c3   | dmrt99B    | eag              |
| corto   | Cyp4d20  | DNapol-eta | eap              |
| Cp1     | Cyp4p2   | DNasell    | ebd2             |
| cpb     | Cyp6a14  | dnc        | EcR              |
| Cpn     | Cyp6a18  | dnk        | ed               |
| cpo     | Cyp6t1   | Doa        | edl              |
| Cpr100A | Cyp6v1   | Doc1       | EF-G2            |
| Cpr49Ab | Cyp9b1   | Dop1R1     | Ef1alpha48D      |
| Cpr49Ac | Cyt-c-d  | Dop1R2     | EF2              |
| Cpr50Ca | D        | Dop2R      | Efa6             |
| Cpr65Ay | d-cup    | dpn        | eg               |
| Cpr65Az | d4       | dpr10      | Egfr             |
| Cpr65Ea | Dab      | dpr12      | egg              |
| Cpr65Eb | Dad      | dpr16      | egl              |
| Cpr66D  | dah      | dpr17      | egr              |
| Cpr76Ba | dan      | dpr4       | Eh               |
| Cpr97Ea | danr     | dpr5       | eIF-4a           |
| Cpsf160 | dap      | dpr8       | eIF4E-4          |
| Crc     | Dbp80    | dpr9       | eIF4E-7          |
| CrebA   | Dbx      | Dr         | eIF5B            |
| CrebB   | Ddr      | Drep-3     | eIF6             |
| crim    | Debcl    | Drip       | Eip63E           |
| crol    | Der-1    | Drl-2      | Eip63F-1         |
| crp     | Df31     | drm        | Eip74EF          |
| cry     | Dfd      | ds         | Eip75B           |
| CrzR    | Dgk      | Dscam1     | Ela              |
| Csp     | Dh31-R   | Dscam2     | elav             |
| ct      | Dh44-R1  | Dscam3     | eIB              |
| CTPsyn  | Dhc36C   | Dscam4     | Elba2            |
| Ctr1C   | Dhc64C   | dsx        | emc              |
| ctrip   | Dhc98D   | dsx-c73A   | en               |
| cue     | Diap1    | dve        | ena              |
| Cul2    | dib      | dyn-p25    | EndoB            |
| cv      | Dic1     | Dyrk2      | Eno              |

|         |              |             |         |
|---------|--------------|-------------|---------|
| Ent2    | Frq1         | Gr77a       | hng2    |
| Epac    | fru          | Gr92a       | hng3    |
| eRF1    | fs(1)h       | Gr93a       | hoip    |
| ergic53 | fs(1)M3      | Gr98a       | HP1e    |
| erm     | fs(2)ltoPP43 | Gr98d       | HP4     |
| esg     | ft           | grh         | HP6     |
| esn     | fu12         | grim        | hppy    |
| Esyt2   | Fur1         | Grip        | Hr4     |
| ETHR    | fuss         | Grip128     | Hs6st   |
| Ets65A  | futsch       | Grip163     | Hsc70Cb |
| Ets98B  | fw           | grn         | Hsp27   |
| ewg     | fz2          | grp         | Hsp60C  |
| ex      | fz3          | grsm        | Hsp70Bc |
| exex    | fzy          | Grx-1       | hth     |
| exu     | Gad1         | gry         | Hug     |
| ey      | galectin     | gsb         | hyd     |
| eya     | GalNAc-T1    | gsb-n       | I-3     |
| Fad2    | Gasp         | GstD3       | IA-2    |
| fas     | GATAd        | Gug         | ldgf1   |
| Fas2    | Gbs-70E      | gukh        | ldgf4   |
| Fatp    | Gbs-76A      | gus         | ldh     |
| Fbp1    | Gclc         | gw          | ifc     |
| fd59A   | gdl          | Gyc76C      | igl     |
| fd96Cb  | gek          | Gyc88E      | llp2    |
| fdy     | gem          | Gycbeta100B | llp6    |
| FeCH    | Gem2         | h           | llp7    |
| Fem-1   | Gfrl         | H15         | llp8    |
| fend    | GILT1        | haf         | Imp     |
| Fer1    | gl           | ham         | ImpL2   |
| Fer1HCH | Gld2         | hang        | inaC    |
| Fer2    | glec         | hb          | inc     |
| Fhos    | glob2        | hbn         | ind     |
| Fib     | Glt          | HDAC4       | InR     |
| Fife    | GluRIB       | hdc         | insb    |
| Fim     | GluRIIA      | hdly        | insc    |
| Fis1    | Glut1        | heph        | insv    |
| Fkbp14  | Glut4EF      | Hers        | Int6    |
| fkh     | Glycogenin   | Hey         | IntS12  |
| Flo1    | Gnf1         | HGTX        | IntS3   |
| fne     | gogo         | hid         | IntS4   |
| fng     | gol          | hipk        | Inx2    |
| fog     | Gp150        | hiw         | Inx3    |
| for     | Gp210        | hkb         | Inx6    |
| foxo    | Gr21a        | HLH4C       | IP3K1   |
| frac    | Gr22d        | HmgD        | lpod    |
| fray    | Gr22f        | Hmgs        | lr25a   |
| fred    | Gr39b        | Hmu         | lr41a   |
| FRG1    | Gr68a        | Hmx         | lr47a   |

|          |            |         |             |
|----------|------------|---------|-------------|
| lr56a    | Kr         | lola    | Miro        |
| lr56d    | Kr-h1      | lov     | mirr        |
| lr64a    | KrT95D     | lox     | Mlc-c       |
| lr67a    | ksh        | lox2    | Mlc2        |
| lr75d    | ktub       | LpR2    | mld         |
| lr7a     | L          | LRP1    | Mmp2        |
| lr92a    | l(1)G0007  | Lrr47   | Mnt         |
| lre1     | l(1)G0193  | LS2     | Mob2        |
| ltp-r83A | l(1)G0222  | LysP    | mod         |
| Jafrac1  | l(1)G0320  | Mad     | Moe         |
| jar      | l(1)sc     | mad2    | mos         |
| jdp      | l(2)09851  | mael    | Mp          |
| jeb      | l(2)35Bd   | Maf1    | mrj         |
| Jheh2    | l(2)37Cg   | MAGE    | mRpL52      |
| jigr1    | l(2)k01209 | Magi    | mRpS22      |
| jim      | l(3)05822  | mas     | mRpS6       |
| jing     | l(3)72Dp   | mbc     | Mrtf        |
| Jon65Ai  | l(3)L1231  | mbl     | ms(3)76Ba   |
| jumu     | l(3)mbt    | Mcm10   | msi         |
| jv       | l(3)neo38  | Mdh2    | msn         |
| Jwa      | lab        | Mdr49   | Msp300      |
| Kah      | Lac        | me31B   | mspo        |
| kay      | lace       | MED10   | MsR2        |
| KCNQ     | laf        | MED11   | Mst85C      |
| Kdm4B    | lama       | Mef2    | Mst87F      |
| kdn      | lambdaTry  | mei-P26 | MTA1-like   |
| Keap1    | LamC       | Meics   | mtd         |
| kek3     | Las        | melt    | mthl10      |
| kek5     | Lasp       | Meltrin | mthl8       |
| kek6     | lbk        | Membrin | MtnC        |
| ken      | Lcp1       | Men     | mtt         |
| kibra    | Lcp65Af    | Menl-1  | mub         |
| kirre    | lea        | Menl-2  | Muc68Ca     |
| kl-2     | Letm1      | Mes2    | Muc68E      |
| klar     | Lgr1       | MESR4   | Muc96D      |
| klg      | Lgr3       | metl    | Mur82C      |
| Klp3A    | lgs        | mew     | Mur89F      |
| Klp54D   | lid        | Mf      | mura        |
| Klp59C   | lig        | MFS15   | Myo31DF     |
| klu      | lilli      | mGluR   | Myo61F      |
| kn       | Lim1       | mid     | MYPT-75D    |
| kni      | Lim3       | mil     | mys         |
| knrl     | lin-28     | milt    | N           |
| ko       | Lin29      | mino    | Naam        |
| koko     | Lip4       | Mio     | nab         |
| kon      | Lis-1      | miple   | nAChRalpha1 |
| KP78a    | Lk6        | miple2  | nAChRalpha2 |
| KP78b    | Lmpt       | mira    | nAChRbeta2  |

|           |           |             |                 |
|-----------|-----------|-------------|-----------------|
| NaCP60E   | Obp56g    | Pcd         | Pli             |
| NaPi-T    | Obp57a    | pcl         | pll             |
| natalisin | Obp85a    | Pde11       | plx             |
| Ncc69     | Obp99c    | Pde1c       | Pmp70           |
| Nep1      | Oct-TyrR  | Pde8        | Pms2            |
| Nep3      | Octbeta1R | Pdfr        | pnt             |
| nerfin-1  | Octbeta2R | Pdi         | pnut            |
| net       | Oda       | Pdk1        | Poc1            |
| NetA      | odd       | pdm2        | pog             |
| NetB      | ogre      | Pdp1        | poly            |
| Neto      | olf186-M  | Pdxk        | pon             |
| neur      | olf413    | peb         | Poxn            |
| Nhe2      | Oli       | PEK         | Pp1-Y2          |
| NijA      | ome       | pelo        | Ppa             |
| NimC2     | opa       | pes         | ppk12           |
| NimC4     | Optix     | Pex7        | ppk27           |
| nkd       | Or24a     | Pfrx        | ppk7            |
| Nlg1      | Or30a     | pgant2      | ppk8            |
| Nlg2      | Or43a     | PGAP5       | PpN58A          |
| Nlg4      | Or45a     | Pgk         | Ppr-Y           |
| Nmdar2    | Or59b     | PGRP-LA     | PpV             |
| Nmdmc     | Or63a     | PGRP-LB     | PPYR1           |
| nmo       | Or65c     | ph-d        | Prat            |
| noc       | Or67d     | ph-p        | Prat2           |
| Nox       | Or83c     | PH4alphaEFB | pre-mod(mdg4)-B |
| Npc1b     | Or85e     | PH4alphaNE2 | pre-mod(mdg4)-G |
| Npc2b     | Or92a     | PH4alphaSG2 | pre-mod(mdg4)-H |
| Npc2d     | Or98b     | phl         | pre-mod(mdg4)-I |
| NPFR      | Orco      | phyl        | pre-mod(mdg4)-J |
| Nplp1     | Orct2     | Pi4KIIalpha | pre-mod(mdg4)-K |
| Nrt       | Oscillin  | pico        | pre-mod(mdg4)-L |
| nrv1      | Oseg2     | Piezo       | pre-mod(mdg4)-P |
| Nrx-IV    | Osi12     | Pif1A       | Proc            |
| nSyb      | Osi17     | Pig1        | pros            |
| Ntf-2     | Osi19     | pigs        | Prosalpha3T     |
| nub       | Osi3      | pip         | Prosap          |
| Nuf2      | osk       | PIP82       | Prosbeta3       |
| numb      | osp       | pita        | Prosbeta5R1     |
| Nup154    | otk       | pk          | Prx2540-2       |
| Nup214    | otk2      | PK2-R2      | Prx3            |
| Nup37     | ovo       | Pka-C1      | Psa             |
| Nup98-96  | p130CAS   | Pka-C2      | PsGEF           |
| nyo       | pain      | Pka-C3      | Psn             |
| Oamb      | pan       | Pkc53E      | psq             |
| Oatp30B   | Pat1      | Pkd2        | ptc             |
| Obp28a    | path      | Pkn         | Ptp10D          |
| Obp47a    | pb        | Plc21C      | Ptp99A          |
| Obp51a    | pbl       | Pld         | Ptpmeg          |

|         |            |          |            |
|---------|------------|----------|------------|
| ptr     | Rh5        | S-Lap4   | shn        |
| puc     | Rh50       | S-Lap8   | shot       |
| pum     | rha        | sa       | Shroom     |
| Pvf2    | rhea       | SA-2     | sick       |
| Pvf3    | rho        | sala     | sif        |
| px      | Rho1       | salm     | Sik3       |
| pyd     | RhoGAP100F | sals     | sima       |
| pyr     | RhoGAP18B  | Samuel   | Sin3A      |
| pyx     | RhoGDI     | sano     | SIP3       |
| Rab1    | RhoGEF2    | Sap47    | siz        |
| Rab11   | RhoGEF3    | sba      | SK         |
| Rab18   | Rhp        | sbb      | Skadu      |
| RabX2   | rib        | Sbp2     | SKIP       |
| RabX4   | Rich       | sbr      | SkpA       |
| RabX6   | Rif1       | SC35     | SkpD       |
| Rac2    | rk         | sca      | SkpE       |
| Rad1    | rl         | scb      | SkpF       |
| RAF2    | RnrL       | Scgdelta | sktl       |
| RanBP3  | robo3      | scro     | sli        |
| Ranbp9  | rod        | scrt     | slif       |
| rap     | rols       | scw      | slim       |
| Rap2l   | Rpb12      | scyl     | Slip1      |
| RapGAP1 | RpL10Aa    | sd       | Slob       |
| ras     | RpL13      | Sdc      | slp1       |
| RasGAP1 | RpL15      | SdhB     | slp2       |
| Rassf   | RpL18A     | sdk      | sm         |
| rau     | RpL21      | Sema-1a  | SMC1       |
| Rbbp5   | RpL22-like | Sema-2a  | smg        |
| Rbp6    | Rpn7       | Sema-5c  | smt3       |
| Rca1    | rpr        | seq      | Smu1       |
| rdgA    | RpS11      | Ser      | sna        |
| rdgC    | RpS2       | Ser7     | Snap25     |
| Rdl     | RpS26      | serp     | SNF4Agamma |
| rdo     | Rpt3       | Set2     | Snm1       |
| rdx     | Rpt5       | sff      | Snoo       |
| Reck    | Rrp40      | Sfp24Bc  | sNPF-R     |
| RecQ4   | Rrp47      | Sfp65A   | sns        |
| RecQ5   | rst        | Sfp84E   | Snx3       |
| Ref2    | RtGEF      | Sfp93F   | Socs36E    |
| Rel     | ru         | sgg      | Socs44A    |
| repo    | run        | Sh       | sosie      |
| RFeSP   | RunxA      | Shab     | sowah      |
| Rfx     | RunxB      | shakB    | sowi       |
| Rgk1    | rut        | Shal     | Sox15      |
| Rgk2    | rux        | Shawl    | Sox21a     |
| Rgl     | Rx         | shd      | Sox21b     |
| rgr     | RyR        | shep     | SoxN       |
| Rh3     | S          | shg      | Sp1        |

|            |           |          |                      |
|------------|-----------|----------|----------------------|
| SP1173     | Sulf1     | tna      | Unc-115a             |
| SP2353     | sunz      | toc      | unc-13-4A            |
| SP2637     | sv        | Toll-4   | unc-4                |
| spartin    | svp       | Toll-6   | unc-5                |
| spas       | svr       | Toll-9   | Unc-76               |
| spdo       | sws       | Tollo    | unpg                 |
| SpdS       | Sxl       | Tom      | ush                  |
| spen       | syd       | tomboy20 | uzip                 |
| spg        | Syn       | Top1     | v                    |
| sphinx2    | Syp       | tos      | VACHT                |
| spn-B      | Syalpha   | TotB     | Vap-33A              |
| Spn28B     | Syx1A     | tou      | Vap-33B              |
| Spn28Db    | Taf12L    | tow      | veil                 |
| Spn38F     | tai       | toy      | ventrally-expressed- |
| Spn43Aa    | Tak1      | TpnC41C  | protein-D            |
| Spn75F     | tal-1A    | trbd     | vfl                  |
| spok       | tal-2A    | Trc8     | Vha100-1             |
| SPR        | tal-3A    | Treh     | Vha100-2             |
| Spred      | tal-AA    | Tret1-1  | Vha100-3             |
| spri       | Tango13   | Trim9    | Vha13                |
| sprt       | tap       | trio     | Vha26                |
| Spt3       | tara      | TrissinR | Vha55                |
| spz5       | Tb        | Trl      | Vha68-2              |
| sqa        | TBCB      | Trpm     | VhaM9.7-c            |
| sr         | tbrd-1    | Trx-2    | VhaSFD               |
| Sr-CIII    | Teh1      | Trxr-2   | vih                  |
| sra        | Ten-a     | tsh      | vir-1                |
| Src42A     | Ten-m     | Tsp      | vnd                  |
| Src64B     | Tengl4    | Tsp39D   | Vps16A               |
| srl        | TER94     | Tsp42Ea  | Vps35                |
| Srp72      | Tet       | Tsp42Ee  | Vsx1                 |
| Ssb-c31a   | tey       | Tsp42Eo  | Vsx2                 |
| ssp3       | TfAP-2    | Tsp74F   | Vti1                 |
| st         | TfIIA-S-2 | ttk      | vvl                  |
| ST6Gal     | Tg        | tud      | w                    |
| stai       | ths       | tun      | wake                 |
| Stam       | Timp      | Tusp     | wal                  |
| stan       | Tis11     | TwdIM    | wdp                  |
| Stat92E    | tj        | TwdIQ    | wech                 |
| stau       | TkR86C    | TwdIT    | wg                   |
| step       | TkR99D    | tyn      | wgn                  |
| stet       | tkv       | TyrR     | Wnt2                 |
| stops      | Tl        | TyrRII   | Wnt4                 |
| Strica     | tlk       | U2A      | wor                  |
| sty        | tll       | Ucrh     | wrapper              |
| Su(var)205 | TM9SF4    | Ugt37b1  | wts                  |
| su(w[a])   | Tmhs      | Ugt37c1  | wun                  |
| Su(z)2     | tmod      | Ugt86Dd  | wun2                 |

Xrp1  
y  
yip3

yrt  
zfh1  
zfh2

Zip89B  
Zir  
Ziz

ZnT35C  
ZnT63C  
Zw

### Appendix 3:

#### *Drosophila* genotypes and temperature conditions

| Figure   | Panel        | GAL4 line                                                                                                                     | Crossed to                                                                                                            | Temperature                                     |
|----------|--------------|-------------------------------------------------------------------------------------------------------------------------------|-----------------------------------------------------------------------------------------------------------------------|-------------------------------------------------|
| Fig. 2.1 | C – E        | <i>w</i> ; +; <i>pntP1</i> -GAL4                                                                                              | <i>w</i> ; <i>tll</i> -EGFP,UAS- <i>myr-mRFP</i> (CyOact-GFP); +                                                      | 25 °C                                           |
|          | F – G'       | N/A                                                                                                                           | <i>w</i> ; +; <i>tll</i> - <i>lacZ</i>                                                                                | 25 °C                                           |
| Fig. 2.2 | A – B        | <i>yw</i> ,UAS- <i>mCD8</i> -GFP;<br><i>pntP1</i> -GAL4                                                                       | N/A                                                                                                                   | 25 °C                                           |
| Fig. 2.3 | B            | <i>w</i> ; +; GMR39A01-GAL4                                                                                                   | <i>yw</i> ; UAS- <i>mCD8</i> -GFP; +                                                                                  | 25 °C                                           |
|          | C            | <i>w</i> ; +; GMR31H09-GAL4                                                                                                   | <i>yw</i> ; UAS- <i>mCD8</i> -GFP; +                                                                                  | 25 °C                                           |
|          | D            | <i>w</i> ; +; GMR31F04-GAL4                                                                                                   | <i>yw</i> ; UAS- <i>mCD8</i> -GFP; +                                                                                  | 25 °C                                           |
|          | E            | <i>w</i> ; +; GMR31D09-GAL4                                                                                                   | <i>yw</i> ; UAS- <i>mCD8</i> -GFP; +                                                                                  | 25 °C                                           |
|          | F            | <i>w</i> ; +; VT151-GAL4                                                                                                      | <i>yw</i> ; UAS- <i>mCD8</i> -GFP; +                                                                                  | 25 °C                                           |
|          | G            | <i>w</i> ; +; VT152-GAL4                                                                                                      | <i>yw</i> ; UAS- <i>mCD8</i> -GFP; +                                                                                  | 25 °C                                           |
|          | H            | <i>w</i> ; +; VT153-GAL4                                                                                                      | <i>yw</i> ; UAS- <i>mCD8</i> -GFP; +                                                                                  | 25 °C                                           |
|          | I            | <i>w</i> ; +; VT156-GAL4                                                                                                      | <i>yw</i> ; UAS- <i>mCD8</i> -GFP; +                                                                                  | 25 °C                                           |
|          | J            | <i>w</i> ; +; VT157-GAL4                                                                                                      | <i>yw</i> ; UAS- <i>mCD8</i> -GFP; +                                                                                  | 25 °C                                           |
|          | K            | <i>w</i> ; +; VT158-GAL4                                                                                                      | <i>yw</i> ; UAS- <i>mCD8</i> -GFP; +                                                                                  | 25 °C                                           |
|          | L            | <i>w</i> ; +; VT159-GAL4                                                                                                      | <i>yw</i> ; UAS- <i>mCD8</i> -GFP; +                                                                                  | 25 °C                                           |
|          | Fig. 2.4     | B                                                                                                                             | <i>w</i> ; +; GMR31F04-GAL4                                                                                           | <i>yw</i> ; UAS- <i>mCD8</i> -GFP; +            |
| C        |              | <i>w</i> ; +; VT153-GAL4                                                                                                      | <i>yw</i> ; UAS- <i>mCD8</i> -GFP; +                                                                                  | 25 °C                                           |
| D        |              | <i>w</i> ; +; VT151-GAL4                                                                                                      | <i>yw</i> ; UAS- <i>mCD8</i> -GFP; +                                                                                  | 25 °C                                           |
| E        |              | <i>w</i> ; +; VT159-GAL4                                                                                                      | <i>yw</i> ; UAS- <i>mCD8</i> -GFP; +                                                                                  | 25 °C                                           |
| Fig. 2.5 | C, C'        | <i>w</i> ; <i>wor</i> -GAL4,UAS- <i>mCD8</i> -GFP; <i>tub</i> -GAL80 <sup>ts</sup>                                            | Control: <i>w</i> <sup>1118</sup> ; +; +<br><i>tll</i> -miRNA[s]; <i>w</i> ; UAS- <i>tll</i> -miRNA[s]; +             | 18 °C until hatching, shift to 29 °C for 3 days |
|          | D, D'        | <i>w</i> ; <i>wor</i> -GAL4,UAS- <i>mCD8</i> -GFP; <i>tub</i> -GAL80 <sup>ts</sup>                                            | Control: <i>w</i> <sup>1118</sup> ; +; +<br><i>tll</i> -shRNA; <i>w</i> ; <i>tll</i> -shRNA; +                        | 18 °C until hatching, shift to 29 °C for 3 days |
| Fig. 2.6 | B, B'        | <i>yw</i> , <i>hsFLP</i> <sup>122</sup> ; <i>wor</i> -GAL4,UAS- <i>mCD8</i> - <i>mCherry</i> (CyO); FRT82B. <i>tub</i> -GAL80 | <i>w</i> ; 9D11- <i>lacZ</i> ; FRT82B                                                                                 | 25 °C<br>37 °C heat shock 24 hours ALH          |
|          | C            | <i>yw</i> , <i>hsFLP</i> <sup>122</sup> ; <i>wor</i> -GAL4,UAS- <i>mCD8</i> - <i>mCherry</i> (CyO); FRT82B. <i>tub</i> -GAL80 | <i>w</i> ; 9D11- <i>lacZ</i> ; FRT82B, <i>tll</i> <sup>49</sup>                                                       | 25 °C<br>37 °C heat shock 24 hours ALH          |
| Fig. 2.7 | A            | <i>yw</i> ,UAS- <i>mCD8</i> -GFP;<br><i>pntP1</i> -GAL4                                                                       | <i>w</i> ; +; R9D11- <i>CD4</i> - <i>tdTomato</i>                                                                     | 25 °C                                           |
|          | C, C', E, E' | <i>w</i> ; <i>Ay</i> -GAL4,UAS-GFP;<br><i>pntP1</i> -GAL4,R9D11- <i>CD4</i> - <i>tdTomato</i>                                 | <i>w</i> ; +; UAS- <i>FLP</i>                                                                                         | 25 °C until hatching then shift to 29 °C        |
|          | D, D'        | <i>w</i> ; <i>Ay</i> -GAL4,UAS-GFP;<br><i>pntP1</i> -GAL4                                                                     | <i>w</i> ; +; UAS- <i>FLP</i>                                                                                         | 25 °C until hatching then shift to 29 °C        |
| Fig. 2.8 | A, C         | <i>w</i> ; <i>Ay</i> -GAL4,UAS-GFP;<br><i>pntP1</i> -GAL4,R9D11- <i>CD4</i> - <i>tdTomato</i>                                 | Control: <i>w</i> ; +; UAS- <i>FLP</i><br><i>tll</i> -miRNA[s]; <i>w</i> ; UAS- <i>tll</i> -miRNA[s]; UAS- <i>FLP</i> | 25 °C until hatching then shift to 29 °C        |

|                  |         |                                                                 |                                                                                                                                                                                                 |                                          |
|------------------|---------|-----------------------------------------------------------------|-------------------------------------------------------------------------------------------------------------------------------------------------------------------------------------------------|------------------------------------------|
|                  | B       | <i>w; Ay-GAL4,UAS-GFP; pntP1-GAL4</i>                           | <u>Control:</u> <i>w; +; UAS-FLP tll-miRNA[s]; w; UAS-tll-miRNA[s]; UAS-FLP</i>                                                                                                                 | 25 °C until hatching then shift to 29 °C |
|                  | D(i)    | <i>w; Ay-GAL4,UAS-GFP; pntP1-GAL4,R9D11-CD4-tdTomato</i>        | <u>Control:</u> <i>w; +; UAS-FLP tll-miRNA[s]; w; UAS-tll-miRNA[s]; UAS-FLP</i>                                                                                                                 | 25 °C until hatching then shift to 29 °C |
|                  | D(ii)   | <i>w; Ay-GAL4,UAS-GFP; pntP1-GAL4</i>                           | <u>Control:</u> <i>w; UAS-FLP/(CyOact-GFP); UAS-p35 tll-miRNA[s]; w; UAS-tll-miRNA[s],UAS-FLP/(CyOact-GFP); UAS-p35</i>                                                                         | 25 °C until hatching then shift to 29 °C |
| <b>Fig. 2.9</b>  | B       | <i>w; wor-GAL4,UAS-mCD8-GFP; tub-GAL80<sup>ts</sup></i>         | <u>Control:</u> <i>w; UAS-lacZ; UAS-mCD8-GFP</i><br><i>brat</i> RNAi: <i>w; UAS-lacZ; UAS-brat-RNAi</i><br><i>brat</i> RNAi and <i>tll-miRNA[s]</i> : <i>w; UAS-tll-miRNA[s]; UAS-brat-RNAi</i> | 18 °C until hatching then shift to 29 °C |
| <b>Fig. 2.10</b> | A – B   | <i>w; Ay-GAL4,UAS-GFP; pntP1-GAL4,R9D11-CD4-tdTomato</i>        | <u>Control:</u> <i>w; +; UAS-FLP Ase OE:</i> <i>w; UAS-ase; UAS-FLP</i>                                                                                                                         | 25 °C until hatching then shift to 29 °C |
|                  | C       | <i>w; Ay-GAL4,UAS-GFP; pntP1-GAL4,R9D11-CD4-tdTomato</i>        | <u>Control:</u> <i>w; +; UAS-FLP tll-miRNA[s]; w; UAS-tll-miRNA[s]; UAS-FLP</i>                                                                                                                 | 25 °C until hatching then shift to 29 °C |
| <b>Fig. 3.2</b>  | A       | <i>w; +; pntP1-GAL4</i>                                         | <i>yw; UAS-mCD8-GFP; +</i>                                                                                                                                                                      | 25 °C                                    |
|                  | B       | <i>btd-GAL4,FRT19A/FM7act-GFP; +; +</i>                         | <i>yw; UAS-mCD8-GFP; +</i>                                                                                                                                                                      | 25 °C                                    |
| <b>Fig. 3.3</b>  | B       | <i>dpn&gt;KDRTs-stop-KDRTs&gt;GAL4; +; +</i>                    | <i>w; UAS-mCD8-GFP/(CyOact-GFP); stg14-KDI(TM6B)</i>                                                                                                                                            | 25 °C                                    |
|                  | C – D'  | <i>dpn&gt;KDRTs-stop-KDRTs&gt;GAL4; ase-GAL80/CyOact-GFP; +</i> | <i>w; UAS-mCD8-GFP/(CyOact-GFP); stg14-KDI(TM6B)</i>                                                                                                                                            | 25 °C                                    |
| <b>Fig. 3.5</b>  | B, D    | <i>w; Ay-GAL4,UAS-lacZ/CyOact-GFP; pntP1-GAL4</i>               | <u>Control:</u> <i>w; UAS-FLP/(CyOact-GFP); my-GFP tll-miRNA[s]; w; UAS-tll-miRNA[s],UAS-FLP/(CyOact-GFP); my-GFP</i>                                                                           | 25 °C until hatching then shift to 29 °C |
| <b>Fig. 3.7</b>  | B, E    | <i>w; Ay-GAL4,UAS-GFP; pntP1-GAL4,R9D11-CD4-tdTomato</i>        | <u>Control:</u> <i>w; +; UAS-FLP tll-miRNA[s]; w; UAS-tll-miRNA[s]; UAS-FLP</i>                                                                                                                 | 25 °C until hatching then shift to 29 °C |
| <b>Fig. 4.1</b>  | B, C    | <i>btd-GAL4,FRT19A/FM7act-GFP; +; tub-GAL80<sup>ts</sup></i>    | <i>w; R9D11-mCD8-GFP; UAS-myr-mRFP/TM6B</i>                                                                                                                                                     | 18 °C until hatching then shift to 29 °C |
| <b>Fig. 4.2</b>  | A       | <i>btd-GAL4,FRT19A/FM7act-GFP; +; tub-GAL80<sup>ts</sup></i>    | <u>Control:</u> <i>w; R9D11-mCD8-GFP; UAS-myr-mRFP/TM6B</i><br>TII OE: <i>w; R9D11-mCD8-GFP; UAS-tll,UAS-myr-mRFP/TM6B</i>                                                                      | 18 °C until hatching then shift to 29 °C |
|                  | B       | <i>btd-GAL4,FRT19A/FM7act-GFP; +; tub-GAL80<sup>ts</sup></i>    | <u>Control:</u> <i>w; +; UAS-myr-mRFP/TM6B</i><br>TII OE: <i>w; +; UAS-tll,UAS-myr-mRFP/TM6B</i>                                                                                                | 18 °C until hatching then shift to 29 °C |
| <b>Fig. 4.3</b>  | A, C, E | <i>w; +; GMR9D11-GAL4,UAS-mCD8-GFP</i>                          | <u>Control:</u> <i>w<sup>1118</sup>; +; +</i><br>TII OE: <i>w; +; UAS-tll(TM6B)</i>                                                                                                             | 25 °C                                    |

|                  |        |                                                                                                                                                  |                                                                                                                                                                                                                                                                                                 |                                                     |
|------------------|--------|--------------------------------------------------------------------------------------------------------------------------------------------------|-------------------------------------------------------------------------------------------------------------------------------------------------------------------------------------------------------------------------------------------------------------------------------------------------|-----------------------------------------------------|
| <b>Fig. 4.4</b>  | C      | w; +; GMR9D11-GAL4                                                                                                                               | <u>Control:</u> w; UAS- <i>RedStinger</i> ,UAS- <i>FLP</i> , <i>Ubi-p63E</i> ,FRT-STOP-FRT <i>Stinger</i> /( <i>CyOact</i> -GFP); +<br><u>TII OE:</u> w; UAS- <i>RedStinger</i> ,UAS- <i>FLP</i> , <i>Ubi-p63E</i> ,FRT-STOP-FRT <i>Stinger</i> /( <i>CyOact</i> -GFP); UAS- <i>tIII</i> (TM6B) | 25 °C                                               |
| <b>Fig. 4.6</b>  | A – D  | w; <i>Ay</i> -GAL4,UAS- <i>GFP</i> /( <i>CyOact</i> -GFP); GMR9D11-GAL4, <i>tub-GAL80<sup>ts</sup></i>                                           | <u>Control:</u> w; UAS- <i>FLP</i> /( <i>CyOact</i> -GFP); +<br><u>TII OE:</u> w; UAS- <i>FLP</i> /( <i>CyOact</i> -GFP); UAS- <i>tIII</i> (TM6B)                                                                                                                                               | 18 °C until hatching then shift to 29 °C            |
| <b>Fig. 4.8</b>  | A – B' | w; +; GMR9D11-GAL4,UAS- <i>mCD8-GFP</i>                                                                                                          | <u>Control:</u> w <sup>1118</sup> ; +; +<br><u>TLX OE:</u> w; UAS- <i>TLX</i> ; +                                                                                                                                                                                                               | 25 °C                                               |
| <b>Fig. 4.9</b>  | A      | w; +; GMR9D11-GAL4                                                                                                                               | <u>Control:</u> w; +; UAS- <i>RedStinger</i> ,UAS- <i>FLP</i> , <i>Ubi-p63E</i> ,FRT-STOP-FRT <i>Stinger</i> /(TM6B)<br><u>TLX OE:</u> w; UAS- <i>TLX</i> /( <i>CyOact</i> -GFP); UAS- <i>RedStinger</i> ,UAS- <i>FLP</i> , <i>Ubi-p63E</i> ,FRT-STOP-FRT <i>Stinger</i> /(TM6B)                | 25 °C                                               |
| <b>Fig. 4.10</b> | C      | w; <i>wor</i> -GAL4,UAS- <i>mCD8-GFP</i> ; <i>tub-GAL80<sup>ts</sup></i>                                                                         | <u>Control:</u> w <sup>1118</sup> ; +; +<br><u>TII OE:</u> w; +; UAS- <i>tIII</i> (TM6B)                                                                                                                                                                                                        | 18 °C for 6 days then shift to 29 °C until eclosion |
|                  | D      | w; <i>wor</i> -GAL4,R9D11- <i>mCD8-GFP</i> ; <i>tub-GAL80<sup>ts</sup></i>                                                                       | <u>Control:</u> w <sup>1118</sup> ; +; +<br><u>TII OE:</u> w; +; UAS- <i>tIII</i> (TM6B)                                                                                                                                                                                                        | 18 °C until hatching then shift to 29 °C            |
| <b>Fig. 4.11</b> | A-A''' | w; <i>wor</i> -GAL4,UAS- <i>mCD8-GFP</i> ; <i>tub-GAL80<sup>ts</sup></i>                                                                         | <u>Control:</u> w <sup>1118</sup> ; +; +<br><u>TII OE:</u> w; +; UAS- <i>tIII</i> (TM6B)                                                                                                                                                                                                        | 18 °C until hatching then shift to 29 °C            |
| <b>Fig. 4.12</b> | A – B  | w; <i>wor</i> -GAL4; <i>tub-GAL80<sup>ts</sup></i>                                                                                               | <u>Control:</u> w <sup>1118</sup> ; +; +<br><u>TII OE:</u> w; +; UAS- <i>tIII</i> (TM6B)                                                                                                                                                                                                        | 18 °C for 6 days then shift to 29 °C for 24 hours   |
|                  | C – F  | <i>btd</i> -GAL4,FRT19A/FM7 <i>act</i> -GFP; +; <i>tub</i> -GAL80 <sup>ts</sup>                                                                  | <u>Control:</u> w; +; UAS- <i>myr-mRFP</i> /TM6B<br><u>TII OE:</u> w; +; UAS- <i>tII</i> ,UAS- <i>myr-mRFP</i> /TM6B                                                                                                                                                                            | 18 °C for 6.5 days then shift to 29 °C for 16 hours |
| <b>Fig. 4.13</b> | A – B  | FRT19A, <i>tub-GAL80</i> , <i>hsFLP<sup>1</sup></i> ; <i>wor</i> -GAL4,UAS- <i>mCD8-mCherry</i> ,R9D11- <i>mCD8-GFP</i> /( <i>CyOact</i> -GFP);+ | <u>Control clones:</u> FRT19A; +; +<br><u>ase<sup>i</sup> clones:</u> <i>ase<sup>i</sup></i> ,FRT19A/(FM7 <i>Dfd</i> -YFP); +; +                                                                                                                                                                | 25 °C<br>37 °C heat shock 24 hours ALH              |
| <b>Fig. 4.14</b> | A – B  | <i>btd</i> -GAL4,FRT19A/FM7 <i>act</i> -GFP; +; <i>tub</i> -GAL80 <sup>ts</sup>                                                                  | <u>Control:</u> w; +; UAS- <i>myr-mRFP</i> /TM6B<br><u>TII OE:</u> w; +; UAS- <i>tII</i> ,UAS- <i>myr-mRFP</i> /TM6B                                                                                                                                                                            | 18 °C until hatching then shift to 29 °C            |

|                  |                  |                                                                                  |                                                                                                                                                                                         |                                          |
|------------------|------------------|----------------------------------------------------------------------------------|-----------------------------------------------------------------------------------------------------------------------------------------------------------------------------------------|------------------------------------------|
| <b>Fig. 4.15</b> | A – C            | <i>w; wor-GAL4,UAS-mCD8-GFP; tub-GAL80<sup>ts</sup></i>                          | <u>Control:</u> <i>w; UAS-lacZ; UAS-mCD8-GFP</i><br><u>TII OE:</u> <i>w; UAS-lacZ/(CyOact-GFP); UAS-tIII(TM6B)</i><br><u>Ase rescue:</u> <i>w; UAS-ase/(CyOact-GFP); UAS-tIII(TM6B)</i> | 18 °C until hatching then shift to 29 °C |
| <b>Fig. 4.16</b> | A                | <i>w; +; GMR71C09-GAL4, UAS-mCD8-GFP</i>                                         | <u>Control:</u> <i>w<sup>1118</sup>; +; +</i><br><u>TII OE:</u> <i>w; +; UAS-tIII(TM6B)</i>                                                                                             | 25 °C                                    |
|                  | B                | <i>w; vGlut-GAL4<sup>0k371</sup>, UAS-mCD8-GFP, FRTG13/(CyO); +</i>              | <u>Control:</u> <i>w<sup>1118</sup>; +; +</i><br><u>TII OE:</u> <i>w; +; UAS-tIII(TM6B)</i>                                                                                             | 25 °C                                    |
| <b>Fig. 4.17</b> | A – C            | <i>w; wor-GAL4,UAS-mCD8-GFP; tub-GAL80<sup>ts</sup></i>                          | <u>Control:</u> <i>w<sup>1118</sup>; +; +</i><br><u>TLX OE:</u> <i>w; UAS-TLX; +</i>                                                                                                    | 18 °C until hatching then shift to 29 °C |
|                  | D                | <i>w; +; GMR71C09-GAL4, UAS-mCD8-GFP</i>                                         | <u>Control:</u> <i>w<sup>1118</sup>; +; +</i><br><u>TLX OE:</u> <i>w; UAS-TLX; +</i>                                                                                                    | 25 °C                                    |
|                  | E                | <i>w; vGLUT-GAL4<sup>0k371</sup>, UAS-mCD8-GFP, FRTG13/(CyO); +</i>              | <u>Control:</u> <i>w<sup>1118</sup>; +; +</i><br><u>TLX OE:</u> <i>w; UAS-TLX; +</i>                                                                                                    | 25 °C                                    |
| <b>Fig. 5.2</b>  | A – C''          | N/A                                                                              | <i>w; R9D11-mCD8-GFP; +</i>                                                                                                                                                             | 25 °C                                    |
| <b>Fig. 5.4</b>  | Ai-iii<br>Ci-iii | N/A                                                                              | <i>w; R9D11-mCD8-GFP; +</i>                                                                                                                                                             | 25 °C                                    |
| <b>Fig. 5.5</b>  | A, C<br>Ei-iii   | N/A                                                                              | <i>w; R9D11-mCD8-GFP; +</i>                                                                                                                                                             | 25 °C                                    |
|                  | B, B'            | <i>w; +; GMR31H09-GAL4</i>                                                       | <i>w; R9D11-mCD8-GFP; UAS-myr-mRFP/TM6B</i>                                                                                                                                             | 25 °C                                    |
| <b>Fig. 5.6</b>  | C                | N/A                                                                              | <i>w; R9D11-mCD8-GFP; +</i>                                                                                                                                                             | 25 °C                                    |
|                  | D, D'            | N/A                                                                              | <i>w; +; R9D11-CD4-tdTomato x yw,hsFLP<sup>122</sup>; Sp/CyO; hh[p30]/(TM2)</i>                                                                                                         | 25 °C                                    |
|                  | E, E'            | N/A                                                                              | <i>w; R9D11-mCD8-GFP; + x yw; noc<sup>sc0</sup>/CyOen<sup>11</sup>(wg/lacZ); +</i>                                                                                                      | 25 °C                                    |
|                  | F                | N/A                                                                              | <i>w; R9D11-mCD8-GFP; +</i>                                                                                                                                                             | 25 °C                                    |
|                  | G                | N/A                                                                              | <i>w; R9D11-mCD8-GFP; + x yw; dpp-lacZ.Exel.2; +</i>                                                                                                                                    | 25 °C                                    |
| <b>Fig. 5.7</b>  | B                | N/A                                                                              | <i>w; R9D11-mCD8-GFP; +</i>                                                                                                                                                             | 25 °C                                    |
|                  | C, C'            | N/A                                                                              | <i>w<sup>1118</sup>; pnt-GFP.FPTB; +</i>                                                                                                                                                | 25 °C                                    |
|                  | D                | N/A                                                                              | <i>w; +; P{(miR7)EGFP}38R/TM6B</i>                                                                                                                                                      | 25 °C                                    |
|                  | E, E'            | N/A                                                                              | <i>w; +; my-GFP/(TM6B)</i>                                                                                                                                                              | 25 °C                                    |
| <b>Fig. 5.8</b>  | A – D'           | N/A                                                                              | <i>w; R9D11-mCD8-GFP; +</i>                                                                                                                                                             | 25 °C                                    |
| <b>Fig. 5.9</b>  | A – C            | <i>w; 13XLexAop2-mCD8-GFP, tub-GAL80<sup>ts</sup>/CyO act-GFP; GMR31H09-GAL4</i> | <i>yw; tub-GAL80<sup>ts</sup>,UAS-FLP;act &gt;y+&gt; LHv2-86Fb,DeltaRFP/(SM5^TM6B)</i>                                                                                                  | 29 °C                                    |
| <b>Fig. 5.10</b> | A, A'<br>C – D   | N/A                                                                              | <i>w; R9D11-mCD8-GFP; +</i>                                                                                                                                                             | 25 °C                                    |
| <b>Fig. 5.11</b> | A – Cii          | N/A                                                                              | <i>w; R9D11-mCD8-GFP; +</i>                                                                                                                                                             | 25 °C                                    |
| <b>Fig. 5.12</b> | A                | <i>w; +; R9D11-GAL4,UAS-mCD8-GFP</i>                                             | <i>w; +; Fz3-RFP/(TM6B)</i>                                                                                                                                                             | 25 °C                                    |

|                  |             |                                                                                                 |                                                                                                               |                                          |
|------------------|-------------|-------------------------------------------------------------------------------------------------|---------------------------------------------------------------------------------------------------------------|------------------------------------------|
|                  | B, B'       | <i>w</i> ; <i>Ay-GAL4,UAS-GFP/(CyOact-GFP)</i> ; <i>GMR9D11-GAL4,tub-GAL80<sup>ts</sup></i>     | <i>w</i> ; <i>UAS-FLP/(CyOact-GFP)</i> ; +                                                                    | 29 °C                                    |
|                  | Ci, Cii     | <i>w</i> ; <i>13XLexAop2-mCD8-GFP, tub-GAL80<sup>ts</sup>/CyOact-GFP</i> ; <i>GMR31H09-GAL4</i> | <i>yw</i> ; <i>tub-GAL80<sup>ts</sup>,UAS-FLP;act &gt;y+</i> + <i>LHv2-86Fb,DeltaRFP/(SM5<sup>TM</sup>6B)</i> | 29 °C until hatching then shift to 18 °C |
| <b>Fig. 5.13</b> | Ai, Aii     | N/A                                                                                             | <i>w</i> ; <i>R9D11-mCD8-GFP</i> ; +                                                                          | 25 °C                                    |
| <b>Fig. 5.14</b> | A – D'      | N/A                                                                                             | <i>w</i> ; <i>R9D11-mCD8-GFP</i> ; +                                                                          | 25 °C                                    |
| <b>Fig. 5.15</b> | A, B, E, E' | <i>w</i> ; <i>wg[ND382]-GAL4/CyOact-GFP</i> ; +                                                 | <i>w</i> ; <i>R9D11-mCD8-GFP</i> ; <i>UAS-myr-mRFP/TM6B</i>                                                   | 25 °C                                    |
|                  | C           | N/A                                                                                             | <i>w</i> ; <i>R9D11-mCD8-GFP</i> ; + x <i>w</i> ; <i>noc<sup>sco</sup>/CyOen<sup>11</sup>(wg/lacZ)</i> ; +    | 25 °C                                    |
|                  | D           | N/A                                                                                             | <i>w</i> ; <i>R9D11-mCD8-GFP</i> ; +                                                                          | 25 °C                                    |

**Appendix Table 1: *Drosophila* genotypes and experimental conditions**



# A newly discovered neural stem cell population is generated by the optic lobe neuroepithelium during embryogenesis in *Drosophila melanogaster*

Anna E. Hakes<sup>‡</sup>, Leo Otsuki<sup>\*-‡</sup> and Andrea H. Brand<sup>§</sup>

## ABSTRACT

Neural stem cells must balance symmetric and asymmetric cell divisions to generate a functioning brain of the correct size. In both the developing *Drosophila* visual system and mammalian cerebral cortex, symmetrically dividing neuroepithelial cells transform gradually into asymmetrically dividing progenitors that generate neurons and glia. As a result, it has been widely accepted that stem cells in these tissues switch from a symmetric, expansive phase of cell divisions to a later neurogenic phase of cell divisions. In the *Drosophila* optic lobe, this switch is thought to occur during larval development. However, we have found that neuroepithelial cells start to produce neuroblasts during embryonic development, demonstrating a much earlier role for neuroblasts in the developing visual system. These neuroblasts undergo neurogenic divisions, enter quiescence and are retained post-embryonically, together with neuroepithelial cells. Later in development, neuroepithelial cells undergo further cell divisions before transforming into larval neuroblasts. Our results demonstrate that the optic lobe neuroepithelium gives rise to neurons and glia over 60 h earlier than was thought previously.

**KEY WORDS:** Neural stem cell, Neuroepithelium, Neuroblast, Stem cell divisions, Symmetric/Asymmetric division, Brain

## INTRODUCTION

Neural stem cells in the developing brain must regulate their proliferation precisely to generate a functional nervous system. An imbalance between symmetric and asymmetric stem cell divisions can lead to the inadequate production of differentiated progeny or, conversely, to tumour formation. Importantly, work in *Drosophila* has shown that specific brain tumours arise from the mis-regulation of distinct populations of neural stem cells. In *brain tumour (brat)* mutants, asymmetrically dividing Type II neuroblasts generate aberrant lineages, whereas symmetrically dividing neuroepithelial cells are the tumour cells of origin in *lethal(3)malignant brain tumour [l(3)mb1]* mutants (Bowman et al., 2008; Richter et al.,

2011). Thus, identifying different types of neural stem cells and their functions is central to understanding both normal brain development and the diverse causes of tumourigenesis.

The *Drosophila* optic lobe, which forms the visual processing system of the adult brain, is an established system for studying neural stem cells *in vivo* (Egger et al., 2011). The development of the medulla, the largest visual ganglion, shares many parallels with the development of the mammalian cerebral cortex (Brand and Livesey, 2011; Egger et al., 2011). In both tissues, symmetrically dividing neural stem cells (neuroepithelial cells) expand the stem cell pool before transforming into asymmetrically dividing neural stem cells (also called neuroblasts in *Drosophila*) that produce neurons and glia (Fig. S1A) (Egger et al., 2007; Noctor et al., 2004). Previous studies of neuroepithelial cells and neuroblasts in the optic lobe have focussed largely on larval stages (Egger et al., 2011, 2010; Yasugi et al., 2010, 2008). Neuroepithelial cells divide symmetrically in the early larva before a proneural wave sweeps across the neuroepithelium at mid-larval stages, converting neuroepithelial cells into neuroblasts (Yasugi et al., 2008). Here, we demonstrate that this transition begins much earlier, and that neuroepithelial cells and neuroblasts co-exist from embryonic stages.

## RESULTS AND DISCUSSION

### Neuroepithelial cells divide in the embryo

The optic lobe primordium is first apparent as a dense patch of cells in the head ectoderm of stage 11 embryos (Hartenstein and Campos-Ortega, 1984; Poulsen, 1950; Turner and Mahowald, 1979). These cells undergo four cell divisions before invaginating from the ectoderm as a neuroepithelial sheet and attaching to the lateral surface of the brain between embryonic stages 12 and 13 (Fig. 1A) (Green et al., 1993).

Neuroepithelial cells can be identified by their expression of Fasciilin II (FasII), the orthologue of neural cell adhesion molecule (NCAM) (Grenningloh et al., 1991; Younossi-Hartenstein et al., 1997). To determine the proliferation pattern of neuroepithelial cells in the embryo, we co-stained for FasII and the cell division marker phospho-histone H3 (pH3). We found pH3<sup>+</sup> neuroepithelial cells at all developmental stages between optic primordium invagination and the end of embryogenesis (Fig. 1Bi-iii and Fig. S1B). Thus, the neuroepithelium divides throughout embryogenesis, in contrast to a previous suggestion that the optic primordium is dormant in the embryo (Green et al., 1993).

Why was the embryonic neuroepithelium suggested to be dormant? BrdU incorporation assays had shown that neuroepithelial cells do not undergo S phase after invagination (Green et al., 1993). We tested the phase of the cell cycle in which neuroepithelial cells reside as they undergo invagination. We assessed expression of Cyclin A (CycA), a G2-phase cyclin protein, and found that neuroepithelial cells were all CycA<sup>+</sup> when they

The Gurdon Institute and Department of Physiology, Development and Neuroscience, University of Cambridge, Tennis Court Road, Cambridge CB2 1QN, UK.

\*Present address: Research Institute of Molecular Pathology (IMP), Vienna Biocenter (VBC), Campus-Vienna-Biocenter 1, 1030 Vienna, Austria.

‡These authors contributed equally to this work

§Author for correspondence (a.brand@gurdon.cam.ac.uk)

 L.O., 0000-0001-6107-2508; A.H.B., 0000-0002-2089-6954

This is an Open Access article distributed under the terms of the Creative Commons Attribution License (<http://creativecommons.org/licenses/by/3.0>), which permits unrestricted use, distribution and reproduction in any medium provided that the original work is properly attributed.

Received 29 March 2018; Accepted 24 August 2018

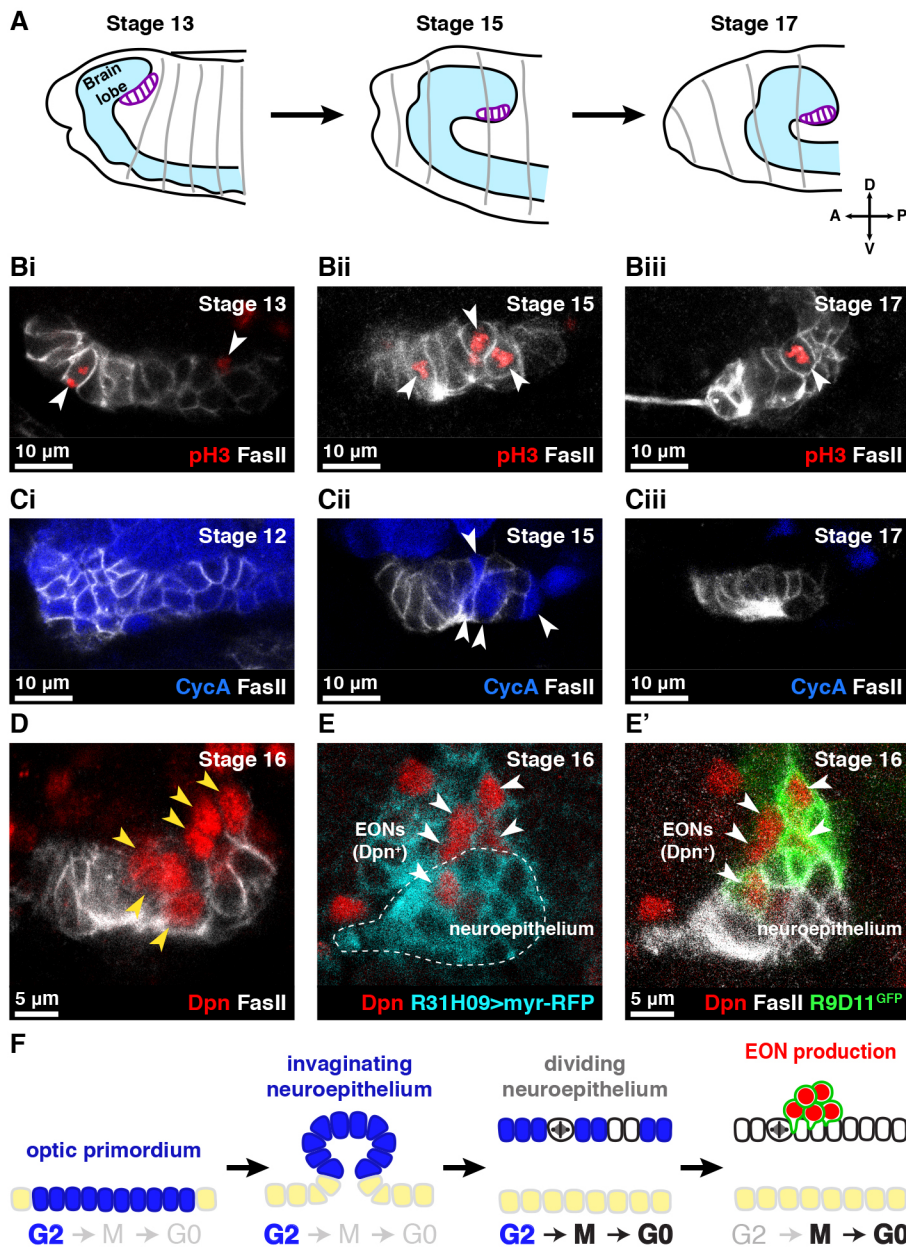


**Fig. 1. Embryonic neuroepithelial cells divide and generate EONs.** (A) Schematic depicting the position of the neuroepithelium (purple) as it invaginates from the head ectoderm and attaches to the side of the brain lobe in the embryo. A, anterior; P, posterior; D, dorsal; V, ventral. (Bi-iii) Neuroepithelial cells (FasII<sup>+</sup>, white) co-stained for the mitosis marker pH3 (red) at the indicated embryonic stages. Arrowheads indicate dividing neuroepithelial cells. (Ci-iii) Neuroepithelial cells (white) co-stained for the S/G2 cyclin CycA (blue) at the indicated embryonic stages. Neuroepithelial cells lose CycA expression progressively. Arrowheads in Cii indicate individual neuroepithelial cells that express CycA. (D) Dpn<sup>+</sup> cells (red, arrowed) appear in close proximity to the neuroepithelium (white) during embryogenesis. (E,E') RFP expressed using R31H09-GAL4 (cyan in E) labels the embryonic neuroepithelium (white in E'). RFP is inherited by neighbouring Dpn<sup>+</sup> cells (red, arrowed). These Dpn<sup>+</sup> cells express R9D11-mCD8-GFP (green). (F) EON production from the embryonic neuroepithelium. The optic primordium invaginates while in G2 (CycA<sup>+</sup>, blue) to give rise to the embryonic neuroepithelium. Neuroepithelial cells undergo mitosis once, losing CycA expression, to produce EONs (green and red). Surface ectoderm cells are indicated in yellow. Brain surface is downwards; interior is upwards. (Bi-E') Single section confocal images.

invaginated from the ectoderm (Fig. 1Ci). Neuroepithelial cells lost CycA expression over time, concomitant with cell divisions, until they were all CycA<sup>-</sup> at the end of embryogenesis (Fig. 1Ci-iii). Thus, we found that neuroepithelial cells invaginate in G2 before dividing, explaining both our results and previous observations (Green et al., 1993). As neuroepithelial cells do not undergo S phase in the embryo after invagination (Green et al., 1993), we infer that they divide once each (Fig. 1F).

### The embryonic neuroepithelium generates neuroblasts

We next assessed the role of neuroepithelial cell divisions in the embryo. We found no significant increase in the number of neuroepithelial cells over time (Fig. S1C), indicating that these cell divisions do not serve to increase the size of the neuroepithelium. We therefore tested whether the embryonic neuroepithelium produces neuroblasts, in a similar manner to the late larval neuroepithelium.

We stained for the Hes family transcription factor Deadpan (Dpn), which labels all identified neuroblasts in the *Drosophila*

brain (Bier et al., 1992). We found Dpn<sup>+</sup> cells in close proximity to the neuroepithelium beginning at embryonic stage 12 (Fig. 1D). To test the lineage relationship between neuroepithelial cells and these neuroblasts, we expressed red fluorescent protein (RFP) in the neuroepithelium and assessed whether RFP was inherited by the Dpn<sup>+</sup> cells. Interestingly, we found that GAL4<sup>855a</sup> and *ogre*-GAL4, two GAL4 drivers that label the larval neuroepithelium (Dillard et al., 2018; Egger et al., 2007), did not express in the embryonic neuroepithelium (data not shown). We therefore identified a GAL4 driver, R31H09-GAL4, that labels the embryonic neuroepithelium (Fig. 1E). When we expressed RFP using R31H09-GAL4, we found that RFP was inherited by the Dpn<sup>+</sup> cells (Fig. 1E). We conclude that the embryonic neuroepithelium produces neuroblasts, and refer to these neuroblasts as EONs (embryonic optic neuroblasts).

We identified a ~4 kb fragment of the *earmuff* (*erm*) enhancer (R9D11) that drives expression in EONs consistently, allowing us to track the production of EONs from the embryonic neuroepithelium. (Fig. 1E'). Using R9D11-mCD8-GFP (R9D11 driving expression

of membrane-targeted GFP) (Pfeiffer et al., 2008; Zhu et al., 2011), we found that EONs are produced continuously between stage 12 and stage 17 of embryogenesis, with a final number of  $8.6 \pm 0.7$  EONs per brain lobe (Fig. S1D,Ei-iii). EONs were first apparent in the neuroepithelial layer (FasII<sup>+</sup> Dpn<sup>+</sup> R9D11<sup>+</sup>) and were extruded medially into the brain, where they downregulated FasII expression (Fig. S1Ei-iii). Importantly, our results demonstrate that neuroepithelial cells produce neuroblasts much earlier (~60 h earlier) than thought previously (mid-larval stage) (Fig. 1F).

### EONs derive from two spatial domains of the neuroepithelium

We noticed that EONs were generated at specific discontinuous points along the embryonic neuroepithelium. In the larval brain, the neuroepithelium is patterned into spatial domains along the anterior-posterior axis by expression of *Vsx1*, *Optix*, *decapentaplegic* (*dpp*) and *wingless* (*wg*) (Fig. S2A) (Erclik et al., 2008; Gold and Brand, 2014; Kaphingst and Kunes, 1994; reviewed by Bertet, 2017). In addition, the ventral (but not dorsal) half of the neuroepithelium expresses *hedgehog* (*hh*) (Fig. S2A) (Chen et al., 2016; Evans et al., 2009). All spatial domains of the neuroepithelium generate neuroblasts in the larva. As we did not find a continuous band of EONs in the embryo, we reasoned that they might arise from a subset of spatial domains of the neuroepithelium.

We found that almost all EONs are produced by the *Vsx1*<sup>+</sup> (central) domain of the embryonic neuroepithelium, straddling the presumptive dorsal-ventral boundary (Fig. 2A-B, Fig. S2B,B'). These EONs themselves expressed *Vsx1* (Fig. 2B). We observed that the *wg*<sup>+</sup> tips of the neuroepithelium produce a minority of EONs as assessed using *wg-LacZ*, a reporter inserted at the endogenous *wg* locus (Kassis et al., 1992) (Fig. S2C,C'). Thus, we conclude that the central domain, and to a lesser extent the tips of the embryonic neuroepithelium, produces neuroblasts. Interestingly, we found no evidence for *Optix* or *dpp* expression in the embryonic neuroepithelium (Fig. 2A, Fig. S2D-E'), suggesting that these domains become patterned and start to produce neuroblasts later in development.

### The embryonic neuroepithelium expresses transition zone markers

In the larval brain, neuroepithelial cells are transformed into neuroblasts at a transition zone. The transition zone expresses the proneural gene *lethal of scute* [*l(1)sc*] and the microRNA *miR-7* and is regulated by signalling pathways, including the EGFR and Notch pathways (Fig. S3A) (Caygill and Brand, 2017; Egger et al., 2010; Yasugi et al., 2008, 2010). We found discrete regions of *L(1)sc* expression in the embryonic neuroepithelium that corresponded spatially with EON production (Fig. 2C). *L(1)sc*<sup>+</sup> cells exhibited many features of the larval transition zone: they were positive for EGFR signalling (Fig. 2D-D'), had low Notch signalling (Fig. 2E-E') and expressed *miR-7* (Fig. S3B). Consistent with a neuroepithelium to neuroblast transition, EONs expressed the neuroepithelial cell markers E-Cadherin (E-Cad) and FasII as they were generated but later downregulated expression of these genes (Fig. S3C-D').

### EONs generate neurons and glia

Neuroblasts in the larval brain divide asymmetrically to generate intermediate progenitor cells (called ganglion mother cells, GMCs) that, in turn, divide once to produce neurons and glia. We found that, like larval neuroblasts, EONs were positive for *Wor* (Wormiu, Fig. S4A,A') and *Mira* (Miranda, Fig. 3A,A'), localised *Pros* (Prospero) and *Mira* asymmetrically at mitosis (Ikeshima-Kataoka et al., 1997) (Fig. S4B,B'), and divided asymmetrically to generate *Dpn*<sup>-</sup> progeny (Fig. 3B,B'). EON lineages were identifiable as R9D11-mCD8-GFP<sup>+</sup> cells contacting EONs (Fig. 3B,B'). To identify the cell types produced by EONs, we stained for markers specific to GMCs, neurons or glia. We found cells with nuclear *Pros* (Fig. S4C,C'), *Elav* (Embryonically lethal abnormal vision, Fig. 3C,C') or *Repo* (Reversed polarity, Fig. 3D-D') next to EONs, corresponding to GMCs, neurons and glia, respectively. By the end of embryogenesis, we found an average of  $16.1 \pm 1.7$  neurons and  $3.7 \pm 1.4$  glia per brain lobe that were in contact with EONs and expressed R9D11-mCD8-GFP ( $n=10$  brain lobes).

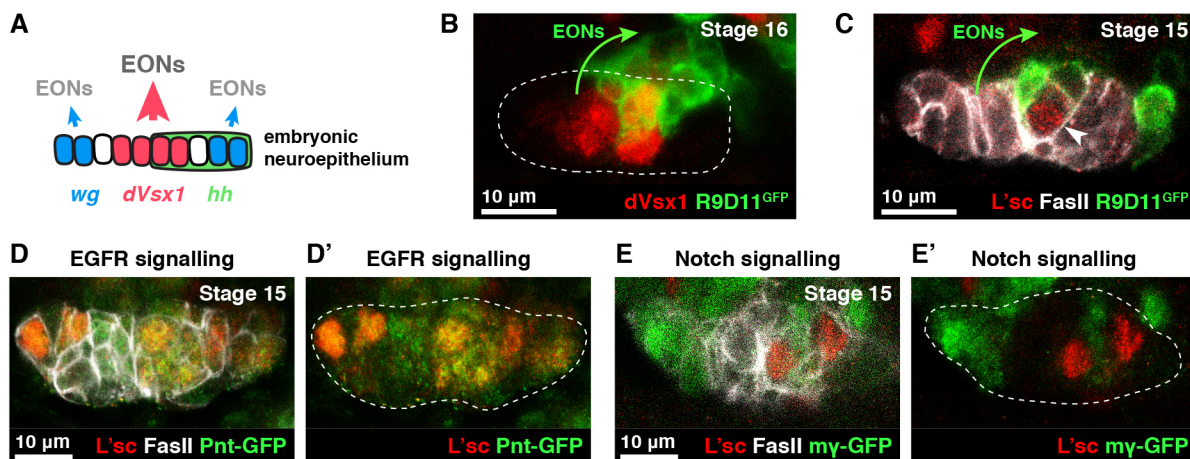


**Fig. 2. The embryonic neuroepithelium expresses transition zone markers and produces EONs at specific spatial domains.** (A) Spatial patterning domains in the embryonic neuroepithelium and neuroblast generation (compare with Fig. S2A). The *Vsx1*<sup>+</sup>, *wg*<sup>+</sup> and *hh*<sup>+</sup> domains are present, but the *Optix*<sup>+</sup> and *dpp*<sup>+</sup> domains are not yet established. The *Vsx1*<sup>+</sup> domain generates most EONs; the *wg*<sup>+</sup> tips generate a minority of EONs. Axes as in Fig. 1F. (B) EONs (R9D11-mCD8-GFP<sup>+</sup>, green) are produced from the *Vsx1*<sup>+</sup> domain (red) of the neuroepithelium (outlined). Arrow indicates EON generation. Maximum intensity projection of five 1 μm slices in z. (C) Neuroepithelial cells (FasII<sup>+</sup>, white) express *L(1)sc* (red, arrowhead) in close proximity to EONs (green, arrow). (D,D') *L(1)sc*<sup>+</sup> cells (red) in the neuroepithelium (white) have high EGFR signalling, as assessed using the Pnt-GFP reporter (green) (Boisclair Lachance et al., 2014). (E,E') *L(1)sc*<sup>+</sup> cells (red) in the neuroepithelium (white) have low Notch signalling, as assessed using the HLHmγ-GFP reporter (green) (Almeida and Bray, 2005). (B-E') Single section confocal images.

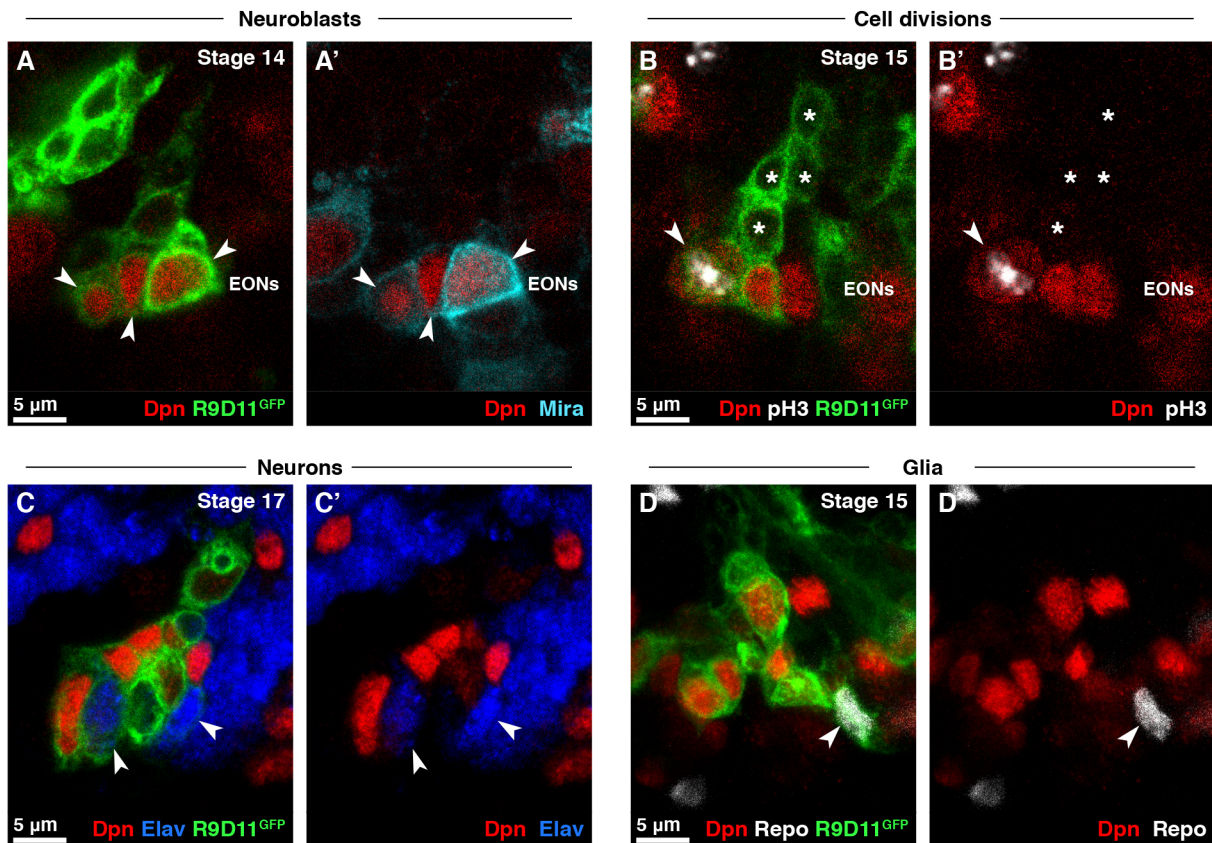


**Fig. 3. EONs generate neurons and glia.** (A,A') EONs ( $Dpn^+/R9D11\text{-}mCD8\text{-}GFP^+$ , red and green, arrowheads) express the gene *Mira* (cyan), which is expressed by neuroblasts. (B,B') EONs (red and green) divide and generate  $Dpn^-$  progeny (asterisks). Arrowheads indicate a dividing EON, assessed by co-staining for pH3 (white). (C,C') EONs (red and green) generate *Elav*<sup>+</sup> neurons (blue, arrowheads). (D,D') EONs (red and green) generate *Repo*<sup>+</sup> glia (white, arrowheads). Maximum intensity projection of three 1  $\mu\text{m}$  slices in z. (A-C') Single section confocal images.

We confirmed the lineage relationship between EONs and neurons using the FLEXAMP (flip-out LexA amplification) technique, a memory cassette tool (Bertet et al., 2014). We found that neurons were labelled when we expressed FLEXAMP in EONs during embryogenesis (Fig. S4D-E). We conclude that, like canonical neuroblasts, EONs undergo neurogenic divisions and generate differentiated progeny.

### EONs undergo G0 quiescence and persist into the larval brain

At the end of embryogenesis, the majority of neuroblasts in the central brain and ventral nerve cord enter mitotic quiescence or are eliminated by apoptosis (Maurange and Gould, 2005; Truman and Bate, 1988; White et al., 1994). Quiescent neuroblasts persist into the larval brain and later become reactivated in a nutrition-dependent manner to generate neurons and glia in a second round of neurogenesis (Britton and Edgar, 1998; Chell and Brand, 2010; Otsuki and Brand, 2018; Sousa-Nunes et al., 2011; Spéder and Brand, 2014; Truman and Bate, 1988). We assessed whether EONs undergo quiescence or apoptosis at the end of embryogenesis.

We found that EONs persist into the larval brain, identifiable as a cluster of  $Dpn^+ R9D11\text{-}mCD8\text{-}GFP^+$  cells. As in the embryo, EONs are located below the neuroepithelium, medial in the brain (Fig. 4A-B, Movie 1). We observed  $10.4 \pm 0.6$  EONs per brain lobe at 0 h after larval hatching (ALH) ( $n=31$  brain lobes), in close agreement with the final number detected in the embryo. The only neuroblasts known to proliferate at larval hatching are the mushroom body and lateral neuroblasts (Ito and Hotta, 1992; Prokop and

Technau, 1991; Truman and Bate, 1988), indicating that EONs are quiescent at this stage. It has been shown that quiescent neuroblasts in the brain lobes and ventral nerve cord do not express *Wor* or *Mira* (Lai and Doe, 2014; Otsuki and Brand, 2018; Tomancak et al., 2007). In agreement with this, we found that EONs did not express *Wor* or *Mira* at 0 h ALH (Fig. S5A-B'), despite expressing these genes previously in the embryo (Fig. 3A,A', Fig. S4A,A').

We discovered recently that neuroblasts can undergo two types of quiescence (Otsuki and Brand, 2018). Most quiescent neuroblasts arrest in G2, and only a minority in G0 in the ventral nerve cord. G2 and G0 are two functionally distinct types of stem cell quiescence, as G2 neuroblasts become activated faster than G0 neuroblasts in response to nutritional inputs (Otsuki and Brand, 2018). We found that all EONs undergo G0 quiescence, as they did not express the G2 marker *CycA* at 0 h ALH (Fig. S5C,C'). We also found that neuroepithelial cells, having divided throughout embryogenesis, eventually become G0 quiescent prior to larval hatching (Fig. S5D). Thus, all neural stem cells in the visual system undergo G0 quiescence, which is otherwise uncommon in the *Drosophila* brain.

### EONs reactivate post-embryonically

The neuroepithelial cells that were generated in the embryo reactivate and begin symmetric divisions during the first larval instar (12-15 h ALH) (Datta, 1995; Nassif et al., 2003). We tested when EONs, which lie below the plane of the neuroepithelium, reactivate. We found that EONs were among the last neuroblasts to reactivate in the brain, consistent with our previous finding that G0 neuroblasts reactivate after G2 neuroblasts (Otsuki and Brand,

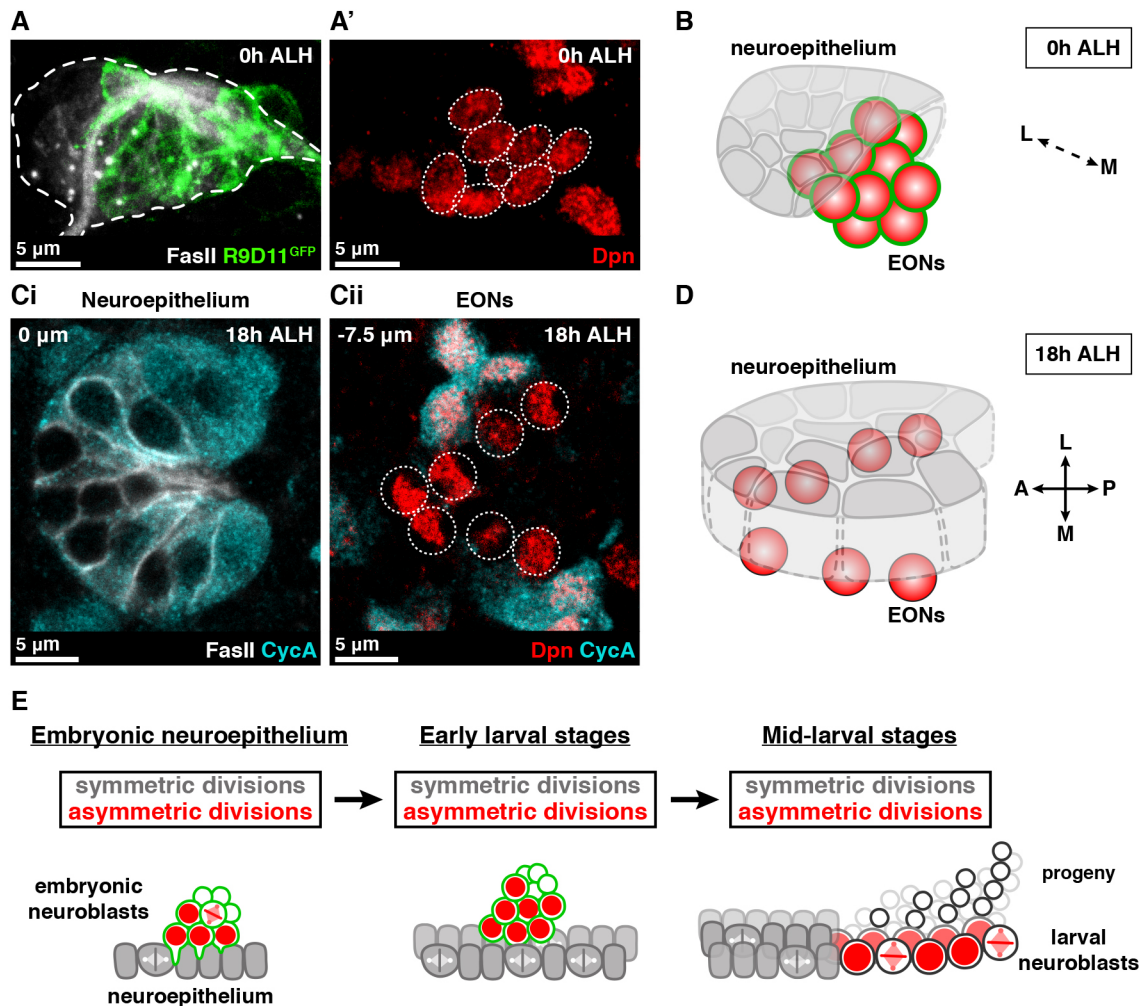


**Fig. 4. EONs persist into the post-embryonic brain.** (A,A') At 0 h ALH, EONs are associated closely with the neuroepithelium (FasII<sup>+</sup>, white and outlined). EONs express R9D11-mCD8-GFP (green) in A and Dpn (red, circled) in A'. Single frame of a 3D reconstruction over a 17  $\mu$ m confocal stack. The entire 3D reconstruction is available as Movie 1. (B) 3D schematic depicting the spatial relationship between the neuroepithelium and EONs at 0 h ALH. L, lateral; M, medial. (Ci,ii) Single section confocal images taken at indicated depths relative to the neuroepithelium at 18 h ALH. EONs are located medial to the neuroepithelium. (Ci) The neuroepithelium (white) has reactivated and expresses CycA (cyan). (Cii) EONs (red, circled) do not express CycA and are G0 quiescent, in contrast to neighbouring neuroblasts (red and cyan). (D) 3D schematic depicting the spatial relationship between the neuroepithelium and EONs at 18 h ALH. A, anterior; P, posterior; L, lateral; M, medial. (E) Revised model of optic lobe medulla development. Neuroepithelial cells (grey) divide and generate neuroblasts (red and green) in the embryo. After larval hatching, these neuroepithelial cells begin symmetric divisions. From mid-larval stages neuroepithelial cells transform into asymmetrically dividing larval neuroblasts (red and not green). Medial-lateral axis is left-right; brain surface is towards the bottom of the schematic. Compare to Fig. S1A.

2018). EONs were quiescent (small, CycA<sup>-</sup> and pH3<sup>-</sup>) at 18 h ALH, in contrast to most other neuroblasts in the brain (Fig. 4Ci,ii, D). EONs no longer expressed R9D11-mCD8-GFP at this stage; however, they were readily identifiable based on their position relative to the neuroepithelium. We found that EONs reactivate by 30 h ALH, as all neuroblasts surrounding the neuroepithelium have re-entered the cell cycle (Fig. S5Ei,ii). Thus, we have shown that EONs generate progeny in the embryo, undergo quiescence and become reactivated post-embryonically.

Switches in stem cell division mode are thought to drive the development of both the mammalian cerebral cortex and the *Drosophila* visual system (Fig. S1A). Symmetrically dividing neuroepithelial cells transform into asymmetrically dividing neuroblasts in the *Drosophila* optic lobe during larval development. Here, we have shown that neuroepithelial cells begin to produce neuroblasts in the embryo, demonstrating a much earlier function for both types of neural stem cell in the developing

visual system (Fig. 4E). Our discovery that both symmetrically and asymmetrically dividing stem cells are present in the embryo is important given that the mis-regulation of each type of stem cell gives rise to tumours through distinct mechanisms (Bowman et al., 2008; Richter et al., 2011). Our results have implications for understanding the susceptibility of the brain to different types of tumours during embryonic development, with relevance for the progression of childhood tumours (Marshall et al., 2014).

Although embryonic neuroepithelial cells appear to generate neuroblasts in a similar manner to larval neuroepithelial cells, we uncovered several striking differences between the embryonic and larval neuroepithelia. We found that GAL4 drivers commonly used to label the larval neuroepithelium (GAL4<sup>c855a</sup> and *ogre*-GAL4) are not expressed in the embryonic neuroepithelium. Larval neuroepithelial cells divide repeatedly and are eventually depleted, in contrast to embryonic neuroepithelial cells that divide once each before becoming quiescent. The larval neuroepithelium

produces neuroblasts from all spatial domains, whereas only the *Vsx1<sup>+</sup>* and *wg<sup>+</sup>* domains produce neuroblasts in the embryo.

Importantly, our results explain recent observations that the larval neuroepithelium expresses L(1)sc, which marks the transition zone, much before the generation of larval neuroblasts (Dillard et al., 2018; Sato et al., 2016). It has been proposed that the transition zone is established at an early stage, ready to induce the neuroepithelium to neuroblast transition later in development (Dillard et al., 2018). Instead, our results demonstrate that L(1)sc expression in the early larval neuroepithelium is a continuation of a neuroepithelium to neuroblast transition that commenced in the embryo.

EONs express R9D11-mCD8-GFP as they are generated by neuroepithelial cells, but later downregulate expression. Intriguingly, we found that R9D11-mCD8-GFP is also expressed at the transition zone in the late larval brain (Fig. S6A). Thus, R9D11-mCD8-GFP expression is common to newly born optic lobe neuroblasts in both the embryo and larva. As R9D11 is a fragment of the *erm* enhancer (Pfeiffer et al., 2008), *erm* might have a function in the transition from neuroepithelial cell to neuroblast.

We have discovered an embryonic phase of neurogenesis originating from the optic lobe neuroepithelium. Although the identities of the neurons born during this embryonic phase are as yet unknown, we find that they lie in close proximity to Bolwig's nerve: part of the larval visual system (Fig. S7A). Tracking the contribution of EONs to the adult brain was not possible in this study because the genetic tools that label EONs, although specific in early development, become widely expressed later in development. The functional contributions of EON lineages to the larval and adult visual systems will be an intriguing topic for future study.

## MATERIALS AND METHODS

### Fly stocks and husbandry

*Drosophila melanogaster* were reared in cages at 25°C, unless indicated otherwise. Embryos were collected onto freshly yeasted apple juice plates overnight and staged according to Campos-Ortega and Hartenstein (1985). For larval experiments, larvae were picked within 1 h of hatching [designated 0 h after larval hatching (ALH)], transferred to a yeasted food plate and reared to the desired stage before dissection.

The following stocks were used: *w<sup>1118</sup>*, *GAL4<sup>c855a</sup>* (Manseau et al., 1997), R9D11-mCD8-GFP (Zhu et al., 2011), R9D11-CD4-tdTomato (Han et al., 2011), (*miR-7*)E>GFP (Li et al., 2009), *wg-LacZ* (*1-en-11*) (Kassis et al., 1992), *hh<sup>P30</sup>* (Lee et al., 1992) and HLHmy-GFP (Almeida and Bray, 2005). The following stocks were obtained from the Bloomington *Drosophila* Stock Center: *dpp-lacZ<sup>Exel.2</sup>* (#8411), UAS-myr-mRFP (#7119), R31H09-GAL4 (#49694), R29C07-GAL4 ('ogre-GAL4', #49340) and pnt-GFP.FPTB (#42680). To perform FLEXAMP, we crossed flies carrying *yw*; *tub-Gal80<sup>ts</sup>*, UAS-*flp*; *act>y<sup>+</sup>*>LHV2<sup>deltaRFP</sup>-86Fb (LexA) (Yagi et al., 2010) to flies carrying 13XLexAOp2-mCD8-GFP (Bloomington #32205), R31H09-GAL4 and *tub-GAL80<sup>ts</sup>* (Bloomington #7019).

### Sample fixation

Embryos were washed into a nitex basket with distilled water and dechorionated in 50% bleach/water for 3 min. After rinsing with water, embryos were fixed on a rolling shaker for 20 min in a 6 ml glass bottle containing 3 ml of 4% formaldehyde/PBS and 3 ml heptane. Fixed embryos were washed and stored in methanol at -20°C until ready to immunostain.

Larval brains were dissected in PBS and fixed on a shaker for 20 min in 4% formaldehyde/PBS. Fixed brains were washed well with PBS containing 0.3% Triton-X (PBTx) before immediate immunostaining.

### Immunostaining

Fixed embryos were re-hydrated in 0.3% PBTx and blocked on a shaker for at least 15 min in 10% normal goat serum/PBS. Embryos were incubated overnight at 4°C with primary antibodies diluted in 0.3% PBTx. Embryos were washed well with 0.3% PBTx, then incubated overnight at 4°C with

secondary antibodies diluted in 0.3% PBTx. Embryos were washed well with 0.3% PBTx then mounted in 50% glycerol/PBS. Larval brains were processed identically to embryos, with the following alterations: (1) the re-hydration step was omitted and (2) brains were mounted in Vectashield (Vector laboratories).

The following primary antisera were used: mouse 22C10 1:50 (DSHB), chicken anti-βgal 1:1000 (Abcam, ab9361), rabbit anti-CycA 1:100 (Whitfield et al., 1990; rb270), guinea pig anti-Dpn 1:5000 (Caygill and Brand, 2017), rat anti-Dpn 1:100 (Abcam, 11D1BC7, ab195173), rat anti-E-Cad 1:20 (DSHB, DCAD2 conc.), rat anti-Elav 1:100 (DSHB, 7E8A10 conc.), mouse anti-FasII 1:20 (DSHB, 1D4 conc.), chick anti-GFP 1:2000 (Abcam, ab13970), rat anti-Mira 1:500 (a kind gift from C. Q. Doe, University of Oregon, USA), rabbit anti-Optix 1:500 (Kenyon et al., 2005), mouse anti-Pros 1:30 (DSHB, MR1A conc.), rabbit anti-pH3 1:100 (Merck Millipore, 06-570), rat anti-pH3 1:200 (Abcam, ab10543), rabbit anti-Repo 1:10,000 (a kind gift from B. Altenhein, University of Cologne, Germany), guinea pig anti-Vsx1 1:1000 (Erclik et al., 2008) and rat anti-Wor 1:100 (Abcam, 5A3AD2, ab196362). Guinea pig anti-L(1)sc (1:1000) was generated by C. M. Davidson, E. E. Caygill and A.H.B. using constructs that were a kind gift from J. Skeath (Washington University, USA). Primary antibodies were detected using Alexa Fluor-conjugated secondary antibodies (Thermo Fisher Scientific) diluted 1:500 in 0.3% PBTx.

### Lineage tracing with FLEXAMP

To perform FLEXAMP, we crossed flies carrying *yw*; *tub-Gal80<sup>ts</sup>*, UAS-*flp*; *act>y<sup>+</sup>*>LHV2<sup>deltaRFP</sup>-86Fb (LexA) to flies carrying 13XLexAOp2-mCD8-GFP, R31H09-GAL4 and *tub-GAL80<sup>ts</sup>*. Embryos were collected for 3 h at room temperature, then raised at 29°C (test) or 18°C (control) until larval hatching. Larval brains were dissected at 0 h ALH and stained for GFP, Dpn, Elav and/or 22C10 as appropriate.

### Image acquisition and processing

Fluorescent images were acquired using a Leica SP8 confocal microscope. Images were analysed using Fiji (Schindelin et al., 2012). Adobe Photoshop was used to adjust brightness and contrast in images. Adobe Illustrator was used to compile figures.

### Quantification and statistical analysis

R was used for statistical analysis. No data were excluded.

### Acknowledgements

We thank B. Altenhein, K. Basler, S. Bray, R. Carthew, J. Casal, E. E. Caygill, C. M. Davidson, C. Doe, T. Erclik, A. Gould, L. Jan and Y. N. Jan, Y. Kimata, G. Kolahgar, F. Pignoni, I. Salecker, J. Skeath, R. Yagi, S. Zhu, Bloomington *Drosophila* Stock Center, the Asian Distribution Centre for Segmentation Antibodies, and the Developmental Studies Hybridoma Bank (DSHB) for reagents. We thank T. Suzuki and J. van den Ameele for helpful discussion.

### Competing interests

The authors declare no competing or financial interests.

### Author contributions

Conceptualization: A.E.H., L.O., A.H.B.; Methodology: A.E.H., L.O.; Formal analysis: A.E.H., L.O., A.H.B.; Investigation: A.E.H., L.O., A.H.B.; Resources: A.H.B.; Writing - original draft: A.E.H., L.O., A.H.B.; Writing - review & editing: A.E.H., L.O., A.H.B.; Supervision: A.H.B.; Project administration: A.H.B.; Funding acquisition: A.H.B.

### Funding

This work was funded by the Royal Society Darwin Trust Research Professorship and a Wellcome Trust Senior Investigator Award (103792) to A.H.B., and by Wellcome Trust PhD Studentships (102454 to A.E.H. and 097423 to L.O.). A.H.B. acknowledges core funding to The Gurdon Institute from the Wellcome Trust (092096) and Cancer Research UK (C6946/A14492). Deposited in PMC for immediate release.

### Supplementary information

Supplementary information available online at <http://dev.biologists.org/lookup/doi/10.1242/dev.166207.supplemental>

## References

- Almeida, M. S. and Bray, S. J. (2005). Regulation of post-embryonic neuroblasts by *Drosophila* Grainyhead. *Mech. Dev.* **122**, 1282-1293.
- Bertet, C. (2017). The developmental origin of cell type diversity in the *Drosophila* visual system. In *Decoding Neural Circuit Structure and Function* (ed. A. Celik and M. F. Wernet), pp. 419-435. Cham, Switzerland: Springer.
- Bertet, C., Li, X., Erclik, T., Cavey, M., Wells, B. and Desplan, C. (2014). Temporal patterning of neuroblasts controls Notch-mediated cell survival through regulation of Hid or Reaper. *Cell* **158**, 1173-1186.
- Bier, E., Vaessin, H., Younger-Shepherd, S., Jan, L. Y. and Jan, Y. N. (1992). deadpan, an essential pan-neural gene in *Drosophila*, encodes a helix-loop-helix protein similar to the hairy gene product. *Genes Dev.* **6**, 2137-2151.
- Boisclair Lachance, J.-F., Peláez, N., Cassidy, J. J., Webber, J. L., Rebay, I. and Carthew, R. W. (2014). A comparative study of Pointed and Yan expression reveals new complexity to the transcriptional networks downstream of receptor tyrosine kinase signaling. *Dev. Biol.* **385**, 263-278.
- Bowman, S. K., Rolland, V., Betschinger, J., Kinsey, K. A., Emery, G. and Knoblich, J. A. (2008). The tumor suppressors Brat and Numb regulate transit-amplifying neuroblast lineages in *Drosophila*. *Dev. Cell* **14**, 535-546.
- Brand, A. H. and Livesey, F. J. (2011). Neural stem cell biology in vertebrates and invertebrates: more alike than different? *Neuron* **70**, 719-729.
- Britton, J. S. and Edgar, B. A. (1998). Environmental control of the cell cycle in *Drosophila*: nutrition activates mitotic and endoreplicative cells by distinct mechanisms. *Development* **125**, 2149-2158.
- Campos-Ortega, J. A. and Hartenstein, V. (1985). *The Embryonic Origin of Drosophila melanogaster*. Berlin, Germany: Springer-Verlag.
- Caygill, E. E. and Brand, A. H. (2017). miR-7 buffers differentiation in the developing *Drosophila* visual system. *Cell Rep.* **20**, 1255-1261.
- Chell, J. M. and Brand, A. H. (2010). Nutrition-responsive Glia control exit of neural stem cells from quiescence. *Cell* **143**, 1161-1173.
- Chen, Z., Del Valle Rodriguez, A., Li, X., Erclik, T., Fernandes, V. M. and Desplan, C. (2016). A unique class of neural progenitors in the *Drosophila* optic lobe generates both migrating neurons and Glia. *Cell Rep.* **15**, 774-786.
- Datta, S. (1995). Control of proliferation activation in quiescent neuroblasts of the *Drosophila* central nervous system. *Development* **121**, 1173-1182.
- Dillard, C., Narbonne-Reveau, K., Foppolo, S., Lanet, E. and Maurice, C. (2018). Two distinct mechanisms silence chimo in *Drosophila* neuroblasts and neuroepithelial cells to limit their self-renewal. *Development* **145**, dev154534.
- Egger, B., Boone, J. Q., Stevens, N. R., Brand, A. H. and Doe, C. Q. (2007). Regulation of spindle orientation and neural stem cell fate in the *Drosophila* optic lobe. *Neural Dev.* **2**, 1.
- Egger, B., Gold, K. S. and Brand, A. H. (2010). Notch regulates the switch from symmetric to asymmetric neural stem cell division in the *Drosophila* optic lobe. *Development* **137**, 2981-2987.
- Egger, B., Gold, K. S. and Brand, A. H. (2011). Regulating the balance between symmetric and asymmetric stem cell division in the developing brain. *Fly* **5**, 237-241.
- Erclik, T., Hartenstein, V., Lipshitz, H. D. and McInnes, R. R. (2008). Conserved role of the *Vsx* genes supports a monophyletic origin for bilaterian visual systems. *Curr. Biol.* **18**, 1278-1287.
- Evans, C. J., Olson, J. M., Ngo, K. T., Kim, E., Lee, N. E., Kuoy, E., Patananan, A. N., Sitz, D., Tran, P., Do, M.-T. et al. (2009). G-TRACE: rapid Gal4-based cell lineage analysis in *Drosophila*. *Nat. Publishing Group* **6**, 603-605.
- Gold, K. S. and Brand, A. H. (2014). Optix defines a neuroepithelial compartment in the optic lobe of the *Drosophila* brain. *Neural Dev.* **9**, 18.
- Green, P., Hartenstein, A. Y. and Hartenstein, V. (1993). The embryonic development of the *Drosophila* visual system. *Cell Tissue Res.* **273**, 583-598.
- Grenningloh, G., Rehm, E. J. and Goodman, C. S. (1991). Genetic analysis of growth cone guidance in *Drosophila*: fasciclin II functions as a neuronal recognition molecule. *Cell* **67**, 45-57.
- Han, C., Jan, L. Y. and Jan, Y.-N. (2011). Enhancer-driven membrane markers for analysis of nonautonomous mechanisms reveal neuron-glia interactions in *Drosophila*. *Proc. Natl. Acad. Sci. USA* **108**, 9673-9678.
- Hartenstein, V. and Campos-Ortega, J. A. (1984). Early neurogenesis in wild-type *Drosophila melanogaster*. *Wilehm Roux Arch. Dev. Biol.* **193**, 308-325.
- Ikeshima-Kataoka, H., Skeath, J. B., Nabeshima, Y., Doe, C. Q. and Matsuzaki, F. (1997). Miranda directs Prospero to a daughter cell during *Drosophila* asymmetric divisions. *Nature* **390**, 625-629.
- Ito, K. and Hotta, Y. (1992). Proliferation pattern of postembryonic neuroblasts in the brain of *Drosophila melanogaster*. *Dev. Biol.* **149**, 134-148.
- Kaphingst, K. and Kunes, S. (1994). Pattern formation in the visual centers of the *Drosophila* brain: wingless acts via decapentaplegic to specify the dorsoventral axis. *Cell* **78**, 437-448.
- Kassis, J. A., Noll, E., VanSickle, E. P., Odenwald, W. F. and Perrimon, N. (1992). Altering the insertional specificity of a *Drosophila* transposable element. *Proc. Natl. Acad. Sci. U.S.A.* **89**, 1919-1923.
- Kenyon, K. L., Li, D. J., Clouser, C., Tran, S. and Pignoni, F. (2005). Fly Six-type homeodomain proteins *Sine oculis* and *Optix* partner with different cofactors during eye development. *Dev. Dyn.* **234**, 497-504.
- Lai, S.-L. and Doe, C. Q. (2014). Transient nuclear Prospero induces neural progenitor quiescence. *eLife* **3**, e03366.
- Lee, J. J., von Kessler, D. P., Parks, S. and Beachy, P. A. (1992). Secretion and localized transcription suggest a role in positional signaling for products of the segmentation gene hedgehog. *Cell* **71**, 33-50.
- Li, X., Cassidy, J. J., Reinke, C. A., Fischboeck, S. and Carthew, R. W. (2009). A microRNA imparts robustness against environmental fluctuation during development. *Cell* **137**, 273-282.
- Manseau, L., Baradaran, A., Brower, D., Budhu, A., Elefant, F., Phan, H., Philp, A. V., Yang, M., Glover, D., Kaiser, K. et al. (1997). GAL4 enhancer traps expressed in the embryo, larval brain, imaginal discs, and ovary of *Drosophila*. *Dev. Dyn.* **209**, 310-322.
- Marshall, G. M., Carter, D. R., Cheung, B. B., Liu, T., Mateos, M. K., Meyerowitz, J. G. and Weiss, W. A. (2014). The prenatal origins of cancer. *Nat. Rev. Cancer* **14**, 277-289.
- Maurange, C. and Gould, A. P. (2005). Brainy but not too brainy: starting and stopping neuroblast divisions in *Drosophila*. *Trends Neurosci.* **28**, 30-36.
- Nassif, C., Noveen, A. and Hartenstein, V. (2003). Early development of the *Drosophila* brain: III. The pattern of neuropile founder tracts during the larval period. *J. Comp. Neurol.* **455**, 417-434.
- Noctor, S. C., Martínez-Cerdeño, V., Ivic, L. and Kriegstein, A. R. (2004). Cortical neurons arise in symmetric and asymmetric division zones and migrate through specific phases. *Nat. Neurosci.* **7**, 136-144.
- Otsuki, L. and Brand, A. H. (2018). Cell cycle heterogeneity directs the timing of neural stem cell activation from quiescence. *Science* **360**, 99-102.
- Pfeiffer, B. D., Jenett, A., Hammonds, A. S., Ngo, T.-T. B., Misra, S., Murphy, C., Scully, A., Carlson, J. W., Wan, K. H., Laverly, T. R. et al. (2008). Tools for neuroanatomy and neurogenetics in *Drosophila*. *Proc. Natl. Acad. Sci. USA* **105**, 9715-9720.
- Poulsen, D. F. (1950). Histogenesis, organogenesis and differentiation in the embryo of *Drosophila melanogaster* Meigen. In *Biology of Drosophila* (ed. M. Demerec), pp. 168-274. New York: Wiley.
- Prokop, A. and Technau, G. M. (1991). The origin of postembryonic neuroblasts in the ventral nerve cord of *Drosophila melanogaster*. *Development* **111**, 79-88.
- Richter, C., Oktaba, K., Steinmann, J., Müller, J. and Knoblich, J. A. (2011). The tumour suppressor L(3)mbt inhibits neuroepithelial proliferation and acts on insulator elements. *Nat. Cell Biol.* **13**, 1029-1039.
- Sato, M., Yasugi, T., Minami, Y., Miura, T. and Nagayama, M. (2016). Notch-mediated lateral inhibition regulates proneural wave propagation when combined with EGF-mediated reaction diffusion. *Proc. Natl. Acad. Sci. USA* **113**, E5153-E5162.
- Schindelin, J., Arganda-Carreras, I., Frise, E., Kaynig, V., Longair, M., Pietzsch, T., Preibisch, S., Rueden, C., Saalfeld, S., Schmid, B. et al. (2012). Fiji: an open-source platform for biological-image analysis. *Nat. Publishing Group* **9**, 676-682.
- Sousa-Nunes, R., Yee, L. L. and Gould, A. P. (2011). Fat cells reactivate quiescent neuroblasts via TOR and glial insulin relays in *Drosophila*. *Nature* **471**, 508-512.
- Spéder, P. and Brand, A. H. (2014). Gap junction proteins in the blood-brain barrier control nutrient-dependent reactivation of *Drosophila* neural stem cells. *Dev. Cell* **30**, 309-321.
- Tomancak, P., Berman, B. P., Beaton, A., Weiszmam, R., Kwan, E., Hartenstein, V., Celniker, S. E. and Rubin, G. M. (2007). Global analysis of patterns of gene expression during *Drosophila* embryogenesis. *Genome Biol.* **8**, R145.
- Truman, J. W. and Bate, M. (1988). Spatial and temporal patterns of neurogenesis in the central nervous system of *Drosophila melanogaster*. *Dev. Biol.* **125**, 145-157.
- Turner, F. R. and Mahowald, A. P. (1979). Scanning electron microscopy of *Drosophila melanogaster* embryogenesis: III. Formation of the head and caudal segments. *Dev. Biol.* **68**, 96-109.
- White, K., Grether, M. E., Abrams, J. M., Young, L., Farrell, K. and Steller, H. (1994). Genetic control of programmed cell death in *Drosophila*. *Science* **264**, 677-683.
- Whitfield, W. G., Gonzalez, C., Maldonado-Codina, G. and Glover, D. M. (1990). The A- and B-type cyclins of *Drosophila* are accumulated and destroyed in temporally distinct events that define separable phases of the G2-M transition. *EMBO J.* **9**, 2563-2572.
- Yagi, R., Mayer, F. and Basler, K. (2010). Refined LexA transactivators and their use in combination with the *Drosophila* Gal4 system. *Proc. Natl. Acad. Sci. U.S.A.* **107**, 16166-16171.
- Yasugi, T., Umetsu, D., Murakami, S., Sato, M. and Tabata, T. (2008). *Drosophila* optic lobe neuroblasts triggered by a wave of proneural gene expression that is negatively regulated by JAK/STAT. *Development* **135**, 1471-1480.
- Yasugi, T., Sugie, A., Umetsu, D. and Tabata, T. (2010). Coordinated sequential action of EGFR and Notch signaling pathways regulates proneural wave progression in the *Drosophila* optic lobe. *Development* **137**, 3193-3203.
- Younossi-Hartenstein, A., Green, P., Liaw, G.-J., Rudolph, K., Lengyel, J. and Hartenstein, V. (1997). Control of early neurogenesis of the *Drosophila* brain by the head gap *Genestill*, *otd*, *ems*, and *btd*. *Dev. Biol.* **182**, 270-283.
- Zhu, S., Barshow, S., Wildonger, J., Jan, L. Y. and Jan, Y.-N. (2011). Ets transcription factor Pointed promotes the generation of intermediate neural progenitors in *Drosophila* larval brains. *Proc. Natl. Acad. Sci. USA* **108**, 20615-20620.



## REFERENCE LIST

- Almeida, M. S. and Bray, S. J.** (2005). Regulation of post-embryonic neuroblasts by *Drosophila* Grainyhead. *Mechanisms of Development* **122**, 1282–1293.
- Alvarez, A. D., Shi, W., Wilson, B. A. and Skeath, J. B.** (2003). *pannier* and *pointedP2* act sequentially to regulate *Drosophila* heart development. *Development* **130**, 3015–3026.
- Ashraf, S. I., Ganguly, A., Roote, J. and Ip, Y. T.** (2004). Worniu, a Snail family zinc-finger protein, is required for brain development in *Drosophila*. *Dev. Dyn.* **231**, 379–386.
- Ashraf, S. I., Hu, X., Roote, J. and Ip, Y. T.** (1999). The mesoderm determinant snail collaborates with related zinc-finger proteins to control *Drosophila* neurogenesis. *The EMBO Journal* **18**, 6426–6438.
- Aughey, G. N., Estacio Gomez, A., Thomson, J., Yin, H. and Southall, T. D.** (2018). CATaDa reveals global remodelling of chromatin accessibility during stem cell differentiation in vivo. *Elife* **7**, 6061.
- Awasaki, T., Kao, C.-F., Lee, Y.-J., Yang, C.-P., Huang, Y., Pfeiffer, B. D., Luan, H., Jing, X., Huang, Y.-F., He, Y., Schroeder, M. D., Kuzin, A., Brody, T., Zugates, C. T., Odenwald, W. F. & Lee, T.** (2014). Making *Drosophila* lineage-restricted drivers via patterned recombination in neuroblasts. *Nature Neuroscience* **17**, 631–637.
- Álvarez, J.-A. and Díaz-Benjumea, F. J.** (2018). Origin and specification of type II neuroblasts in the *Drosophila* embryo. *Development* **145**, dev158394.
- Bangi, E., Murgia, C., Teague, A. G. S., Sansom, O. J. and Cagan, R. L.** (2016). Functional exploration of colorectal cancer genomes using *Drosophila*. *Nat Commun* **7**, 13615.
- Baumgardt, M., Karlsson, D., Salmani, B. Y., Bivik, C., MacDonald, R. B., Gunnar, E. and Thor, S.** (2014). Global programmed switch in neural daughter cell proliferation mode triggered by a temporal gene cascade. *Dev. Cell* **30**, 192–208.
- Bayraktar, O. A., Boone, J. Q., Drummond, M. L. and Doe, C. Q.** (2010). *Drosophila* type II neuroblast lineages keep Prospero levels low to generate large clones that contribute to the adult brain central complex. *Neural Dev* **5**, 26.
- Bello, B. C., Izergina, N., Caussinus, E. and Reichert, H.** (2008). Amplification of neural stem cell proliferation by intermediate progenitor cells in *Drosophila* brain development. *Neural Dev* **3**, 5.
- Bello, B., Reichert, H. and Hirth, F.** (2006). The *brain tumor* gene negatively regulates neural progenitor cell proliferation in the larval central brain of *Drosophila*. *Development* **133**, 2639–2648.
- Benod, C., Villagomez, R., Filgueira, C. S., Hwang, P. K., Leonard, P. G., Poncet-Montange, G., Rajagopalan, S., Fletterick, R. J., Gustafsson, J.-Å. and Webb, P.** (2014). The Human Orphan Nuclear Receptor Tailless (TLX, NR2E1) Is Druggable. *PLoS ONE* **9**, e99440.
- Bertet, C.** (2017). The Developmental Origin of Cell Type Diversity in the *Drosophila* Visual System. In *Decoding Neural Circuit Structure and Function*, pp. 419–435. Cham:

Springer, Cham.

- Bertet, C., Li, X., Erclik, T., Cavey, M., Wells, B. and Desplan, C.** (2014). Temporal Patterning of Neuroblasts Controls Notch-Mediated Cell Survival through Regulation of Hid or Reaper. *Cell* **158**, 1173–1186.
- Bertrand, N., Castro, D. S. and Guillemot, F.** (2002). Proneural genes and the specification of neural cell types. *Nat. Rev. Neurosci.* **3**, 517–530.
- Bier, E., Vaessin, H., Younger-Shepherd, S., Jan, L. Y. and Jan, Y. N.** (1992). *deadpan*, an essential pan-neural gene in *Drosophila*, encodes a helix-loop-helix protein similar to the *hairy* gene product. *Genes Dev.* **6**, 2137–2151.
- Blanpain, C.** (2013). Tracing the cellular origin of cancer. *Nat. Cell Biol.* **15**, 126–134.
- Bonaguidi, M. A., Wheeler, M. A., Shapiro, J. S., Stadel, R. P., Sun, G. J., Ming, G.-L. and Song, H.** (2011). In Vivo Clonal Analysis Reveals Self-Renewing and Multipotent Adult Neural Stem Cell Characteristics. *Cell* **145**, 1142–1155.
- Bondy, M. L., Scheurer, M. E., Malmer, B., Sloan, J. S. B., Davis, F. G., Il'yasova, D., Kruchko, C., McCarthy, B. J., Rajaraman, P., Schwartzbaum, J. A., Sadetzki, S., Schlehofer, B., Tihan, T., Wiemels, J. L., Wrensch, M. and Buffler, P. A.** (2008). Brain Tumor Epidemiology: Consensus from the Brain Tumor Epidemiology Consortium. *Cancer* **113**, 1953–1968.
- Boone, J. Q. and Doe, C. Q.** (2008). Identification of *Drosophila* Type II Neuroblast Lineages Containing Transit Amplifying Ganglion Mother Cells. *Dev Neurobiol* **68**, 1185–1195.
- Bowman, S. K., Rolland, V., Betschinger, J., Kinsey, K. A., Emery, G. and Knoblich, J. A.** (2008). The Tumor Suppressors Brat and Numb Regulate Transit-Amplifying Neuroblast Lineages in *Drosophila*. *Dev. Cell* **14**, 535–546.
- Boyle, E. I., Weng, S., Gollub, J., Jin, H., Botstein, D., Cherry, J. M. and Sherlock, G.** (2004). GO::TermFinder--open source software for accessing Gene Ontology information and finding significantly enriched Gene Ontology terms associated with a list of genes. *Bioinformatics* **20**, 3710–3715.
- Brand, A. H. and Livesey, F. J.** (2011). Neural stem cell biology in vertebrates and invertebrates: more alike than different? *Neuron* **70**, 719–729.
- Brand, A. H. and Perrimon, N.** (1993). Targeted gene expression as a means of altering cell fates and generating dominant phenotypes. *Development* **118**, 401–415.
- Brand, M., Jarman, A. P., Jan, L. Y. and Jan, Y. N.** (1993). *asense* is a *Drosophila* neural precursor gene and is capable of initiating sense organ formation. *Development* **119**, 1–17.
- Britton, J. S. and Edgar, B. A.** (1998). Environmental control of the cell cycle in *Drosophila*: nutrition activates mitotic and endoreplicative cells by distinct mechanisms. *Development* **125**, 2149–2158.
- Buescher, M., Yeo, S. L., Udolph, G., Zavortink, M., Yang, X., Tear, G. and C, W.** (1998). Binary sibling neuronal cell fate decisions in the *Drosophila* embryonic central nervous system are nonstochastic and require inscuteable-mediated asymmetry of

ganglion mother cells. *Genes Dev.* **12**, 1858–1870.

- Calof, A. L., Mumm, J. S., Rim, P. C. and Shou, J.** (1998). The neuronal stem cell of the olfactory epithelium. *J. Neurobiol.* **36**, 190–205.
- Campos-Ortega, J. A. and Hartenstein, V.** (1985). *The Embryonic Development of Drosophila Melanogaster*. Springer.
- Carney, T. D., Miller, M. R., Robinson, K. J., Bayraktar, O. A., Osterhout, J. A. and Doe, C. Q.** (2012). Functional genomics identifies neural stem cell sub-type expression profiles and genes regulating neuroblast homeostasis. *Dev. Biol.* **361**, 137–146.
- Caygill, E. E. and Brand, A. H.** (2017). *miR-7* Buffers Differentiation in the Developing *Drosophila* Visual System. *Cell Reports* **20**, 1255–1261.
- Chavali, P. L., Saini, R. K. R., Zhai, Q., Vizlin-Hodzic, D., Venkatabalasubramanian, S., Hayashi, A., Johansson, E., Zeng, Z.-J., Mohlin, S., Pählman, S., Hansford, L., Kaplan, D. R., and Funa, K.** (2014). TLX activates MMP-2, promotes self-renewal of tumor spheres in neuroblastoma and correlates with poor patient survival. *Cell Death Dis* **5**, e1502.
- Cheetham, S. W., Gruhn, W. H., van den Aamele, J., Krautz, R., Southall, T. D., Kobayashi, T., Surani, M. A. and Brand, A. H.** (2018). Targeted DamID reveals differential binding of mammalian pluripotency factors. *Development* **145**, dev170209.
- Chell, J. M. and Brand, A. H.** (2010). Nutrition-Responsive Glia Control Exit of Neural Stem Cells from Quiescence. *Cell* **143**, 1161–1173.
- Chen, J., Li, Y., Yu, T.-S., McKay, R. M., Burns, D. K., Kernie, S. G. and Parada, L. F.** (2012). A restricted cell population propagates glioblastoma growth following chemotherapy. *Nature* **488**, 522–526.
- Chen, Z., del Valle Rodriguez, A., Li, X., Erclik, T., Fernandes, V. M. and Desplan, C.** (2016). A Unique Class of Neural Progenitors in the *Drosophila* Optic Lobe Generates Both Migrating Neurons and Glia. *Cell Reports* **15**, 774–786.
- Choksi, S. P., Southall, T. D., Bossing, T., Edoff, K., de Wit, E., Fischer, B. E., van Steensel, B., Micklem, G. and Brand, A. H.** (2006). Prospero acts as a binary switch between self-renewal and differentiation in *Drosophila* neural stem cells. *Dev. Cell* **11**, 775–789.
- Corso-Díaz, X., de Leeuw, C. N., Alonso, V., Melchers, D., Wong, B. K. Y., Houtman, R. and Simpson, E. M.** (2016). Co-activator candidate interactions for orphan nuclear receptor *NR2E1*. *BMC Genomics* **17**, 832.
- Cui, Q., Yang, S., Ye, P., Tian, E., Sun, G., Zhou, J., Sun, G., Liu, X., Chen, C., Murai, K., Zhao, C., Azizian, K. T., Yang, L., Warden, C., Wu, X., Massimo D'Apuzzo, M., Brown, C., Badie, B., Peng, L., Riggs, A. D., John J. Rossi, J. J. & Shi, Y.** (2016). Downregulation of TLX induces TET3 expression and inhibits glioblastoma stem cell self-renewal and tumorigenesis. *Nat Commun* **7**, 10637.
- Daniel, A., Dumstrei, K., Lengyel, J. A. and Hartenstein, V.** (1999). The control of cell fate in the embryonic visual system by *atonal*, *tailless* and EGFR signaling. *Development* **126**, 2945–2954.

- Das, T. K. and Cagan, R. L.** (2013). A *Drosophila* approach to thyroid cancer therapeutics. *Drug Discov Today Technol* **10**, e65–71.
- Das, T. K., Sangodkar, J., Negre, N., Narla, G. and Cagan, R. L.** (2013). Sin3a acts through a multi-gene module to regulate invasion in *Drosophila* and human tumors. *Oncogene* **32**, 3184–3197.
- Datta, S.** (1995). Control of proliferation activation in quiescent neuroblasts of the *Drosophila* central nervous system. *Development* **121**, 1173–1182.
- Davis, S. M., Thomas, A. L., Nomie, K. J., Huang, L. and Dierick, H. A.** (2014). Tailless and Atrophin control *Drosophila* aggression by regulating neuropeptide signalling in the *pars intercerebralis*. *Nat Commun* **5**, 1–10.
- del Valle Rodriguez, A., Didiano, D. and Desplan, C.** (2011). Power tools for gene expression and clonal analysis in *Drosophila*. *Nature Methods* **9**, 47–55.
- Diaz, R. J., Harbecke, R., Singer, J. B., Pignoni, F., Janning, W. and Lengyel, J. A.** (1996). Graded effect of *tailless* on posterior gut development: molecular basis of an allelic series of a nuclear receptor gene. *Mechanisms of Development* **54**, 119–130.
- Dick, D. M., Foroud, T., Flury, L., Bowman, E. S., Miller, M. J., Rau, N. L., Moe, P. R., Samavedy, N., El-Mallakh, R., Manji, H., Glitz, D. A., Meyer, E. T., Smiley, C., Hahn, R., Widmark, C., McKinney, R., Sutton, L., Ballas, C., Grice, D., Berrettini, W., Byerley, W., Coryell, W., DePaulo, R., MacKinnon, D. F., Gershon, E. S., Kelsoe, J. R., McMahon, F. J., McInnis, M., Murphy, D. L., Reich, T., Scheftner, W., and Nurnberger Jr., J. I.** (2003). Genomewide linkage analyses of bipolar disorder: a new sample of 250 pedigrees from the National Institute of Mental Health Genetics Initiative. *Am. J. Hum. Genet.* **73**, 107–114.
- Dillard, C., Narbonne-Reveau, K., Foppolo, S., Lanet, E. and Maurange, C.** (2018). Two distinct mechanisms silence *chinmo* in *Drosophila* neuroblasts and neuroepithelial cells to limit their self-renewal. *Development* **145**, dev154534.
- Doe, C. Q.** (2008). Neural stem cells: balancing self-renewal with differentiation. *Development* **135**, 1575–1587.
- Doe, C. Q.** (2017). Temporal Patterning in the *Drosophila* CNS. *Annu Rev Cell Dev Biol* **33**, 219-240.
- Doe, C. Q., Chu-LaGraff, Q., Wright, D. M. and Scott, M. P.** (1991). The *prospero* Gene Specifies Cell Fates in the *Drosophila* Central Nervous System. *Cell* **65**, 451–464.
- Doetsch, F., Caillé, I., Lim, D. A., García-Verdugo, J. M. and Alvarez-Buylla, A.** (1999). Subventricular Zone Astrocytes Are Neural Stem Cells in the Adult Mammalian Brain. *Cell* **97**, 703–716.
- Ebens, A. J., Garren, H., Cheyette, B. N. and Zipursky, S. L.** (1993). The *Drosophila anachronism* Locus: a Glycoprotein Secreted by Glia Inhibits Neuroblast Proliferation. *Cell* **74**, 15–27.
- Egger, B., Boone, J. Q., Stevens, N. R. and Brand, A. H.** (2007). Regulation of spindle orientation and neural stem cell fate in the *Drosophila* optic lobe. *Neural Dev* **2**.

- Egger, B., Gold, K. S. and Brand, A. H.** (2010). Notch regulates the switch from symmetric to asymmetric neural stem cell division in the *Drosophila* optic lobe. *Development* **137**, 2981–2987.
- Egger, B., Gold, K. S. and Brand, A. H.** (2011). Regulating the balance between symmetric and asymmetric stem cell division in the developing brain. *Fly (Austin)* **5**, 237–241.
- Elmi, M., Matsumoto, Y., Zeng, Z.-J., Lakshminarasimhan, P., Yang, W., Uemura, A., Nishikawa, S.-I., Moshiri, A., Tajima, N., Ågren, H. and Funa, K.** (2010). TLX activates MASH1 for induction of neuronal lineage commitment of adult hippocampal neuroprogenitors. *Molecular and Cellular Neuroscience* **45**, 121–131.
- Erclik, T., Hartenstein, V., Lipshitz, H. D. and McInnes, R. R.** (2008). Conserved role of the *Vsx* genes supports a monophyletic origin for bilaterian visual systems. *Curr. Biol.* **18**, 1278–1287.
- Estella, C., Rieckhof, G., Calleja, M. and Morata, G.** (2003). The role of *buttonhead* and *Sp1* in the development of the ventral imaginal discs of *Drosophila*. *Development* **130**, 5929–5941.
- Estruch, S. B., Buzón, V., Carbó, L. R., Schorova, L., Lüders, J. and Estébanez-Perpiñá, E.** (2012). The Oncoprotein BCL11A Binds to Orphan Nuclear Receptor TLX and Potentiates its Transrepressive Function. *PLoS ONE* **7**, e37963.
- Evans, C. J., Olson, J. M., Ngo, K. T., Kim, E., Lee, N. E., Kuoy, E., Patananan, A. N., Sitz, D., Tran, P., Do, M.-T., Yackle, K., Cespedes, A., Hartenstein, V., Call, G. B., and Banerjee, U.** (2009). G-TRACE: rapid Gal4-based cell lineage analysis in *Drosophila*. *Nature Methods* **6**, 603–605.
- Ferlay, J., Shin, H.-R., Bray, F., Forman, D., Mathers, C. and Parkin, D. M.** (2010). Estimates of worldwide burden of cancer in 2008: GLOBOCAN 2008. *Int. J. Cancer* **127**, 2893–2917.
- Galas, D. J. and Schmitz, A.** (1978). DNase footprinting: a simple method for the detection of protein-DNA binding specificity. *Nucleic Acids Res.* **5**, 3157–3170.
- Gerlitz, O. and Basler, K.** (2002). Wingful, an extracellular feedback inhibitor of Wingless. *Genes Dev.* **16**, 1055–1059.
- Gold, K. S. and Brand, A. H.** (2014). Optix defines a neuroepithelial compartment in the optic lobe of the *Drosophila* brain. *Neural Dev* **9**.
- González, F., Romani, S., Cubas, P., Modolell, J. and Campuzano, S.** (1989). Molecular analysis of the *asense* gene, a member of the *achaete-scute* complex of *Drosophila melanogaster*, and its novel role in optic lobe development. *The EMBO Journal* **8**, 3553–3562.
- Gordon, M. K., Mumm, J. S., Davis, R. A., Holcomb, J. D. and Calof, A. L.** (1995). Dynamics of MASH1 Expression *in Vitro* and *in Vivo* Suggest a Non-Stem Cell Site of MASH1 Action in the Olfactory Receptor Neuron Lineage. *Mol. Cell. Neurosci.* **6**, 363–379.
- Götz, M., Nakafuku, M. and Petrik, D.** (2016). Neurogenesis in the Developing and Adult Brain - Similarities and Key Differences. *Cold Spring Harbor Perspectives in Biology* **8**,

a018853.

- Green, P., Younossi-Hartenstein, A. and Hartenstein, V.** (1993). The embryonic development of the *Drosophila* visual system. *Cell Tissue Res.* 583–598.
- Grenningloh, G., Rehm, E. J. and Goodman, C. S.** (1991). Genetic Analysis of Growth Cone Guidance in *Drosophila*: Fasciclin II Functions as a Neuronal Recognition Molecule. *Cell* **67**, 45–57.
- Guillemot, F. and Joyner, A. L.** (1993). Dynamic expression of the murine *Achaete-Scute* homologue *Mash-1* in the developing nervous system. *Mechanisms of Development* **42**, 171–185.
- Guillemot, F., Lo, L. C., Johnson, J. E., Auerbach, A., Anderson, D. J. and Joyner, A. L.** (1993). Mammalian *achaete-scute* Homolog 1 Is Required for the Early Development of Olfactory and Autonomic Neurons. *Cell* **75**, 463–476.
- Guillermin, O., Perruchoud, B., Sprecher, S. G. and Egger, B.** (2015). Characterization of *tailless* functions during *Drosophila* optic lobe formation. *Dev. Biol.* **405**, 202–213.
- Haecker, A., Qi, D., Lilja, T., Moussian, B., Andrioli, L. P., Luschnig, S. and Mannervik, M.** (2007). *Drosophila* Brakeless Interacts with Atrophin and Is Required for Tailless-Mediated Transcriptional Repression in Early Embryos. *PLoS Biol* **5**, e145.
- Haenfler, J. M., Kuang, C. and Lee, C.-Y.** (2012). Cortical aPKC kinase activity distinguishes neural stem cells from progenitor cells by ensuring asymmetric segregation of Numb. *Dev. Biol.* **365**, 219–228.
- Hakes, A. E., Ostuki, L. and Brand, A. H.** (2018). A newly discovered neural stem cell population is generated by the optic lobe neuroepithelium during embryogenesis in *Drosophila melanogaster*. *Development* **145**, dev166207.
- Han, C., Jan, L. Y. and Jan, Y.-N.** (2011). Enhancer-driven membrane markers for analysis of nonautonomous mechanisms reveal neuron-glia interactions in *Drosophila*. *PNAS* **108**, 9673–9678.
- Hartenstein, V. and Campos-Ortega, J. A.** (1984). Early neurogenesis in wild-type *Drosophila melanogaster*. *Wilhelm Roux' Archiv* **193**, 308–325.
- Hartmann, B., Reichert, H. and Walldorf, U.** (2001). Interaction of gap genes in the *Drosophila* head: *tailless* regulates expression of *empty spiracles* in early embryonic patterning and brain development. *Mechanisms of Development* **109**, 161–172.
- Hass, M. R., Liow, H.-H., Chen, X., Sharma, A., Inoue, Y. U., Inoue, T., Reeb, A., Martens, A., Fulbright, M., Raju, S., et al.** (2015). SpDamID: Marking DNA Bound by Protein Complexes Identifies Notch-Dimer Responsive Enhancers. *Mol. Cell* **59**, 685–697.
- Hippenmeyer, S.** (2013). Dissection of gene function at clonal level using mosaic analysis with double markers. *Front. Biol.* **8**, 557–568.
- Hoch, M., Gerwin, N., Taubert, H. and Jäckle, H.** (1992). Competition for overlapping sites in the regulatory region of the *Drosophila* gene *Krüppel*. *Science* **256**, 94–97.

- Hoch, M., Seifert, E. and Jäckle, H.** (1991). Gene expression mediated by *cis*-acting sequences of the *Krüppel* gene in response to the *Drosophila* morphogenes *bicoid* and *hunchback*. *The EMBO Journal* **10**, 2267–2278.
- Hofbauer, A. and Campos-Ortega, J. A.** (1990). Proliferation and early differentiation of the optic lobes in *Drosophila melanogaster*. *Roux's Arch Dev Biol* **198**, 264–274.
- Holleman, T., Bellefroid, E. and Pieler, T.** (1998). The *Xenopus* homologue of the *Drosophila* gene *tailless* has a function in early eye development. *Development* **125**, 2425–2432.
- Hu, Y., Flockhart, I., Vinayagam, A., Bergwitz, C., Berger, B., Perrimon, N. and Mohr, S. E.** (2011). An integrative approach to ortholog prediction for disease-focused and other functional studies. *BMC Bioinformatics* **12**, 357.
- Ikeshima-Kataoka, H., Skeath, J. B., Nabeshima, Y., Doe, C. Q. and Matsuzaki, F.** (1997). Miranda directs Prospero to a daughter cell during *Drosophila* asymmetric divisions. *Nature* **390**, 625–629.
- Ito, K. and Hotta, Y.** (1992). Proliferation pattern of postembryonic neuroblasts in the brain of *Drosophila melanogaster*. *Dev. Biol.* **149**, 134–148.
- Ito, K., Awano, W., Suzuki, K., Hiromi, Y. and Yamamoto, D.** (1997). The *Drosophila* mushroom body is a quadruple structure of clonal units each of which contains a virtually identical set of neurones and glial cells. *Development* **124**, 761–771.
- Iwahara, N., Hisahara, S., Hayashi, T. and Horio, Y.** (2009). Transcriptional activation of NAD<sup>+</sup>-dependent protein deacetylase SIRT1 by nuclear receptor TLX. *Biochem. Biophys. Res. Commun.* **386**, 671–675.
- Jackson, A., Panayiotidis, P. and Foroni, L.** (1998). The Human Homologue of the *Drosophila tailless* Gene (TLX): Characterization and Mapping to a Region of Common Deletion in Human Lymphoid Leukemia on Chromosome 6q21. *Genomics* **50**, 34–43.
- Janssens, D. H., Komori, H., Grbac, D., Chen, K., Koe, C. T., Wang, H. and Lee, C.-Y.** (2014). Earmuff restricts progenitor cell potential by attenuating the competence to respond to self-renewal factors. *Development* **141**, 1036–1046.
- Jenett, A., Rubin, G. M., Ngo, T.-T. B., Shepherd, D., Murphy, C., Dionne, H., Pfeiffer, B. D., Cavallaro, A., Hall, D., Jeter, J., Iyer, N., Fetter, D., Hausenfluck, J. H., Peng, H., Trautman, E. T., Svirskas, R. R., Myers, E. W., Iwinski, Z. R., Aso, Y., DePasquale, G. M., Enos, A., Hulamm, P., Lam, S. C. B., Li H.-H., Lavery, T. R., Long, F., Qu, L., Murphy, S. D., Rokicki, K., Safford, T., Shaw, K., Simpson, J. H., Sowell, A., Tae, S., Yu, Y., and Zugates, C. T.** (2012). A GAL4-driver line resource for *Drosophila* neurobiology. *Cell Rep* **2**, 991–1001.
- Johnson, B. E., Mazor, T., Hong, C., Barnes, M., Aihara, K., McLean, C. Y., Fouse, S. D., Yamamoto, S., Ueda, H., Tatsuno, K., Asthana, S., Jalbert, L. E., Nelson, S. J., Bollen, A. W., Gustafson, W. C., Charron, E., Weiss, W. A., Smirnov, I. V., Song, J. S., Olshen, A. B., Cha, S., Zhao, Y., Moore, R. A., Mungall A. J., Jones, S. J. M., Hirst, M., Marra, M. A., Saito, N., Aburatani, H., Mukasa, A., Berger, M. S., Chang, S. M., Taylor, B. S. and Costello, J. F.** (2014). Mutational analysis reveals the origin and therapy-driven evolution of recurrent glioma. *Science* **343**, 189–193.

- Johnson, J. E., Birren, S. J. and Anderson, D. J.** (1990). Two rat homologues of *Drosophila achaete-scute* specifically expressed in neuronal precursors. *Nature* **346**, 858–861.
- Jürgens, G., Wieschaus, E., Nüsslein-Volhard, C. and Kluding, H.** (1984). Mutations affecting the pattern of the larval cuticle in *Drosophila melanogaster*: II. Zygotic loci on the third chromosome. *Wilhelm Roux' Archiv* **193**, 283–295.
- Kaphingst, K. and Kunes, S.** (1994). Pattern Formation in the Visual Centers of the *Drosophila* Brain: *wingless* Acts via *decapentaplegic* to Specify the Dorsoventral Axis. *Cell* **78**, 437–448.
- Karcavich, R. and Doe, C. Q.** (2005). *Drosophila* neuroblast 7-3 cell lineage: A model system for studying programmed cell death, Notch/Numb signaling, and sequential specification of ganglion mother cell identity. *Journal of Comparative Neurology* **481**, 240–251.
- Kassis, J. A., Noll, E., VanSickle, E. P., Odenwald, W. F. and Perrimon, N.** (1992). Altering the insertional specificity of a *Drosophila* transposable element. *Proc. Natl. Acad. Sci. U.S.A.* **89**, 1919–1923.
- Kawamori, H., Tai, M., Sato, M., Yasugi, T. and Tabata, T.** (2011). Fat/Hippo pathway regulates the progress of neural differentiation signaling in the *Drosophila* optic lobe. *Dev. Growth Differ.* **53**, 653–667.
- Kenyon, K. L., Yang-Zhou, D., Cai, C. Q., Tran, S., Clouser, C., Decene, G., Ranade, S. and Pignoni, F.** (2005). Partner specificity is essential for proper function of the SIX-type homeodomain proteins *Sine oculis* and *Optix* during fly eye development. *Dev. Biol.* **286**, 158–168.
- Klaes, A., Menne, T., Stollewerk, A., Scholz, H. and Klämbt, C.** (1994). The *Ets* transcription factors encoded by the *Drosophila* gene *pointed* direct glial cell differentiation in the embryonic CNS. *Cell* **78**, 149–160.
- Klämbt, C.** (1993). The *Drosophila* gene *pointed* encodes two ETS-like proteins which are involved in the development of the midline glial cells. *Development* **117**, 163–176.
- Knoblich, J. A., Jan, L. Y. and Jan, Y. N.** (1995). Asymmetric segregation of *Numb* and *Prospero* during cell division. *Nature* **377**, 624–627.
- Komori, H., Xiao, Q., Janssens, D. H., Dou, Y. and Lee, C.-Y.** (2014a). *Trithorax* maintains the functional heterogeneity of neural stem cells through the transcription factor *Buttonhead*. *Elife* **3**, 183.
- Komori, H., Xiao, Q., McCartney, B. M. and Lee, C.-Y.** (2014b). Brain tumor specifies intermediate progenitor cell identity by attenuating  $\beta$ -catenin/*Armadillo* activity. *Development* **141**, 51–62.
- Kosman, D., Small, S. and Reinitz, J.** (1998). Rapid preparation of a panel of polyclonal antibodies to *Drosophila* segmentation proteins. 1–5.
- Kumar, R. A., Everman, D. B., Morgan, C. T., Slavotinek, A., Schwartz, C. E. and Simpson, E. M.** (2007a). Absence of mutations in *NR2E1* and *SNX3* in five patients with MMEP (microcephaly, microphthalmia, ectrodactyly, and prognathism) and related

phenotypes. *BMC Med. Genet.* **8**, 48.

- Kumar, R. A., Leach, S., Bonaguro, R., Chen, J., Yokom, D. W., Abrahams, B. S., Seaver, L., Schwartz, C. E., Dobyns, W., Brooks-Wilson, A. and Simpson, E. M.** (2007b). Mutation and evolutionary analyses identify *NR2E1*-candidate-regulatory mutations in humans with severe cortical malformations. *Genes Brain Behav.* **6**, 503–516.
- Kurusu, M., Maruyama, Y., Adachi, Y., Okabe, M., Suzuki, E. and Furukubo-Tokunaga, K.** (2009). A conserved nuclear receptor, Tailless, is required for efficient proliferation and prolonged maintenance of mushroom body progenitors in the *Drosophila* brain. *Dev. Biol.* **326**, 224–236.
- Lai, S.-L., Miller, M. R., Robinson, K. J. and Doe, C. Q.** (2012). The Snail Family Member Worniu Is Continuously Required in Neuroblasts to Prevent Elav-Induced Premature Differentiation. *Dev. Cell* **23**, 849–857.
- Larderet, I., Fritsch, P. M., Gendre, N., Neagu-Maier, G. L., Fetter, R. D., Schneider-Mizell, C. M., Truman, J. W., Zlatić, M., Cardona, A. and Sprecher, S. G.** (2017). Organization of the *Drosophila* larval visual circuit. *Elife* **6**, 450.
- Lee, C.-Y., Wilkinson, B. D., Siegrist, S. E., Wharton, R. P. and Doe, C. Q.** (2006). Brat is a Miranda Cargo Protein that Promotes Neuronal Differentiation and Inhibits Neuroblast Self-Renewal. *Dev. Cell* **10**, 441–449.
- Lee, J. J., Kessler, von, D. P., Parks, S. and Beachy, P. A.** (1992). Secretion and Localized Transcription Suggest a Role in Positional Signaling for Products of the Segmentation Gene *hedgehog*. *Cell* **71**, 33–50.
- Lee, T. and Luo, L.** (1999). Mosaic Analysis with a Repressible Cell Marker for Studies of Gene Function in Neuronal Morphogenesis. *Neuron* **22**, 451–461.
- Levine, B. D. and Cagan, R. L.** (2016). *Drosophila* Lung Cancer Models Identify Trametinib plus Statin as Candidate Therapeutic. *Cell Reports* **14**, 1477–1487.
- Li, H.-H., Kroll, J. R., Lennox, S. M., Ogundeyi, O., Jeter, J., Depasquale, G. and Truman, J. W.** (2014). A GAL4 driver resource for developmental and behavioral studies on the larval CNS of *Drosophila*. *Cell Reports* **8**, 897–908.
- Li, S., Sun, G., Murai, K., Ye, P. and Shi, Y.** (2012). Characterization of TLX Expression in Neural Stem Cells and Progenitor Cells in Adult Brains. *PLoS ONE* **7**, e43324.
- Li, W., Sun, G., Yang, S., Qu, Q., Nakashima, K. and Shi, Y.** (2008). Nuclear Receptor TLX Regulates Cell Cycle Progression in Neural Stem Cells of the Developing Brain. *Molecular Endocrinology* **22**, 56–64.
- Li, X., Cassidy, J. J., Reinke, C. A., Fischboeck, S. and Carthew, R. W.** (2009). A MicroRNA Imparts Robustness against Environmental Fluctuation during Development. *Cell* **137**, 273–282.
- Li, X., Chen, R. and Zhu, S.** (2017). bHLH-O proteins balance the self-renewal and differentiation of *Drosophila* neural stem cells by regulating Earmuff expression. *Dev. Biol.* **431**, 239–251.
- Li, X., Xie, Y. and Zhu, S.** (2016). Notch maintains *Drosophila* type II neuroblasts by

suppressing expression of the Fez transcription factor Earmuff. *Development* **143**, 2511–2521.

**Liaw, G. J., Rudolph, K. M., Huang, J. D., Dubnicoff, T., Courey, A. J. and Lengyel, J. A.** (1995). The torso response element binds GAGA and NTF-1/Elf-1, and regulates *tailless* by relief of repression. *Genes Dev.* **9**, 3163–3176.

**Liaw, G. J., Steingrímsson, E., Pignoni, F., Courey, A. J. and Lengyel, J. A.** (1993). Characterization of downstream elements in a Raf-1 pathway. *Proc. Natl. Acad. Sci. U.S.A.* **90**, 858–862.

**Liaw, G.-J. and Lengyel, J. A.** (1992). Control of *tailless* expression by *bicoid*, *dorsal* and synergistically interacting terminal system regulatory elements. *Mechanisms of Development* **40**, 47–61.

**Lin, S., Huang, Y. and Lee, T.** (2009). Nuclear Receptor Unfulfilled Regulates Axonal Guidance and Cell Identity of *Drosophila* Mushroom Body Neurons. *PLoS ONE* **4**, e8392.

**Liu, C., Sage, J. C., Miller, M. R., Verhaak, R. G. W., Hippenmeyer, S., Vogel, H., Foreman, O., Bronson, R. T., Nishiyama, A., Luo, L. and Zong, H.** (2011). Mosaic analysis with double markers reveals tumor cell of origin in glioma. *Cell* **146**, 209–221.

**Liu, H.-K., Belz, T., Bock, D., Takacs, A., Wu, H., Lichter, P., Chai, M. and Schütz, G.** (2008). The nuclear receptor *tailless* is required for neurogenesis in the adult subventricular zone. *Genes Dev.* **22**, 2473–2478.

**Liu, H.-K., Wang, Y., Belz, T., Bock, D., Takacs, A., Radlwimmer, B., Barbus, S., Reifenberger, G., Lichter, P. and Schütz, G.** (2010). The nuclear receptor *tailless* induces long-term neural stem cell expansion and brain tumor initiation. *Genes Dev.* **24**, 683–695.

**Louis, D. N., Perry, A., Reifenberger, G., Deimling, Von, A., Figarella-Branger, D., Cavenee, W. K., Ohgaki, H., Wiestler, O. D., Kleihues, P. and Ellison, D. W.** (2016). The 2016 World Health Organization Classification of Tumors of the Central Nervous System: a summary. *Acta Neuropathol* **131**, 803–820.

**Mahr, A. and Aberle, H.** (2006). The expression pattern of the *Drosophila* vesicular glutamate transporter: a marker protein for motoneurons and glutamatergic centers in the brain. *Gene Expr. Patterns* **6**, 299–309.

**Manseau, L., Baradaran, A., Brower, D., Budhu, A., Elefant, F., Phan, H., Philp, A. V., Yang, M., Glover, D., Kaiser, K., Palter, K. and Selleck, S.** (1997). GAL4 enhancer traps expressed in the embryo, larval brain, imaginal discs, and ovary of *Drosophila*. *Dev. Dyn.* **209**, 310–322.

**Margolis, J. S., Borowsky, M. L., Steingrímsson, E., Shim, C. W., Lengyel, J. A. and Posakony, J. W.** (1995). Posterior stripe expression of *hunchback* is driven from two promoters by a common enhancer element. *Development* **121**, 3067–3077.

**Marshall, O. J., Southall, T. D., Cheetham, S. W. and Brand, A. H.** (2016). Cell-type-specific profiling of protein-DNA interactions without cell isolation using targeted DamID with next-generation sequencing. *Nat Protoc* **11**, 1586–1598.

**Maurange, C. and Gould, A. P.** (2005). Brainy but not too brainy: starting and stopping

neuroblast divisions in *Drosophila*. *Trends in Neurosciences* **28**, 30–36.

- McQueen, M. B., Devlin, B., Faraone, S. V., Nimgaonkar, V. L., Sklar, P., Smoller, J. W., Abou Jamra, R., Albus, M., Bacanu, S.-A., Baron, M., Barrett, T. B., Berrettini, W., Blacker, D., Byerley, W., Cichon, S., Coryell, W., Craddock, N., Daly, M. J., DePaulo, J. R., Edenberg, H. J., Foroud, T., Gill, M., Gilliam, T. C., Hamshere, M., Jones, I., Jones, L., Juo, S.-H., Kelsoe, J. R., Lambert, D., Lange, C., Lerer, B., Liu, J., Maier, W., MacKinnon, J. D., McInnis, M. G., McMahon, F. J., Murphy, D. L., Nöthen, M. M., Nurnberger Jr., J. I., Pato, C. N., Pato, M. T., Potash, J. B., Propping, P., Pulver, A. E., Rice, J. P., Rietschel, M., Scheftner, W., Schumacher, J., Segurado, R., Steen, K. V., Xie, W., Zandi, P. P. and Laird, N. M.** (2005). Combined Analysis from Eleven Linkage Studies of Bipolar Disorder Provides Strong Evidence of Susceptibility Loci on Chromosomes 6q and 8q. *Am. J. Hum. Genet.* **77**, 582–595.
- Middleton, F. A., Pato, M. T., Gentile, K. L., Morley, C. P., Zhao, X., Eisener, A. F., Brown, A., Petryshen, T. L., Kirby, A. N., Medeiros, H., Carvalho, C., Macedo, A., Dourado, A., Coelho, I., Valente, J., Soares, M. J., Ferreira, C. P., Lei, M., Azevedo, M. H., Kennedy, J. L., Daly, M. J., Sklar, P. and Pato, C. N.** (2004). Genomewide Linkage Analysis of Bipolar Disorder by Use of a High-Density Single-Nucleotide–Polymorphism (SNP) Genotyping Assay: A Comparison with Microsatellite Marker Assays and Finding of Significant Linkage to Chromosome 6q22. *Am. J. Hum. Genet.* **74**, 886–897.
- Monaghan, A. P., Bock, D., Gass, P., Schwäger, A., Wolfer, D. P., Lipp, H. P. and Schütz, G.** (1997). Defective limbic system in mice lacking the tailless gene. *Nature* **390**, 515–517.
- Monaghan, A. P., Grau, E., Bock, D. and Schütz, G.** (1995). The mouse homolog of the orphan nuclear receptor *tailless* is expressed in the developing forebrain. *Development* **121**, 839–853.
- Mumm, J. S., Shou, J. and Calof, A. L.** (1996). Colony-forming progenitors from mouse olfactory epithelium: Evidence for feedback regulation of neuron production. *Proc. Natl. Acad. Sci. U.S.A.* **93**, 11167–11172.
- Murray, R. C., Navi, D., Fesenko, J., Lander, A. D. and Calof, A. L.** (2003). Widespread Defects in the Primary Olfactory Pathway Caused by Loss of *Mash1* Function. *J. Neurosci.* **23**, 1769–1780.
- Nakamura, Y., Sakakibara, S. I., Miyata, T., Ogawa, M., Shimazaki, T., Weiss, S., Kageyama, R. and Okano, H.** (2000). The bHLH Gene *Hes1* as a Repressor of the Neuronal Commitment of CNS Stem Cells. *J. Neurosci.* **20**, 283–293.
- Neumüller, R. A., Richter, C., Fischer, A., Novatchkova, M., Neumüller, K. G. and Knoblich, J. A.** (2011). Genome-wide analysis of self-renewal in *Drosophila* neural stem cells by transgenic RNAi. *Cell Stem Cell* **8**, 580–593.
- Niu, W., Zou, Y., Shen, C. and Zhang, C.-L.** (2011). Activation of Postnatal Neural Stem Cells Requires Nuclear Receptor TLX. *J. Neurosci.* **31**, 13816–13828.
- Noctor, S. C., Martínez Cerdeño, V., Ivic, L. and Kriegstein, A. R.** (2004). Cortical neurons arise in symmetric and asymmetric division zones and migrate through specific phases. *Nat Neurosci* **7**, 136–144.

- Obernier, K., Simeonova, I., Fila, T., Mandl, C., Hölzl-Wenig, G., Monaghan-Nichols, P. and Ciccolini, F.** (2011). Expression of *Tlx* in Both Stem Cells and Transit Amplifying Progenitors Regulates Stem Cell Activation and Differentiation in the Neonatal Lateral Subependymal Zone. *Stem Cells* **29**, 1415–1426.
- Ohtsuka, T., Sakamoto, M., Guillemot, F. and Kageyama, R.** (2001). Roles of the Basic Helix-Loop-Helix Genes *Hes1* and *Hes5* in Expansion of Neural Stem Cells of the Developing Brain. *J. Biol. Chem.* **276**, 30467–30474.
- Oliver, G., Sosa-Pineda, B., Geisendorf, S., Spana, E. P., Doe, C. Q. and Gruss, P.** (1993). Prox 1, a *prospero*-related homeobox gene expressed during mouse development. *Mechanisms of Development* **44**, 3–16.
- Otsuki, L. and Brand, A. H.** (2018). Cell cycle heterogeneity directs the timing of neural stem cell activation from quiescence. *Science* **360**, 99–102.
- O’Leary, J. D., Kozareva, D. A., Hueston, C. M., O’Leary, O. F., Cryan, J. F. and Nolan, Y. M.** (2016). The nuclear receptor *Tlx* regulates motor, cognitive and anxiety-related behaviours during adolescence and adulthood. *Behavioural Brain Research* **306**, 36–47.
- Pandey, U. B. and Nichols, C. D.** (2011). Human Disease Models in *Drosophila melanogaster* and the Role of the Fly in Therapeutic Drug Discovery. *Pharmacol. Rev.* **63**, 411–436.
- Pankratz, M. J., Busch, M., Hoch, M., Seifert, E. and Jäckle, H.** (1992). Spatial control of the gap gene *knirps* in the *Drosophila* embryo by posterior morphogen system. *Science* **255**, 986–989.
- Park, H.-J., Kim, J.-K., Jeon, H.-M., Oh, S.-Y., Kim, S.-H., Park, M.-J., Soeda, A., Nam, D.-H. and Kim, H.** (2010). The Neural Stem Cell Fate Determinant *TLX* Promotes Tumorigenesis and Genesis of Cells Resembling Glioma Stem Cells. *Mol Cells* **30**, 403–408.
- Park, N. I., Guilhamon, P., Desai, K., McAdam, R. F., Langille, E., O’Connor, M., Lan, X., Whetstone, H., Coutinho, F. J., Vanner, R. J., Ling, E., Prinos, P., Lee, L., Selvadurai, H., Atwal, G., Kushida, M., Clarke, I. D., Voisin V., Cusimano, M. D., Bernstein, M., Das, S., Bader, G., Arrowsmith, C. H., Angers, S., Huang, X., Lupien, M. and Dirks, P. B.** (2017). *ASCL1* Reorganizes Chromatin to Direct Neuronal Fate and Suppress Tumorigenicity of Glioblastoma Stem Cells. *Stem Cell* 1–24.
- Pfeiffer, B. D., Jenett, A., Hammonds, A. S., Ngo, T.-T. B., Misra, S., Murphy, C., Scully, A., Carlson, J. W., Wan, K. H., Lavery, T. R., Mungall, C., Svirskas, R., Kadonaga, J. T., Doe, C. Q., Eisen, M. B., Celniker, S. E. and Rubin, G. M.** (2008). Tools for neuroanatomy and neurogenetics in *Drosophila*. *PNAS* **105**, 9715–9720.
- Pignoni, F., Baldarelli, R. M., Steingrímsson, E., Diaz, R. J., Patapoutian, A., Merriam, J. R. and Lengyel, J. A.** (1990). The *Drosophila* gene *tailless* is expressed at the embryonic termini and is a member of the steroid receptor superfamily. *Cell* **62**, 151–163.
- Pisapia, D. J.** (2017). The Updated World Health Organization Glioma Classification: Cellular and Molecular Origins of Adult Infiltrating Gliomas. *Arch. Pathol. Lab. Med.* **141**, 1633–1645.
- Poulson, D. F.** (1950). Histogenesis, organogenesis, and differentiation in the embryo of

*Drosophila melanogaster* Meigen. *Biology of Drosophila* 168–274.

- Prokop, A. and Technau, G. M.** (1991). The origin of postembryonic neuroblasts in the ventral nerve cord of *Drosophila melanogaster*. *Development* **111**, 79–88.
- Prokop, A. and Technau, G. M.** (1994). Normal Function of the *mushroom body defect* Gene of *Drosophila* is Required for the Regulation of the Number and Proliferation of Neuroblasts. *Dev. Biol.* **161**, 321–337.
- Qu, Q., Sun, G., Li, W., Yang, S., Ye, P., Zhao, C., Yu, R. T., Gage, F. H., Evans, R. M. and Shi, Y.** (2010). Orphan nuclear receptor TLX activates Wnt/beta-catenin signalling to stimulate neural stem cell proliferation and self-renewal. *Nat. Cell Biol.* **12**, 31–40– sup pp 1–9.
- Reddy, B. V. V. G., Rauskolb, C. and Irvine, K. D.** (2010). Influence of fat-hippo and notch signaling on the proliferation and differentiation of *Drosophila* optic neuroepithelia. *Development* **137**, 2397–2408.
- Reya, T., Morrison, S. J., Clarke, M. F. and Weissman, I. L.** (2001). Stem cells, cancer, and cancer stem cells. *Nature* **414**, 105–111.
- Reynolds, B. A. and Weiss, S.** (1992). Generation of neurons and astrocytes from isolated cells of the adult mammalian central nervous system. *Science* **255**, 1707–1710.
- Richter, C., Oktaba, K., Steinmann, J., Müller, J. and Knoblich, J. A.** (2011). The tumour suppressor L(3)mbt inhibits neuroepithelial proliferation and acts on insulator elements. *Nat. Cell Biol.* **13**, 1029–1039.
- Ringrose, L.** (2009). Transgenesis in *Drosophila melanogaster*. In *Transgenesis Techniques*, pp. 3–19. Totowa, NJ: Humana Press.
- Roy, K., Thiels, E. and Monaghan, A. P.** (2002). Loss of the *tailless* gene affects forebrain development and emotional behavior. *Physiol. Behav.* **77**, 595–600.
- Rudolph, K. M., Liaw, G. J., Daniel, A., Green, P., Courey, A. J., Hartenstein, V. and Lengyel, J. A.** (1997). Complex regulatory region mediating *tailless* expression in early embryonic patterning and brain development. *Development* **124**, 4297–4308.
- San-Juán, B. P. and Baonza, A.** (2011). The bHLH factor *deadpan* is a direct target of Notch signaling and regulates neuroblast self-renewal in *Drosophila*. *Dev. Biol.* **352**, 70–82.
- Sanai, N., Alvarez-Buylla, A. and Berger, M. S.** (2005). Neural Stem Cells and the Origin of Gliomas. *N Engl J Med* **353**, 811–822.
- Sato, M., Yasugi, T., Minami, Y., Miura, T. and Nagayama, M.** (2016). Notch-mediated lateral inhibition regulates proneural wave propagation when combined with EGF-mediated reaction diffusion. *PNAS* **113**, E5153–62.
- Schindelin, J., Arganda-Carreras, I., Frise, E., Kaynig, V., Longair, M., Pietzsch, T., Preibisch, S., Rueden, C., Saalfeld, S., Schmid, B., Tinevez, J.-Y., White, D. J., Hartenstein, V., Eliceiri, K., Tomancak, P. and Cardona, A.** (2012). Fiji: an open-source platform for biological-image analysis. *Nature Methods* **9**, 676–682.

- Schmucker, D., Jäckle, H. and Gaul, U.** (1997). Genetic analysis of the larval optic nerve projection in *Drosophila*. *Development* **124**, 937–948.
- Schmucker, D., Taubert, H. and Jäckle, H.** (1992). Formation of the *Drosophila* Larval Photoreceptor Organ and Its Neuronal Differentiation Require Continuous *Krüppel* Gene Activity. *Neuron* **9**, 1025–1039.
- Seri, B., García-Verdugo, J. M., McEwen, B. S. and Alvarez-Buylla, A.** (2001). Astrocytes Give Rise to New Neurons in the Adult Mammalian Hippocampus. *J. Neurosci.* **21**, 7153–7160.
- Shi, Y., Chichung Lie, D., Taupin, P., Nakashima, K., Ray, J., Yu, R. T., Gage, F. H. and Evans, R. M.** (2004). Expression and function of orphan nuclear receptor TLX in adult neural stem cells. *Nature* **427**, 78–83.
- Singh, S. K., Clarke, I. D., Terasaki, M., Bonn, V. E., Hawkins, C., Squire, J. and Dirks, P. B.** (2003). Identification of a Cancer Stem Cell in Human Brain Tumors. *Cancer Res* **63**, 5821–5828.
- Singh, S. K., Hawkins, C., Clarke, I. D., Squire, J. A., Bayani, J., Hide, T., Henkelman, R. M., Cusimano, M. D. and Dirks, P. B.** (2004). Identification of human brain tumour initiating cells. *Nature* **432**, 396–401.
- Skeath, J. B. and Carroll, S. B.** (1994). The *achaete-scute* complex: generation of cellular pattern and fate within the *Drosophila* nervous system. *FASEB J.* **8**, 714–721.
- Sonoshita, M. and Cagan, R. L.** (2017). Modeling Human Cancers in *Drosophila*. *Curr Top Dev Biol* **121**, 287–309.
- Sottoriva, A., Spiteri, I., Piccirillo, S. G. M., Touloumis, A., Collins, V. P., Marioni, J. C., Curtis, C., Watts, C. and Tavaré, S.** (2013). Intratumor heterogeneity in human glioblastoma reflects cancer evolutionary dynamics. *PNAS* **110**, 4009–4014.
- Sousa-Nunes, R., Yee, L. L. and Gould, A. P.** (2011). Fat cells reactivate quiescent neuroblasts via TOR and glial insulin relays in *Drosophila*. *Nature* **471**, 508–512.
- Southall, T. D., Davidson, C. M., Miller, C., Carr, A. and Brand, A. H.** (2014). Dedifferentiation of neurons precedes tumor formation in Lola mutants. *Dev. Cell* **28**, 685–696.
- Southall, T. D., Gold, K. S., Egger, B., Davidson, C. M., Caygill, E. E., Marshall, O. J. and Brand, A. H.** (2013). Cell-type-specific profiling of gene expression and chromatin binding without cell isolation: assaying RNA Pol II occupancy in neural stem cells. *Dev. Cell* **26**, 101–112.
- Spana, E. P. and Doe, C. Q.** (1995). The prospero transcription factor is asymmetrically localized to the cell cortex during neuroblast mitosis in *Drosophila*. *Development* **121**, 3187–3195.
- Spéder, P. and Brand, A. H.** (2014). Gap Junction Proteins in the Blood-Brain Barrier Control Nutrient-Dependent Reactivation of *Drosophila* Neural Stem Cells. *Dev. Cell* **30**, 309–321.
- Stiles, C. D. and Rowitch, D. H.** (2008). Glioma Stem Cells: A Midterm Exam. *Neuron* **58**,

- Strecker, T. R., Kongsuwan, K., Lengyel, J. A. and Merriam, J. R.** (1986). The zygotic mutant *tailless* affects the anterior and posterior ectodermal regions of the *Drosophila* embryo. *Dev. Biol.* **113**, 64–76.
- Strecker, T. R., Merriam, J. R. and Lengyel, J. A.** (1988). Graded requirement for the zygotic terminal gene, *tailless*, in the brain and tail region of the *Drosophila* embryo. *Development* **102**, 721–734.
- Sun, G., Alzayady, K., Stewart, R., Ye, P., Yang, S., Li, W. and Shi, Y.** (2010). Histone Demethylase LSD1 Regulates Neural Stem Cell Proliferation. *Mol. Cell. Biol.* **30**, 1997–2005.
- Sun, G., Ye, P., Murai, K., Lang, M.-F., Li, S., Zhang, H., Li, W., Fu, C., Yin, J., Wang, A., Ma, X. and Shi, Y.** (2011). miR-137 forms a regulatory loop with nuclear receptor TLX and LSD1 in neural stem cells. *Nat Commun* **2**, 529.
- Sun, G., Yu, R. T., Evans, R. M. and Shi, Y.** (2007). Orphan nuclear receptor TLX recruits histone deacetylases to repress transcription and regulate neural stem cell proliferation. *Proc. Natl. Acad. Sci. U.S.A.* **104**, 15282–15287.
- Tix, S., Minden, J. S. and Technau, G. M.** (1989). Pre-existing neuronal pathways in the developing optic lobes of *Drosophila*. *Development* **105**, 739–746.
- Torii, M. A., Matsuzaki, F., Osumi, N., Kaibuchi, K., Nakamura, S., Casarosa, S., Guillemot, F. and Nakafuku, M.** (1999). Transcription factors Mash-1 and Prox-1 delineate early steps in differentiation of neural stem cells in the developing central nervous system. *Development* **126**, 443–456.
- Truman, J. W. and Bate, M.** (1988). Spatial and temporal patterns of neurogenesis in the central nervous system of *Drosophila melanogaster*. *Dev. Biol.* **125**, 145–157.
- Turner, F. R. and Mahowald, A. P.** (1979). Scanning electron microscopy of *Drosophila melanogaster* embryogenesis. III. Formation of the head and caudal segments. *Dev. Biol.* **68**, 96–109.
- Ulvklo, C., MacDonald, R., Bivik, C., Baumgardt, M., Karlsson, D. and Thor, S.** (2012). Control of neuronal cell fate and number by integration of distinct daughter cell proliferation modes with temporal progression. *Development* **139**, 678–689.
- Urbach, R. and Technau, G. M.** (2003). Molecular markers for identified neuroblasts in the developing brain of *Drosophila*. *Development* **130**, 3621–3637.
- Vaessin, H., Grell, E., Wolff, E., Bier, E., Jan, L. Y. and Jan, Y.-N.** (1991). *prospero* is Expressed in Neuronal Precursors and Encodes a Nuclear Protein That Is Involved in the Control of Axonal Outgrowth in *Drosophila*. *Cell* **67**, 941–953.
- van Steensel, B. and Henikoff, S.** (2000). Identification of *in vivo* DNA targets of chromatin proteins using tethered dam methyltransferase. *Nat Biotechnol* **18**, 424–428.
- van Steensel, B., Delrow, J. and Henikoff, S.** (2001). Chromatin profiling using targeted DNA adenine methyltransferase. *Nat Genet* **27**, 304–308.

- Venken, K. J. T., Carlson, J. W., Schulze, K. L., Pan, H., He, Y., Spokony, R., Wan, K. H., Koriabine, M., de Jong, P. J., White, K. P., Bellen, H. J. and Hoskins R. A.** (2009). Versatile P[acman] BAC libraries for transgenesis studies in *Drosophila melanogaster*. *Nat Meth* **6**, 431–434.
- Wallace, K., Liu, T. H. and Vaessin, H.** (2000). The Pan-Neural bHLH Proteins DEADPAN and ASENSE Regulate Mitotic Activity and cdk Inhibitor *dacapo* Expression in the *Drosophila* Larval Optic Lobes. *genesis* **26**, 77–85.
- Wang, L., Charroux, B., Kerridge, S. and Tsai, C.-C.** (2008). Atrophin recruits HDAC1/2 and G9a to modify histone H3K9 and to determine cell fates. *EMBO Rep* **9**, 555–562.
- Wang, L., Rajan, H., Pitman, J. L., McKeown, M. and Tsai, C.-C.** (2006). Histone deacetylase-associating Atrophin proteins are nuclear receptor corepressors. *Genes Dev.* **20**, 525–530.
- Wang, T. and Xiong, J.-Q.** (2016). The Orphan Nuclear Receptor TLX/NR2E1 in Neural Stem Cells and Diseases. *Neurosci Bull* 1–7.
- Wang, Y.-C., Yang, J. S., Johnston, R., Ren, Q., Lee, Y.-J., Luan, H., Brody, T., Odenwald, W. F. and Lee, T.** (2014). *Drosophila* intermediate neural progenitors produce lineage-dependent related series of diverse neurons. *Development* **141**, 253–258.
- Weng, M., Golden, K. L. and Lee, C.-Y.** (2010). dFzef/Earmuff maintains the restricted developmental potential of intermediate neural progenitors in *Drosophila*. *Dev. Cell* **18**, 126–135.
- White, K. and Kankel, D. R.** (1978). Patterns of Cell Division and Cell Movement in the Formation of the Imaginal Nervous System in *Drosophila melanogaster*. *Dev. Biol.* **65**, 296–321.
- White, K., Grether, M. E., Abrams, J. M., Young, L., Farrell, K. and Steller, H.** (1994). Genetic control of programmed cell death in *Drosophila*. *Science* **264**, 677–683.
- Whitfield, W. G., González, C., Maldonado-Codina, G. and Glover, D. M.** (1990). The A- and B-type cyclins of *Drosophila* are accumulated and destroyed in temporally distinct events that define separable phases of the G2-M transition. *The EMBO Journal* **9**, 2563–2572.
- Wong, E. H. F., Tarazi, F. I. and Shahid, M.** (2010). The effectiveness of multi-target agents in schizophrenia and mood disorders: Relevance of receptor signature to clinical action. *Pharmacol. Ther.* **126**, 173–185.
- Wu, H.-H., Ivkovic, S., Murray, R. C., Jaramillo, S., Lyons, K. M., Johnson, J. E. and Calof, A. L.** (2003). Autoregulation of neurogenesis by GDF11. *Neuron* **37**, 197–207.
- Xie, Y., Li, X., Deng, X., Hou, Y., O'Hara, K., Urso, A., Peng, Y., Chen, L. and Zhu, S.** (2016). The Ets protein Pointed prevents both premature differentiation and dedifferentiation of *Drosophila* intermediate neural progenitors. *Development* **143**, 3109–3118.
- Xie, Y., Li, X., Zhang, X., Mei, S., Li, H., Urso, A. and Zhu, S.** (2014). The *Drosophila* Sp8 transcription factor Buttonhead prevents premature differentiation of intermediate neural progenitors. *Elife* **3**, 26.

- Yagi, R., Mayer, F. and Basler, K.** (2010). Refined LexA transactivators and their use in combination with the *Drosophila* Gal4 system. *PNAS* **107**, 16166–16171.
- Yang, C.-P., Fu, C.-C., Sugino, K., Liu, Z., Ren, Q., Liu, L.-Y., Yao, X., Lee, L. P. and Lee, T.** (2016). Transcriptomes of lineage-specific *Drosophila* neuroblasts profiled by genetic targeting and robotic sorting. *Development* **143**, 411–421.
- Yasugi, T., Sugie, A., Umetsu, D. and Tabata, T.** (2010). Coordinated sequential action of EGFR and Notch signaling pathways regulates proneural wave progression in the *Drosophila* optic lobe. *Development* **137**, 3193–3203.
- Yasugi, T., Umetsu, D., Murakami, S., Sato, M. and Tabata, T.** (2008). *Drosophila* optic lobe neuroblasts triggered by a wave of proneural gene expression that is negatively regulated by JAK/STAT. *Development* **135**, 1471–1480.
- Yokoyama, A., Takezawa, S., Schüle, R., Kitagawa, H. and Kato, S.** (2008). Transrepressive function of TLX requires the histone demethylase LSD1. *Mol. Cell. Biol.* **28**, 3995–4003.
- Young, K. A., Berry, M. L., Mahaffey, C. L., Saionz, J. R., Hawes, N. L., Chang, B., Zheng, Q. Y., Smith, R. S., Bronson, R. T., Nelson, R. J., R. J. and Simpson, E. M.** (2002). Fierce: a new mouse deletion of Nr2e1; violent behaviour and ocular abnormalities are background-dependent. *Behavioural Brain Research* **132**, 145–158.
- Younossi-Hartenstein, A., Green, P., Liaw, G.-J., Rudolph, K., Lengyel, J. and Hartenstein, V.** (1997). Control of Early Neurogenesis of the *Drosophila* Brain by the Head Gap Genes *tll*, *otd*, *ems*, and *btd*. *Dev. Biol.* **182**, 270–283.
- Yu, R. T., Chiang, M. Y., Tanabe, T., Kobayashi, M., Yasuda, K., Evans, R. M. and Umesono, K.** (2000). The orphan nuclear receptor Tlx regulates Pax2 and is essential for vision. *Proc. Natl. Acad. Sci. U.S.A.* **97**, 2621–2625.
- Yu, R. T., McKeown, M., Evans, R. M. and Umesono, K.** (1994). Relationship between *Drosophila* gap gene *tailless* and a vertebrate nuclear receptor Tlx. *Nature* **370**, 375–379.
- Zacharioudaki, E., Magadi, S. S. and Delidakis, C.** (2012). bHLH-O proteins are crucial for *Drosophila* neuroblast self-renewal and mediate Notch-induced overproliferation. *Development* **139**, 1258–1269.
- Zeng, Z.-J., Johansson, E., Hayashi, A., Chavali, P. L., Akrap, N., Yoshida, T., Kohno, K., Izumi, H. and Funa, K.** (2012). TLX controls angiogenesis through interaction with the von Hippel-Lindau protein. *Biol Open* **1**, 527–535.
- Zhang, C.-L., Zou, Y., He, W., Gage, F. H. and Evans, R. M.** (2008). A role for adult TLX-positive neural stem cells in learning and behaviour. *Nature* **451**, 1004–1007.
- Zhang, C.-L., Zou, Y., Yu, R. T., Gage, F. H. and Evans, R. M.** (2006). Nuclear receptor TLX prevents retinal dystrophy and recruits the corepressor atrophin1. *Genes Dev.* **20**, 1308–1320.
- Zhang, S., Xu, L., Lee, J. and Xu, T.** (2002). *Drosophila* Atrophin homolog functions as a transcriptional corepressor in multiple developmental processes. *Cell* **108**, 45–56.
- Zhi, X., Zhou, X. E., He, Y., Searose-Xu, K., Zhang, C.-L., Tsai, C.-C., Melcher, K. and**

- Xu, H. E.** (2015). Structural basis for corepressor assembly by the orphan nuclear receptor TLX. *Genes Dev.* **29**, 440–450.
- Zhu, S., Barshow, S., Wildonger, J., Jan, L. Y. and Jan, Y.-N.** (2011). Ets transcription factor Pointed promotes the generation of intermediate neural progenitors in *Drosophila* larval brains. *Proc. Natl. Acad. Sci. U.S.A.* **108**, 20615–20620.
- Zhu, S., Wildonger, J., Barshow, S., Younger, S., Huang, Y. and Lee, T.** (2012). The bHLH repressor Deadpan regulates the self-renewal and specification of *Drosophila* larval neural stem cells independently of Notch. *PLoS ONE* **7**, e46724.
- Zhu, Z., Khan, M. A., Weiler, M., Blaes, J., Jestaedt, L., Geibert, M., Zou, P., Gronych, J., Bernhardt, O., Korshunov, A., Bugner, V., Lichter, P., Radlwimmer, B., Heiland, S., Bendszus, M., Wick, W. and Liu, H.-K.** (2014). Targeting Self-Renewal in High-Grade Brain Tumors Leads to Loss of Brain Tumor Stem Cells and Prolonged Survival. *Cell Stem Cell* **15**, 185–198.
- Zong, H., Espinosa, J. S., Su, H. H., Muzumdar, M. D. and Luo, L.** (2005). Mosaic Analysis with Double Markers in Mice. *Cell* **121**, 479–492.
- Zong, H., Verhaak, R. G. and Canoll, P.** (2012). The cellular origin for malignant glioma and prospects for clinical advancements. *Expert Rev. Mol. Diagn.* **12**, 383–394.
- Zou, Y., Niu, W., Qin, S., Downes, M., Burns, D. K. and Zhang, C.-L.** (2012). The nuclear receptor TLX is required for gliomagenesis within the adult neurogenic niche. *Mol. Cell Biol.* **32**, 4811–4820.